# Examination of the potential for glass-containing gunshot residues to improve forensic gunshot residue interpretation

by

**Kelsey Elaine Seyfang, BSc(Hons)**

Thesis

Submitted to Flinders University

for the degree of

Doctor of Philosophy

**College of Science and Engineering**

December 2019

# Table of Contents

Table of Contents ..... i

Abstract ..... vi

Statement of Originality ..... vii

Acknowledgements ..... viii

Funding Sources and Instrumental Access ..... ix

Publications resulting from this research ..... x

Presentations given about this research ..... xi

Table of Tables ..... xii

Table of Figures ..... xiv

Table of Abbreviations/Acronyms ..... xix

Periodic Table ..... xxi

1. Introduction and Literature Review ..... 1

1.1. General Introduction ..... 1

1.1.1. Firearms and Society ..... 1

1.1.2. The Firearm ..... 2

1.1.3. Introduction to Firearm Science: ..... 4

1.1.4. General Introduction to Gunshot Residue (GSR) ..... 5

1.2. Review of the Classification and Discrimination of GSRs ..... 9

1.3. Early History of the Classification of GSR ..... 9

1.4. Review of the Classification of GSR by Bulk Instrumental Analysis Techniques ..... 10

1.4.1. General Limitations of Bulk Analysis Techniques for GSR Applications ..... 11

1.5. Review of Classification and Discrimination of GSR by Particle Analysis ..... 12

1.5.1. The Use of SEM-EDS for Particle Analysis ..... 12

1.5.2. GSR Interpretation using SEM-EDS ..... 15

1.5.3. Alternative Techniques for GSR Particle Analysis ..... 17
1.6. Previous work involving glass-containing GSR ..... 20
1.7. Glass, the analysis of glass, and the analysis of gGSR ..... 21
1.7.1. Glass elemental composition analysis methods ..... 21
2. Objectives and Experimental Theory ..... 23
2.1. Contextual Statement ..... 23
2.2. Overarching Aims ..... 23
2.3. Thesis Outline of Experimental Chapters ..... 24
2.3.1. Chapter 3: Glass-containing gunshot residues and similar particles of industrial and occupational origins: considerations for evaluating GSR traces ..... 24
2.3.2. Chapter 4: Analysis of elemental and isotopic variation in glass frictionators from 0.22 rimfire primers ..... 25
2.3.3. Chapter 5: Methods for Analysis of Glass in Glass-Containing Gunshot Residue (gGSR) Particles ..... 25
2.4. Experimental Theory ..... 26
2.4.1. Refractive index measurements by GRIM ..... 26
2.4.2. Scanning electron microscopy and related techniques ..... 27
2.4.3. Mass spectrometry techniques ..... 30
3. Glass-containing gunshot residues and similar particles of industrial and occupational origins: considerations for evaluating GSR traces ..... 33
3.1. Preface ..... 33
3.2. Chapter Summary ..... 33
3.3. Introduction ..... 34
3.3.1. Literature Review of Particles Originating from Fireworks ..... 37
3.3.2. Literature Review of Particles Originating from Nail Guns ..... 39
3.3.3. Literature Review of Particles Originating from Matches ..... 40
3.3.4. Literature Review of Particles Originating from Brake Pads ..... 40

3.4. Methods ..... 41
3.4.1. Sample Collection ..... 41
3.4.2. Analysis by SEM-EDS and automated particle searching ..... 44
3.4.3. Review of real-world casework data for GSR and gGSR ..... 44
3.5. Results ..... 45
3.5.1. Examination of Firework Particles and Populations ..... 45
3.5.2. Examination of Nail Gun Particles and Populations ..... 50
3.5.3. Examination of Match Particles and Populations ..... 56
3.5.4. Examination of Brake Pad Particles and Populations ..... 59
3.5.5. Comparison of Particles from Different Sources ..... 63
3.5.6. Review of real-world casework data for GSR and gGSR ..... 65
3.6. Conclusions ..... 68
3.7. Supplementary information for Chapter 3 ..... 71
4. Analysis of elemental and isotopic variation in glass frictionators from 0.22 rimfire primers ..... 72
4.1. Preface ..... 72
4.2. Chapter Summary ..... 72
4.3. Introduction ..... 74
4.3.1. Samples and Reference Materials ..... 78
4.4. Methods ..... 82
4.4.1. Identification of glass in frictionator and gGSR ..... 82
4.4.2. Isotopic Composition of Li and B in CRMs ..... 83
4.4.3. Frictionator Extraction Process ..... 88
4.4.4. ToF-SIMS ..... 90
4.4.5. SHRIMP ..... 91
4.4.6. SEM-EDS ..... 92
4.4.7. GRIM ..... 94

4.5. Results and Discussion ..... 95
4.5.1. Isotopic Composition of Li and B in CRMs ..... 95
4.5.2. ToF-SIMS Analysis ..... 102
4.5.1. SHRIMP Elemental Composition Analysis ..... 107
4.5.2. SHRIMP Isotope Analysis ..... 108
4.5.3. SEM-EDS Analysis ..... 110
4.5.4. Comparison and Contrast of Techniques. ..... 113
4.5.5. Refractive Index Measurement ..... 115
4.6. Comparison to Previous Results ..... 119
4.7. Summary and Conclusions ..... 121
5. Methods for Analysis of Glass in Glass-Containing Gunshot Residue (gGSR) Particles ..... 124
5.1. Preface ..... 124
5.2. Chapter Summary ..... 124
5.3. Introduction ..... 126
5.4. Materials and Methods ..... 129
5.4.1. Sample Collection ..... 129
5.4.2. SEM EDS Identification of GSR particles ..... 132
5.4.3. Sample Preparation by Focussed Ion Beam (FIB) ..... 132
5.4.4. Preparation for X-ray Spot Analyses and Mapping and SEM-EDS Analysis of FIB Slices 135
5.4.5. ToF-SIMS Analysis of FIB-prepared slices of gGSR ..... 136
5.5. Results and Discussion ..... 136
5.5.1. SEM-EDS analysis of FIB Slice – X-ray Spot Analyses and Mapping ..... 136
5.5.2. Comparison of gGSR to extracted frictionator using SEM-EDS ..... 143
5.5.3. Comparison of gGSR to extracted frictionator using ToF-SIMS ..... 144
5.6. Conclusions ..... 147
6. Conclusions and Future Works ..... 150

6.1.1. Occupational residue sources and gunshot residues .....150

6.1.2. Concluding comments concerning Glass-containing residues.....151

6.1.3. Concluding comments regarding particles characteristic of GSR .....152

6.2. Analysis of Glass Frictionators ..... 153

6.3. Glass-Containing Gunshot Residues ..... 154

6.4. Recommendations and Future Works ..... 155

6.5. Impacts of this Research ..... 158

7. References..... **Error! Bookmark not defined.**

8. Appendices ..... 175

8.1. Plots of ToF-SIMS data with Average Abundance and 99% Confidence Intervals 175

8.2. Plots of SEM-EDS data with Average Abundance and 99% Confidence Intervals 176

8.3. Particle Count Data from stubs from GSR, automotive sources, nail guns, fireworks and matches..... 177

8.4. Manuscripts published associated with work from this thesis ..... 178

# Abstract

Guns were used in crimes amassing over 24 thousand victims in Australia between 1995 and 2012, including 859 homicides [4]. A common trace evidence in these cases is gunshot residue (GSR), a mix of vapours and particulates that are deposited onto the shooter, victim and surrounds during a firing event.

There is currently difficulty in distinguishing between residues from different sources, such as from a firearm and fireworks or nail guns, or GSR from two different ammunitions. A potentially highly characteristic particle 'glass-containing GSR' (gGSR) has been discovered previously, and in order to improve fundamental understanding of this type of GSR, and to explore novel capabilities offered through analysis of these particles, a three-pronged project was undertaken.

The first examined the probative value of glass-containing GSR by investigating potential sources of similar particles, including from brake pads, fireworks and nail guns. This project focussed on incorporating gGSR particles into GSR investigations using techniques currently used in research and casework, and improving the detection of and discrimination between samples of GSR using the glass-containing GSR.

Secondly, a market survey was undertaken on glass particles taken from different ammunitions. The variation of frictionator glass and glass-containing GSR from ammunitions across the Australian market was assessed, focussing on 0.22 rimfire weapons. It was found that with 99% confidence over 94% of glass samples from ammunitions from different brands could be distinguished.

In the third sub-project, genuine glass-containing GSR particles were located, and methods for the analysis and comparison of these samples were investigated. It was found that different glass-containing particles had different morphologies, and different incorporation of other GSR components. It was also demonstrated, as a proof-of-concept, that pre-fired and post-fired residues from the same ammunition could not be discriminated, while residues from different sources could potentially be discriminated.

The results from each of these parallel prongs have inter-connecting and overlapping consequences for interpretation of GSR evidence and could lead to the development of new capabilities and opportunities in forensic laboratories.

# Statement of Originality

I certify that this thesis does not incorporate without acknowledgement any material previously submitted for a degree or diploma in any university, and to the best of my knowledge and belief, does not contain any material previously published or written by another person except where due reference is made in the text or preface.

Signed:

Kelsey E Seyfang 19th December 2019

# Acknowledgements

Firstly, I would like to thank my family, for their support, for looking after me during the stressful times, and for all their help over the years. I wouldn't be here without you. Mum, Jess, Beth, you are all a daily source of strength and inspiration for me.

Thanks to Kim Wong for teaching me about the falling of glass from the sky after the meteor that killed the dinosaurs hit the Earth. It's good to know some things are timeless.

Thanks to all my co-workers at FASS for their patience, support and for traveling the last part of this journey with me.

Thank you to the all regular visitors to ElNicSey, who always made our office bright, and feel a little like Grand Central Station. You have made the last few years fun as well as productive, and filled with tea, games and desserts. Love going out to our regulars, Ruby, Tristan, Jo, Ryan and Caroline, and Alex.

To Claire Lenehan, thanks for your support in a thousand different ways, I probably wouldn't have pursued a PhD if I had never met you. Thank you to the staff, students and alumni of the analytical chemistry research group (PopelKirkPringEhan) at Flinders University.

Thanks to Lachlan Arentz, for his counsel, for always being only a call or message away, and for excellent support through all of the personal and professional ups-and-downs over the last five years. I promise to visit more.

Thank you to Eliza and Nick, for everything. I couldn't have asked for better people to share an office with. You guys have kept me sane, let me bounce ideas, and have taught me more about life than I might have learned in 20 years without you. I'll be keeping my post-its forever.

To Hilton and Kahlee, thank you for always giving such great perspective, and for all the reads, chats and feedback.

To Rachel, for always asking more of me, and inspiring me to do better. For demonstrating how to succeed in academia, and for always having a handy textbook.

To Paul, for your unwavering support, your belief that I have what it takes, and for all the excellent discussions we have had in meetings over the past few years. For your always thoughtful comments and insights, for always frowning during presentations, and for improving analytical group barbecues since '15.

# Funding Sources and Instrumental Access

This project was supported by a Premier's Research and Industry Fund grant provided by the South Australian Government Department of State Development. I acknowledge financial contributions from an Australian Government Research Training Program Scholarship. I acknowledge the travel scholarship I received from the Australian and New Zealand Forensic Science Society (ANZFSSS) SA Branch to attend the 23rd ANZFSS Symposium held in Auckland in 2016.

This project also received contributions from the Ross Vining Fund, provided by the South Australian Government Department of Justice. Many thanks go to my supervisor, Kahlee Redman, from Forensic Science SA, for her support, advice and her thoughtful and timely suggestions that improved this thesis. I would also like to extend thanks to Michael Cook, and the rest of the Chemistry – Trace Evidence team for their expert comments, provision of standard methods and samples, and technical support.

I acknowledge the support of Australian Scientific Instruments (ASI) and Geoscience Australia (GA), for the access to their SHRIMP instrument and equipment, their methods, and their staff, specifically Charles W Magee Jr., David DiBugnara, Keith Sircombe, and Geoff Fraser.

I would like to acknowledge Ivan Sarvas for sharing his expertise in FIB methodology for GSR analyses, Jim Wallace for providing the PMC Zapper residue, and South Australia Police for supplying cartridge cases, and assisting in collection of Federal Premium residue.

I acknowledge the expertise, equipment, and support provided by Australian Microscopy and Microanalysis Research Facility (AMMRF), including the South Australian Research Facility (SARF) at the University of South Australia, Adelaide Microscopy at the University of Adelaide, and the AMMRF and Australian National Fabrication Facilities (ANFF) at Flinders University. I would specifically like to acknowledge expertise and assistance of Dr Animesh Basak from Adelaide Microscopy for assistance with FIB analysis, and Dr Jason Gascooke for his assistance with the SEM EDS system. I would also like to specifically acknowledge the assistance of Dr John Denman and Dr Alex-Anthony Cavallaro, of the University of South Australia and the AMMRF for assistance with the ToF-SIMS analysis.

I acknowledge the support received from Simone Kasemann and Anette Meixner from Marum, at the University of Bremen, for their analysis of isotopic ratios of borosilicate glass standards by MC-ICPMS, and for their assistance in data interpretation, their expertise, and for providing a description of their methods for my work.

# Publications resulting from this research

[1] W. Tucker, N. Lucas, K.E. Seyfang, K.P. Kirkbride, R.S. Popelka-Filcoff, Gunshot residue and brake pads: Compositional and morphological considerations for forensic casework, Forensic Science International 270 (2017) 76-82.

[2] K.E. Seyfang, H.J. Kobus, R.S. Popelka-Filcoff, A. Plummer, C.W. Magee, K.E. Redman, K.P. Kirkbride, Analysis of elemental and isotopic variation in glass frictionators from 0.22 rimfire primers, Forensic Science International 293 (2018) 47-62.

[3] K.E. Seyfang, N. Lucas, K.E. Redman, R.S. Popelka-Filcoff, H.J. Kobus, K.P. Kirkbride, Glass-containing gunshot residues and particles of industrial and occupational origins: Considerations for evaluating GSR traces, Forensic Science International 298 (2019) 284-297.

[4] K.E. Seyfang, N. Lucas, R.S. Popelka-Filcoff, H.J. Kobus, K.E. Redman, K.P. Kirkbride, Methods for analysis of glass in glass-containing gunshot residue (gGSR) particles, Forensic Science International 298 (2019) 359-371.

# Presentations given about this research

*Royal Australian Chemical Institute: Research and Development 2015*

Poster presentation: Forensic Identification and Discrimination of Gunshot Residue (GSR)

*Royal Australian Chemical Institute: Analytical and Environmental Division Meeting 2016*

Poster presentation: Combining Morphology and Composition for the Differentiation between GSR and Environmental Particles

*The 23rd International Symposium on the Forensic Sciences of the Australian and New Zealand Forensic Science Society (ANZFSS 2016)*

Oral Presentation: Glass in primer GSR: can it revolutionise how we interpret gunshot residue evidence?

*Flinders University Higher Degree Research Conference 2017*

Oral Presentation: Novel Capabilities for Gunshot Residue Analyses through the Exploitation of Glass from Primer Mixes

*The 70th Annual Meeting of the American Academy of the Forensic Sciences (AAFS 2018)*

Oral Presentation: Novel Capabilities for Forensic Gunshot Residue Analysis through Exploitation of Glass found in Primer Mixes

Poster presentation: Analysis of Standard Glass Reference Materials via Advanced Chemical Techniques for Forensic Applications

*The 24th International Symposium on the Forensic Sciences of the Australian and New Zealand Forensic Science Society (ANZFSS 2018)*

Oral Presentation: Glass-Containing Gunshot Residues: Exploitation for Forensic Purposes

# Table of Tables

Table 1: Inorganic compounds associated with primers and their functions ..... 6
Table 2: Compounds associated with Heavy Metal Free primers and their functions [28-31] ..... 7
Table 3: Organic compounds associated with propellant GSR and their functions ..... 7
Table 4: Original Aerospace Report guidelines for the identification of GSR ..... 13
Table 5: Current 2017 ASTM guidelines for GSR classification ..... 14
Table 6: A summary of the findings of existing literature in atmospheric pollution of heavy metals attributable to firework displays. [203-213] ..... 38
Table 7: Total number of selected particle types automatically categorised by software from *n* samples from fireworks with average 30 < Z < 82 by BSE-SEM-EDS. ..... 46
Table 8: Results of a manual review of 1000 fireworks particles for magnalium indicators. Particles were identified using BSE-SEM-EDS GSR particle searching. ..... 50
Table 9: Total number of selected particle types automatically categorised by software for particles from *n* samples from nail guns with average 30 < Z < 82 by BSE-SEM-EDS. ..... 53
Table 10: Absolute number (n) and frequency (%) of selected particle types automatically categorised by Magnum software for particles from matches with average 30 < Z < 82 by BSE-SEM-EDS. ..... 58
Table 11: Total number of selected particle types automatically categorised by software for particles from *n* samples from automotive/brake pad samples with average 30 < Z < 82 by BSE-SEM-EDS, and average number of particles per stub (Total/*n*). ..... 61
Table 12: Pertinent figures from a meta-analysis of Si-containing GSR particles on casework stubs from Forensic Science SA ..... 66
Table 13: A summary of the findings of existing literature in the area of atmospheric pollutions of heavy metals attributable to firework displays. ..... 71
Table 14: Collected standards for glass analysis, detailing name, source, and variant of glass. ..... 79
Table 15: Collected samples of glass frictionator, with elements from the primer for each as determined by SEM ..... 80
Table 16: Certified concentrations of constituents in CRMs NIST 93a and NCS DC61104, and approximate concentrations of constituents in typical frictionator samples. ..... 81
Table 17: Typical run parameters for SHRIMP analysis ..... 91
Table 18: Parameters for final SEM-EDS analyses ..... 93

Table 19: Mean null temperature, refractive index and standard deviation of NIST 93a, as measured by two independent GRIM3 systems, identified by location. ..... 94
Table 20: Boron reference materials and samples, concentrations and $\delta^{11}B$ (‰), shown for individual solutions, and averaged for each sample Boron concentration and isotope composition for standards reference materials and samples ..... 96
Table 21: Lithium isotopic composition and concentrations as determined by Isotope Geochemistry Laboratory at University of Bremen, for both isotopic standards and the samples of borosilicate reference materials. ..... 98
Table 22: Summary of SHRIMP measurements showing the homogeneity of the boron isotopic composition of NIST SRM 93a from SPI, NIST SRM 93a from NIST and NCS DC61104. ..... 100
Table 23: Summary of SHRIMP measurements showing the homogeneity of the lithium isotopic composition of NIST SRM 93a from SPI, NIST SRM 93a from NIST, NIST SRM 612 and NCS CRM DC61104. ..... 101
Table 24: Successive discrimination pairs of frictionator brands added by ToF-SIMS ions ..... 105
Table 25: SEM-EDS (weight %) quantification results for the analysis of 29 samples of frictionator by brand, and 3 reference materials, shown as average ± 3σ ..... 112
Table 26: Summary of discrimination power of each analytical technique ..... 114
Table 27: Discrimination power of various combinations of the techniques used in this study, compared to ToF-SIMS ..... 114
Table 28: Results of GRIM analysis for frictionator samples successfully extracted from cartridges or 0.22 calibre rimfire ammunitions. ..... 118
Table 29: Ammunitions available from nine online retailers based in Australia ..... 120
Table 30: Inorganic compounds associated with primer GSR and their functions, with compounds in bold being reported as the most common for 0.22 calibre [17, 35] ..... 127
Table 31: Elements present in a Winchester Powerpoint ammunition slice, by region, organised by intensity. ..... 137
Table 32: Elements present in the particle of PMC Zapper ammunition, divided by region and then ordered approximately in decreasing intensity ..... 139
Table 33: Elements present in the various regions of the particle slice from Federal Premium centrefire ammunition ..... 141

# Table of Figures

Figure 1: A inter-jurisdictional comparison of weapons associated with all coronial firearm deaths from 2006-2015. ..... 2

Figure 2: Labelled diagram showing common firearm components. Modified from http://sutur.info/wp-content/uploads/2019/01/nerf-coloring-pages-gun-coloring-pages-gun-coloring-pages-gun-coloring-pages-pixel-pistol-2-a-gun-coloring-gun-coloring-pages-nerf-stryfe-coloring-pages.jpg Accessed 1 June 2019 ..... 3

Figure 3: Structure of an ammunition cartridge (rimfire). Modified from, owned by Hmaag [CC BY-SA 3.0 (https://creativecommons.org/licenses/by-sa/3.0) or GFDL (http://www.gnu.org/copyleft/fdl.html)], from Wikimedia Commons, accessed 21 June 2015. ..... 3

Figure 4: The expulsion of gunshot residue onto surroundings [3] accessed 30 Mar 2017 ..... 5

Figure 5: A typical GSR particle with distinctive morphology indicative of condensation ..... 5

Figure 6: Part of the Bayesian Network for the evaluation of GSR Results first proposed by [1], reproduced and modified from [2]. ..... 17

Figure 7: Part of the Bayesian Network for the evaluation of GSR Results first proposed by [1], reproduced and modified from [2]. ..... 35

Figure 8: Number and percentage of locations at which each combination of Pb, Ba and Sb were found to have significantly increased after a firework event compared to a 'normal day'. ..... 38

Figure 9: A diagram of gGSR PET collector, created using images from https://owips.com/clipart-9778231 and https://owips.com/clipart-11540676, access date 10 NOV 2019. ..... 42

Figure 10: Secondary electron image (left) and an elemental map (right) of a 'Pb/Ba' particle containing Pb, Ba, Ca, Si, Al, and S. ..... 48

Figure 11: EDS spectrum showing elements detected in the particle shown in Figure 10, which included low levels of Mg and Al ..... 49

Figure 12: A comparison of particle types observed (%) from GSR from two-component ammunition mixtures (left) caught in a PET collector (n=11) and particles from two-component nail gun residues (right) collected from hands (n=14) ..... 51

Figure 13: Secondary electron image (left) and EDS elemental map (right) showing a Pb/Ba/Si/Ca particle from a nail gun. ..... 51

Figure 14: Secondary electron image (left) and EDS elemental map (right) of a glass-containing nail gun particle with Ca and Fe inclusions, and an exposed glass surface ..... 52
Figure 15: Three-component Pb/Ba/Sb particle as observed from the hands of an individual who had used a Hilti powder actuated nail gun ..... 54
Figure 16: SEM image and an elemental map of a Si containing particle (presumably $SiO_2$) from matches, encrusted with Al, P, K and Cl. ..... 57
Figure 17: SEM images showing round and globular particles sourced from matches ..... 59
Figure 18: A SE image of a typical particle from a brake pad (left) and an elemental map showing the composition of that particle (right) ..... 60
Figure 19: A comparison of the distribution of particle classifications on hands after exposure to brake pads (top left), fireworks (top centre), a nail gun (top right), GSR (bottom left) and safety matches (bottom right) ..... 64
Figure 20: Images of exemplar spectra of silicon-containing gunshot residue particles, labelled A-C (top to bottom), A showing a spectrum that was considered consistent with what would be expected from a glass-containing particle, B is a spectrum that was inconsistent with what would be expected from a glass-containing particle, and C shows a spectrum that was inconclusive, as it was unable to be classified into either category from this data. ..... 67
Figure 21: Typical optical microscopy image (with reflected light) of glass frictionator collected after solvent extraction and spin-filtration, specifically showing residue from Swartklip ammunition. Scale bar represents 500 µm ..... 89
Figure 22: Mean boron ($^{11}B^+$) signal as a percent of silicon ($^{28}Si^+$) signal for the 17 brands of ammunition examined, with 99% confidence intervals ..... 102
Figure 23: Plot showing mean counts of $^{41}K^+$ per 100 counts of $^{28}Si^+$ ±3σ for all brands ..... 103
Figure 24: 99% discrimination plot for ToF-SIMS analysis of the $^{41}K^+$ ion ..... 104
Figure 25: Discrimination plot of frictionator brands showing successively compiled ToF-SIMS ions .... 104
Figure 26: 99% confidence plot showing pair-wise discrimination of ToF-SIMS for Winchester Samples (by sample number from Table 15) ..... 106
Figure 27 Mean boron ($^{41}K^+$) signal as a percent of silicon ($^{28}Si^+$) signal for the 13 Winchester items examined, with 99% confidence intervals ..... 106
Figure 28: $^{7}Li^+$ elements analysed by SHRIMP, presented as counts relative to oxygen ($^{16}O$+) ..... 107
Figure 29: 99% discrimination plot compiled from SHRIMP elemental composition analyses ..... 107
Figure 30: Average $\delta^{11}B$ ± 2σ for borosilicate glass frictionators (relative to LSVEC) ..... 108

Figure 31: Average $\delta^7$Li [‰], ± 2σ for glass frictionators (relative to LSVEC) ..... 109
Figure 32: Mean $Na_2O$ concentrations with 99% confidence intervals showing which pairs can be discriminated by $Na_2O$ concentration ..... 111
Figure 33: 99% discrimination plot for SEM-EDS analysis created by successively layering individual discrimination factors ..... 113
Figure 34: Mean refractive indices ±3σ of frictionator samples which had a null temperature in the B oil ..... 117
Figure 35: RI Values for the 13 Winchester samples, including 7 different 0.22 variants ..... 117
Figure 36: Mean refractive indices ±3σ of frictionator samples (by brand) which had a null temperature in the C oil. The Winchester value indicates an average of all the samples measured ..... 119
Figure 37: Total power of discrimination including macro-characteristics of primer (i.e. one-, two-, or three-component, or Hg-based) as an added variable ..... 121
Figure 38: Left. Diagram of the aluminium holder designed to safely discharge disassembled ammunition cartridges, with a cartridge placed in the holder. The diameter of the hole through which the cartridge is place is smaller than the diameter of the cartridge case base but sufficient to allow cases to be inserted easily and removed after discharge. Right. Typical particles of Winchester Powerpoint GSR, the arrow indicates a particle that was later sectioned using the FIB. ..... 129
Figure 39: Particles collected from PMC Zapper ammunition that were chosen for sectioning by FIB, intended for further analysis. The left particle is the one for which analytical results are presented in this chapter ..... 130
Figure 40: gGSR particle collected from Federal Premium (centrefire) particle from hands that was sectioned by FIB for further analysis ..... 131
Figure 41: Top-down view (left) of gGSR particle from PMC Zapper taken using BSE-SEM-EDS on the FEI F50 instrument (note the typical glass choncoidal fracture evident), and an SE-SEM-EDS (right) image of the same particle taken at a 52° stage tilt and a clockwise rotation of about 45° on the FEI helios dualbeam nanolab 600 instrument. n.b. The white arrow on the BSE image (Left) indicates the viewpoint for the SE image (Right). The view of the exposed glass is obscured by the bulk of the particle in the view on the right ..... 133
Figure 42: Troughs milled around the slice in the region of interest in a PMC Zapper gGSR particle (left) and needle from the nanomanipulator welded to top of the slice, to allow *in situ* transfer of it to a holder (right) ..... 133

Figure 43: A slice of GSR welded to the copper peg (above the “B”) of a sample holder. Inset is an electron photomicrograph image of the slice at 2,500 x magnification. Note that the specimen on the right is rotated about its vertical axis compared to the one on the left. ..... 135
Figure 44: SE-SEM Image of a sliced Winchester Powerpoint particle showing clearly the glassy interior, and crusted exterior (left), and the 9 selected regions analysed by electron dispersive X-ray spectroscopy (right). ..... 137
Figure 45: SEM-EDS mapping of particle sliced with a FIB. Overlay of elements showing Cu (lightest green, sample holder), Pt (dark green, weld and coating), Pb (brown-yellow, primer residue) and Si (pink, glass, area also contained significant O, Na), and Al (blue, stub surface) ..... 138
Figure 46: Left BSE image showing the various regions and voids in the PMC Zapper particle, and right, the regions examined via EDS analysis. ..... 138
Figure 47: Map showing overlay of phases found by SEM-EDS mapping of a particle of PMC Zapper sliced open using FIB ..... 139
Figure 48: EDS spectra of the 2 glassy phases from the slice of PMC Zapper, the blue region showing less incorporation of Pb and barium, and the pink region showing a greater incorporation of Pb and Ba into the glass ..... 140
Figure 49: SE-SEM image showing the sliced particle from the Federal Premium (centrefire) particle (top left), showing two regions, a core and a crust. BSE image (top right) showing four distinct regions in the core, and an outer rim with Pb and Ba incorporated, Diagram (bottom) labelling the various regions of the particle examined corresponding to the compositions listed in Table 33. ..... 141
Figure 50: Single element maps of particle of Federal Premium (centrefire), showing a silicon containing glassy core (right), with incorporated Pb nodules (left), and a Pb/Ba incorporation on the outer rim of the particle (Ba, centre). ..... 142
Figure 51: Phase overlay diagram of SEM-EDS map of Federal Premium centrefire ammunition sliced open using FIB ..... 142
Figure 52: SEM-EDS comparison of glass frictionator fragment populations from PMC Zapper samples of various manufacture and a gGSR particle from a PMC Zapper particle of unknown manufacture. It is important to note that the two populations of Mexican frictionator present originated from one cartridge, where all other samples represent separate cartridges. Inset: a close-up of the low concentration elements. X-axis shows the X-ray lines for each element used for quantitation. ..... 144
Figure 53: Mean intensities of fragments ±3σ, as a percentage of total counts of, comparing extracted frictionator and FIB-prepared gGSR samples from Winchester ..... 145

Figure 54: Mean intensities of fragments ±3σ, as a percentage of total counts, comparing extracted frictionator and FIB-prepared gGSR samples from PMC Zapper ..... 146

# Table of Abbreviations/Acronyms

| Abbreviation | Meaning |
|---|---|
| AAS/FAAS | Atomic Absorption Spectroscopy/ Flame Atomic Absorption Spectroscopy |
| AES | Auger Electron Spectroscopy |
| AFM | Atomic Force Microscopy |
| ANOVA | Analysis of Variance |
| BSE | Backscattered electron |
| CDR | Cartridge Discharge Residue |
| cps | Counts Per Second |
| CRM | Certified Reference Material |
| DC | Direct Current |
| DESI-MS | Desorption Electro-Spray Ionisation – Mass Spectrometry |
| EBSD | Electron Back Scatter Diffraction |
| EDX/EDS | Energy Dispersive X-ray Spectrometry |
| FDR | Firearm Discharge Residue |
| FIB | Focussed Ion Beam |
| FTIR | Fourier Transform Infrared |
| GCMS | Gas Chromatography Mass Spectrometry |
| gGSR | Glass-containing Gunshot Residue |
| GIS | Gas injection system |
| GRIM | Glass Refractive Index Measurements |
| GSR | Gunshot Residue |
| HMF | Heavy Metal Free |
| Hd/Hp | Defence Hypothesis/Prosecution Hypothesis |
| IBA | Ion Beam Analysis |
| ICPMS | Inductively Coupled Plasma Mass Spectrometry |
| ICP-OES | Inductively Coupled Plasma – Optical Emission Spectrometry |
| IGSR/OGSR | Inorganic Gunshot Residue/Organic Gunshot Residue |
| INLO | *In situ* Lift Out |
| IR | Infrared |
| IUPAC | International Union of Pure and Applied Chemistry |
| keV | Kilo-electron volts |
| LA-ICPMS | Laser Ablation – Inductively Coupled Plasma Mass Spectrometry |
| LIBS | Laser Induced Breakdown Spectroscopy |
| LMIS/LMIG | Liquid Metal Ion Source/Liquid Metal Ion Gun |

| | |
|---|---|
| LOD | Limit of Detection |
| LR | Likelihood Ratio |
| M&P | Military and Police |
| MALDI | Matrix Assisted Laser Desorption Ionisation |
| MC-ICPMS | Multi-Collector – Inductively Coupled Plasma Mass Spectrometry |
| n | Number of |
| NAA | Neutron Activation Analysis |
| NIST | National Institute of Science and Technology |
| Pa | Pascals |
| PC | Principal Component |
| PCA | Principal Component Analysis |
| PIXE | Particle Induced X-ray Emission (some older references use Proton Induced X-ray Emission) |
| PM | Particulate Matter |
| ppm/ppb/ppt | Parts per Million, billion or trillion |
| Pr | Probability of |
| RI | Refractive Index |
| RSD | Residual Standard Deviation |
| RM | Reference Material |
| rpm | Revolutions per minute |
| SAM | Scanning Auger Microscope |
| SE | Secondary Electron |
| SEM | Scanning Election Microscopy |
| SHRIMP | Sensitive High-Resolution Ion Micro-Probe |
| SIM | Scanning Ion Microscope |
| SIMS | Secondary Ion Mass Spectrometry |
| SP-ICPMS | Single Particle- Inductively Coupled Plasma Mass Spectrometry |
| SRM | Standard Reference Material |
| TEM | Transmission Electron Microscopy |
| TERS | Tip Enhanced Raman Spectroscopy |
| ToF SIMS | Time of Flight – Secondary Ion Mass Spectrometry |
| wt % | Percent by Weight |
| (m- or μ-) XRF | (Milli- or micro-) X-ray Fluorescence |
| XPS | X-ray Photoelectron Spectroscopy |
| Z | Atomic/Proton number |
| σ | Standard deviation |

# Periodic Table

In this thesis, elemental symbols and mass numbers are frequently used in discussions. For brevity, elemental symbols and mass numbers to designate isotopes, where relevant, have been used. The Periodic Table of the Elements presented on the following page was taken from the IUPAC website, who provide periodic tables for the public. This may be used as a reference to allow for interpretation of any elemental symbols.

Image removed due to copyright restriction.

# 1. Introduction and Literature Review

## 1.1. General Introduction

### 1.1.1. Firearms and Society

Due to the particularly heinous nature of gun crime, society places hefty punishments on those who commit gun crimes, and significant police and forensic resources are committed to these cases. Firearm crime investigations can involve tool mark comparisons of striations on bullets and cartridge cases, the use of chemical tests to look at patterns left by weapons on hands, or the analysis of organic or inorganic residues deposited on the shooter, victim and scene during a firing incident. This project will focus on improving the methods for the identification and discrimination of inorganic gunshot residue samples, to support forensic practitioners' conclusions in court.

There are approximately 3 million legally owned firearms in Australia, of which an overwhelming majority are shotguns or long rifles [5]. The illicit market is conservatively estimated to represent another 250,000 long rifles and 10,000 handguns [5]. The prevalence of 0.22 calibre long rifles and shotguns, associated with the strong firearms legislation in Australia, has also caused them to be the most common types associated with crimes or deaths. This is quite different to other developed countries, where revolvers, pistols or other weapons are more popular, and more frequently associated with crime or deaths [6-8]. A comparison of firearm deaths by weapon type between Australia and the USA, (Figure 1) shows that long rifles and shotguns are involved in more than 70% of cases in Australia, but only 11% of cases of cases in the USA [6, 9]. Between 2002 and 2018, hand guns were used in approximately 45% of all crimes involving a firearm in the UK, whereas rifles were used in only 0.8% (excluding air weapons) [7]. In the UK, however, three out of every four deaths associated with firearms were self-inflicted, with 43% of all firearms deaths coming from a rifle or shotgun, which are not distinguished by the international coroners codes. [10]. Previous research has indicated that although firearms-related suicides are relatively rare in the UK, when they occur, shotguns are mostly used ([11] and Armour 1996, Chapman and Milroy 1992, Moug *et al.*, 2001 and Nowers 2002 as cited in Haw *et al.* 2004 .

The variance in firearm usage between Australia and other jurisdictions means that Australia may see different patterns of forensic firearms evidence compared to the other jurisdictions.

Image removed due to copyright restriction.

**Figure 1: A inter-jurisdictional comparison of weapons associated with all coronial firearm deaths from 2006-2015.**

### 1.1.2. The Firearm

Firearms in the 21st century are available in various calibres, arrangements and styles, including those that are 3D printed, or improvised out of easily sourced components [8]. For something to be classed as a firearm, it must have a chamber to hold ammunition, a mechanism to discharge the ammunition, and a barrel to direct projectiles (bullets) towards a target [8]. Other common firearm components are shown in Figure 2.

Each make and model of ammunition will have its own combination of features such as cartridge composition, primer formulation, and projectile type, composition and jacket to optimise the ammunition for its purpose. A diagram showing components of ammunition is presented in Figure 3. A round of ammunition is comprised of a cartridge and a projectile. A projectile, generally a bullet, is the component that is discharged through the firearm towards the target [8]. The projectile sits in a cartridge case, the base of which holds a primer, a sensitive, inorganic explosive that sets off the main explosive compound (the propellant) which is held in the bulk of the cartridge. The primer can be held in a rim at the base, in which case the cartridge is discharged by crushing the rim, or it can be contained in a cup, which is discharged by percussive force punching the centre of the cup [8]. Rimfire ammunitions are cheaper, and more common than their centrefire counterparts in small calibre ammunitions, such as 0.22, but rimfire configurations are not suitable for larger calibre ammunition [8].

Image removed due to copyright restriction.

**Figure 2: Labelled diagram showing common firearm components. Modified from http://sutur.info/wp-content/uploads/2019/01/nerf-coloring-pages-gun-coloring-pages-gun-coloring-pages-gun-coloring-pages-pixel-pistol-2-a-gun-coloring-gun-coloring-pages-nerf-stryfe-coloring-pages.jpg Accessed 1 June 2019**

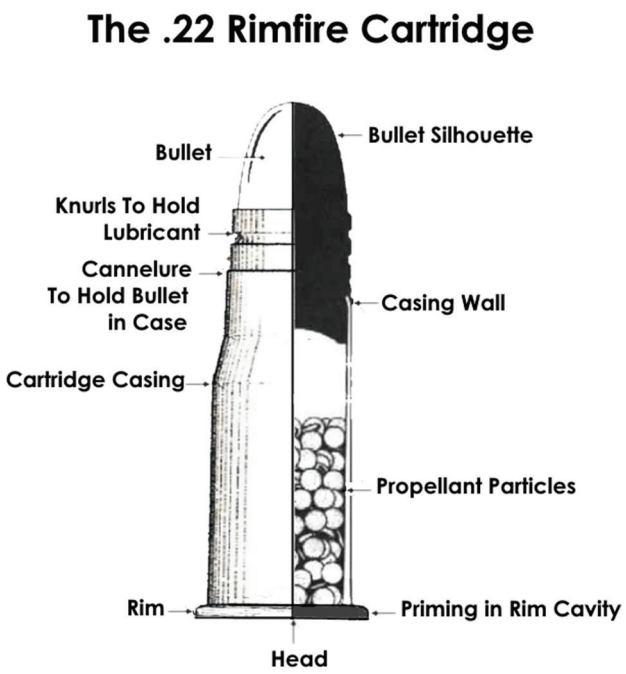


**Figure 3: Structure of an ammunition cartridge (rimfire). Modified from, owned by Hmaag [CC BY-SA 3.0 (https://creativecommons.org/licenses/by-sa/3.0) or GFDL (http://www.gnu.org/copyleft/fdl.html)], from Wikimedia Commons, accessed 21 June 2015.**

### 1.1.3. Introduction to Firearm Science:

There are three types of evidence evaluation in cases involving firearms. The first is a comparative analysis of a cartridge case/projectile collected from a scene to one test-fired in the laboratory. This is a well-used technique in cases of crime but can only be completed when the weapon is known and present and when the offending projectile/cartridge case is recovered; this can connect ammunition to a gun, but not to a shooter.

The second type of evidence evaluation is that which connects a weapon to a shooter. This evidence could consist of fingermarks or DNA left on the firearm. Alternatively, in limited jurisdictions, a method has been applied to detect and compare patterns left by Fe ions from firearm components on the hands of a shooter, theoretically enabling the linking of a person to a weapon [12]. This has been met with some success in determining who has held the firearm, especially in cases of suicide or murder-suicide, but cannot prove that a person fired the weapon [12].

A third approach is also commonly used to determine whether a suspect has been involved in or associated with the discharge of a firearm. This approach involves linking an individual with firearm activity by analysis of organic and inorganic gunshot residues (GSR) that are deposited onto the shooter, victim, bystanders and the surrounding scene during a firing incident [8, 13-15]. It can be very powerful, as GSR is microscopic and not visible to the naked eye, it is highly specific to firearms exposure, and can inform an investigation even if the firearm is not recovered [8, 13].

GSR evidence evaluation does however, have several limitations; these residues can also be found on the hands of people who have handled or cleaned, but not fired, a weapon [8, 14, 15]. Furthermore, using GSR examination, it is not possible to accurately infer when the suspect might have discharged a gun nor is it currently possible to determine whether the suspect was involved in a particular shooting incident [8, 14, 15]. The time interval between firearm exposure and GSR collection is difficult to estimate because the quantity of GSR particles deposited on hands is highly variable shot-to-shot, dependent on the combination of firearm and ammunition used and heavily influenced by environmental factors [16]. Because there is a complex relationship between recovered GSR composition and primer composition, the ratios of elements found in the primer cannot be used to accurately discriminate between ammunition used with small differences in quantitative composition.

### 1.1.4. General Introduction to Gunshot Residue (GSR)

Projectiles are propelled from a firearm by the rapid expulsion of gases, which drive the ammunition from the barrel with great acceleration [17-21]. When this occurs, particles are ejected from the barrel, the ejection port and any additional openings of the weapon (Figure 4). These transfer to the surrounding area, including onto the clothes, hair and skin of the shooter and any close bystanders [17-21].

Image removed due to copyright restriction.

**Figure 4: The expulsion of gunshot residue onto surroundings [3] accessed 30 Mar 2017**

This mixture of gases and particles is commonly referred to as gunshot residue (GSR), but also as cartridge discharge residue (CDR) or firearm discharge residue (FDR) [19]. These terms are often used interchangeably, but CDR has a slightly different meaning, as it specifically includes residues from cartridges other than ammunition cartridges, such as from powder-actuated nail guns, or similar. Broadly, GSR is defined as the burnt and unburnt particles, of both organic (OGSR) and inorganic compositions (IGSR), originating from the primer, propellant, projectile, cartridge and the interior of the barrel [19] that are deposited onto surroundings from a firing event. As these deposits are formed *via* condensation, the mixing of vapours in the firing process can cause some particles to have inclusions from a combination of these sources [17, 22].

GSR particles have distinctive morphologies because of their formation through rapid condensation [22]. An example is shown in Figure 5. GSR particles are generally spherical or globular and form by rapid cooling of the gaseous GSR into a solid state [22]. Larger particles (>10 µm in diameter) are thought to form by agglomeration of these particles or by gaseous components coalescing around a nucleus of metallic, glass, or other solid particles.

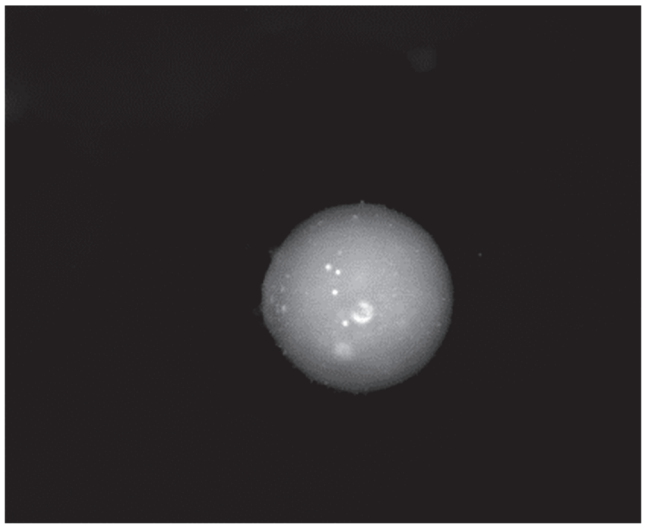

**Figure 5: A typical GSR particle with distinctive morphology indicative of condensation**

Inorganic compounds found in GSR are principally sourced from the primer, with minor additions from the cartridge, ammunition and the weapon. The purpose of a primer is to provide extremely hot gasses which initiate combustion of the propellants [23]. Composition is variable between manufacturer and calibre of ammunitions; however, the primers will contain compounds which will initiate, oxidise and fuel the reaction. Primers often contain extra compounds that increase the sensitivity of the reaction, or that will act as a 'frictionator', a compound that assists with shock transfer and improves the reliability of the ammunition [24]. Specific elements and inorganic compounds commonly encountered in ammunition primers with their respective functions are shown in Table 1.

**Table 1: Inorganic compounds associated with primers and their functions**

| Compound | Function |
|---|---|
| Barium nitrate (most common)<br>Barium peroxide<br>Lead nitrate<br>Lead peroxide | Oxidiser |
| Lead styphnate (current, common)<br>Lead azide (historical)<br>Mercury fulminate (historical, Europe only) | Initiator |
| Antimony sulfide (common for ammunitions other than 0.22s)<br>Calcium silicide (usual for 0.22s)<br>Lead thiocyanate<br>Powdered zirconium | Fuel |
| Tetrazene (common)<br>Pentaerythritol tetranitrate<br>Trinitrotoluene | Sensitisers |
| Antimony sulfide (common for ammunitions other than 0.22s)<br>Calcium silicide (common)<br>Ground glass (usual for 0.22s)<br>Powdered aluminium | Frictionator (most have dual purpose) |

Research [25-27] has shown that chronic exposure of humans and animals to heavy metals from firearms can have significant health effects, which has been a major factor in the proliferation of heavy metal free (HMF) ammunitions. Compounds and their functions found in HMF ammunitions are seen in Table 2.

**Table 2: Compounds associated with Heavy Metal Free primers and their functions [28-31]**

| Compounds Associated with HMF Primers | Function |
|---|---|
| DDNP (Diazo dinitrophenol)<br>KDNBF Powder (Potassium dinitrohydroxyhydrobenzofuroxan) | Initiator |
| Potassium nitrate<br>Manganese dioxide<br>Zinc peroxide<br>Cupric oxide<br>Ferric oxide<br>Strontium nitrate<br>Ascorbic acid<br>A metal salicylate<br>A metal peroxide | Oxidiser |
| aluminium powder<br>calcium silicide<br>sulfur<br>sieved ball propellant powder<br>iron powder<br>magnesium powder<br>zinc powder | Fuel |
| Tetrazene | Sensitiser |
| Glass powder<br>Boron particles | Frictionator |

Organic substances in GSR generally originate from the propellant [17], which is a secondary, more stable explosive that is initiated by the primary explosive, the primer mix. Common organic inclusions of the propellant and their functions are presented in Table 3.

**Table 3: Organic compounds associated with propellant GSR and their functions**

| Compound | Function |
|---|---|
| Nitrocellulose (common)<br>Nitroglycerine (double base)<br>Nitroguanidine (triple base, dual role) | Smokeless powder base |
| Diphenylamine (most common)<br>Ethyl centralite<br>Methyl centralite<br>Resorcinol | Stabilisers |
| glyceryl triacetate (triacetin)<br>Dimethyl phthalate<br>Diethyl phthalate<br>Dibutyl phthalate | Plasticisers |
| Dinitrotoluene<br>Nitroguanidine (dual role) | Flash suppresser |

In traditional ammunitions, the main components of primer (inorganic) GSR are lead (Pb), antimony (Sb) and barium (Ba) compounds. For this reason, particles are considered 'characteristic' [32] or most likely originating from a cartridge source if they contain these three elements.

In Australia, 0.22 rimfire weapons are very common, and these tend to fire ammunition that does not contain Sb in the primer and uses powdered glass as a frictionator instead of calcium silicide, which is more common in high calibre ammunition primer. This is problematic, as these ammunitions will then produce less, or negligible quantities of the three-component Pb/Ba/Sb particles and would not be classified as 'characteristic' of GSR. Therefore, in cases involving 0.22 rimfire ammunition, GSR evidence would be of intrinsically lower probative value.

The foci of this thesis will centre on IGSR analysis; however, it must be noted that significant progress has been made using OGSRs [17, 19, 33-39]. Works have included use of infrared spectroscopy (IR) [40-42], Raman spectroscopy [37-39, 42-44], various forms of gas [45-51] and liquid chromatography [41, 51] and desorption electrospray ionisation – mass spectrometry (DESI-MS) [33, 52, 53] in order to characterise organic GSR components. OGSR analysis can provide complementary information to IGSR analysis, and if propellant particles are recovered, the shape, colour and composition of the particles can allow discrimination between different ammunitions.

However, OGSR has several limitations. There is no universally accepted method for the collection and analysis of OGSR at this time, although research is ongoing in this area. The main components of propellants, such as nitrocellulose and nitroglycerine, are generally degraded in OGSR samples, and are used in other applications, including medical, and cosmetic products [17, 53-55]. This means that low percentage components of the primer have to be detected in OGSR samples (where intact propellant particles are not recovered) to prevent false positive results. Another limitation is that there is no method available currently for sampling for OGSR without potentially losing IGSR evidence.

Some work has included attempts to incorporate IGSR and OGSR analyses into one process, to increase the evidentiary value of GSR [39, 47, 56-58], but these processes involve compromise, as the methods either involve two sampling processes, such as a stub and a swab, or using only half of a GSR stub for IGSR analysis. A limitation of both OGSR and IGSR for forensic scientists is that it is very hard to link pre- and post- firing samples (e.g., link GSR with its suspected source ammunition), as the composition undergoes complex reactions when the firearm is discharged. As the scope of this thesis excludes OGSR, GSR will henceforth refer to IGSR unless specifically stated otherwise.

## 1.2. Review of the Classification and Discrimination of GSRs

There are two main objectives in performing analysis on GSR. The first is 'classification'; the process of finding and categorising residues as being most likely sourced from a firearm discharge event and not from other environmental, industrial or occupational sources. The other objective, 'discrimination,' will refer to the differentiation of different samples of GSR, such as by exploiting differences in composition due to manufacturer, age or calibre.

In order to enable simple, definitive classification of GSR, and enable discrimination between GSR samples, several researchers have advocated for the tagging of ammunition in a way to allow the differentiation of manufacturer and/or calibre [59-62]. Some manufacturers offer a range of tagged ammunitions, such as used by German police [63, 64]. However, as this recommendation would have to be taken on by all manufacturers to be effective, the most practical option for forensic scientists is to look for existing variation between different types and brands of ammunition.

## 1.3. Early History of the Classification of GSR

GSR analysis has been performed for over 100 years, and the methods employed have adapted with the changing understanding of GSR and the advancement of chemical analysis technologies.

An early chemical test used for GSR detection was the Griess Test [65, 66] (or various modifications of it [67]). The Griess Test produces brightly coloured solutions by reacting nitrites (organic components) with sulfanilic acid to form nitrous acids and diazonium ions [20, 67]. If this then reacted with α-naphthylamine, a brightly coloured orange azo dye would form [20, 67]. This test suffers from issues, as nitrites are specific to burnt particles, and if there was very little burning, which was a problem with some types of ammunition, false negative results could occur [67]. Furthermore, nitrites are not only found associated with shootings, but are also associated with other sources, such as preservatives in cured meats, therefore the test is subject to false positives. A widely used application for the Griess test is range determination, as this test can show patterns of GSR distribution on the target, which allows determination of muzzle-to-target distances up to a range of 1-2 m [20, 68], and it is currently used for this purpose in many jurisdictions.

In 1933, Teodoro Gonzalez of the Mexico City Police Laboratory introduced the paraffin test to America [19]; however, it was reported (by Castellanos [69] as cited in Schlesinger's report [70]) to have been used by Iturrioz as early as 1914. This test, also referred to as the dermal nitrate test [19], involved removing GSR deposits from a suspect's hand by taking a cast with paraffin wax, and then testing for nitro-compounds. The test was generally performed by examining the cast under a microscope and applying a 0.25% solution of *N*,N′-diphenyl-benzidine or diphenylamine in

concentrated sulfuric acid to areas of interest (e.g. thumb webbing). A positive result was indicated by a deep blue colouration; however, this test suffers from a range of issues. This test gave a simple, strong result for a positive, but many other oxidisers [19, 35, 70], present in various substances including medicines, nail polishes, and urine, give positive results. The Schlesinger work [70] also indicated that there was evidence that the rate of false negatives was high.

In 1934, a surgeon noted the presence of metallic gunshot residues on the bodies of gunshot victims, and acknowledged their potential usefulness if examined by X-ray imaging and spectroscopic chemical techniques [71]. Although this had been known for some time, and Feigl had begun using sodium rhodizonate to detect various metals by 1924 [72], it wasn't until 1959 that Harrison and Gilroy developed an assay for lead (Pb), barium (Ba) and antimony (Sb), three metals known to occur commonly in GSR [73, 74]. This test was preferable to the paraffin and Griess tests as it tested for three different components of the primer, and thus had a much lower rate of false positives [19]. The test, however, wasn't widely adopted due to its lack of sensitivity, [70, 75] which would have caused false negatives.

## 1.4. Review of the Classification of GSR by Bulk Instrumental Analysis Techniques

In the early 1960s, the new range of instruments available to forensic scientists allowed further development of GSR analysis techniques. After Harrison and Gilroy realised the potential of the inorganic elements associated with GSR, Ruch, Guinn *et al.* [74, 76, 77] worked on detecting GSR *via* neutron activation analysis (NAA). It was found that using NAA, Sb and Ba could be routinely detected at higher concentrations on the backs of hands of people who had recently fired a weapon than on people who had not.

Two out of the three elements chosen by Harrison and Gilroy, Ba and Sb, could be detected using NAA, although Pb could not, as the limits of detection (LODs) for Pb using NAA are three, or four orders of magnitude higher than Ba or Sb, respectively [76]. Disadvantages with NAA include the requirement for a nuclear reactor [19], the inability to detect Pb effectively [19], the expense of sending samples and having the samples analysed by suitably trained personnel [19, 78] and the expense and hassle of the disposal of the samples, which emit low-to-medium, or sometimes high levels of radiation after neutron activation, making the technique effectively destructive. Other limitations are the long times required to analyse *via* this technique, both from transporting the samples to and from a suitable reactor and from the analysis times of the technique itself. Many researchers used NAA and controversy existed as to whether other elements (e.g. copper (Cu), arsenic (As) ) should be tested for

[35, 79-83] and what concentration ranges for the elements were most indicative of GSR residues as compared to other possible sources [84-87].

The next major technique investigated for the use of identifying gunshot residue was flame atomic absorption spectrometry (FAAS). This technique was first used by Krishnan *et al.* in 1971 [88] and could determine the presence and quantity of Pb, but not Ba or Sb as the LODs for these elements were not low enough [19]. Flameless atomic absorption spectrometry (AAS) was then used by Petty and Stone in 1974 [89], and found to be more sensitive and able to be used for all three elements. However, AAS has several limitations, including its destructive nature, and its inability to detect multiple elements simultaneously. Krishnan in 1973 [81] developed standard protocols using a mixture of NAA and AAS for the detection of Pb, Sb, As, Ba, Cu and silver (Ag). While this potentially enables limited discrimination between GSR samples originating from different source ammunition, these techniques, even in combination, cannot lead to any definitive statements regarding the residues being sourced from firearm-related sources as these various elements have other potential origins of environmental, industrial or occupational exposure.

### 1.4.1. General Limitations of Bulk Analysis Techniques for GSR Applications

It is extremely difficult to prove that any elements examined are artefacts of GSR and not from another source [86] without showing that they are all present in a single particle.

Bulk analysis techniques require concentrations of all three elements, Pb, Ba and Sb, to be measured above a specified background level for a 'positive' identification of as sample as GSR. This can potentially result in a high rate of both false-positive and false-negative results, as some individuals could have picked up extraneous (environmental, industrial or occupational) sources of these elements, and people that have low background concentrations of one or more of these elements may not appear to have raised concentrations after contact with GSR. Havekost *et al.* attempted to evaluate the minimum required concentrations of Pb, Sb, and Ba to determine the presence of GSRs from environmental false-positives, and looked at different occupational exposures [90]. Other researchers studied the relative concentrations of elements observed, to analyse the likelihood of high backgrounds of one or more of the elements ([91] as cited in [87] and [92]). By 1984, Booker *et al.* had begun to question if any definitive statements about the presence of GSRs could be made from the bulk concentrations alone [87].

More sensitive and readily available techniques have been developed, and electrochemical [36, 93-99] and Inductively Coupled Plasma Mass Spectrometry (ICPMS) [39, 100-106] or Inductively Coupled Plasma – Optical Emission Spectrometry (ICP-OES) [107-112] techniques have been consistently used in attempts to identify samples of GSR, and in some cases to determine the number of shots fired

[109]. These are bulk techniques and thus are subject to the same limitations as previously mentioned in regards to exclusively identifying GSR samples, but in spite of this, various research [109-111, 113] has persisted in the hopes of finding the 'silver bullet' protocol to universally identify GSRs by concentrations of Pb/Ba/Sb for the courtroom. This may be due to the large cost associated with obtaining and maintaining an SEM-EDS system, as this instrumentation may not be affordable for some laboratories, but unfortunately, most research suggests that no bulk analysis technique is capable of reliably determining whether samples contain GSR.

It has generally been concluded by the forensic science community that these bulk analysis approaches are severely limited, as no real conclusions as to whether the residue came from a firearm-related source can be made from bulk analysis alone. For this reason, scanning electron microscopy with energy dispersive X-ray spectroscopy (SEM-EDX or SEM-EDS), a particle analysis technique, is the most commonly used technique to identify GSR, and to attempt to discriminate between samples, in current practice.

## 1.5. Review of Classification and Discrimination of GSR by Particle Analysis

### 1.5.1. The Use of SEM-EDS for Particle Analysis

In 1974, a scanning electron microscope with an energy dispersive X-ray spectrometer (SEM-EDS, also known as energy dispersive X-ray analysis) (SEM-EDX)) was used to visualise and analyse gunshot residues [114]. Through this research, the distinct morphology of these particles was discovered and characterised, leading to a proliferation of GSR research using this technique. Wolten *et al.* published this work in 'the Aerospace report' of 1977, which is still considered a landmark review of GSR classification [115]. Wolten *et al.* reviewed previous detection methods of GSR and discussed the formation, detection *via* SEM-EDS and the value of GSR evidence in casework. The bulk of this work was later published a series of peer-reviewed articles about GSR analysis for the scientific literature [116-118]. This work introduced the idea of 'unique' GSR particles being detectable by SEM-EDS. Arising from the work of Wolten *et al.*, the definition of a 'unique' vs. 'characteristic' particles is as seen in Table 4. In subsequent years the definition has been revised several times, as further research has stimulated scientific discussion as to sources that may produce particles that have similar composition and morphology [119-126]. Brake linings, cartridge operated tools and pyrotechnics are commonly discussed as possible sources of particles with similarities to GSR.

At the time of the introduction of SEM-EDS as the main technique to analyse GSR, a major disadvantage was noted as being the large amounts of time and labour required by SEM-EDS operators to gain results [13, 17, 19, 35]. This has been substantially offset by the introduction of automated GSR analysis [21, 127-129] which requires far less user input, although the process is still lengthy.

**Table 4: Original Aerospace Report guidelines for the identification of GSR**

| **Compositions of Gunshot Residue Particles** | | |
|---|---|---|
| Category | Required Composition | Required Absence |
| Unique | Lead (Pb), antimony (Sb), barium (Ba) | |
| | Ba, calcium (Ca), silicon (Si), with trace Sulfur (S) | |
| | Ba, Ca, Si with trace Pb | Copper (Cu), Zinc (Zn) |
| | Sb, Ba | |
| Characteristic (esp. if spheroidal) | Pb, Sb | |
| | Pb, Ba | |
| | Pb | Iron (Fe), Phosphorous (P) |
| | Ba (with trace or no S) | |
| | Sb | |
| **GSR may also contain the following elements, unless specifically excluded above: Si, Ca, Al, Cu, Fe, S, P (rare), Zn (only with Cu), Ni (rare, only with Cu and Zn), K, Cl, Sn (old ammunition only). The presence of other elements indicates non-GSR origin.** | | |

Guidelines for the forensic analysis of inorganic GSR by scanning electronic microscopy with energy dispersive X-ray spectroscopy (SEM-EDS) are issued by ASTM International (Standard E1588) and they have defined a particle classification scheme [32] (See Table 5). At the latest revision, 'characteristic' particles are defined as those that have compositions rarely found in particles other than those originating from a firearm source meaning that they have the highest probative value in shooting investigations. 'Characteristic' particles contain the elements lead (Pb), barium (Ba) and antimony (Sb), or lead (Pb), barium (Ba), calcium (Ca), silicon (Si) and tin (Sn). Non-toxic or heavy metal free ammunition formulations produce their own 'characteristic' GSR particles, which are classed separately within the standard and include particles that contain gadolinium (Gd), titanium (Ti) and zinc (Zn), or gallium (Ga), copper (Cu) and tin (Sn). There are other particle types associated with firearm sources, such as those containing Pb and Ba, but these are considered less strongly supportive of a firearm origin. In the current standard evaluating the significance of these types of particles on a 'case-by-case' basis is advocated.

Table 5: Current 2017 ASTM guidelines for GSR classification

| Compositions of Gunshot Residue Particles | | |
|---|---|---|
| **Category** | **Required Composition [1]** | |
| | Standard ammunitions | |
| **Characteristic of GSR** | Lead (Pb), antimony (Sb), barium (Ba) | Pb, Ba, silicon (Si), calcium (Ca), tin (Sn) |
| **Consistent with GSR** | Pb, Ba, Ca, Si<br>Ba, Ca, Si<br>Pb, Sb | Sb, Ba<br>Pb, Ba<br>Ba, aluminium (Al) |
| **Commonly associated with GSR** | Pb<br>Sb | Ba |
| | Lead-free/ non-toxic ammunitions | |
| **Characteristic** | Gadolinium (Gd), titanium (Ti), zinc (Zn) | Gallium (Ga), copper (Cu), Sn |
| **Consistent** | Ti, Zn | Strontium (Sr) |

[1]GSR may also contain, but are not limited to, one or more of the following elements: Al, Si, P, S, Cl, K, Ca, Fe, Ni, Cu, Zn, Zr, and Sn.

When the current ASTM guidelines (E1588-17) are applied, genuine GSR particles derived from many 0.22 calibre ammunitions will be categorised as consistent with GSR, at best, due to the absence of antimony in most rimfire primers. The same situation applies for particles derived from HMF ammunition, which is becoming more widely used. In both the cases of the HMF ammunitions and ammunitions not containing antimony, GSR particles of the morphology considered 'GSR-like' (i.e., round or globular, consistent with condensation from the gaseous phase) are still formed, as the primers are still subjected to very high pressures and temperatures [22], despite the variance in elemental composition.

There is a relevant exception to the preceding discussion. It is possible for residues from certain ammunitions with two-component primers to produce particles containing Pb, Ba and Sb, and to thus be categorised as characteristic, but these are probably the results of the weapon memory effect, or residues that arise from mixture between primer components (Pb and Ba) and projectile components (Pb and Sb, and sometimes Cu or Cu and Zn) [17].

When ammunition is discharged through a firearm, most of the gases and particles formed are expelled through various gaps in the firearm. However, some proportion of the residues remain inside the firearm, especially for small calibre firearms such as 0.22s [130-132]. These can be expelled on subsequent firings and can mix with gases and particles from the subsequent firings to produce mixed composition particles. This phenomenon is known as the weapon memory effect, and is one reason that two-component primers could produce, or appear to produce 3-component residues [130-132].

It has been suggested that the other method of formation of three-component particles from two-component primers is through incorporation of Sb from the projectile. Pb, Ba and Sb are usually present as compounds (such as lead styphnate, barium nitrate and antimony trisulfide) in primer mixes, and therefore may be present as compounds in GSR. As the projectile is generally an alloy of Pb, Sb and other metals, it might be possible to chemically differentiate between characteristic particles that are derived only from the primer and 'characteristic' particles that arise from mixture of primer and projectile components.

The current ASTM method (Table 5) includes characteristic and consistent classes for HMF GSR, but the composition of HMF primers are quite variable, containing combinations of elements such as Sr, Al, Cu, Gd, Sn and Ga [133], so there are types of GSR from HMF primers not yet covered by this standard, for example Federal American Eagle MFP ammunition, which produces an abundance of Sr/Al containing particles.

After a residue is identified as GSR, meaning that it has originated from a firearm, there exists the possibility that the residue is from a shooting incident other than the offence under investigation. For this reason, it is desirable that there is the scope in GSR analysis for sub-source classification. Attempts have previously been made to discriminate between samples of GSR *via* several methods. Some studies have involved trying to link GSR found on cartridge cases to the GSR found on hands, grouping ammunitions by the quantity of GSR produced [134], and using SEM-EDS to examine the relative proportions of different types of GSR particles present [135, 136]. Each of these studies has shown that results largely depended on environmental factors, and thus have not been considered suitable methods for discriminating between ammunitions or linking residues with source ammunition. This leaves a significant capability gap for the analysis of GSR compared to other traces and represents an area that warrants further research.

### 1.5.2. GSR Interpretation using SEM-EDS

The approaches discussed above are examples of a 'formal' or 'traditional' approach, where particles and particle populations are compared to a pre-defined classification scheme. However, the prevalence of various known ammunition formulations that do not conform to this scheme, such as those that do not contain primer sources of antimony, or some HMF formulations, have led to many practitioners advocating a 'case-by-case' or Bayesian approach [32].

The Bayesian methodology allows details relevant to the specific case to be used to determine the meaning and strength of the evidence, numerically [19, 21, 35, 120]. In this way, GSR residues, or ingredient lists, from relevant 'known' sources, such as from discarded cartridge cases, or seized

firearms, could be compared to the results from the hand-stubs to assist in the determination as to the identity of the sample.

The probative value of GSR is inversely related to the prevalence of occupational, industrial and environmental sources of particles that could be confused with those originating from a firearm source. It is hoped, that in the future, the forensic interpretation of GSR will be weighed and reported using evaluative methods much like those employed in glass casework and be able to incorporate both source-level and activity-level information. The formation of a likelihood ratio (LR) and Bayesian networks depends on the context of a case and the formulation of the prosecution hypothesis (*Hp*) and alternate or defence hypothesis (*Hd*). *Hp* and *Hd* are required to be mutually exclusive hypotheses that exhaust all possibilities, i.e. Pr(*Hp*) + Pr(*Hd*) = 1. Each case will have its own hypothesis and factors that need to be considered, but a proposed generalised LR for the assessment of GSR is shown in Equation 1.

$$V = \frac{\Pr(x|Hp)}{\Pr(x|Hd)} \text{ or}$$

$$Value = \frac{\text{The probability of observing } x \text{ GSR particles given the suspect was associated with the matter under investigation}}{\text{The probability of observing } x \text{ GSR particles given the suspect was not associated with the matter under investigation}}$$

**Equation 1: A likelihood ratio for GSR evidence evaluation, as based on Lucas et al. 2018 [2]**

One method of evaluating these probabilities is through analysing the factors contributing to the situation through a Bayesian network. A network structure (Figure 6) informed by experimental data has been proposed by, Biedermann, Bozza and Taroni [1] and further adapted by Lucas et al. 2018 [2]. A Bayesian network includes 'nodes' representing variables in an evaulation, with the relationships between the variables illustrated by the connections between them. A conditional probability is associated with each node, allowing for a logical and systematic evaluation of the probabilities and variables under consideration. For GSR analysis, nodes often relate to the possibility that a particular number of GSR particles were deposited onto the person of interest due to a specific association or activity. These may include contact with a firearm under the circumstances proposed by the prosecution, the possibility that the person of interest had contact with the firearm as proposed by the prosecution yet did not acquire the GSR particles found, the possibility of cross-contamination taking place during sampling, and the factors affecting efficiency of particle detection.

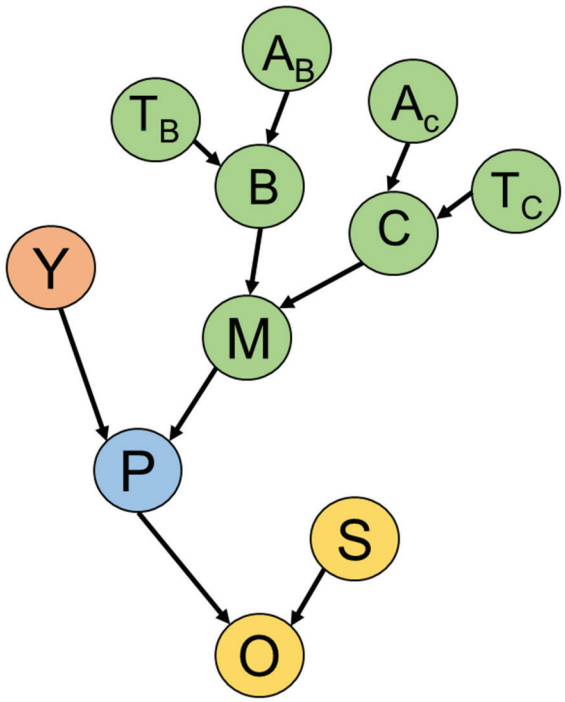


| Variable | Description |
|---|---|
| **Y** | Number of GSR particles present if Hp is assumed to be true |
| **M** | Particles present originating from sources other than Hp |
| **B** | *Background levels of 'GSR' Particles* |
| **C** | *Contamination levels of 'GSR' Particles* |
| $A_{x_{1-n}}$ | *Nature of exposure to* $x_1, x_2, \ldots x_n$ |
| $T_{x_{1-n}}$ | *Time since exposure to* $x_1, x_2, \ldots x_n$ |
| **P** | Total GSR present on subject's hands |
| **S** | Effects of sampling procedures, particle lifting efficiency, instrumental settings, etc. |
| **O** | Total GSR Reported |

**Figure 6: Part of the Bayesian Network for the evaluation of GSR Results first proposed by [1], reproduced and modified from [2].**

### 1.5.3. Alternative Techniques for GSR Particle Analysis

SEM-EDS is currently the main technique used by practitioners to identify and discriminate between samples of GSR; however, research has been undertaken to find suitable additional or complementary techniques. This is desirable for several reasons including: the high cost associated with obtaining and maintaining a SEM-EDS with particle searching abilities, the long times required for analysis of GSR stubs, and the lack of understanding that currently exists about the fundamental nature of GSR.

In 1982, Sen *et al.* used (proton) particle-induced X-ray emission (PIXE), an ion beam analysis (IBA) technique, to investigate GSR particles and recommended it for further investigation. Sen *et al.* reported results similar to what is obtainable by SEM-EDS except that PIXE has a LOD more than two magnitudes (i.e. at least 100 x) lower than the former technique [137]. Work by Bailey et al. [138] also used PIXE and found results comparable to Sen *et al.*, with PIXE having much greater sensitivity for trace element analysis. Although the technique would be undesirable for routine analysis due to the relatively high cost and lack of availability of particle accelerator facilities required for analysis using PIXE, it could be used to great advantage for further analysis of some particles in some critical cases, and for fundamental research studies.

Later works by Romolo *et al.* [139] and Christopher *et al.* [140] simplified and streamlined the previous approach, and reported that using IBA techniques (such as μ-PIXE) gave 'unprecedented characterisation and discrimination power' to samples of GSR [139]. Drawbacks of IBA techniques

include the significant expertise required to use PIXE or μ-PIXE instrumentation and the relatively high costs required to access particle accelerator facilities.

When compared to SEM-EDS, the current industry standard, SEM-EDS appears favourable due to its capability for backscattered election (BSE) imaging, which allows automated searching over a large area at high-spatial resolution. Although mapping is possible with IBA techniques, it would likely be difficult to search larger areas with a similar resolution to what is achieved using BSE-SEM-EDS automated searching.

Niewöhner *et al.* used [141] a focussed ion beam (FIB) to slice open GSR particles, and a scanning ion microscope (SIM) to image the interior and exterior of the particles. SIM was used to create high quality images, and had the added advantage of not requiring any sample coating. It was noted that a system incorporating an *in situ* SEM-EDS, secondary ion mass spectrometer (SIMS) or scanning auger microscope (SAM) would allow elemental composition determination, which was not possible by the instrument used. This work has been followed up by Sarvas *et al.* and Wuhrer *et al.* [142, 143] who also sectioned several particles of GSR. Although FIB coupled with SEM-EDS, SIM, SIMS or SAM would not be suitable for routine GSR casework, fin casework, these techniques offer the possibility of providing further information after particles are located by SEM-EDS, and could be invaluable in advancing the fundamental understanding of GSR particle formation, heterogeneity, and internal morphology and composition.

Hellmiss *et al.* [144] reported the use of Auger electron spectroscopy (AES) for GSR analysis. AES is a technique similar to SEM, except that instead of measuring the secondary electron, the 'Auger' electron is targeted. When the inner shell (secondary) electron is ejected, outer shell electron moves to a lower energy shell, generating energy that is usually released in the form of a photon. However, sometimes, that energy is transferred to an outer shell electron, and upon ejection of that electron, the kinetic energy of the electron can be measured to give information about the element and chemical environment from which the electron originated. That second ejected electron is known as the Auger electron. AES was found to be capable of detecting GSR and to have better surface-sensitivity and lateral resolution in comparison to SEM-EDS. It also has the potential to discriminate between GSRs from different sources, which could lead to new capabilities in GSR analysis although it is more expensive and time-consuming than SEM-EDS and is not a suitable technique for routine screening.

Some works have investigated the use of milli- or micro- X-ray fluorescence (m- or μ-XRF) [145] for detection/classification [146, 147] and discrimination [148] of GSRs, and for the estimation of shooting distance [149]. This has shown reasonable success in laboratory examples and suicides, but as the

technology was limited to particles larger than 10 µm, and particles of 10 µm or larger are lost very quickly from hands, it was accepted that in most cases XRF-based techniques would be unsuitable for GSR analysis in casework.

Laser ablation – inductively coupled plasma mass spectrometry (LA-ICPMS) was first applied to the analysis of GSR in 2012 [100], and it was found to be a potential alternative to SEM-EDS, as it had a reduced analysis time, and much lower LODs whilst still detecting multiple elements. Unfortunately, this technique may not be entirely suitable, as it will likely obliterate many case-sized GSR particles.

A related technique, laser induced breakdown spectroscopy (LIBS) has been investigated as a screening technique for GSR in several studies [150-155]. It was found to be able to detect Pb, Ba and Sb signals under some circumstances, however, the spot size of the beam is unable to be focussed for single particle analysis (typical beam sizes reported as 60-100 µm) [152, 154], and the technique does not have imaging capabilities. This means that it would not be possible to distinguish between a sample of GSR (particles containing all of Pb, Ba, Sb) and a population of particles of Pb, Ba, and Sb, similarly to a bulk technique. In one study, LIBS was not able to detect a signal from a small number (<3 in a field) of particles, and was found to completely obliterate particles less than 1 µm in diameter [155]. This could impact confirmatory testing using SEM-EDS particle analysis and therefore, it is not a technique suitable for GSR analysis of shooters. LIBS would be more suitable for use in ballistics, as it could potentially be used for the analysis of patterns on targets and/or muzzle-to-target distance determinations.

Melo *et al.* [156] used high-resolution transmission electron microscopy (TEM) to investigate GSR formation. They showed that some of the 'regular spheroid' particles between 0.5 and 3 µm (common to GSR) are actually made up of agglomerates of nanoparticles. Lead oxide (PbO) nanoparticles of 2-10 nm were the most common, with traces of barium oxide or carbonate (BaO, $BaCO_3$) and antimony metal (Sb) present in various samples. This contrasts to earlier work in this field, which claimed that all submicron particles are metallic, and that the spheroid nature of these particles infers that they formed from condensation [22].

In 2001, Coumbaros *et al.* applied time of flight – secondary ion mass spectrometry (ToF-SIMS) to GSR and found that this technique has several advantages, namely its surface sensitivity and etching capabilities, which allows for high resolution imaging of internal structures of GSR particles [18]. The determination of the location of Pb and Ba within GSR particles was studied in a later Coumbaros *et al.* paper [157]. These works focussed primarily on 0.22 calibre ammunition, as this is the most common weapon type in Australia. 0.22 calibre ammunition can present an issue regarding GSR

classification and discrimination, as they rarely contain Sb (antimony), and thus tend not to produce characteristic GSR particles.

In 2003, Collins *et al.* [158] discovered the presence of glass particles with Pb and Ba fused to the surface in 0.22 calibre ammunition. It was postulated that this could be a new type of highly characteristic GSR particles, worthy of further investigation.

## 1.6. Previous work involving glass-containing GSR

Collins' and Coumbaros' work [18, 157-159], concerned the discovery of glass-containing gunshot residue particles in 0.22 rimfire ammunition of traditional (Stabanate/Sinoxid) composition. It was noted that the majority of glass discovered was borosilicate, although the presence of soda lime glass was detected in some frictionators. Coumbaros [159] also undertook a compositional analysis of individual particles within his work using SEM-EDS and ToF-SIMS, but the method chosen to expose clean sections of glass was ToF-SIMS milling using direct current (DC) mode. Sputtering using ToF-SIMS is only capable of removing 0.2 nm/s, and depth profiles were taken, so hours were required for sample analysis, and only a small sample of representative particles from Winchester, CCI and Federal ammunition were chosen for analysis.

In later work, involving SEM-EDS only, Coumbaros [159] examined 11 brands of ammunition and 1 type of nail gun cartridge and found 9 brands contained glass frictionators (Fiocchi and Lapua Pistol did not contain glass at all). Of the 9 brands containing glass only Remington contained soda lime glass, borosilicate glass was present in all the others. A combination of borosilicate and soda lime glass was observed, either within or between batches, in two brands, RWS and PMC Zapper.

The discovery of glass-containing GSR and the existence of a Pb/Ba/glass particle type was reported in the Dalby review [35], and since the completion of their study, a few other people have directly or indirectly reported on these particles. Henderson [160] investigated the possibility of discriminating between frictionators from different sources in his thesis, by digesting large quantities of frictionator and analysing them by ICP-AES. Unfortunately, this method allows only a bulk analysis, and cannot account for any variation within a glass-containing particle, between particles within a cartridge, or between cartridges within a box.

Particles with some similarity to glass-containing GSR have been observed, but not reported as such, in other literature articles, including in Oomen and Pierce [133], where a particle containing Si, Al and Na (amongst S, C, O, Fe) was reported, and Martiny *et al.* [161], where particles were observed containing various combinations of Si, Al, Na and K (amongst Cu, Zn, Mg, S, Sr, Ca, Fe).

## 1.7. Glass, the analysis of glass, and the analysis of gGSR

Glass is a non-crystalline (or amorphous), isotropic solid material and in common usage the word glass refers to a transparent, silica-based material, which has several sub-classes depending on composition. The most common type of glass is soda lime glass, which is characterised by relatively high concentrations of sodium (Na) and calcium (Ca). Other classes of glass have high boron, lead or aluminium (known as borosilicate, lead-glass or aluminosilicate, respectively).

Identifying a substance as being glass can be accomplished using a combination of physical and chemical properties. Polarising light can show whether a material displays birefringence, or whether the material is isotropic and therefore could be glass. Similarly, diffraction-based techniques can show whether a compound is amorphous or non-crystalline. The refractive indices of various categories of glass are well known. Refractive index is related to the density of the material, and can be determined with great accuracy and precision using a refractometer, or for small samples, oil-immersion/temperature-variation analyses. Elemental composition can give information about the makeup of a material, what elements are present, and indicate whether they are present in ratios that would be expected for glass.

### 1.7.1. Glass elemental composition analysis methods

Although limited literature directly concerning the analysis of gGSR exists, glass itself is a well-studied trace evidence type. Several researchers [162-176] have developed methods to analyse glass fragments that are less than 1 mm in diameter, which are common for casework including glass. The first analytical method used for glass in many labs are refractive index measurements, usually analysed *via* temperature variation/oil immersion methods. Many jurisdictions now use elemental composition analysis in addition to, or replacing RI measurements.

SEM-EDS has been used to analyse glass elemental compositions, but is not considered a preferred technique, as the homogeneous structure of glass means that only the major and minor glass forming elements tend to be present above the relatively high LODs (~1000 ppm) [176]. However, in forensic GSR analysis, SEM-EDS is the preferred technique and at the present time the vast majority of suspected GSR traces would be examined using that technique. Therefore, the particular application of SEM-EDS to the detection and analysis of glass present in GSR may be useful, despite limitations to the number of detectable elements.

X-ray fluorescence (XRF) techniques have been successfully used to analyse glass, and have provided good quality semi-quantitative or quantitative data for numerous elements [165, 168, 176]. However, even μ-XRF techniques may not have the required spatial resolution to analyse post-discharge glass

from frictionators, which can be expected to be less than 20 µm in diameter (i.e., of the size typical IGSR particles).

ToF-SIMS [174] has been used to profile and discriminate between glass from different sources, is only micro-destructive (removes a few nm per analysis), and it measures a wide mass range, meaning that elements or molecules of interest do not have to be pre-identified, and data can be retrospectively interrogated for specific elements. ToF-SIMS is, however, only useful for semi-quantitative analyses.

The most commonly used elemental analysis technique for forensic glass examination is LA-ICPMS [164, 165, 175-180], a technique that can quickly quantify a range of pre-identified elements, but that can be highly destructive to microscopic samples. It has been used by forensic researchers and is used for casework using the ASTM guide E2330 – 04 [180] in many jurisdictions. Although it has had success with casework sized glass particles, the particles of glass expected to be found in glass-containing GSR are smaller again, and as 3 replicate analyses at a spot size of at least 50 µm is recommended for analysis of glass by LA-ICPMS [180], most casework GSR samples, including glass containing particles would be obliterated prior to any meaningful elemental analysis having occurred.

# 2. Objectives and Experimental Theory

## 2.1. Contextual Statement

The work by Coumbaros and Collins [18, 158, 159] raised several interesting possibilities and avenues of research. The presence of these lead (Pb)/barium (Ba)/glass particles, or the potentially equally significant Pb/glass and Ba/glass, could, as hypothesised by Collins, be a highly specific indicator to infer firearms involvement. It is also possible that, following on from Collins' and Coumbaros' work [18, 158, 159], given the differences in elemental composition observed a method could be developed which would allow these differences to be quantified and exploited for the discrimination of GSR samples from different sources. The presence of glass-containing particles in a GSR sample could therefore be exploited for the improvement of GSR interpretation.

After considering the commonly used glass analysis techniques, RI, SEM-EDS and ToF-SIMS appear to be the most practicable techniques to implement, and these were chosen for the initial work with glass frictionators, and glass containing GSR.

## 2.2. Overarching Aims

The overarching aims of this project were to assess the feasibility and added value of incorporating these glass-containing GSR particles into GSR evidence examination and evaluation. This thesis assesses whether the presence of glass-containing GSR, or 'gGSR' in GSR residues increases the evidentiary, or probative value of the residue, and whether the presence of these particles would strengthen the identification of a residue as being associated with a firearm. Glass-containing GSR (gGSR) shall be defined as particles containing Pb/Ba/glass, however, Pb/glass and Ba/glass particles could also be considered gGSR, although perhaps less probative. An investigation into the prevalence of particles containing glass with Pb and/or Ba has not been attempted before and if they are found to be sufficiently rare, gGSR may be a useful addition to the current investigative toolkit and the ASTM classification scheme.

This thesis assessed the possibility that the presence of gGSR in a residue could be exploited to add a new dimension to GSR analysis, the ability to distinguish between GSR samples from various sinoxid, or other similar formulations. This thesis aimed to develop a method for demonstrating links between residues or links between residue samples and potential source ammunition. To assess these possibilities, three research areas were investigated, with interdependent results and impacts. To assess the first, whether gGSR could strengthen the identity of a residue as being associated with a firearm source, it must first be considered what the likelihood of finding gGSR particle in a GSR residue

is. Then, the possibility of the existence of other sources of particles indistinguishable from gGSR (glass with condensed Pb and Ba, smaller than 50 µm) was assessed.

The second area investigated methods for analysing microscopic pieces of glass, and a survey was undertaken to assess whether frictionator samples from different sources could be differentiated using refractive index, and elemental and isotopic composition analyses.

In the third area, a method was then developed to extend the analysis to genuine, post-discharge residues, and used to discern whether the elemental composition of glass was sufficiently stable through a firearm discharge to allow the linking of samples from a single source, and the differentiation of samples from different sources.

These research areas are covered in following chapters, where each is separately investigated to inform the bigger picture- the first comprehensive study of glass-containing GSR from 0.22 calibre ammunitions. Major original contributions to knowledge made by this work include:

- *the first substantial database of glass frictionator elemental profiles where individual grains were analysed,*
- *the first attempt to investigate Coumbaros' assertion that glass/Pb/Ba may be 'unique' to GSR*
- *the first methods described to visualise the interior of gGSR particles and to transfer particle fragments to secondary sample holders for simpler analysis by secondary techniques.*
- *the first $\delta^{11}B$ and $\delta^{7}Li$ measurements for two borosilicate RMs, NIST SRM 93a and NCS DC 61104.*

The following section describes the outline of this thesis and the novel contributions to forensic science that are presented in each.

## 2.3. Thesis Outline of Experimental Chapters

### 2.3.1. Chapter 3: Glass-containing gunshot residues and similar particles of industrial and occupational origins: considerations for evaluating GSR traces

In order for the work undertaken in this thesis to have practical value in casework, it was necessary to show that glass-containing GSR particles were collected in routine casework examinations. Casework particle searching data from Forensic Science SA was re-processed and reviewed to search for glass containing particles and a meta-analysis was undertaken.

After verifying whether these particles can be detected, the value of these particles in a forensic GSR investigation is dependent on the prevalence of alternate sources of glass/Pb/Ba residues that could be confused with particles from a firearm source. Thus, an investigation of fireworks, nail guns, brake linings and matches was undertaken, to determine whether these sources contained any combination

of Pb, Ba and glass, and whether particles from these sources could be confused for GSR or gGSR in casework. This was undertaken through using SEM-EDS particle searching and mapping, to determine characteristics of particles and particle populations from the various sources discussed.

### 2.3.2. Chapter 4: Analysis of elemental and isotopic variation in glass frictionators from 0.22 rimfire primers

This experimental chapter investigated the potential for novel information to be generated for GSR analysis by comparing unfired, cleaned frictionator samples, to determine the extent of elemental and isotopic variation across the South Australian ammunitions market. In this chapter, boron and lithium isotopic composition data were generated for two certified reference materials, to allow them to be used as standards in isotopic examinations of frictionator samples. Several techniques including SEM-EDS, ToF-SIMS and SHRIMP were investigated to determine what techniques are appropriate for the analysis of case-sized glass pieces (<20 µm in diameter), and to determine the relative discrimination power of these techniques. And finally, a survey of different ammunition was undertaken, creating the first substantial database of primer and frictionator composition information for 0.22 rimfire calibre ammunition.

### 2.3.3. Chapter 5: Methods for Analysis of Glass in Glass-Containing Gunshot Residue (gGSR) Particles

The final experimental chapter investigated methods to overcome the experimental difficulties associated with glass-containing GSR analysis. In this chapter, methods were examined and developed to expose clean glass surfaces, and analyse the glass-containing GSR particles. This chapter investigated the compositional and morphological properties of this particle type, specifically the metal incorporation into the glass nucleus of several particles, and the elemental homogeneity of the glass within a post-fired residue. Using this information, an investigation was then undertaken to determine whether pre-fired and post-fired glass from a single source can be linked, and those from different sources discriminated, similarly to the unfired residues.

## 2.4. Experimental Theory

This thesis has used a number of advanced analytical techniques, including several beam techniques based on SEM-EDS and various mass-spectrometry based techniques. The techniques used and discussed in this thesis include some that are common and familiar to operational forensic laboratories, and some which have been used in unrelated fields, or only in research. A comprehensive or nuanced discussion of the principles and operation of each of these techniques could be a book in itself. However, a basic overview of techniques used and the differences between the, along with references to more nuanced discussions of these techniques is presented below.

### 2.4.1. Refractive index measurements by GRIM

Refraction is the phenomenon of the change in direction of light at the interface of two media, and is a property of the different velocity of light between the media. Refractive Index (RI) is a measure of the relative velocity of light in a medium compared to another (usually a vacuum).This property is closely related to the media's density. The RI of a vacuum is defined as 1 and glasses have a RI of approximately 1.5.

A refractometer is used to measure RI for most applications, such as for gemmology, minerology or quality assurance in manufacturing. However, in forensic casework, glass fragments as small as 150 µm in diameter can be collected, and the RI needs to be determined accurately (usually to at least the $4^{th}$ decimal place). For this reason, other techniques have been developed, the one currently preferred being the automated oil immersion-temperature variation method. This automated measurement is controlled by glass refractive index measurement (GRIM) apparatus [169, 181, 182].

A Foster and Freeman GRIM3 instrument is a combination of a phase contrast compound microscope, a Mettler Toledo hotstage model FP82HT and a computer [182].

This method involves immersing a glass fragment in a refined silicone oil on a microscope slide. The silicone oil used has an accurately known, stable and calibrated refractive index variation over a temperature range. The calibration is performed using Locke glass reference materials which have known RIs. (Note: the glasses have slightly different RIs at room temperature vs. match temperature, but corrected values are available from Locke and Locke [175].) The glass slides are placed into the hotstage under the microscope. The microscope is used to find glass particles of interest, and sharp broken edges of the glass are chosen for analysis. Original edges can have different RIs from the bulk of the glass, and so are not usually chosen. Once the edges of interest are selected, the computer heats and cools the glass according to an automated program to determine the RI of the glass.

Phase contrast microscopy is used to visualise differences in RI between different phases. With colourless items such as glass and the silicone oils, the edges between two phases are visible when

the RIs of the phases are different. However, the closer in RI the two phases are, the more difficult it is to visualise the edge between in the phases. In RI determination by the automated oil immersion-temperature variation method (as used in the GRIM3) the temperature is varied between room temperature and ~120 degrees and the oils change in RI much faster than the glass [175]. When the RI of the oil reaches that of the glass, the edges of the glass fragments are no longer visible,, which is called the 'null point temperature' of the glass [182]. The computer monitors the precise temperature where the glass disappears and based on the calibration of the oil by glasses of known RI, calculates the RI of the oil at the null point temperature.

RI measurement through this method has very high precision, with 99% confidence intervals (±3σ) usually in the 5$^{th}$ decimal place [169, 182]. Because of this high precision, and the relatively low cost of this technique, in both resources and time, RI measurement is the first quantitative test undertaken by most forensic laboratories to determine whether two glass samples could have originated from the same source.

This technique is described in more detail in many published resources, and further reading about this technique should include:

[169] J. Locke, M. Underhill, Automatic refractive index measurement of glass particles, Forensic Science International 27(4) (1985) 247-260.

[181] J. Locke, H.V. Locke, Refractive Index Standards for the Forensic Scientist.

[182] Foster and Freeman, Grim3 Overview, 2007.

### 2.4.2. Scanning electron microscopy and related techniques

At a very basic level, scanning electron microscopy is like a light microscope, in that a source of illumination is focussed onto a sample to magnify an image of interest. In electron microscopy, however, the source of illumination used is an electron beam, not visible light [183]. Visible light cannot readily achieve magnifications higher than ~1000 x because the resolution of a light microscope is fundamentally limited by the wavelengths of visible light. Therefore, when high magnification, high resolution imaging is required, electron microscopy-based techniques are a better choice.

The electron source is focussed into a highly condensed, directed beam using a series of magnetic lenses [183]. The properties of this beam including voltage, amperage, spot size and focal distance can be varied for optimal visualisation/interrogation of a sample of interest. The electron beam is rastered over the sample, and the electrons interact with the sample to produce various signals [183]. Different signals produced from the sample can be detected using specialised detection systems, interpreted using computer software packages and displayed as an image, spectrum, or other information. The

images are displayed on the computer screen as a fixed size, and thus the magnification is a product of the raster area. The smaller the area rastered by the beam, the larger the magnification of the image produced.

SEM is a technique with many applications [184], both in forensic science and generally. It is a technique frequently used for high resolution imaging that is not possible using light microscopy, but with the wide array of detectors and hyphenated techniques available, many different types of information can be produced about almost any conceivable sample of interest. The three main types of detectors used generally detect secondary electrons, backscattered electrons and X-rays.

#### *2.4.2.1. Secondary electron (SE) imaging*

When the incident beam of electrons interacts with the atoms in the sample, loosely bound outer shell electrons can absorb sufficient energy from inelastic scattering of the beam to be ejected from the atom. These ejected electrons are known as secondary electrons (SE) [184]. These SE have very low energies (<50 eV) and are therefore only able to travel a short distance before being absorbed by the sample [184]. Therefore, they will generally only be able to escape from the top ~10 nm of the sample, and the probability of the electrons reaching the SE detector is mainly dependent on the angles on which the electrons can escape. The number of electrons that reach the detector from a point is converted to a grey value, with lighter values equivalent to more electrons. The beam is rapidly rastered over the area of interest, and a grey value is produced for every point (which becomes a pixel), gradually building up an image of the sample surface. SE imaging provides mainly topographical information about the surface of the sample [184].

#### *2.4.2.2. Backscattered electron (BSE) imaging*

When the primary incident beam enters the sample surface, it is as a coherent beam of negatively – charged electrons. The positively charged protons of the atoms in the sample are highly concentrated in the nucleus, whereas the electrons are more widely dispersed [184]. The beam electron- specimen atom interactions can cause elastic scattering, where the electrons of the primary beam are deflected without losing energy and deflected several times before re-escaping the sample surface – which is called 'backscattering' [178]. Back-scattered electrons (BSE) can be much higher in energy than secondary electrons, and therefore the signal can originate from a greater depth than SE [177]. BSE imaging gives compositional information, as the probability of electrons being backscattered from a sample is dependent on the atomic number (Z) of the atoms in the sample surface, with materials of a higher atomic number producing more BSE. Therefore, when the beam is rastered, and the signals

are converted to grey values, the areas where more BSE signal is observed will represent areas of higher average atomic number.

#### *2.4.2.3. Energy dispersive X-ray analysis*

When the incident beam interacts with the sample, electrons are not the only kinds of signal ejected. Incident electrons can interact with and eject inner shell electrons [183]. When this occurs, it creates an inner shell vacancy. Electrons tend to revert to the lowest possible energy state (called the ground state), so when the inner shell electron is ejected, the atom is left in an excited state [183]. To return to the ground state, an electron from a higher shell will move to fill the inner shell vacancy, and will release the excess energy. That energy is released in the form of an X-ray [184]. Depending on which electron was ejected, and which electron filled the vacancy, X-rays of different energies could be produced for most elements. Because the difference in energy between different shells is a function of the atomic number of the atom, each element has a characteristic set of X-rays (known as X-ray lines) that could be produced, with more theoretically possible X-rays for elements with higher atomic number (and more shells) [183, 184]. An EDS detector collects the X-ray signals and sorts them by energy, which allows the elemental composition of a sample to be determined.

#### *2.4.2.4. Focussed ion beam – scanning electron microscope (FIB-SEM)*

SE, BSE and EDS detectors are three of the most commonly used detectors with a SEM system. However, there are numerous other detectors available. SEM systems can also be dual beam (or multi-beam) instruments, incorporating other sources of incident energy and detectors. Although there are numerous combinations available, a dual beam focussed ion beam – scanning electron microscope (FIB-SEM) was the type used in this thesis. A FIB-SEM has all the components of a SEM, but also incorporates a liquid metal ion source (LMIS). A LMIS is similar to an electron source, except that it focuses a beam of ions (such as $Ga^+$) onto a sample. This ion beam can be used for several purposes. The FIB-SEM incorporated both a secondary electron and a secondary ion detector (which works by converting secondary ions to secondary electrons) allowing imaging from 2 different angles/orientations [185]. An ion beam can be advantageous because it has a smaller interaction volume compared to an electron beam of similar energy [185]. An ion beam, unlike an electron beam is inherently destructive (albeit micro-destructive) to the sample, which can be both an advantage and a disadvantage. If the intent of the analysis is only for imaging or compositional analysis, an electron beam is a better choice. However, the destructive capabilities of the ion beam can be harnessed for

etching, micromachining, depth profiling analyses, or for the preparation of thinned samples for analysis by transmission electron microscopy (TEM).

Scanning electron microscopy, micro-analysis, and focussed ion beam analysis are complicated, sophisticated techniques, which require a thoughtful consideration and compromise of conditions and parameters to generate meaningful data. Further reading in these subject areas should begin with the following:

[183] Microscopy Australia, Scanning Electron Microscopy. <https://myscope.training/#/SEMlevel_3_1>, 2019 (accessed 11 Nov 2019.).

[184] J.I. Goldstein, D.E. Newbury, J.R. Michael, N.W. Ritchie, J.H.J. Scott, D.C. Joy, Scanning electron microscopy and X-ray microanalysis, Third Edition ed., Springer 2003.

[186] L.A. Giannuzzi, Introduction to Focused Ion Beams: Instrumentation, Theory, Techniques and Practice, Springer Science & Business Media 2004.

[187] A.T. Ampere, Recent developments in micromilling using focused ion beam technology, Journal of Micromechanics and Microengineering 14(4) (2004) R15.

### 2.4.3. Mass spectrometry techniques

The remainder of the techniques used in this thesis are based in mass spectrometry. Mass spectrometry requires ionisation of the sample, which can be accomplished using variety of approaches. Then the ionised species are detected and their mass to charge ratios determined, again,this can be accomplished  of the ions is measured. The mass to charge ratio of the ionic species can allow the determination of the chemical composition of a sample. The ionisation process may or may not cause fragmentation or atomisation of species within the sample.

#### *2.4.3.1. Time of flight – secondary ion mass spectrometry (ToF-SIMS)*

In time of flight – secondary ion mass spectrometry (ToF-SIMS) a primary beam of energetic ions (can be a LMIS similar to in FIB) is focussed onto a sample surface. The bombardment of the surface with ions produces sputtered particles, including positive, neutral and negatively charged species, that can be atomic or polyatomic species [188]. The species that are created flow through to the time of flight mass spectrometer.

A time of flight mass spectrometer (ToF) separates secondary ions based on their flight time in a flight tube [188]. The ions are all accelerated with the same potential at the entrance to the flight tube, and

therefore the lighter ions will flow through the tube at a higher velocity than the heavier ions [188]. From the time of flight, the mass to charge ratio of the ion can be determined.

ToF-SIMS has advantages over other mass spectrometry techniques in that the ion-sputtering means that the MS is not limited to volatile samples, as many heavier elements can atomised into the gas phase, and because the mass to charge ratio of all species is measured simultaneously, ToF-SIMS does not require pre-identification of elements of interest [189]. It also has high spatial resolution, high mass resolution, high sensitivity (ppm-ppb) and can detect all elements (H to U) in addition to molecular species [189]. However, ToF-SIMS is very sensitive to matrix-effects and this means it is very hard to perform quantitative analyses with this technique [188].

#### *2.4.3.2. Sensitive High-Resolution Ion Microprobe (SHRIMP)*

Similar to ToF-SIMS, SHRIMP is a secondary ion mass spectrometry technique, but it exclusively uses an oxygen ion gun to ionise material sputtered from the sample, and it uses a high-resolution double-focussing mass analyser instead of a ToF MS [190]. The high-resolution double-focussing mass analyser uses an electrostatic sector and quadrupoles to select ions based on their mass to charge ratio [190]. Unlike the ToF MS, the isotopes (or ions) of interest must be known, but the SHRIMP can use electron multiplier detectors or Faraday cups for extremely sensitive trace element or stable isotope ratio analyses, and can be used quantitatively when used with appropriately matrix-matched reference materials [190].

#### *2.4.3.3. Multi-collector inductively coupled plasma mass spectrometry (MC-ICP-MS)*

All of the techniques thus far are micro-analytical or beam techniques. However, all beam techniques are subject to some level of matrix effects. For quantitative or semi-quantitative analysis of samples by beam techniques, matrix-matched reference materials with known properties are necessary for interpretation. For the stable isotope analyses performed on frictionators by SHRIMP, there were no borosilicate glasses with known isotopic properties for reference. Therefore, some reference materials were analysed by multi-collector inductively coupled plasma mass spectrometry (MC-ICP-MS), a bulk analysis technique. This means that the glasses had to be finely homogenised and dissolved into solution for analysis. A portion of the solution was injected onto the instrument.

MC-ICP-MS uses an inductively coupled plasma torch to ionise the sample and force it into the gas phase [191, 192]. A quadrupole mass spectrometer is used to select mass-to-charge ratios of interest, and Faraday cups are used to detect isotopes of interest [191].

For more information regarding the various mass spectrometry techniques discussed, please refer to some of the following references:

[188] S. Fearn, An Introduction to Time-of-Flight Secondary Ion Mass Spectrometry (ToF-SIMS) and its Application to Materials Science, Morgan & Claypool Publishers, 2015.

[189] A. Schnieders, Time-of-Flight Secondary Ion Mass Spectrometry, Microscopy Today 19(2) (2011) 30-33.

[190] The ASI website: https://asi-pl.com.au/ accessed 20 Nov 2015, 9 Nov 2019.

[191] D. Beauchemin, Inductively Coupled Plasma Mass Spectrometry, Analytical Chemistry 82(12) (2010) 4786-4810.

[193] S. Benson, C. Lennard, P. Maynard, C. Roux, Forensic applications of isotope ratio mass spectrometry—A review, Forensic Science International 157(1) (2006) 1-22.

# 3. Glass-containing gunshot residues and similar particles of industrial and occupational origins: considerations for evaluating GSR traces

## 3.1. Preface

In this chapter, a survey has been undertaken of sources which may produce particles similar to glass-containing GSR (gGSR). This chapter contributes to the overall aims of this work by assessing the probative value that could be added to GSR evidence if gGSR particles are present. The original contribution of this chapter is primarily that this is the first directed survey that aimed to support or refute the hypothesis that gGSR is characteristic of an association with a firearm. This survey is also a significant analysis of brake pads, fireworks, matches and nail guns as available in South Australia, and one of few analyses of particles similar to GSR to be undertaken using modern definitions of GSR.

This chapter is based upon and significantly similar to the papers describing this work, which have been published in Forensic Science International [194, 195].

## 3.2. Chapter Summary

In an ideal case, the value of evidentiary traces such as paint, glass or GSR would be determined numerically and presented through the use of likelihood ratios or verbal-equivalent scales. The problem in the evaluation of gunshot residue (GSR) evidence using these models is that in many shooting scenarios insufficient data exist to support a quantitative model of interpretation. The complex relationship that exists between ammunition composition and post-firing residues makes quantitative interpretation more difficult for GSR than for other traces such as glass. When evaluating the significance of traces in a quantitative model, the value of a trace is reduced as the number of random sources that could produce the trace increases.

Previously published work [158] has suggested that glass-containing GSR (gGSR), which is glass encrusted with lead (Pb) barium (Ba), and/or antimony (Sb) residues, are a new type of GSR not already classified under ASTM E1588 – 17 [196]. If random sources of particles resembling gGSR are rare, then gGSR may be valuable evidentiary traces. In order to potentially incorporate these particles into a future model, the general background prevalence of gGSR and specific sources capable of producing similar particles must be understood.

Therefore, particles from fireworks, brake pads, matches, and cartridge actuated nail guns were assessed on an individual basis and at a population level. These sources, known to produce particles resembling GSR, were assessed using backscattered electron – scanning electron microscopy – energy dispersive X-ray spectroscopy analysis (BSE-SEM-EDS) for the presence of glass-containing particles that resemble gGSR.

In the experiments described in this chapter the nail gun produced particles compositionally indistinguishable from gGSR, due to the primer in the brand of nail gun cartridges used containing glass as the frictionator in addition to Pb and Ba compounds.

In this study, no particles were located from fireworks, brake pads or matches that were indistinguishable from gGSR, nor was any evidence observed that would suggest that such particles could be formed.

## 3.3. Introduction

Guidelines for the forensic analysis of inorganic GSR by scanning electronic microscopy with energy dispersive X-ray spectroscopy (SEM-EDS) are issued by the American Society for Testing and Materials (ASTM) and define a hierarchical particle classification scheme [32]. At the latest revision, 'characteristic' particles are defined as those that have compositions rarely found in particles other than those originating from a firearm source, meaning that they have the highest probative value in shooting investigations. 'Characteristic' particles commonly contain the elements lead (Pb), barium (Ba) and antimony (Sb), or less commonly containing lead (Pb), barium (Ba), calcium (Ca), silicon (Si) and tin (Sn). Non-toxic or lead-free ammunition formulations produce their own 'characteristic' GSR particles, which are classified separately within the standard and include particles that contain gadolinium (Gd), titanium (Ti) and zinc (Zn), or also could contain gallium (Ga), copper (Cu) and tin (Sn). However, there are many different non-toxic or lead-free ammunition formulations available, and many may not produce 'characteristic' particles. There are other particle types associated with firearm sources, such as those containing Pb and Ba, or Ti and Zn for non-toxic or lead-free ammunitions, but these are considered less supportive of a firearm origin and are referred to as particles "consistent" with a firearm source. This means that it is important to evaluate the significance of GSR particles on a case-by-case basis, and as per the current standard, where appropriate compare recovered particulate matter to "case-specific known source items" [32].

As part of this thesis, it has been asserted that glass-containing GSR (gGSR) particles, defined as particles with a glass core encrusted with Pb and/or Ba, are a highly specific indicator of the origin of the particles being a firearm or cartridge source.

The probative value of GSR is inversely related to the prevalence of occupational, industrial and environmental sources of particles that could be mis-identified as those originating from a firearm source. Accordingly, the prevalence of gGSR particles such as Pb/glass, Ba/glass, or Pb/Ba/glass in the environment is related to the probative value of these particles.

It is hoped, that in the future, the forensic interpretation of GSR will be weighted and reported using evaluative methods much like those employed in glass casework and be able to incorporate both source-level and activity-level information. Each case will have its own hypothesis and factors that need to be considered, which can be represented through various methods, one of which is a Bayesian network. The formation of a Bayesian network structure depends on the context of a case and the formulation of the prosecution hypothesis (*Hp*) and alternate or defence hypothesis (*Hd*).

A network structure for the interpretation of GSR, informed by experimental data, was proposed by Biedermann, Bozza and Taroni [1] and further adapted by Lucas *et al.* 2018 [2]. An expansion of that network was described in the introduction to this thesis. The part relevant to this chapter is reproduced in Figure 7.

The work described in this chapter focuses upon factors that contribute to the particles that are GSR (or gGSR), or indistinguishable from GSR, present on a person of interest (node 'M' in Figure 7) *via* means that are unrelated to *Hp*. The work presented here is an investigation of several sources that could potentially contribute background levels of particles indistinguishable from GSR and in particular gGSR ('B'/'$A_B$' nodes, in Figure 7), and will use results of a literature review and a survey of the chemical composition of particles which come from sources potentially capable of producing particles similar to GSR or gGSR.

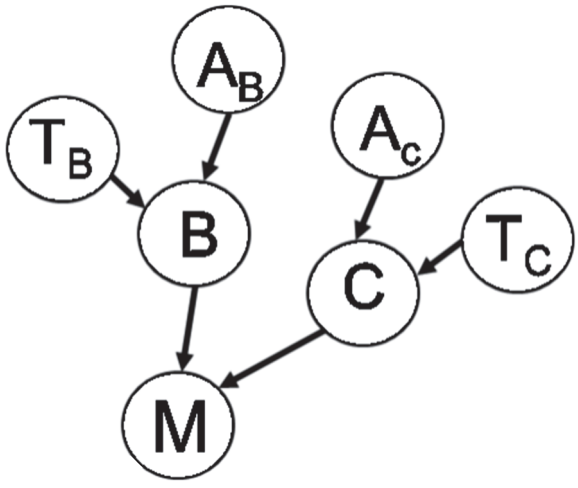


| Variable | Description |
|---|---|
| M | Particles present originating from sources other than Hp |
| B | *Background levels of 'GSR' Particles* |
| C | *Contamination levels of 'GSR' Particles* |
| $A_{x_{1-n}}$ | *Nature of exposure to $x_1, x_2, \ldots x_n$* |
| $T_{x_{1-n}}$ | *Time since exposure to $x_1, x_2, \ldots x_n$* |

**Figure 7: Part of the Bayesian Network for the evaluation of GSR Results first proposed by [1], reproduced and modified from [2].**

Efforts have been made previously to assess 'M', or the number of particles on a person's hands from sources other than *Hp* through either general or specific surveys. General surveys aim to quantify the prevalence of GSR particles (or, more correctly, particles indistinguishable from GSR) on a 'random man' (i.e., background levels of GSR in the general population, and 'B' on Figure 7) [197, 198], whereas specific surveys assess the possibility that there are industrial or other non-firearm sources of particles indistinguishable from GSR that could contribute to this frequency ('$A_B$' on Figure 7). The most recent general study of the prevalence of GSR in Australia showed that very few particles similar to GSR on the hands of the general public [198].

In her specific survey, Brożek-Mucha investigated the possibility that welding fumes [199] could produce particle populations similar to GSR, but found that whilst particles indistinguishable from lead-free primer particles are present in welding fumes, the abundance of other particles unlike GSR should allow the differentiation of welding fumes from GSR when the entire population of particles in a residue is considered. Berk [200] investigated airbags, another automotive source, and found that some airbag residues from side passenger airbags could produce three-component Pb/Ba/Sb particles that would be classified as 'characteristic' under current guidelines. However, it was noted that the three-component particles made up less than 0.2% of particles in the dataset, and that the overwhelming population of Zr-, Cu-, and Co-containing particles are good indicators for airbag residues. Berk also advocated for including 'Zr-rich' and 'Co' as categories within particle searching software packages to aid in the correct identification of airbag residues. A recent study by Laflèche *et al.* [201] also examined airbags, and found that approximately 5% of the passenger side airbags surveyed in Canada (2/38) tested positive for GSR-similar Pb/Ba/Sb particles, although no relationship could be ascertained between location or time of manufacture and the likelihood of the airbag testing positive. Additionally, they noted that no brake pads were able to be sourced that appeared capable of producing Pb/Ba/Sb particles.

Several works [158, 159, 202] have suggested that the presence of glass particles encrusted with Pb and/or Ba may be an indicator for residues associated with a firearm discharge. However, a specific or directed survey of particles of occupational or industrial sources for the presence of glass and elements of relevance to GSR investigation and a survey of particles on 'random man' are needed to determine whether particles of this type may be considered 'characteristic' under the ASTM classification. The work in this chapter relates to such a survey involving particles and particle populations sourced from fireworks, nail gun cartridges, brake pads and safety matches that resemble gGSR. The impact that these findings have on forensic analyses of GSR from conventional primers, and GSR originating from non-toxic, or heavy metal free (HMF) primers, is also presented.

### 3.3.1. Literature Review of Particles Originating from Fireworks

A review was conducted of papers in environmental science journals concerning particulate matter attributable to fireworks. Sixteen papers [203-218] were found where the impacts of fireworks on air pollution were studied and where changes in concentration of airborne particles less than 10 µm in diameter following firework events were reported. This particle size domain is directly comparable to particle sizes found in GSR casework. The 16 literature sources reported on air samples collected at a total of 21 distinct locations and it was found that airborne particulate matter (PM, analysed as bulk material rather than as discrete particles) showed higher concentrations of various elements on days with firework events compared to control days.

Table 6 provides a compilation of the data from these 16 articles (individual site data are shown in the supplementary information at the end of this chapter) regarding elements that were reported to be associated with fireworks events in more than one site. As shown in Figure 8, bulk Pb and Ba concentrations in airborne particulate matter were observed to increase in 19 of the 21 locations, and in 17 of the 21 locations both Ba and Pb were detected above normal concentrations. Sb was found to have increased in 7 locations, and in these 7 locations increases in Pb and Ba were also found. This indicates that one-third of the firework events studied in these international contexts have at least the potential to produce particles with similar elemental composition to GSR. It is important to note, however, that this is a minimum estimate, as a different a suite of elements was reported in each study, and it cannot be determined whether elements were not reported because an increase was not detected, or simply whether no attempt was made to measure them. This is most relevant to Sb, as an increase was noted in 7 of 21 locations, but Sb was only reported in 8 locations. It is unknown whether there was an increase in the other 13 locations. Of the studies examined, none mentioned glass particles amongst the residues, but 4 studies mentioned Si, and each noticed a modest increase of Si residues attributable to firework displays.

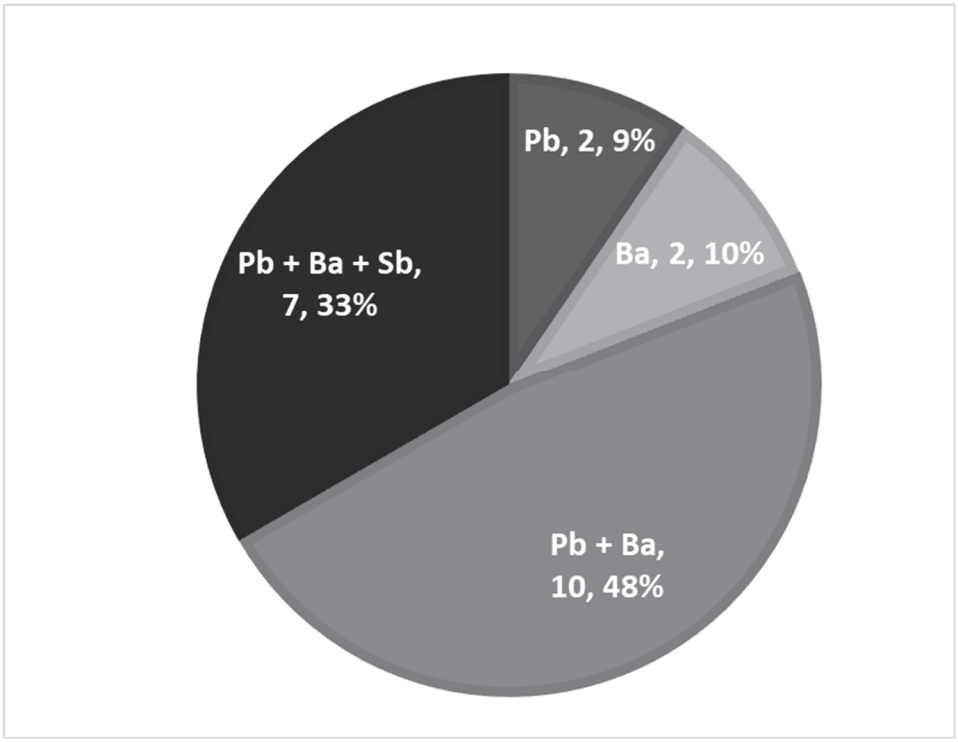


**Figure 8: Number and percentage of locations at which each combination of Pb, Ba and Sb were found to have significantly increased after a firework event compared to a 'normal day'.**

**Table 6: A summary of the findings of existing literature in atmospheric pollution of heavy metals attributable to firework displays. [203-213]**

| Element Measured | Total Number of locations where element was reported | Number of locations where increase due to fireworks were reported |
|---|---|---|
| Pb | 19 | 19 |
| Ba | 19 | 19 |
| Sb | 8 | 7 |
| Sr | 18 | 18 |
| Cu | 21 | 20 |
| P | 8 | 6 |
| S | 3 | 3 |
| Cd | 16 | 13 |
| K | 18 | 18 |
| Mn | 14 | 12 |
| Mg | 17 | 17 |
| Cr | 12 | 12 |
| Bi | 6 | 6 |
| Zn | 18 | 17 |
| As | 10 | 10 |

Several previous works have looked at firework residues in a GSR context. Mosher *et al.* [219], Grima *et al.* [126, 220] and Trimpe [221], concluded that the possibility of observing small, round, three-component particles was remote yet possible, but further concluded that GSR could usually be distinguished from firework residues by considering the particle population as a whole. Grima *et al.* [220] highlighted that there could be difficulty recognizing 'consistent' particles as such in a mixed sample of GSR and fireworks. Garafano *et al.* [121] concluded that Pb/Ba/Sb characteristic particles were 'unique' (what is now called characteristic) to firearms discharge, and that the particles from fireworks containing some of these elements were composites that could "easily be distinguished from GSR". None of the afore-mentioned studies reported searching for, or observing, either silicon or glass in their residues.

In the study reported in this thesis, residues from firework displays in South Australia were examined for GSR-like particles, and especially those with glass inclusions. As the fireworks involved in the study originated from overseas, the findings have a wider relevance than South Australia.

### 3.3.2. Literature Review of Particles Originating from Nail Guns

The vast majority of modern nail guns, at least in Australia, use pneumatic or electrical actuation, rather than the once-popular explosive cartridges containing smokeless powder and primer. Particulate matter arising from the use of explosive nail gun cartridges has been previously studied in the literature. Wolten *et al.* [115] looked at nail gun residues, of both "wad-type construction" charges and crimped charges. They found that the crimped charges were capable of producing particles of "possible interest" but concluded that the populations of particles arising from the use of nail guns were inconsistent with gunshot residues. This conclusion was based on the presence of Fe, Mn, Cr and Zn (in the absence of Cu) observed in an overwhelming majority of particles, which can be attributed from the nail. Wallace and McQuillan from Northern Ireland [119] investigated nail gun particulate matter on hands through bulk analysis and particle analysis. This work agreed with Wolten *et al.,* finding that although 2- and 3- component particles can be found, the population of particles produced by nail guns could be differentiated from GSR by other factors, including high Fe concentration, and a reversed Cu to Zn concentration ratio compared to GSR. Both studies concluded that although a small number of particles consistent with GSR could be found, the overwhelming number of inconsistent particles would allow a trained examiner to disregard nail gun residue as being gunshot residue.

Garafano [121] also looked at cartridge-operated industrial tools, and agreed with Wolten that the presence of the three-component GSR particles, and many spherical or nodular particles, were "fully compatible with GSR" but then claimed that it is possible for these residues and GSR to be

differentiated, without explanation. The true challenge in interpreting genuine casework samples is that there is rarely an ideal sample to work with, and the number of particles of potential firearm origin are small, so the significance of the samples must be determined from only a few particles. Additionally, elements that have been previously suggested to invalidate residues as being from a firearm source (e.g., Zr, Co, Bi) are not considered exclusionary elements by the current definitions from the ASTM. Consequently, this study includes results of an investigation of nail gun residues within the context of the current guidelines.

### 3.3.3. Literature Review of Particles Originating from Matches

A limited amount of literature exists concerning the composition of matches. Kasamatsu *et al.* [222] detected and quantified six elements in match heads using ICP-MS; which included Mg, Al, Ca, Fe, Zn and Ba. In a second study, the elements Cl, K, Si, Al, S, P, Fe, Mn, Cr, Zn and Mg were detected in matches using energy dispersive X-ray analysis [223]. HMF formulations can include a number of these elements. As the strike surface can include glass, it is possible that particles like those seen from GSR from HMF formulations could arise from matches, therefore the research carried out for this thesis also includes an examination of residues from matches.

### 3.3.4. Literature Review of Particles Originating from Brake Pads

Automobiles and the brake pads that are fitted to them are abundant in the community. Many members of the community can be regularly exposed to particles produced by braking, through activities such as changing tyres, cleaning their car or performing car maintenance. Therefore, if even a small percentage of these braking-related particles resemble GSR that could result in a large number of particles similar to GSR present in the environment, which would decrease the probative value of the detection of GSR particles.

Several studies have been conducted investigating the probability that brake pads could generate particles that contain combinations of Pb, Ba and Sb [121, 123, 201, 224], and found that although these particles were sometimes present, they were located amongst numerous particles that are rarely found in association with firearm discharge. Additionally, these Pb, Ba and Sb-containing particles lacked the spheroidal morphology that is characteristically associated with GSR and tended to be angular and/or irregular. It was concluded that while individual braking-related particles, considered in isolation, may share similarities with individual GSR particles from firearm sources, that at a population level, it was possible to determine whether a sample was sourced from brake pads rather from firearms.

In spite of these findings, the fact that brake pads could possibly produce particles that resemble GSR has been used to suggest, occasionally [225, 226], that GSR examination was not reliable or specific, and could be prone to producing false positive results. This view is exemplified by an article in a popular science magazine [225] and alluded to even in more scholarly articles [226]. Contrastingly, modern population surveys have not revealed widespread occurrences of GSR-like particles on members of the public [197, 198].

Therefore, an investigation of the types of particles produced by modern brake pads in modern vehicles in light of the latest ASTM definitions of GSR was warranted, as Pb, Ba and Sb have plausible sources in samples associated with brakes/automobiles.

Barium sulfate is a commonly used friction material used to control heat stability in brake pads (Cardolite Specialty Chemicals, personal communication, as cited in [194]). Other metal sulfides are used as additives in brake pads in order to modify the frictional characteristics of brake materials, in particular antimony trisulfide is used as a solid lubricant [227]. Although many countries have recognised the health risks associated with Pb [228-232], and Pb has been largely removed from many automotive components, including fuel and brake pads, there are a number of currently existing automotive sources of lead. Current automotive sources of Pb include some air bags [200, 201], lead-acid batteries, automotive paints and wheel weights, which could be incorporated into particles collected from brake pads.

The work presented in this chapter is an evaluation of particles generated from a number of brake pads and an assessment of their significance to GSR examinations.

## 3.4. Methods

### 3.4.1. Sample Collection

Aluminium pin stubs covered in carbon adhesive (Tri-Tech Forensics Inc., North Carolina, USA.) were used to collect all samples. These stubs are industry standard for GSR collection. Samples were coated with 20 nm of carbon using a Cressington 108C (Watford, England) evaporative carbon coater to minimise charging effects during analyses.

#### *3.4.1.1. Collection of GSR and non-toxic GSR samples*

Samples of GSR from traditional and HMF ammunition were collected from a South Australia Police training centre during an exercise demonstrating a range of firearms and ammunitions. Samples were collected by pressing a GSR stub onto both hands of the officers 50 times, or until the stubs were no

longer sticky, commencing with the volunteer's dominant hand and focussing on the region between the thumb and forefinger. Samples were collected immediately after a session where the officers had fired between two and ten shots.

The collection method used to collect GSR from 2-component primers was based on that used by Lucas *et al.* 2016 [233], which was a modification of a method developed by JS Wallace (Personal Communication between JS Wallace and HJ Kobus, 2014). Briefly, at least 30 shots of 0.22 LR PMC Zapper ammunition were shot with a Ruger model 77 bolt-action long rifle. Then the officer's hands were washed, and two more shots were fired through a GSR collector constructed out of a 1.25 L PET soft-drink bottle with cap removed, the neck of which was slipped over the end of the barrel and secured with duct tape. Samples were subsequently taken from hands and the interior of the PET collector.

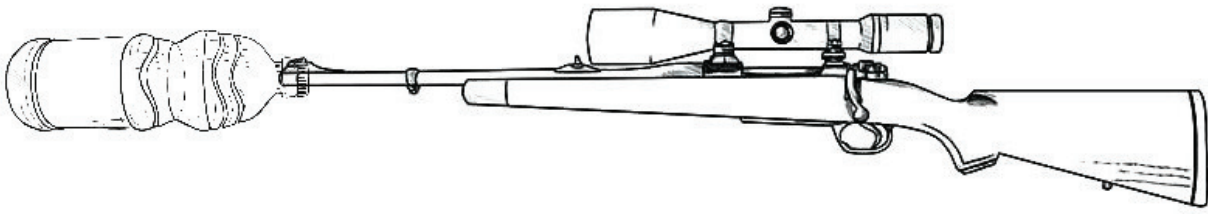

**Figure 9: A diagram of gGSR PET collector, created using images from https://owips.com/clipart-9778231 and https://owips.com/clipart-11540676, access date 10 NOV 2019.**

#### *3.4.1.2. Collection of firework samples*

Firework residues were collected at public firework displays. Air samples were collected from one show by exposing stubs to air for the period of the firework display and air blanks were collected by exposing GSR stubs in the firework region for approximately 45 minutes prior to the show. Hand samples were collected by pressing stubs, as per normal GSR sampling procedures, onto hands of spectators and technicians and onto firework components and surfaces around the display. Hand samples were collected at 3 different displays, from 2 different firework companies. Blanks of hands were collected from spectators before the display for comparison. The spectators sampled were approximately 50 m from the source of the fireworks. The technicians and surfaces sampled were in the direct vicinity of the fireworks. All technicians were sampled after the display and each of the technicians and spectators indicated that they had had no contact with a firearm in the previous week and were non-smokers. Twenty samples from firework components, surfaces and the hands of technicians and members of the crowd were used in this study.

#### *3.4.1.3. Collection of nail gun samples*

Hilti nail gun cartridges were obtained (Hilti Red: 0.27 Cal. Short, crimped, part # 50353; Hilti Yellow: 0.27 Cal. Short, crimped, part # 50352) from the Hilti Store Adelaide (Keswick, South Australia). Samples of particulate matter sourced from these cartridges were collected onto an adhesive covered microscope slide *via* manual detonation of primer using a square head centre punch and a hammer, in the same manner as described in Chapters 4 and 5. Initial SEM-EDS results indicated that these cartridges appeared to produce particles like GSR. Therefore, a semi-automatic cartridge-actuated nail gun was sourced to discharge cartridges in a conventional fashion (Hilti DX 460, leased from Kennard's Hire, Morphett Vale, South Australia). Each of fourteen operators using the nail gun fired ten cartridges and operator's hands were subsequently stubbed. The participants were asked to wash their hands prior to handling the nail gun. Samples were additionally taken from interior and exterior nail gun components and from associated surfaces such as the packaging for the tool and the target surface, adding to a total of 23 samples associated with nail guns.

#### *3.4.1.4. Collection of match samples*

Four types of safety matches were sourced; Redhead Extra-Long Safety Matches, Hanna Matches promotional matchbooks, Coghlan's Waterproof Matches and Coghlan's Windproof/Waterproof Storm Matches. Strike-anywhere matches are prohibited for sale in Australia and were therefore not considered in this study. Match samples were collected by two methods. In the first, a match was struck over a stub, and the head of the match and the strike surface were then stubbed with the same stub. In the second method, particles from hands were collected by having volunteers each light a box (~45 matches) of Redhead matches and then stub their own hands. Redhead matches were chosen because they are the most commonly used in Australia. Eight samples from matches were used in this study.

#### *3.4.1.5. Collection of brake pad samples*

Particulate samples were collected from the direct stubbing of used brake pads (n=12), brake rotors (n=3), wheel rims (n=22) and the hands of individuals who had handled brake pads or wheels (n=11). The brake pads were sampled by dabbing across the entire surface of the pad until the stub was no longer sticky. . Samples from brake rotors were collected by directly sampling from the rotor surface. Samples were collected by applying the adhesive stub to the rotor surface at a point directly accessible from between the wheel spokes. Wheel samples were taken directly from vehicles in a car park. They were collected by dabbing wheel rims with a stub. The cars sampled were from various manufacturers and models, but the brake pad types present on the vehicles were unknown. The hands of a number

of mechanics who had handled brakes and other automotive components were also sampled. An undergraduate student aided in the collection of samples.

### 3.4.2. Analysis by SEM-EDS and automated particle searching

SEM-EDS analysis of all samples was carried out using a FEI Inspect F50 SEM-EDS system (FEI Inc., Oregon, USA) equipped with an EDAX brand EDS detector operating in Backscattered Electron Mode (BSE). An accelerating voltage of 25 keV was selected. Particles were detected *via* the automated particle searching software 'Magnum' with minimum particle size set to 0.5 µm. Settings for spot size, brightness and contrast were optimised and X-ray energies and Z-values were calibrated using a mixed metal standard containing flakes of carbon, silicon, germanium, niobium and gold (Ardennes Analytique sprl, Belgium) and the Microvalidator software. The settings were optimised to filter out as many large flakes of iron as possible. Three-component particles were manually re-acquired using TEAM EDS software to verify classifications. Spectra for consistent particle types were manually reviewed, but not manually re-acquired unless they contained antimony.

Negative sample controls (blank carbon coated stubs) and negative process controls (blanks of the experimenters' or subjects' hands) were analysed and showed no evidence of sample cross-contamination. A positive control (PLANO W Plannet GmbH, Wetzlar, Germany, SPS-5P-2A), consisting of deliberately deposited Pb/Sb/ Ba films of known size between 0.5 µm and 10 µm, was analysed bracketing every run.

SEM-EDS X-ray maps were collected using 25 KeV accelerating voltage, also on the FEI F50 Inspect and within the TEAM EDS Software, with dwell time and number of scans optimised for each particle to maximise counts and minimise drift.

### 3.4.3. Review of real-world casework data for GSR and gGSR

In most of the work undertaken in this thesis, when gGSR was examined it was collected under unrealistic conditions. This included manual discharge of disassembled ammunition through an aluminium holder and having a police officer with clean hands, firing multiple shots of the same ammunition through a relatively clean firearm, and GSR being collected from hands immediately post-firing. Although these methods were effective in collecting GSR and gGSR for analysis, it was not considered to representative of what would be seen in casework.

For the work undertaken in this chapter to be applicable, and this thesis more broadly, it was deemed necessary to determine the rate at which gGSR was found in casework and the number of particles found on a stub if gGSR were present.

Therefore, 10 cases analysed by Forensic Science SA from the 2017-2018 financial year were selected for review. In this review, the previously collected data was interrogated but the stubs were not re-analysed, and particles were not able to be manually reacquired, which introduces a limitation to any conclusions drawn from the analysis.

The data for the cases examined was collected using a Zeiss Evo 50 SEM with Oxford EDX system and INCA Aztec particle analysis software. The automated particle search system brightness and contrast settings were calibrated through use of a Gold/Cobalt/Rhodium (Au/Co/Rh) standard. A positive control for the Zeiss system, a synthetic particle standard (PLANO W. Plannet GmbH, Wetzlar, Germany, SPS-A521-2(27C)), consisting of accurately deposited particles of known sizes (1-5 µm) was analysed bracketing each one for quality control.

Twenty-six stubs were analysed from these 10 cases, each stub being from suspect hands where consistent or characteristic particles were found. Several blank samples and those negative for GSR were removed from the sample set. Of those remaining, 17 were positive for characteristic Pb/Ba/Sb GSR, and 9 had only consistent particles present. The data from these stubs were re-processed to look for particles containing Pb/Ba/Sb/Si, Pb/Ba/Si, Pb/Si. Ba/Si, in addition to existing classifications (of note, Pb/Ba/Si was an existing category).

The data for all of the Si-containing particles were then individually reviewed, comparing the spectra collected for these particles (through automatic particle searching) to spectra collected for silicon-containing particles from GSR samples collected from ammunitions found to contain glass frictionator. Specifically, the relative abundance of Si, Al and Na was used to determine whether it was possible that the particles were glass-containing. Some samples had several thousand Pb/Si or Ba/Si particles and it was impractical to review each one, and so were not included for several samples.

## 3.5. Results

### 3.5.1. Examination of Firework Particles and Populations

In this study, fifty-one stubs have been examined using automatic BSE-SEM-EDS particle searching. The first source of particles examined was fireworks. A summary of the results obtained from the particle searching software (excluding particles with low Z elements such as Al and Mg) is shown in Table 7.

**Table 7: Total number of selected particle types automatically categorised by software from *n* samples from fireworks with average 30 < Z < 82 by BSE-SEM-EDS.**

| | Components post display n=7 *(average number per stub)* | Surfaces <3 m away post display n=6 *(average number per stub)* | Technicians' Hands post display n=5 *(average number per stub)* | Observers' Hands n=2 *(average number per stub)* |
|---|---|---|---|---|
| **Characteristic of GSR** | | | | |
| **Pb/Ba/Sb** | 0 (0) | 0 (0) | 0 (0) | 0 (0) |
| **Pb/Ba/Ca/Si/Sn** | 0 (0) | 0 (0) | 0 (0) | 0 (0) |
| **Total characteristic** | 0 (0) | 0 (0) | 0 (0) | 0 (0) |
| **Consistent with GSR** | | | | |
| **Pb/Ba** | 3 (0.4) | 5 (0.8) | 21 (4.2) | 0 (0) |
| **Ba/Sb** | 2 (0.3) | 9 (1.5) | 4 (0.8) | 0 (0) |
| **Pb/Sb** | 0 (0) | 1 (0.2) | 0 (0) | 0 (0) |
| **Ba/Ca/Si** | 18 (2.6) | 75 (12.5) | 113 (22.6) | 4 (2.0) |
| **Ba/Al** | 17 (2.4) | 27 (4.5) | 66 (13.2) | 1 (0.5) |
| **Ti/Zn** | 0 (0) | 0 (0) | 0 (0) | 0 (0) |
| **Total consistent** | 40 (5.7) | 117 (19.5) | 204 (40.8) | 5 (2.5) |
| **Commonly associated with GSR (Single Element)** | | | | |
| **Sb** | 0 (0) | 21 (3.5) | 46 (9.2) | 1 (0.5) |
| **Ba** | 254 (36.3) | 309 (51.5) | 329 (65.8) | 20 (10.0) |
| **Pb** | 164 (23.4) | 128 (2.3) | 582 (116.4) | 4 (2.0) |
| **Total commonly associated** | 418 (59.7) | 458 (76.3) | 957 (191.4) | 25 (12.5) |
| **Other Particles** | | | | |
| **Ba/S** | 464 (66.3) | 449 (74.8) | 2298 (459.6) | 122 (61.0) |
| **Cu/Zn** | 2 (0.3) | 3 (0.5) | 27 (5.4) | 55 (27.5)) |
| **Fe** | 619 (88.4) | 12974 (2162.3) | 5511 (1102.2) | 693 (346.5) |
| **Ni** | 129 (18.4) | 6 (1.0) | 61 (12.2) | 51 (25.5) |
| **Cu** | 8155 (1165.0) | 1821 (303.5) | 368 (73.6) | 36 (18.0) |
| **K/Cl** | 9 (1.3) | 53 (8.8) | 11130 (2226.0) | 4619 (2309.5) |
| **La/Ce** | 85 (12.1) | 2454 (409.0) | 94 (18.8) | 7 (3.5) |
| **Ti** | 33 (4.7) | 6 (1.0) | 321 (64.2) | 77 (38.5) |
| **Bi** | 85 (12.1) | 288 (48.0) | 71 (14.2) | 29 (14.5) |
| **Zn** | 816 (116.6) | 1151 (191.8) | 22 (4.4) | 9 (4.5) |
| **Zr** | 0 (0) | 3 (0.5) | 215 (43.0) | 12 (6.0) |
| **Sr** | 0 (0) | 6 (1.0) | 785 (157.0) | 1 (0.5) |
| **Unclassified** | 10022 (1431.7) | 19768 (3294.7) | 4569 (913.8) | 468 (234.0) |
| **Total** | 22666 (3238.0) | 45468 (7578.0) | 27201 (5440.2) | 6476 (3238.0) |
| **Classified** | 12651 (1807.2) | 25701 (4283.5) | 22647 (4529.4) | 6008 (3004) |

Of the twenty stubs representing residues on hands of firework technicians and observers, direct sampling of firework components and samples taken from surfaces at the venue, over 100 000 particles were detected and over 67 000 of these were classified by the software.

Within the firework particle population, very few particles were automatically detected containing Si. However, software classifications can be incorrectly assigned for a variety of reasons, and automatic classifications are not sensitive to minor concentrations of elements of interest. For this reason, over 3000 particles were manually reviewed. Only a small proportion were found to contain more than a trace of Si, and no particles were observed to have a composition that may indicate that the particle contained glass (i.e., Si with Al, Ca and Na for soda lime glass or Si with Al and Na for borosilicate glass). Although the particle searching parameters were not optimised to identify particles of glass, glass particles associated with heavier elements such as Pb, Ba, Sb, Zn, Cu or La/Ce would have been detected by these parameters. Therefore, based on observations thus far, fireworks do not appear to be capable of generating particles that would resemble glass-containing gunshot residue (gGSR), that is, glass particles encrusted with deposits containing Pb and/or Sb and/or Ba.

The most prevalent particle populations were observed from Ba/S, Fe, Cu, Zn, and La/Ce. No characteristic particles were classified by the software and 0.4% were identified as consistent with GSR. When single element particles were included, 2.5% of the particles were classified as at least commonly associated with GSR.

At the population level, although a small percentage of the particles examined were categorized by the particle recognition software as ‘consistent’ composition, the presence of many particles containing Fe, Cu, Zn, lighter flint (La/Ce) or Bi tend to point to sources of particulate matter other than a firearm. Compounds containing Fe, Cu, Zn and Bi have known uses in fireworks as pigments and effects. Although the observed concentrations Fe and K/Cl on technicians’ hands were observed to be very high (20% and 41%, respectively), there was a lower than expected number of particles containing elements frequently observed in the international studies [203-218], such as Sr (3%), Cr (<1%), Bi (<1%), Zn (<0.1%) and As (0 particles observed), which would have been identified by particle searching.

La and Ce are often found on hands because they are found in lighter flint, which smokers are regularly exposed to. However, in this study all the individuals who were sampled reported being non-smokers. The particles were also found on firework components and on surfaces adjacent to the display, not only on the hands of technicians and observers. This indicates that fireworks may contain their own source of La/Ce particles, possibly associated with the fuse wiring of the fireworks.

Some individual particles do show some similarities to GSR. As an example, a particle that appears to be smaller than 10 µm, rounded, and to be an agglomeration of several distinct phases is shown in Table 8. The particle has a relatively homogenous structure containing Ba and S, with inclusions of other elements including Al, Ca, Pb and Si. Trace levels of Fe and Mg were also observed but not in high enough concentration to be mapped using SEM-EDS. However, Ba particles with more than a trace of S are known to have sources other than from a firearm, and the current ASTM guidelines advise caution when interpreting these particles.

A review of the captured images and spectra of the individual particles was undertaken. From this, it was observed that most particles with composition consistent with GSR had particle morphologies not typical of particles from a firearm source, either appearing angular, flaky or layered, and not appearing to be a product of condensation. The few particles observed in this study to have rounded, condensation-like morphology, which is consistent with GSR, tended to have Fe as the major component. It was determined that the combination of the population containing particle compositions rarely found in GSR and the atypical morphologies would mean that it is highly unlikely that a trained GSR examiner would identify these particles as GSR. This suggests that exposure to fireworks is not likely to affect the $A_B$ and thus B values (Figure 7) for GSR evidence evaluation.

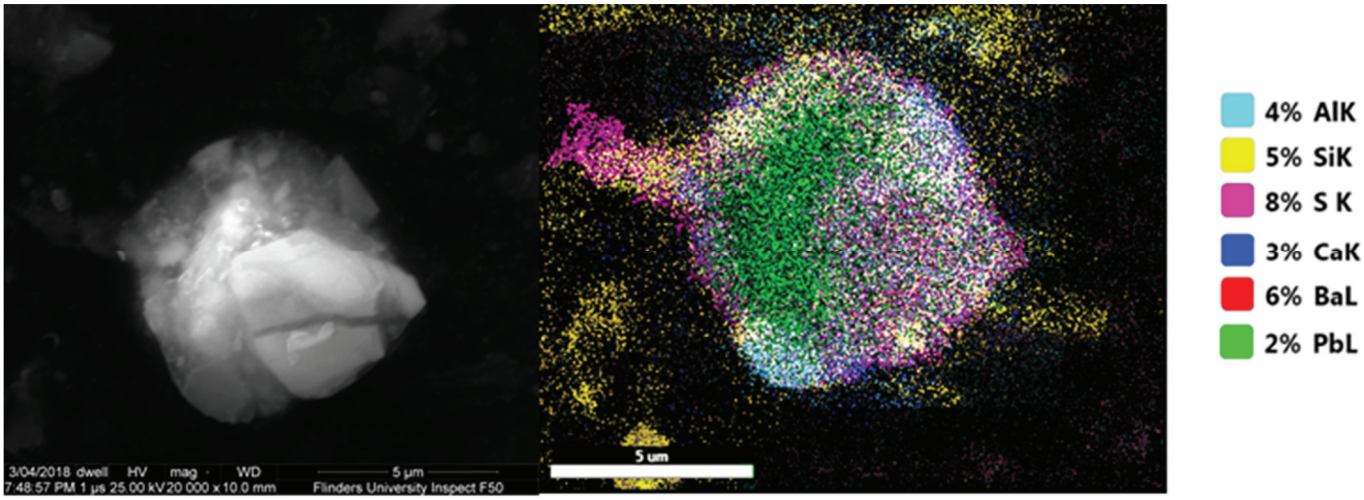


**Figure 10: Secondary electron image (left) and an elemental map (right) of a 'Pb/Ba' particle containing Pb, Ba, Ca, Si, Al, and S**

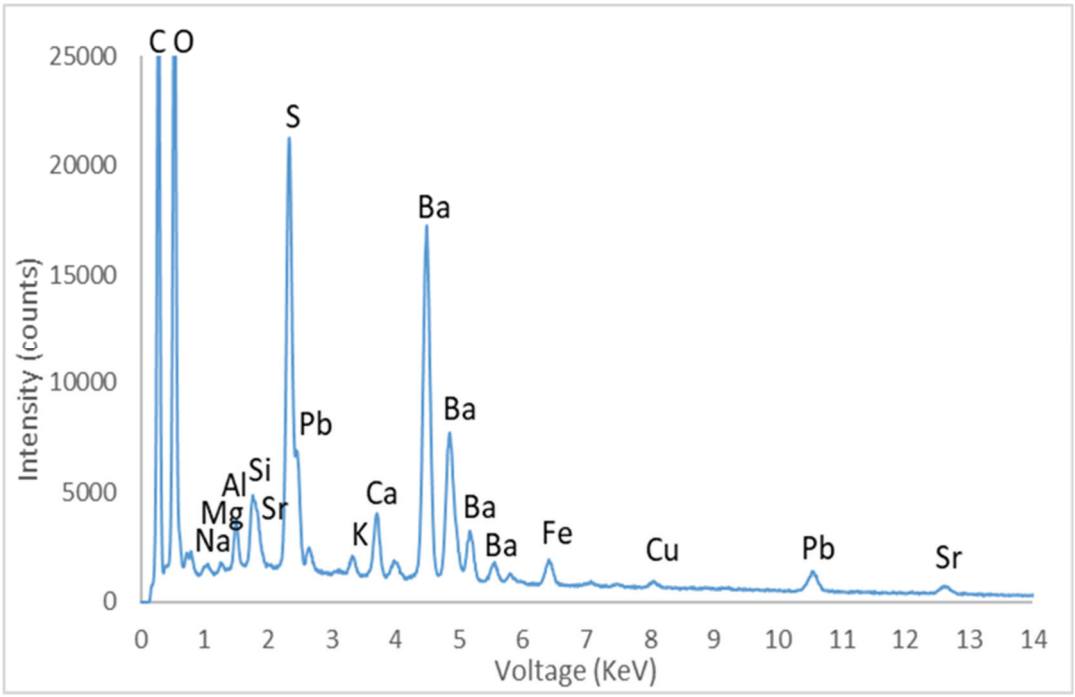


**Figure 11: EDS spectrum showing elements detected in the particle shown in Figure 10, which included low levels of Mg and Al**

The most common type of particle identified in the survey of hands of firework technicians contained K/Cl, with more than 40% of particles from hands being identified as such. This was expected, as potassium perchlorate ($KClO_4$) is used in large quantities in fireworks as an oxidising agent and a chlorine donor [234]. A sample with an extremely high K/Cl particle count is likely to have arisen from a non-firearm source, as match particles also contained many particles containing K and Cl (see Figure 19).

A Mg-Al alloy called magnalium is used in fireworks formulations to improve the brightness of firework colours [234]. Since Mg is not frequently found in ammunition primer mixes, finding these two elements in major or minor concentrations within a particle may indicate that fireworks were the source of the residue [221]. Magnesium and Al have low atomic numbers, and thus a low backscatter signal. Therefore, particles primarily composed of these elements would be filtered out by GSR particle-searching methods used in forensic laboratories. This was the case with the software used this work. A manual review of 1000 of the firework particles classified under other categories was undertaken; 5.7% of particles were found to contain Mg and Al *inter alia* (Table 8). A typical spectrum demonstrating this composition is shown in Figure 11, which depicts the composition of the particle shown in Figure 10.

**Table 8: Results of a manual review of 1000 fireworks particles for magnalium indicators. Particles were identified using BSE-SEM-EDS GSR particle searching.**

| Category | Number observed |
|---|---|
| Al + Mg major | 2 |
| Al + Mg minor | 3 |
| Al major, Mg minor | 1 |
| Al major Mg trace | 4 |
| Mg major Al minor | 1 |
| Al minor Mg trace | 2 |
| Mg minor, no Al | 1 |
| Mg + Al Trace (more Al) | 14 |
| Mg + Al Trace (more Mg) | 14 |
| Mg + Al Trace (~equal) | 15 |
| **Total** | **57** |

*'Major' concentration indicates that the peak was >50% of the height of the highest peak in the spectrum, 'minor' indicates a peak height 10-50% the height of the highest peak and 'trace' indicates a peak height <10% of the highest peak, classifications adapted from [119]*

Care must be taken by examiners who analyse a sample suspected to be of mixed firework/GSR composition. Although a firework particle population can be differentiated from GSR, a false-negative conclusion might be reached by an examiner if a few GSR particles, (especially from cartridges with two-component primers, were present within a sample heavily contaminated with fireworks residue, however the detection of gGSR particles would decrease the risk of such a conclusion being reached.

### 3.5.2. Examination of Nail Gun Particles and Populations

Explosive nail gun cartridges contain primer compositions that are the same as many two-component 0.22LR rimfire cartridges, leading to the formation of residues similar to GSR, which include Pb and Ba [159] and, in the cartridges used in this study, glass as a frictionator was also found to be present. Gevelot cartridges for a nail gun produced by Obo used three-component primers but that nail gun and its cartridges are no longer in production [159]. The glass used in Hilti cartridges appears, by SEM-EDS, to have a similar composition to many of the borosilicate glass frictionators reported in Chapter 4. This means that nail gun cartridges at least have the potential to form GSR-like particles, including gGSR-like particles.

Particles generated from the manual discharge were observed to contain Pb and/or Ba, some of which contained glass, as was expected. Some glass particles were also observed that had little or no

encrustation from the other primer elements, which was presumably due to the lower temperatures reached during discharge using this approach.

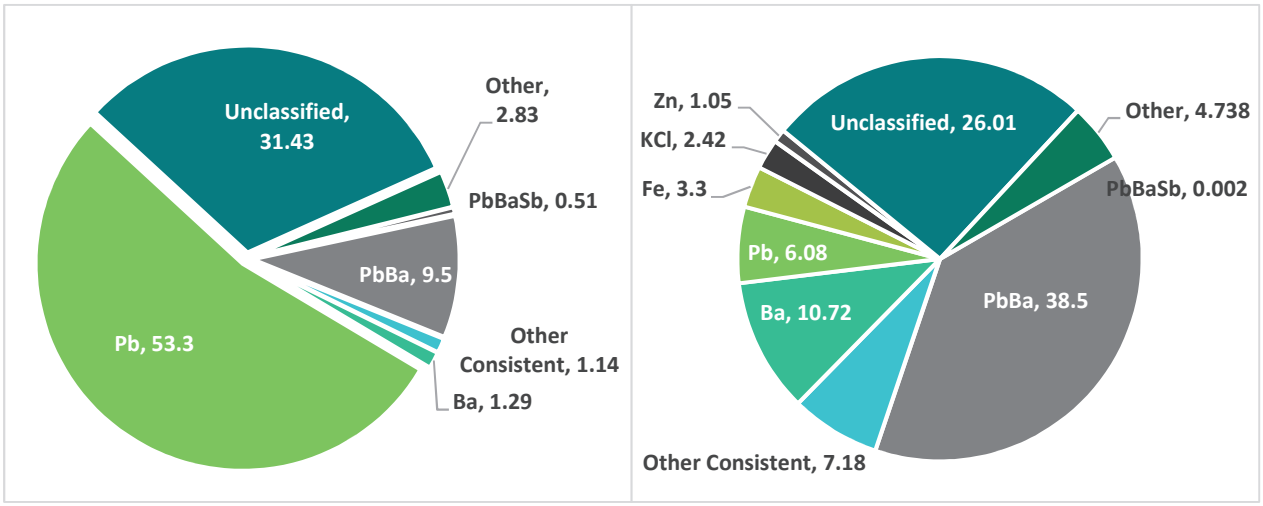


**Figure 12: A comparison of particle types observed (%) from GSR from two-component ammunition mixtures (left) caught in a PET collector (n=11) and particles from two-component nail gun residues (right) collected from hands (n=14)**

As nail gun cartridges and PMC Zapper ammunition both contain glass, the presence and characteristics of glass in residues from firearms and nail guns after conventional discharge were examined. Compared to GSR, residues from nail guns contained a higher proportion of particles containing Ba/Ca/Si; (Table 9 and Figure 12). A round, globular nail gun residue particle containing Pb, Ba, a small amount of Fe and several elements present in glass (Si, Na, Mg and Al) is shown in Figure 13, demonstrating the similarity between gGSR particles and particles from nail guns.

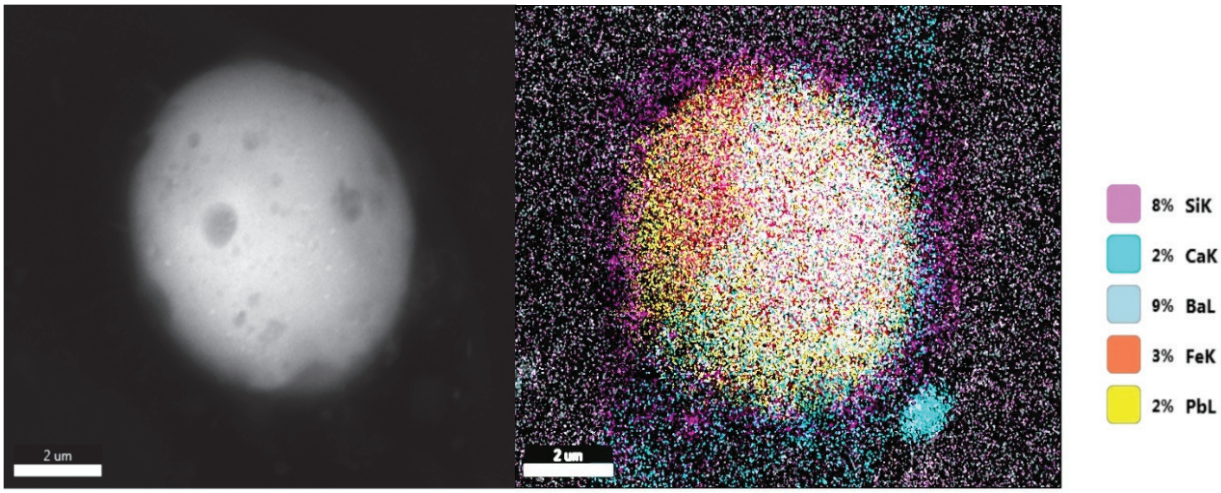


**Figure 13: Secondary electron image (left) and EDS elemental map (right) showing a Pb/Ba/Si/Ca particle from a nail gun.**

It was noticed that when a few of the Ba/Ca/Si particles from nail guns were examined, the Ca signal did not appear to be co-localised with the other glass elements (i.e., Si, Na, Al). This effect is observed in Figure 14, and may indicate an alternative source of Ca, such as calcium silicide.

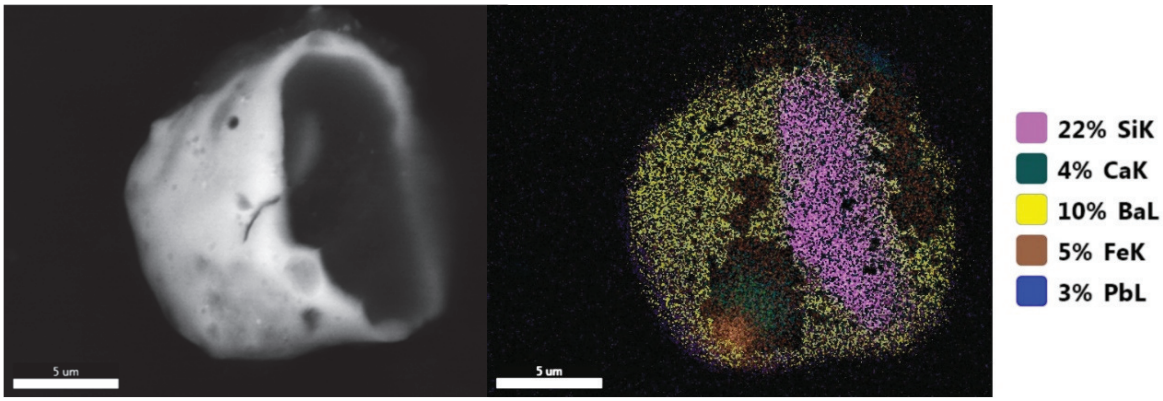


**Figure 14: Secondary electron image (left) and EDS elemental map (right) of a glass-containing nail gun particle with Ca and Fe inclusions, and an exposed glass surface**

Figure 14 shows one of these particles where part of the Si-rich 'core' is exposed within the encrustation of primer components (Pb/Ba) and a small amount of Fe. The darker region in Figure 14 (left) corresponds to the Si signal (right) from an exposed glass surface, and the bottom left part of the particle shows what appears to be a slight discolouration or shadow, which correlates with the Fe and Ca inclusions seen in Figure 14 (right).

**Table 9: Total number of selected particle types automatically categorised by software for particles from *n* samples from nail guns with average 30 < Z < 82 by BSE-SEM-EDS.**

| | Hands of nail gun operators n = 14 *(average number per stub)* | Direct sampling of nail gun residues n = 5 *(average number per stub)* | Sampling of surfaces associated with nail guns n = 4 *(average number per stub)* |
|---|---|---|---|
| **Characteristic of GSR** | | | |
| **Pb/Ba/Sb** | 1 (0.1) | 0 (0) * | 0 (0) |
| **Pb/Ba/Ca/Si/Sn** | 0 (0) | 0 (0) | 0 (0) |
| **Total characteristic** | 1 (0.1) | 0 (0) * | 0 (0) |
| **Consistent with GSR** | | | |
| **Pb/Ba** | 21170 (1512.1) | 8595 (1719.0) | 7157 (1789.3) |
| **Ba/Sb** | 1 (0.1) | 0 (0) | 0 (0) |
| **Pb/Sb** | 1 (0.1) | 0 (0) | 0 (0) |
| **Ba/Ca/Si** | 3926 (280.4) | 514 (102.8) | 670 (167.5) |
| **Ba/Al** | 25 (1.8) | 4 (0.8) | 0 (0) |
| **Ti/Zn** | 0 (0) | 0 (0) | 0 (0) |
| **Total consistent** | 25123 (1794.5) | 9113 (1822.6) | 7827 (1956.8) |
| **Commonly associated with GSR (Single Element)** | | | |
| **Sb** | 1 (0.1) | 1 (0.2) | 0 (0) |
| **Ba** | 5893 (420.9) | 764 (152.8) | 637 (159.3) |
| **Pb** | 3344 (238.9) | 2516 (503.2) | 4361 (1090.3) |
| **Total commonly associated** | 9238 (659.9) | 3281 (656.2) | 4998 (1249.5) |
| **Other Particles** | | | |
| **Ba/S** | 301 (21.5) | 59 (11.8) | 22 (5.5) |
| **Cu/Zn** | 114 (8.1) | 21 (4.2) | 1 (0.3) |
| **Fe** | 1814 (129.6) | 901 (180.2) | 266 (66.5) |
| **Ni** | 48 (3.4) | 7 (1.4) | 0 (0) |
| **Cu** | 229 (16.4) | 14 (2.8) | 4 (1.0) |
| **K/Cl** | 1329 (94.9) | 37 (7.4) | 2 (0.5) |
| **La/Ce** | 9 (0.6) | 5 (1.0) | 1 (0.3) |
| **Ti** | 130 (9.3) | 89 (17.8) | 44 (11.0) |
| **Sn** | 64 (4.6) | 10 (2.0) | 5 (1.3) |
| **Bi** | 16 (1.1) | 1 (0.2) | 0 (0) |
| **Zn** | 576 (41.1) | 431 (86.2) | 195 (48.8) |
| **Zr** | 62 (4.4) | 45 (9.0) | 15 (3.8) |
| **Sr** | 6 (0.4) | 2 (0.4) | 1 (0.3) |
| **Unclassified** | 14304 (1021.7) | 7348 (1469.6) | 7103 (1775.8) |
| **Total** | 54993 (3928.1) | 21901 (4380.2) | 21186 (5296.5) |
| **Classified** | 40689 (2906.4) | 14553 (2910.6) | 14083 (3520.8) |

**There were 2 particles initially flagged as Pb/Ba/Sb, but excluded upon reacquisition, as they were not found to contain Sb*

Both compositional and morphological information could be gained from the whole cartridge when the cartridges were discharged with a nail gun. The particle counting results shown in Table 9 are a summary of the particles observed from usage of the nail gun.

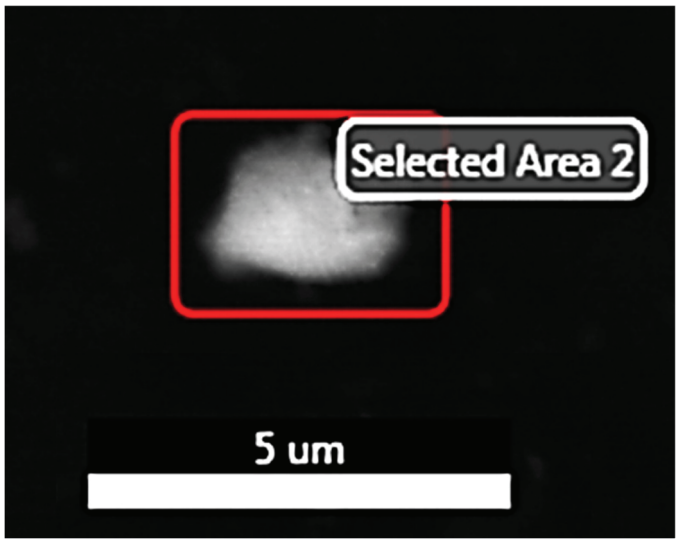


**Figure 15: Three-component Pb/Ba/Sb particle as observed from the hands of an individual who had used a Hilti powder actuated nail gun**

A single particle that contained Pb, Ba and Sb was observed on a GSR stub from one volunteer, representing 0.002% of all particles observed from the hands of individuals after using the nail gun. Data for this particle were manually reacquired, and while it was confirmed to included Pb, Ba and Sb, it did not have a typical morphology for GSR, instead appearing as a flake (Figure 15). The Hilti primers used are not known to contain Sb, and very few particles containing Sb were observed within this particle population. The origin of Sb-containing particles observed on hands of those who had recently used a nail gun, especially the particle containing Sb, Ba and Pb, and the mechanism by which these particles arrived on the stubs remains unknown. No three-component particles were flagged when the nail gun itself was stubbed.

The existence of this single Pb/Ba/Sb particle does highlight the dangers of identifying a residue as GSR based on the presence of a single particle. An experienced GSR examiner should be prompted, upon observing just one 3-component particle amongst a population of thousands of consistent particles, to think of other possible sources of the particles, or another explanation for their observations. A logical assessment of the evidence given the circumstances under investigation and considering both composition and morphology is imperative for distinguishing particles originating from firearms from those derived from occupational sources.

More than 30% of the particles collected from direct sampling of the nail gun, from the hands of the operators and collected from surfaces adjacent to nail gun usage were classified as 'consistent' with GSR. Of these particles, the large majority were Pb/Ba, as expected. Two particles were indicated to be characteristic Pb/Ba/Sb, but when manually reviewing and reacquiring the data, the particles were not found to contain Sb. Based on the limited data observed, the particles collected from hands tended to be smaller than those sampled directly from the nail gun, and approximately 20% of the particles with 'consistent' elemental compositions were round or globular. The majority of 'consistent' particles on hands were flaky in appearance or larger than is typical for GSR (>10 µm) as would be expected given the short delay between discharge and hand sampling. The particles observed by directly sampling the nail gun with compositions 'consistent' with GSR tended to have a flaky or angular appearance, and often contained another element with an equal or higher signal than the Pb and Ba, or Ba, Ca and Si. For example, the particles collected from surfaces surrounding the nail's impact with timber tended to be large Fe flakes that had regions including small Pb, or Pb and Ba nodules. Very few particles from any of the other 'consistent' particle types were observed on hands, the gun itself, or on the 'target.'

Particles collected from hands that had fired Hilti nail gun cartridges were compared to the range of particles ejected from the muzzle of a firearm loaded with PMC Zapper 0.22 calibre rimfire ammunition, which is known to have a primer that contains Pb, Ba and glass, but no Sb; results (as %) are shown in Figure 12. It can be seen that even though the ammunition does not contain Sb in the primer, firearm discharge results in a higher proportion of particles containing Pb/Ba/Sb compared to nail gun discharge. This may have been due to some combination of mixing between primer and projectile components [233, 235] and/or the weapon-memory effect [130-132, 233, 236, 237] despite more than 30 shots of PMC Zapper ammunition being fired through the barrel prior to sample collection. However, it is important to note that the Sb would be less likely to be observed on hands than from the muzzle discharge, as the muzzle emission would have the greatest opportunity for mixing between primer and projectile components, and perhaps have greater opportunity to mix with particulate matter from previous firings [236].

The ammunition used to generate GSR was traditional and thus contained Pb in both the primer and projectile. There was therefore a higher proportion of Pb-only particles than Pb/Ba or Ba-only particles observed in discharge from the ammunition cartridges compared to a higher proportion of Pb/Ba-containing particles than Pb-only particles observed from the nail gun cartridges. This comparison also held true with regards to particles collected from the nail gun 'muzzle' or from the target into which nails were discharged. There was not a high degree of variance in the particle types and their relative

proportions between individual stubs used to collect nail gun residues therefore the populations on individual stubs did not differ greatly from the aggregated data presented in Figure 12. We have not studied other ammunition brands extensively to determine whether the particle population arising from PMC Zapper ammunition is representative, however, it would be worth investigating in future studies.

Other than the presence of multiple Pb/Ba/Sb particles, there does not appear to be a definitive 'signature' that can be used on a particle by particle basis to differentiate GSR from rimfire ammunition with residues from cartridge-actuated nail guns, even when glass-containing particles are under consideration. Glass frictionators from rimfire ammunition are made from either borosilicate glass or soda lime glass [202], and the frictionator observed from Hilti cartridges was borosilicate glass. In Australia, elemental analysis of the glass in a residue may prove fruitful, as Hilti and Ramset nail gun cartridges [159] have both been observed to usually produce heavy metal-encrusted borosilicate glass particles. Therefore, the presence of soda lime glass in particles indicates that they are unlikely to have originated from a Hilti nail gun. We have not been able to carry out analysis of frictionator from other nail gun cartridge brands to determine whether that differentiation holds true beyond Australia. If a higher level of elemental analysis of the frictionator is carried out (for example by using time of flight-secondary ion mass spectrometry [202]) discrimination within the two broad glass types is possible, but then an exemplar of the glass from the particular cartridge (or a spent cartridge) would be necessarily analysed alongside.

### 3.5.3. Examination of Match Particles and Populations

Literature suggests that the strike surface of a matchbox can contain sand or glass as the friction-producing agent [238]. After lighting a whole box of matches, the strike surface of the matchbox was stubbed. The stub, when analysed *via* SEM-EDS, showed very few particles composed primarily of Si. This may indicate that they are not easily removed from the strike surface. Particles containing Si with other elements were few, but one such particle is shown in Figure 16. From the elemental map, it can be seen that P, K, and Cl are co-located in the deposit encrusting the Si. Al and other elements commonly associated with glass (especially Na, Mg, and Ca) were not detected in the Si-rich regions of the particle, indicating that the Si was not from a glass but may have been from a mineral such as quartz. However, even if some match brands other than those used in this study include glass in their products, the lack of Pb, Ba and Sb in matches means that the glass-containing particles would not be mistaken for gGSR arising from conventional Pb-containing primers and the abundance of elements

such as K and Cl in the particle population would not suggest the involvement of Pb-containing and Pb-free ammunition sources.

No characteristic particles were observed from the investigation of match residues as shown in Table 10. Twenty-four 'consistent' particles were observed, twenty-three of which contained Ti and Zn, which is a consistent particle type from Sintox ammunition [3]. However, this represented a very small percentage of the total particle population (0.12%). As expected, particles from hands resembled those collected by direct sampling, but fewer and smaller particles were collected.

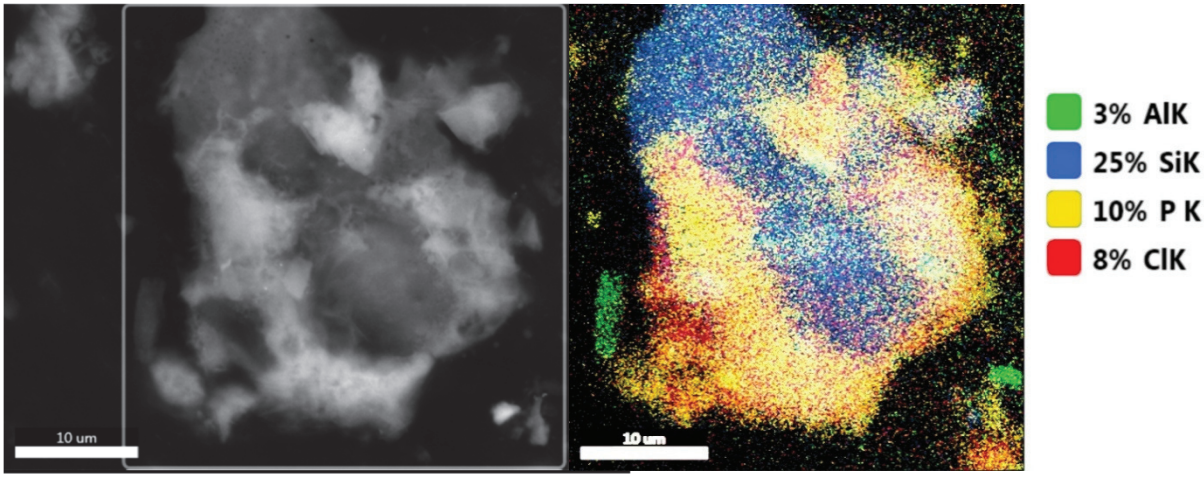


**Figure 16: SEM image and an elemental map of a Si containing particle (presumably $SiO_2$) from matches, encrusted with Al, P, K and Cl.**

Morphologically, the particles produced from matches were similar to GSR particles, which can be seen in Figure 17. There tended to be a majority of round and globular particles and fewer angular or flaky particles than produced by the residues arising from the other sources. Therefore, in GSR case investigations it is possible that match particles on a person's hands may be confused with HMF GSR, but these particles are likely to be associated with much larger numbers of particles containing K, Cl, Ca, Fe, Ti, Zn and Zr, all of which would alert the examiner to the possibility that the source of these particles is not a firearm.

**Table 10: Absolute number (n) and frequency (%) of selected particle types automatically categorised by Magnum software for particles from matches with average 30 < Z < 82 by BSE-SEM-EDS.**

| | Hands of people after striking matches n = 3, (average number per stub) | Surfaces associated with match lighting n = 5, (average number per stub) |
|---|---|---|
| **Characteristic of GSR** | | |
| **Pb/Ba/Sb** | 0 (0) | 0 (0) |
| **Pb/Ba/Ca/Si/Sn** | 0 (0) | 0 (0) |
| **Total characteristic** | 0 (0) | 0 (0) |
| **Consistent with GSR** | | |
| **Pb/Ba** | 0 (0) | 0 (0) |
| **Ba/Sb** | 0 (0) | 1 (0.2) |
| **Pb/Sb** | 0 (0) | 0 (0) |
| **Ba/Ca/Si** | 0 (0) | 0 (0) |
| **Ba/Al** | 0 (0) | 0 (0) |
| **Ti/Zn** | 0 (0) | 23 (4.6) |
| **Total consistent** | 0 (0) | 24 (4.8) |
| **Commonly associated with GSR (Single Element)** | | |
| **Sb** | 2 (0.7) | 0 (0) |
| **Ba** | 1 (0.3) | 2 (0.4) |
| **Pb** | 1 (0.3) | 1 (0.2) |
| **Total commonly associated** | 4 (1.3) | 3 (0.6) |
| **Other Particles** | | |
| **Ba/S** | 25 (8.3) | 9 (1.8) |
| **Cu/Zn** | 13 (4.3) | 0 (0) |
| **Fe** | 19 (6.3) | 146 (29.2) |
| **Ni** | 3 (1) | 0 (0) |
| **Cu** | 11 (3.7) | 0 (0) |
| **K/Cl** | 172 (57.3) | 11531 (2306.2) |
| **La/Ce** | 0 (0) | 0 (0) |
| **Ti** | 0 (0) | 13 (2.6) |
| **Sn** | 8 (2.7) | 0 (0) |
| **Bi** | 3 (1) | 13 (2.6) |
| **Zn** | 6 (2) | 1211 (242.2) |
| **Zr** | 3 (1) | 2500 (500) |
| **Sr** | 1 (0.3) | 0 (0) |
| **Unclassified** | 95 (31.7) | 3344 (668.8) |
| **Total** | 749 (149.8) | 18930 (3786.0) |
| **Classified** | 654 (130.8) | 15586 (3117.2) |

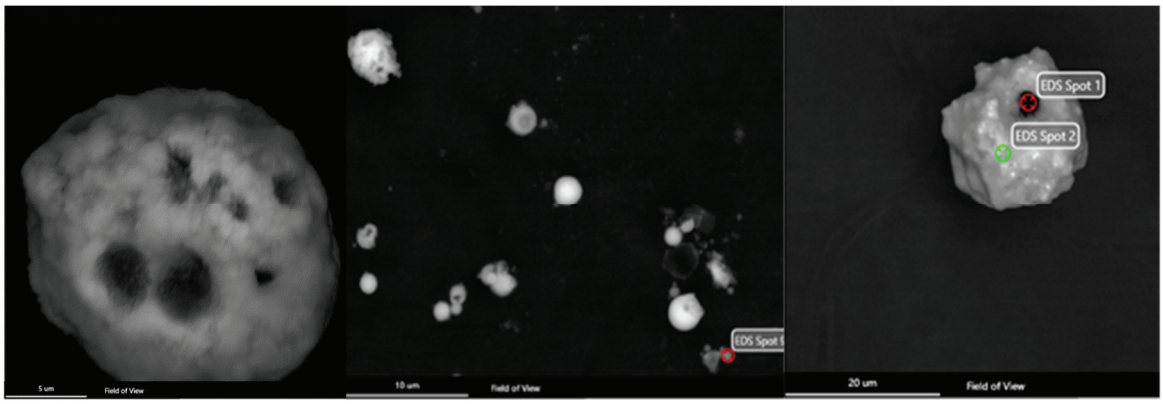


**Figure 17: SEM images showing round and globular particles sourced from matches**

### 3.5.4. Examination of Brake Pad Particles and Populations

Several previous literature studies have highlighted the possibility for characteristic three-component particles to be produced from brake pads [121, 123, 201, 224]. In this study, loose particles were collected from 12 used brake pads found to contain Ba and Sb. The brake pads were stubbed to collect residues off their surfaces, and the particles detected were manually reviewed and reacquired, to determine whether there were particles present similar to GSR.

Particles observed were angular or flaky and not spheroidal or globular, meaning that they exhibited morphological characteristics dissimilar to GSR. GSR particles are formed *via* condensation, from the gasses produced due to the extreme temperatures and pressures during the discharge of a firearm [22]. While automotive braking can generate temperatures in excess of 500 °C under extreme conditions, usual temperatures are in the range of 40–250 °C, at atmospheric pressure [239]. The observed morphology of the particles found from brake pads, and the distinct lack of spheroidal or globular particles, suggest that temperatures and pressures attained during typical braking are insufficient to replicate the formation of the characteristic morphology of particles seen in GSR.

An exemplar brake pad particle is shown in Figure 18, with the left image showing the crumbled morphology seen from many brake pad particles, and the right side showing elemental distribution of the particles. The morphology of the particles shown in Figure 18 are more consistent with particles arising from abrasion rather than through random condensation of elements from a gaseous mixture, as is thought to take place when GSR are produced.

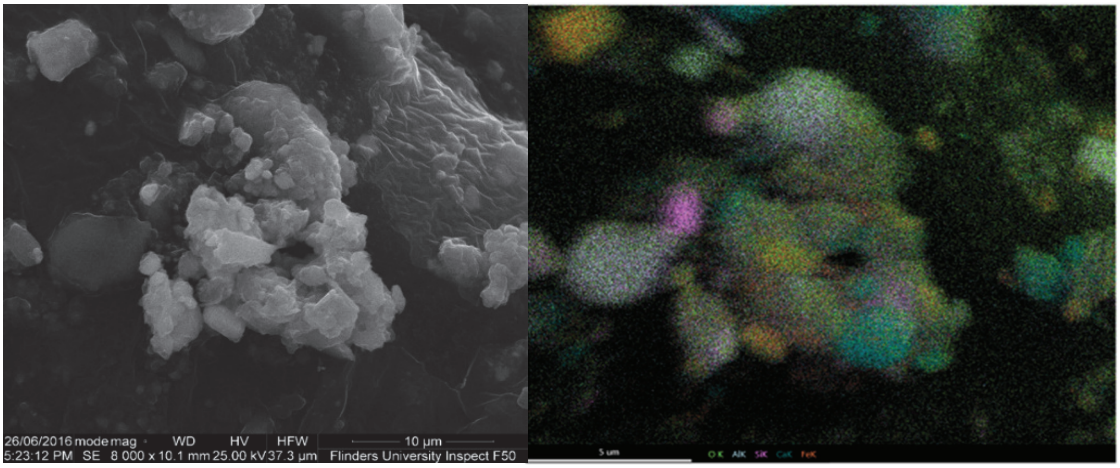


**Figure 18: A SE image of a typical particle from a brake pad (left) and an elemental map showing the composition of that particle (right)**

Table 11 shows particles detected using SEM-EDS from brake pads, hands and wheel rims. The automated particle screening software detected one 'characteristic' Pb/Ba/Sb particle from a direct sample from a brake pad, but upon manual reacquisition, it was discovered that the result was caused by a lead particle that was resting on a larger particle containing both Ba and Sb, amongst other elements, rather than from a single particle containing all three elements.

No characteristic GSR particles were found during this survey of particles from brake pads. However, particles containing Ba and Sb, or just one of those elements, were readily observed. Particles observed from all braking-related sources had both compositional and morphological inconsistencies with GSR; the particles instead being composed of many elements and in many particles classified as Ba or Pb/Ba, elements not commonly associated with GSR were more abundant than the Ba and/or Pb signal. Particle clusters were often found in brake pad samples, appearing to be conglomerates of smaller particles. These particles were not rounded, and the compositional variation between particles from the same pads and different pads was low.

There was a relatively low occurrence of Pb particles found on brake pads, with 0.12% of all particles from direct sampling detected as Pb, and the combined frequency of all particle types containing lead (Pb, Pb/Ba, Pb/Sb, Pb/Sn, Pb/Ti, Pb/Ca, Pb/Cl/Br and Pb/Sb/Sn) was 0.47% of all detected particle from direct sampling. Pb-containing particles were slightly less frequent on hands, with 0.32% of all particles classified as Pb-containing.

**Table 11: Total number of selected particle types automatically categorised by software for particles from *n* samples from automotive/brake pad samples with average 30 < Z < 82 by BSE-SEM-EDS, and average number of particles per stub (Total/*n*).**

| | Direct sampling from used brake pads (n=12) *(average number per stub)* | Sampling from hands of individuals who have recently removed brake pads (n=11) *(average number per stub)* | Sampling from wheel rims of parked cars (n=22) *(average number per stub)* |
|---|---|---|---|
| **Characteristic of GSR** | | | |
| **Pb/Ba/Sb** | 0* (0) | 0 (0) | 0 (0) |
| **Pb/Ba/Ca/Si/Sn** | 0 (0) | 0 (0) | 0 (0) |
| **Total characteristic** | 0* (0) | 0 (0) | 0 (0) |
| **Consistent with GSR** | | | |
| **Pb/Ba** | 566 (47.2) | 8 (0.7) | 23 (1.0) |
| **Ba/Sb** | 9374 (781.2) | 210 (19.1) | 3879 (176.3) |
| **Pb/Sb** | 2 (0.2) | 19 (1.7) | 0 (0) |
| **Ba/Ca/Si** | 977 (81.4) | 1536 (139.6) | 2358 (107.2) |
| **Ba/Al** | 34 (2.8) | 41 (3.7) | 56 (2.5) |
| **Ti/Zn** | 0 (0) | 0 (0) | 0 (0) |
| **Total consistent** | 10953 (912.8) | 1814 (164.9) | 6316 (287.1) |
| **Commonly associated with GSR (Single Element)** | | | |
| **Sb** | 207 (17.3) | 48 (4.4) | 19 (0.9) |
| **Ba** | 2530 (210.8) | 1064 (96.7) | 10722 (487.4) |
| **Pb** | 10 (0.8) | 352 (88.0) | 61 (2.8) |
| **Other Particles** | | | |
| **Ba/S** | 9386 (782.1) | 4399 (399.9) | 9769 (444.0) |
| **Cu/Zn** | 659 (54.9) | 309 (28.1) | 49 (2.2) |
| **Fe** | 45458 (3788.2) | 68064 (6187.6) | 97594 (4436.1) |
| **Ni** | 1 (0.1) | 194 (17.6) | 2 (0.1) |
| **Cu** | 2429 (202.4) | 1466 (133.3) | 57 (2.6) |
| **K/Cl** | 19 (1.6) | 176 (16.0) | 1 (0.0) |
| **La/Ce** | 2 (0.2) | 39 (3.5) | 23 (1.0) |
| **Ti** | 1060 (88.3) | 679 (61.7) | 293 (13.3) |
| **Sn** | 1010 (84.2) | 233 (21.2) | 51 (2.3) |
| **Bi** | 33 (2.8) | 10 (0.9) | 629 (28.6) |
| **Zn** | 78 (6.5) | 1627 (147.9) | 745 (33.9) |
| **Zr** | 1751 (145.9) | 458 (41.6) | 585 (26.6) |
| **Sr** | 2 (0.2) | 1 (0.1) | 2 (0.1) |
| **Unclassified** | 10618 (884.8) | 26120 (2374.5) | 18759 (852.7) |
| **Total** | 89240 (7436.7) | 115314 (10483) | 148211 (6736.9) |
| **Classified** | 78622 (6551.8) | 89194 (8108.5) | 129452 (5884.2) |

** One sample registered a false positive, detecting a singular 3-component particle. On review, it was discovered to be a lead particle sitting on a flake that contained antimony and barium, amongst other elements*

Torre *et al.* in their study in 2002 [123] detected Pb in many particles collected from automotive parts and workers who handle them. In this study, very few particles containing Pb were found on either component (brake pads and wheel rims), or the hands of individuals who had touched them. It would appear that the environmental Pb-reduction initiatives introduced after the work of Torre *et al.* that were aimed at minimizing the usage of lead in automotive components has had an impact on the composition of dust derived from brake pads. This does not mean that Pb couldn't be found on real-world hand samples, as there are still numerous Pb sources associated with automotive. Laflèche *et al.* in their more recent study [201] found no lead in currently commercially available brake pads in Ontario, Ottawa, Canada, which is consistent with the findings from this work.

Particles identified as consistent with GSR by the software were all detected in low to very low frequencies (<2% of detected particles), except for Ba/Sb particles, which were more frequently observed, making up 10% of all detected particles from direct sampling, 2.6% of particles from wheels, and 1.6% of all particles detected from hands. A manual review of a sample of the elemental data and images collected indicated that the majority of Ba/Sb particles would not be classified as being of firearm origin either based on morphology or the presence of elements not usually associated with firearm discharge. For example, one of the particles flagged as "consistent – Ba/Sb" in this study was found to contain Fe, Ti, K, S, Si, Cu, Al and Mg at similar or greater peak levels than Ba and Sb. These data are comparable to the results reported by Torre *et al.* [123] and Garafano *et al.*[121], who also frequently observed particles containing these elements.

Iron was a found on all sample stubs, with 50-70% of the particles detected containing Fe as a major component. This result is comparable with what was observed by Torre *et al.* [123], who found Fe to be present in all brake pad particles, frequently at a major level. The result observed in this study, however, grossly under-represents the true Fe content in the samples, as the particle searching was carried out under parameters that were intended to exclude Fe. Consequently, many particles containing Fe as a major element were classified as other particle types. This quantity of Fe is not generally observed in GSR particles, and in the absence of Pb/Ba/Sb particles, would be viewed with suspicion.

These results indicate that while samples collected from brake pads may result in a few false positive results through the software, a trained analyst would resolve the situation readily. This is in support of the conclusions previously drawn by Garafano *et al.* [121].

Pb-containing particles no longer appear to be a common component of brake-related dust in Australia, and any lead incorporated into the particles may originate from extraneous automotive

sources. The results of this study re-emphasise the importance of both thorough manual review and re-acquisition of EDS data produced by automated particle classification software, before evaluating the overall population of particles recovered in connection with an investigation. If this is undertaken, it is difficult to envisage scenarios in which brake dust could mistakenly be identified as GSR. On the other hand, scenarios that might lead to a false negative result are more plausible. For example, if a surface is sampled that contains a mixed deposit of brake pad dust and a few particles of GSR it is possible that an analyst would identify the obvious presence of the brake pad dust and mistakenly dismiss the GSR particles.

### 3.5.5. Comparison of Particles from Different Sources

Various automotive sources associated with brake linings were investigated for their potential to produce particles or particle populations that could not be reliably differentiated from particles sourced from firearm discharge. In this study, no characteristic particles were observed, and less than 5% of particles were classified as consistent with GSR. As part of the research described in this thesis, the data were analysed to search for glass-containing particles, and it was determined that neither glass nor glass-containing particles originated from brake linings and are therefore they not a source of particles that can be confused with gGSR.

It is important in the comparison of data to minimise the effects of extraneous variables; for the research described here comparing samples collected in a like manner is ideal. For most common GSR analyses, samples are taken from the hands of suspects or people who were alleged to be present during an incident. Therefore, a comparison of particle distribution from samples from hands for each of the four non-firearm sources examined in Tables 2, 4 and 5 and 7 is shown in Figure 19.

Results for a sample of GSR stubs, which were taken from the hands of police officers who had recently fired traditional three-component primed ammunitions, are shown for comparison (Figure 20). The Sr value of 6.1% is most likely an artefact of the weapon memory effect; the guns used in this research are used to fire lead-free ammunition from time to time. In the study of brake pads, it was found that samples taken from the hands of automotive workers have high proportions of particles primarily containing iron, and many particles containing sulfur, which are both usually associated with particle sources other than firearm discharges. Fewer Ba/S and Sb/S particles were observed in samples from nail guns and matches, and Sb/S was very rarely detected in firework samples. Ba can be used to produce a green colour [122, 240], and was found in significant amounts in the firework residues assessed in this study.

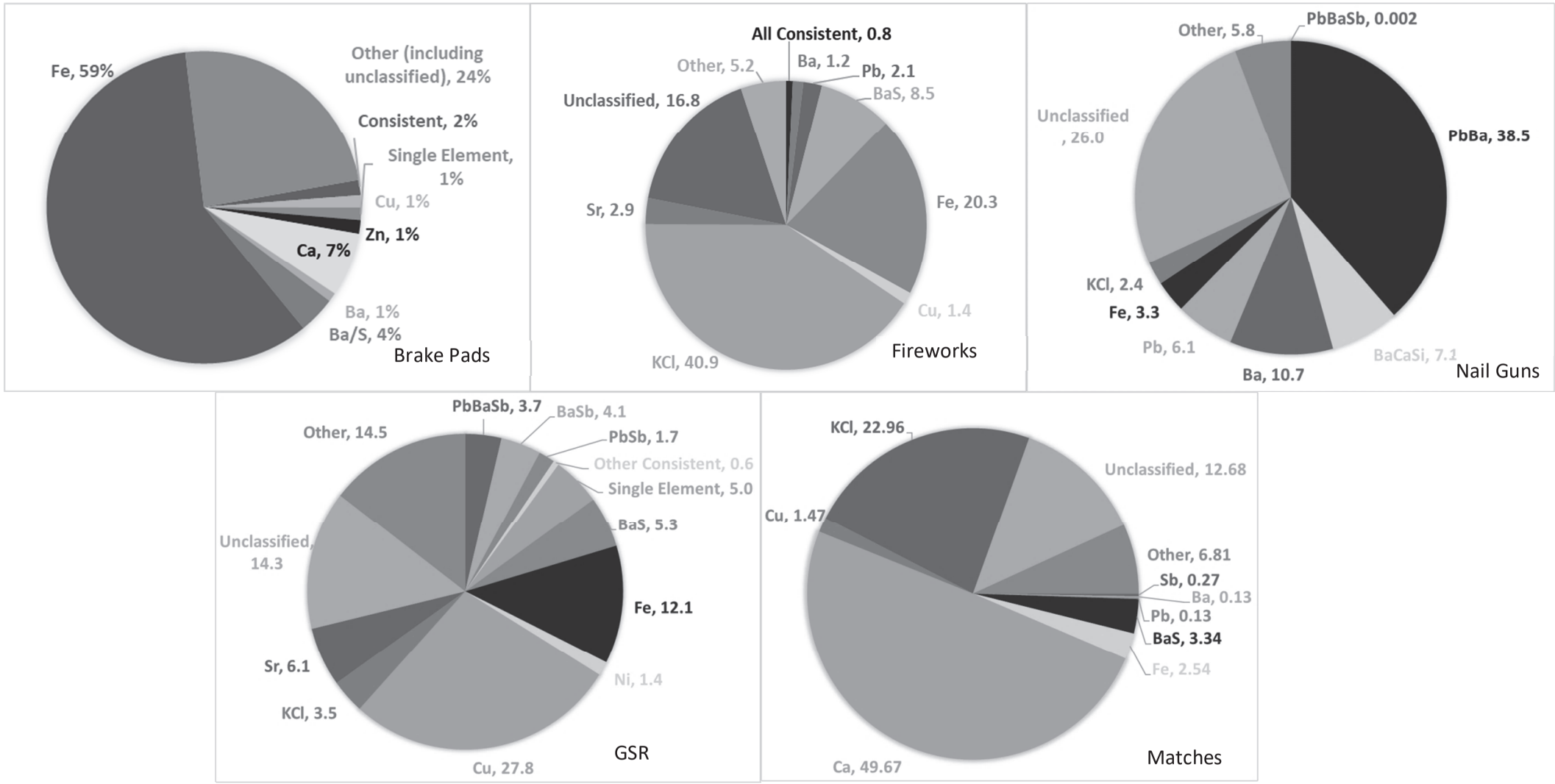


**Figure 19: A comparison of the distribution of particle classifications on hands after exposure to brake pads (top left), fireworks (top centre), a nail gun (top right), GSR (bottom left) and safety matches (bottom right)**

Matches did not appear to be capable of producing particles like traditional GSR and produced very few particles that could be considered compositionally like primer residue from non-toxic ammunition.

### 3.5.6. Review of real-world casework data for GSR and gGSR

Twenty-six stubs from 10 cases were examined as a part of this review. Figures of interest for Si-containing particles are shown in Table 12. Ba/Si was found on 25 out of the 26 stubs, and Pb/Si was found on all 26 stubs. Pb/Ba/Si was found on 18 of the 26 stubs.

Of the 18 stubs that contained Pb/Ba/Si particles, at least 1 particle on each was consistent with what we would see if the particle contained glass. It must be noted though, that there were possibly more glass containing particles, as most Si-containing particles were not able to be classified as 'consistent with gGSR' but would be most appropriately considered 'inconclusive' from the reviewed data. The conditions used routinely for the identification of GSR are not optimal for the collection of X-rays from Si, Na and Al. For the purposes of this investigation, particles that were inconclusive were considered inconsistent, in favour of presenting a conservative estimate in the results discussed below.

shows an exemplar of each type of relevant particle: 'consistent with gGSR', 'inconsistent with gGSR' and 'inconclusive'. It should be noted, however, that in the samples analysed in this work many particles found to be 'consistent with gGSR' using a 30 or 60 second scan during manual reacquisition were 'inconclusive' using the conditions used for general GSR screening, and thus it follows that if each of the Si-containing particles were re-acquired more glass-containing particles could be identified.

In total, approximately 1% of all particles detected across the 26 stubs were 'characteristic' Pb/Ba/Sb particles and 0.24% of particles were consistent with (Pb/Ba/glass) gGSR. Comparatively, in the 'ideal' samples collected from police officers in this study, approximately 4% of particles detected were 'characteristic' Pb/Ba/Sb. Particles consistent with glass were found on 25 of the 26 stubs, although on the remaining 7 the glass was only encrusted with Pb or Ba and these may have a lower probative value than glass encrusted with both Pb and Ba.

Table 12: Pertinent figures from a meta-analysis of Si-containing GSR particles on casework stubs from Forensic Science SA

| Category | Count of stubs with *n* = 0 particles of this type | Count of stubs with *n* > 0 particles of this type | minimum *n* particles of this type (if *n* >0) | Average *n* of this type on a stub (including if *n* = 0) | Average number of particles of this type on a stub (if *n* > 0) | s.d. of number of particles of this type on a stub | maximum *n* particle of this type |
|---|---|---|---|---|---|---|---|
| **Sb Ba Pb** | 9 | 17 | 1 | 21.3 | 32.6 | 46.6 | 157 |
| **Ba Si** | 1 | 25 | 3 | 374.2 | 389.1 | 798.5 | 3306 |
| **Ba Sb** | 12 | 14 | 2 | 11.1 | 20.6 | 23.3 | 102 |
| **Pb Sb** | 4 | 22 | 1 | 31.4 | 37.1 | 46.0 | 177 |
| **Pb Ba** | 15 | 11 | 1 | 6.0 | 14.3 | 22.4 | 115 |
| **Pb Ba Si** | 8 | 18 | 1 | 4.9 | 7.1 | 9.7 | 48 |
| **Pb Si** | 0 | 26 | 1 | 53.0 | 53.0 | 50.0 | 197 |
| **Pb** | 2 | 24 | 1 | 52.4 | 56.8 | 52.0 | 186 |
| **Sb** | 4 | 22 | 2 | 15.1 | 17.8 | 20.5 | 92 |
| **Ba** | 23 | 3 | 1 | 0.7 | 5.7 | 2.9 | 15 |

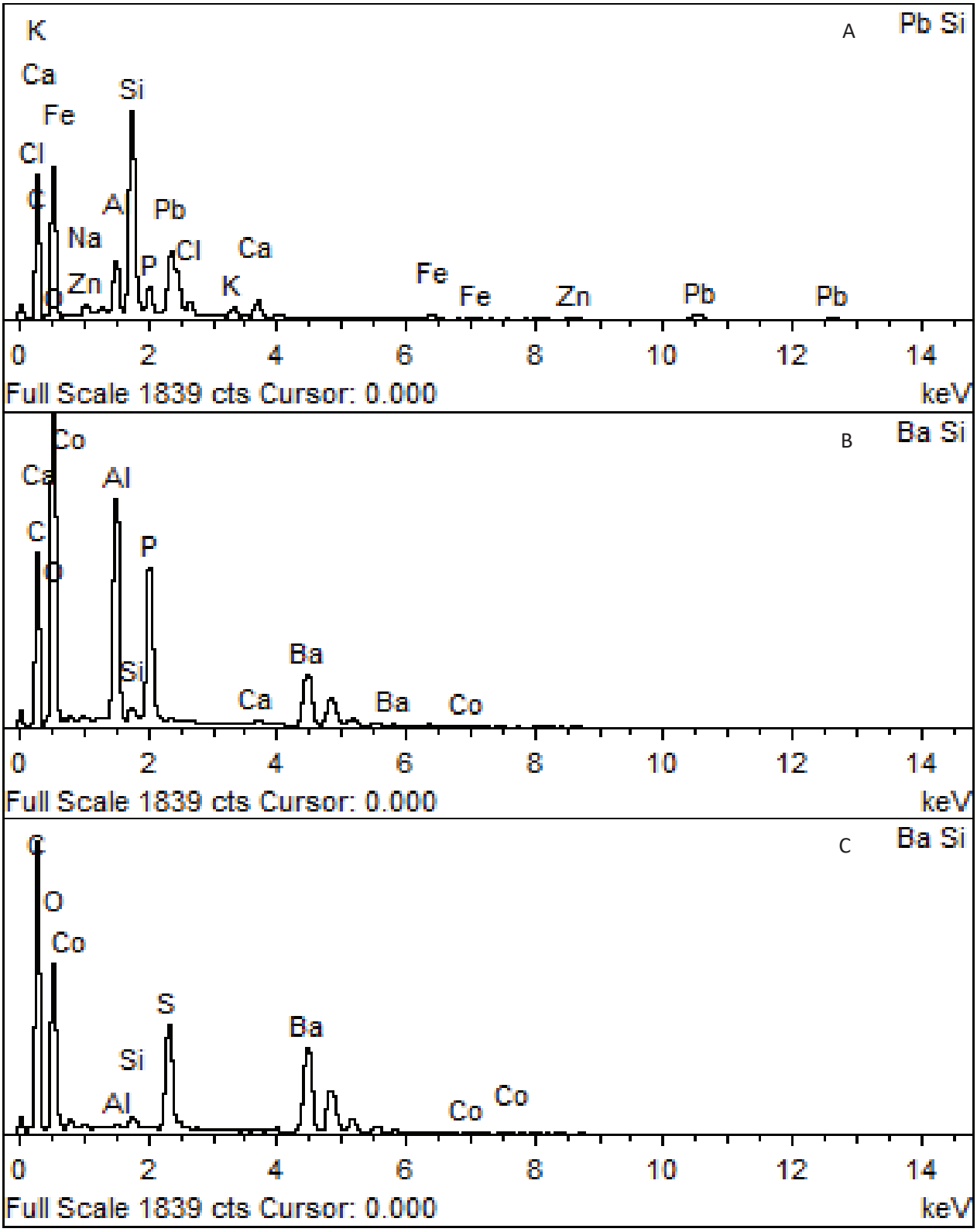


**Figure 20: Images of exemplar spectra of silicon-containing gunshot residue particles, labelled A-C (top to bottom), A showing a spectrum that was considered consistent with what would be expected from a glass-containing particle, B is a spectrum that was inconsistent with what would be expected from a glass-containing particle, and C shows a spectrum that was inconclusive, as it was unable to be classified into either category from this data.**

## 3.6. Conclusions

This study examined samples sourced from several thermo-chemical processes that may produce particles similar to what are observed from the discharge of firearms. The thermo-chemical processes chosen for examination in this study were fireworks, brake pads, nail guns, and matches. Residues from these non-firearm sources were examined for the presence of glass and particles resembling gGSR. In addition, particles from these non-firearm sources, were assessed to determine the likelihood that they may be mistaken for GSR.

As cartridges for nail guns contain primers with conventional firearm cartridge composition, including the presence of glass frictionator, particles from the discharge of cartridge actuated nails guns are practically indistinguishable from particles of GSR and gGSR. It is only when residues are evaluated on the basis of their entire particle population characteristics that their origin may be determined as being either firearm or nail gun. However, the prevalence of nail guns in the community is low, and only a small proportion of those are of the cartridge actuated variety, so all traces should be considered on a case-to-case basis. When relevant, nail gun particles could be a significant contributor to the value of the node $A_{B,}$ contributing to the background level of GSR like particles, if using a Bayesian network in the likelihood ratio evaluation for that case. However, a recent study of the Australian population has shown that the background rate of particles similar to GSR on hands is very low [198].

One particle with composition 'characteristic' of GSR was identified in this study and it was from the hands of a volunteer who had fired a nail gun. This particle was morphologically inconsistent with GSR and the nail gun cartridge primer used did not contain antimony, as is the case with all modern nail gun cartridges. The origin of the particle is unknown but was not from the components of the nail gun. The volunteers were asked to wash their hands immediately before the test firing, so it is unlikely that the particle arose through contact with an object other than the nail gun. This demonstrates that even 'characteristic' particles from obscure origins can be detected on hands and demonstrates the dangers of attributing too much significance to the detection of single particles and the importance of considering particle morphology together with compositional information.

Whilst it is the case that nail gun cartridges and rimfire firearm cartridges share similarities with regards to manufacture, firearms and nail guns are designed for different purposes. The chamber in a nail gun is much larger than in a firearm, meaning that a given quantity of propellant would produce lower pressures and temperatures in a nail gun. Additionally, in the nail gun used in this study, the gases from the primer/propellant were not applying direct force to the projectile. Instead, a piston

propelled by the cartridge pressed the nail into the surface. Therefore, although a certain level of qualitative compositional similarity between the residues from firearms and nail guns can be expected, the high pressures and temperatures involved in the discharge of a gun could rationally explain the differences in morphology observed between particles from the two sources in this study. This subject would appear to warrant further exploration. Depending upon the circumstances surrounding a shooting investigation, it may be very difficult to distinguish between particles from nail gun cartridges and firearm cartridges; as was illustrated in this study by the detection of a three-component particle and a population of two-component particles in the residues from the hands of someone that had operated a nail gun.

Samples from fireworks in Australia were observed to contain minor concentrations of Pb and Ba and trace amounts of Sb and therefore fireworks have at least the potential to produce GSR-Like particles. However, fireworks do not appear to contain glass powder and particles containing glass were not observed within firework residues. Therefore, it appears reasonable to conclude that fireworks cannot produce particles resembling gGSR. Compounds containing Pb and Ba have differing effects in fireworks but do not appear to have combined to produce GSR-like particles when fireworks were discharged. Therefore, the probability of a singular random particle in a firework residue in Australia being characteristic of GSR or resembling gGSR is very low, possibly 0 for gGSR-like particles. The probability of finding a larger population of these particles sourced from firework residues would be even lower. In most cases, the probability of observing a firework particle containing characteristic Pb/Ba/Sb composition is likely to have a zero or insignificant contribution to $A_B$ and thus M (Figure 7) compared to the probability of someone being contaminated with particles from another source, such as from a nail gun, an alternate firearm incident, or contact with law enforcement.

Safety matches available in Australia were found to be incapable of producing particles containing glass. Furthermore, safety matches do not seem to be capable of producing characteristic particles of either GSR or non-toxic GSR and are not likely to be confused with GSR in casework.

No glass containing particles were found from automotive sources associated with brake pads, and this work has indicated that these are also not likely to contribute to the background level of characteristic Pb/Ba/Sb particles on a suspect.

The relevance of gGSR to casework is becoming clearer because of the results presented here. The only sources found so far for particles containing glass encrusted with Pb, Ba and Sb or any combination thereof are firearms cartridges or explosive nail gun cartridges. Given the current rarity of cartridge-operated tools in the community, these are unlikely to be a significant source of residues

in casework but nevertheless the possibility should be considered when evaluating GSR traces on a case-by-case basis.

Under certain circumstances an examination of the elemental composition of the glass present in questioned particles could be informative. For example, glass-containing particles originating from Hilti nail gun cartridges have a borosilicate composition, which does not include Ca. Several ammunition manufacturers use soda lime glass frictionators, which do contain Ca. Therefore, in a shooting involving ammunition with a soda lime glass frictionator, differentiation between nail gun cartridge residue and the firearm cartridge residue would be simple, even using SEM-EDS [202]. On the other hand, if a case involved residue from ammunition that uses borosilicate glass frictionator, a comparison of the elemental composition of the glass in the residue with glass from the putative sources (i.e., nail gun cartridge or the ammunition) would be required. As will be shown in Chapter 4, this can be accomplished using SEM-EDS or, at a higher level of discriminating power, by the use of time of flight-secondary ion mass spectrometry (ToF-SIMS) [158, 159, 202].

## 3.7. Supplementary information for Chapter 3

**Table 13: A summary of the findings of existing literature in the area of atmospheric pollutions of heavy metals attributable to firework displays.**

| Ref | ROI* | Pb | Ba | Sb | Sr | Cu | P | S | Cd | K | Mn | Mg | Cr | Bi | Zn | As | Details |
|---|---|---|---|---|---|---|---|---|---|---|---|---|---|---|---|---|---|
| **[203]** | India (Varanasi) | N/a | 24.7 a | N/a | 2.98 a | 3.18 a | 385% b | 341% b | 0.04-0.13 µg/m$^3$ c | 313% b | 639% b | N/a | N/a | N/a | N/a | N/a | $PM_{10}$ |
| **[204]** | Taiwan Site A (Kaohsiung City) | 10.1 a | 4.63 a | N/a | 9.75 a | 4.25 a | N/a | N/a | 0.67 a | 19.44 a | 0.44 a | 24.4 a | 1.85 a | N/a | 2.15 a | N/a | $PM_{10}$ |
| **[204]** | Taiwan Site B (Kaohsiung City) | 8.95 a | 2.53 a | N/a | 5.75 a | 3.13 a | N/a | N/a | 0 a | 7.55 a | 0.67 a | 12.7 a | 1.42 a | N/a | 2.68 a | N/a | $PM_{10}$ |
| **[205]** | Hawaii (Oahu Pearl City) | 158 a | 7 a | 86 a | 215 a | 49 a | N/a | N/a | 16 a | 94 a | 15 a | 9 a | 14 a | 512 a | 49 a | 7.6 ng/m$^3$ c | $PM_{10}$ |
| **[206]** | China (Shanghai) | ~12 a | ~50 a | N/a | ~50 a | ~12 a | N/a | N/a | N/a | ~50 a | N/a | ~7 | 2-3 a | N/a | ~7 a | N/a | $PM_{2.5}$ |
| **[207]** | Spain (Alicante) | 7.96 a | 4.49 a | N/a | 14.5 a | 17.4 a | N/a | 9.7 a | N/a | 11.8 a | 3.43 a | 8.59 a | 7.24 a | N/a | 6.50 a | 3.91 a | $PM_{10}$ |
| **[208]** | Spain (Girona) Parc Migdia | 6.93 a | 10.9 a | 3.5 a | 86.1 a | 5.05 a | 2.61 a | N/a | 2.00 a | 26.0 a | 1.85 a | >2 a | N/a | 4 a | 3.90 a | 2 a | $PM_{2.5}$ |
| **[208]** | Spain (Girona) Escola Musica | 5.18 a | 5.55 a | 1.89 a | 71.2 a | 1.37 a | 1.04 a | N/a | 2.00 a | 13.0 a | 1.26 a | 2 a | N/a | 4 a | 1.87 a | 2 a | $PM_{2.5}$ |
| **[209]** | Italy (Milan) | 3.7 a | 9.3 a | N/a | 56.0 a | 4.6 a | N/a | 2.1 a | N/a | 6.8 a | 3.0 a | 11.4 a | 2.9 a | N/a | 3.4 a | N/a | $PM_{2.5}$ |
| **[210]** | China (Beijing) | 8 a | 82 a | N/a | 17 a | 6 a | N/a | N/a | N/a | 22 a | 4 a | 8 a | N/a | N/a | 5 a | N/a | Mainly $PM_{2.5}$ |
| **[211]** | Spain (L'alcora) | 12.1 a | 6.36 a | 1 a | 15.0 a | 0 a | 0.6 a | N/a | 3.33 a | 56.2 a | N/a | 5 a | 25.0 a | N/a | 3.76 a | 12.5 a | $PM_{10}$ |
| **[211]** | Spain (Borriana) | 88.6 a | 3.23 a | 0 a | 5.33 a | 4.08 a | 0.6 a | N/a | 19.0 a | 15.6 a | N/a | 5 a | 25.0 a | N/a | 12.85 a | 96.25 a | $PM_{10}$ |
| **[211]** | Spain (Valencia) | 14.5 a | 6.05 a | 27 a | 10.33 a | 5.08 a | 1 a | N/a | 2.0 a | 7.6 a | N/a | 3 a | 6.5 a | N/a | 0.76 a | 2 a | $PM_{10}$ |
| **[212]** | India (Lucknow) | 116.8% b | N/a | N/a | N/a | 217.3% b | N/a | N/a | 158.1% b | N/a | 119.9% b | N/a | 197.5% b | N/a | 154% b | N/a | $PM_{10}$ |
| **[213]** | China (Nanjing) CNY | 2.6 a | 99.1 a | 2.9 a | 79.4 a | 1.3 a | 1.5 a | N/a | 1.6 a | 9.3 a | 1.9 a | 2.6 a | 2.9 a | 7.2 a | 1.6 a | 2.2 a | $PM_{2.5}$ |
| **[213]** | China (Nanjing) Lantern Festival | 1.0 a | 9.7 a | 1.7 a | 5.7 a | 1.3 a | 1.4 a | N/a | 0.6 a | 1.8 a | 1.3 a | 1.3 a | 1.3 a | 2.3 a | 1.3 a | 1.3 a | $PM_{2.5}$ |
| **[214]** | India (Hyderabad) | N/a | 1091 a | N/a | 15 a | 9 a | N/a | N/a | N/a | 25 a | 2 a | 6 a | N/a | 3 a | N/a | 16 a | ? |
| **[215]** | India (Salkia) | 14.9 a | 56.72 a | N/a | N/a | 79 a | N/a | N/a | 16.7 a | N/a | N/a | N/a | N/a | N/a | N/a | N/a | $PM_{2.5}$ |
| **[216]** | India (Kolkata) | 10-12 a | N/a | N/a | N/a | 25 a | N/a | N/a | 10-12 a | N/a | 40 a | N/a | N/a | N/a | 5-6 a | N/a | $PM_{10}$ |
| **[217]** | China (Beijing) | 6.00 a | 67.0 a | N/a | 25.1 a | 1.35 a | N/a | N/a | 1.24 a | 11.5 a | N/a | 6.24 a | N/a | N/a | 1.85 a | N/a | $PM_{10}$ |
| **[218]** | UK (London, Marylebone Rd) | 19 a | 28 a | N/a | 25 a | ~1 a | N/a | N/a | N/a | ~8 a | N/a | ~4 a | N/a | N/a | ~2 a | N/a | $PM_{10}$ |
| **Total** | 21 | 19 | 19 | 7 | 18 | 20 | 6 | 2 | 11 | 18 | 12 | 17 | 12 | 6 | 17 | 10 | |

***a*** *Values reported as peak factor over 'normal day'*
***b*** *Values reported as percent increase over 'normal day'*
***c*** *Values reported as concentrations as they are not detectable on normal days (infinite increase)*
**Region of interest (ROI)*

# 4. Analysis of elemental and isotopic variation in glass frictionators from 0.22 rimfire primers

## 4.1. Preface

In this chapter, the second strand of research contributing to the overall aims is investigated. The original contributions of this chapter are as follows:

Firstly, data were generated to provide lithium and boron isotopic compositions for two borosilicate reference materials, because there were found to be no certified reference materials for boron or lithium isotopic composition for use in high-boron borosilicate glasses. The second contribution concerns the investigation of a new technique sensitive high-resolution ion microprobe (SHRIMP), for the forensic analysis of glass frictionator samples. This work also represents the first examination of the discrimination power of various techniques for the analysis of glass frictionator samples for different ammunition samples, batches and brands, and the creation of the first large database of the elemental composition of frictionator samples from various 0.22 rimfire ammunition brands.

This work is based on and substantially similar to a journal article published from this work [202]. Some methodology sections, as noted within the chapter, are as supplied by Drs. Simone A Kasemann, Anette Meixner, and Charles W Magee, Jr.

## 4.2. Chapter Summary

The majority of 0.22 calibre rimfire ammunition available in Australia, and overseas, tends to use glass powder rather than antimony sulfide frictionator in the primer. This glass can be the nucleus of a GSR particle with other primer components condensing around and onto the glass structure. As the composition of glass frictionator remains largely unaltered during ammunition discharge [159] there is the possibility that frictionator composition could be used in GSR examinations to either correlate or discriminate between samples, thereby providing valuable information to an investigation.

The small particle size (~100 µm) of glass frictionator samples mean that it is necessary to use *in situ* microanalysis techniques for the analysis of the elemental or isotopic composition of single particles. There are currently no appropriate certified reference materials for boron (B) and lithium (Li) isotopic composition available with a similar composition to the high boron borosilicate frictionator samples.

Therefore, two samples of borosilicate glass, NIST SRM 93a and NCS DC61104 were obtained, data were produced using multi-collector inductively coupled plasma mass spectrometry (MC-ICPMS) and sample heterogeneity was assessed using secondary ion mass spectrometry (SIMS) for both Li and B composition.

The recommended $\delta^{11}B$ values of borosilicate standards NIST SRM 93a and NCS DC61104 determined in this study are 0.03 ± 0.08‰ and -6.74 ± 0.12‰ (2 σ) respectively. Recommended $\delta^{7}Li$ values for the same glasses were determined to be -21.05 ± 0.32‰ and -3.22 ± 0.25‰ respectively.

In this study, the composition of glass frictionator from a wide variety of 0.22 rimfire ammunition was analysed by time-of-flight – secondary ion mass spectrometry (ToF-SIMS), sensitive high-resolution ion microprobe (SHRIMP) and scanning electron microscopy – energy dispersive X-ray spectrometry (SEM-EDS). Refractive index (RI) was measured using glass refractive index measurement (GRIM).

Across the population of ammunition studied, it was found that the elemental and isotopic composition of frictionator varied. ToF-SIMS was able to discriminate 94.1% of brands in a pairwise comparison and SEM-EDS achieved a pairwise discrimination power of 79.4%. If SHRIMP was combined with the other two techniques, 95.6% of brands could be discriminated. This could be increased to 97.0% discrimination if macro-characteristics of the primer (e.g. 2-component, 3-component) were included. Refractive index measurements supported the elemental data showing that there appeared, in most cases, to be only one population of glass within a cartridge.

The results suggest that there is scope for frictionator analysis to contribute valuable, new capability to forensic GSR examinations.

## 4.3. Introduction

Gunshot residue (GSR) originates both from organic and inorganic substances present in the primer, propellant, projectile, cartridge and the interior of the barrel [19], including the barrel surface itself [19]. Inorganic compounds found in GSR are sourced from the primer, with additions from the cartridge case, projectile and the gun [8, 35].

Primer composition is variable between manufacturer and calibre of ammunitions; however, the primers will contain compounds to fulfil specific, critical functions [8, 35], including fuel, oxidiser and frictionator. A frictionator is a substance that increases the sensitivity of the primer mixture to percussion thereby reducing the chance that the primer will misfire. Some components perform dual functions, for example antimony sulfide and calcium silicide function as fuel and frictionator. Whilst centrefire ammunition predominately contains antimony sulfide and/or calcium silicide, the majority of 0.22 calibre rimfire ammunition does not. Instead, rimfire ammunition usually contains glass powder as frictionator [4], although other materials such as ”granular amorphous carbon which exhibits conchoidal fracture” [241, 242] or metal powders such as bismuth or titanium have been reported in the patent literature [24, 243, 244].

The absence of antimony sulfide in rimfire ammunition primer is relevant during the evaluation of the weight and significance of GSR evidence. The ASTM Standard Guide for Gunshot Residue Analysis by Scanning Electron Microscopy – Energy Dispersive X-ray Spectrometry [32], a document used for guidance by many forensic laboratories around the world, involves a hierarchy whereby particles containing the elements lead (Pb), barium (Ba) and antimony (Sb) carry higher probative value than particles that contain only Pb and Ba. Therefore, primer residues arising from rimfire ammunition can only be assigned a relatively low probative value, unless they have incorporated some Sb from the projectile or *via* the weapon-memory effect [131, 233, 245].

The foregoing discussion has relevance in Australia where, due to the strong jurisdictional gun legislation, most of the three million firearms registered are small calibre rifles or shotguns [5]. This is different to the situation in other countries, where crimes or deaths more often involve revolvers, pistols and automatic weapons. A comparison of firearm deaths by weapon type between Australia and the USA (See Thesis Introduction) demonstrated that long rifles and shotguns are involved in more than 70% of cases in Australia, but only 11% of cases of cases in the USA [6, 9]. In the UK, rifles were only used in 0.8% of crimes involving a firearm, and shotguns in 7.3%. This prevalence of small calibre, long-arm rifles means that Australian jurisdictions usually deal with GSR evidence with different characteristics compared to other jurisdictions.

A theme in the literature has been a search for a way to discriminate between GSR particles arising from different ammunition. For the most part, success has only been achieved when small populations of ammunition have been considered or where the population includes a major difference in formulation (e.g. standard vs heavy metal free (HMF) ammunitions) [135, 140, 161, 246, 247].

However, some previous research indicated that glass frictionator present in rimfire primer can be incorporated into GSR and a small pilot survey of 0.22 calibre ammunition was carried out in order to establish whether the composition of frictionator varied sufficiently between ammunition sources to allow discrimination between GSR particles arising from different ammunition [158-160]. In each of these works, glass frictionator was extracted for analysis from cartridges using an extension of the method developed by Wallace and McQuillan [119] for desensitisation of primer. In one of these works [159], it was shown that glass composition is preserved through firing process, thus confirming that examination of frictionator composition offers potential to link GSR to unfired ammunition or to demonstrate similarity (or difference) between GSR deposits. That work used a small population of ammunition and was limited to particles with exposed glass. Henderson [160], using inductively coupled plasma – optical emission spectroscopy (ICP-OES), carried out another survey of extracted frictionator and showed that cleaned, bulk samples of frictionator from different brands of ammunition had elemental compositions that could be discriminated and that some brands used different glasses in different batches. The work of Coumbaros showed that soda lime glass (commonly used in windows or containers) and borosilicate glass (commonly used in laboratory glassware or in kitchenware such as Pyrex®) both have been used as frictionators [158, 159].

The present research extends the earlier work [158-160]. It describes work driven by two key hypotheses: 1) if it is the case that minute particles containing glass and Ba and/or Pb are quite rare in the community but relatively frequent in GSR then the evidential value that can be attributed to these particles would be greater than that attributed to simple Pb and/or Ba particles; and 2) if the composition of frictionator varies between manufacturers, or between ammunition from a particular manufacturer, then frictionator composition might provide a basis for linking GSR to a particular source of ammunition or to another deposit of glass-containing GSR. This chapter presents a survey of glass frictionators extracted from a wide population of 0.22 calibre ammunition, which provides data directly relevant to hypothesis 2. This chapter also describes an evaluation of time-of-flight – secondary ion mass spectrometry (ToF-SIMS) and sensitive high-resolution ion microprobe (SHRIMP) as techniques applicable to the analysis of raw glass frictionator particles and the strengths and weakness of the techniques if they were to be applied to the analysis of frictionator present in GSR

case samples. These techniques were compared to scanning electron microscopy – energy dispersive X-ray spectrometry (SEM-EDS), as this technique is already used routinely in glass and GSR analyses.

ToF-SIMS has been applied to both glass and GSR in the past [18, 157, 174, 248], and work has previously been done to characterise the glass frictionator samples using this technique [158]. In ToF-SIMS, an ion beam from a liquid metal ion gun causes secondary ionisation of atoms from the surface of the sample (within a few tens of angstroms), meaning that it is very surface-sensitive. When the liquid metal ion source is run in DC mode, it can be used to sputter away layers and mill a surface, thus allowing depth-profiling of a specimen. Another advantage of ToF-SIMS is that the ion separation and detection method used means that all the positively charged ions are collected simultaneously, so that the operator does not need to know which elements will be of interest prior to analysing the sample. ToF-SIMS has many desirable attributes for the analysis of extracted frictionator. These include high spatial resolution (down to about 5 x 5 $\mu m^2$ on the instrument used), low detection limits, high mass resolution, and negligible destruction even in the micro-domain. It can also be used on samples of glass in GSR particles of the size encountered in casework [158, 159].

A technique that was applied during this project, one that has not previously been used for analysis of GSR or trace evidence, is sensitive high-resolution ion micro-probe (SHRIMP). Similar to ToF-SIMS, SHRIMP is a secondary ion mass spectrometry technique, but it uses an oxygen ion gun to ionise material sputtered from the sample and a high-resolution double-focussing mass analyser equipped with multiple detection systems. Previous work using SHRIMP has included the analysis of zircons and other geological samples [249-258]. SHRIMP offers possible advantages for the analysis of GSR and glass in GSR such as the capability to carry out stable isotope ratio measurements to high precision and accuracy (including on B and Pb) and an ability to analyse elements that are difficult to detect using other techniques, such as F, Be, B, and Li [258]. It also has the capability for analysis of particles of the size encountered as glass in GSR [190].

Initial analysis of frictionators using ToF-SIMS indicated that the majority of ammunition manufacturers use high-boron ([B] = 2-5 wt. %) borosilicate glass; therefore, it appeared reasonable to explore whether B isotope measurements offer any potential for forensic examination of frictionators. In addition, Li was found to be present in all types of frictionator. Although the lithium concentrations are low and are probably a result of natural impurities in the glass feedstock, the high instrumental sensitivity of SHRIMP to Li and the similarity in analytical procedures for B and Li analysis made Li isotopic variation a target of opportunity.

The high B content of borosilicate glass requires it to be manufactured from either raw or processed borate products, which are either mined from borate minerals or extracted from boron-rich brines. There is a large range in the boron isotopic composition of borate minerals and brines, with Swihart et al. reporting marine evaporate borates having a range of 25 ± 4 ‰, while non-marine deposits have substantially lower isotopic ratios, in the range of -7 ± 10 ‰ [259]. Kasemann et al. report even lower boron isotopic compositions from the salar deposits of Argentina, with minerals ranging from -29.5 to -0.3‰, and fluids ranging from -18.3 to 0.7‰ [260]. This represents a range of over 50‰, and the boron in borosilicate glass could be included from any variety of these sources. Therefore, it is possible that there are differences in $\delta^{11}B$ composition between frictionators from different brands or between regions of manufacture that could be detected using SHRIMP.

Like B, Li is mined from either minerals or brines. However, none of the glasses analysed aside from NIST SRM 612 intentionally contain Li. Rather, it is a contaminant in the feedstock for the glasses, most likely coming in with the source of Na, Mg, or B. As a result, the entire terrestrial range of Li isotopic compositions, up to 80‰, is possible [261]. Additionally, because Li is a contaminant, it is present in both borosilicate and soda lime glasses, so the isotopic analysis can be used on either type of frictionator. Similar to B, it is expected that there will be isotopic variation between the glass frictionators from various sources, and that the stable isotope ratio analysis of Li composition possible using SHRIMP will generate additional and complementary information.

To collect absolute values for B and Li isotope data using microanalytical *in situ* analyses by secondary ion mass spectrometry (specifically relevant to Sensitive High-Resolution Ion Microprobe (SHRIMP) in this study) it was necessary to source suitable, matrix-matched reference materials to act as calibrants.

This chapter presents the first characterization of NIST SRM 93a and NCS DC1104 with regards to B and Li isotope ratios and Li concentrations. These data are provided to assist calibration of bulk and *in situ* microanalytical measurements for forensic research and analysis. In addition, the data can also serve as initial recommended values to develop these borosilicate glasses as suitable reference materials for routine analysis of the light elements in high B and high Li geological materials.

After determining appropriate methodologies and requirements, ToF-SIMS, SHRIMP and SEM-EDS have been examined in this study to advance the overall aims, which were to gain understanding of the composition and variation amongst glass from frictionators used in 0.22 rimfire ammunitions, and to assess the potential of these techniques for application in future studies and forensic examination of glass frictionators and glass in GSR.

### 4.3.1. Samples and Reference Materials

Due to the increasing interest in B and Li isotope measurement, a range of reference materials for both microanalytical and bulk analytical techniques have been produced, covering a wide range of isotope compositions. In addition, substantial effort has been expended to integrate bulk analytical and microanalytical, *in situ* techniques. This has included the NIST SRM 61x series glasses [261-264] and geological glasses [265]. However, in these previous works, B was invariably present in trace levels in the standards used, with the maximum B concentration being 351 μg $g^{-1}$ [263], which is far below the level required (2-5 wt. % B) for this purpose. High B- and Li-bearing minerals such as tourmaline have been analysed for their light element content and B isotopic composition, but these are crystalline substances (Dyar et al. 2001) and not sufficiently close in matrix (composition and structure) to the borosilicate glass fragments employed as frictionator.

The National Institute of Standards and Technology (NIST) provides a range of different borosilicate glasses, but most of them are intended to serve as calibrants for viscosity (NIST SRM 717a), chemical resistance (NIST SRM 623) or thermal expansion (NIST SRM 731), and only nominal composition values are available. For NIST SRM 1411 a certified chemical composition for 12 elements is available, but it is a high-sodium “soft borosilicate glass”, which did not appear to match the approximate composition of frictionator glass.

Previous work involving analysis of frictionator glass samples using scanning electron microscopy-energy dispersive X-ray spectrometry [158] made use of a borosilicate glass NIST SRM 93a, and this standard proved appropriate for ToF-SIMS analysis. One sample studied was a borosilicate glass with high concentrations of Ti and Al. A borosilicate glass reference material, NCS DC 61104 provided by the National Analysis Centre for Iron and Steel (NCS) was found, which is sold as an industrial reference material according to the supplier’s websites [266], and this material was enriched in both Ti and Al compared to NIST SRM 93a [266]. Both NIST SRM 93a and NCS DC 61104 have certified information on elemental concentrations and are characterized by high-boron concentration [266, 267]. NIST SRM 93a has an elemental composition close to the majority of frictionator samples available to us whereas NCS DC 61104 has higher Ca and Al concentrations (Table 16) that offer a closer matrix match to high Al borosilicate glass frictionator. As can be seen from Table 16, lithium concentrations have not previously been published for NIST SRM 93a or NCS DC61104.

As the compositions of these two borosilicate glasses are close to the typical high-boron borosilicate glass used as frictionator, they appeared to the best available materials that could function as reference materials for this research. Therefore, they were characterised by multi-collector

inductively coupled plasma mass spectrometry (MC-ICP-MS) to determine their B and Li isotopic ratios as well as their lithium concentrations. Homogeneity of the glasses and evidence of isotope fractionation was then evaluated using a Sensitive High-Resolution Ion Microprobe (SHRIMP).

However, not all the glass frictionator samples sourced were borosilicate. NIST SRM 612 was used as a comparative standard for the soda lime glasses, and FGS1 and FGS2 were used as control samples for SEM-EDS and ToF-SIMS.

In total, 37 0.22 calibre rimfire ammunition products and five standard reference glasses were involved in this study. The ammunition products were sourced from the South Australian Police reference collection, and some were manufactured several decades ago. Samples were included from 11 different countries and 25 manufacturers. Glass was recovered from most of the ammunition. The full list of reference materials used is shown in Table 14 and ammunitions examined is shown in Table 15. Table 15 shows each of the ammunition's information, whether glass was found to be present and successfully extracted, and other elements present in the primer.

The elemental concentrations for NIST SRM 612, FGS1 and a typical soda lime frictionator sample are shown in Table 16, along with NIST SRM 93a, NCS DC 61104 and a typical borosilicate frictionator.

**Table 14: Collected standards for glass analysis, detailing name, source, and variant of glass.**

| Standard | Standard Name | Source | Country of Origin | Type |
|---|---|---|---|---|
| **N612** | NIST SRM 612 | NIST | USA | Soda lime Standard |
| **93a** | NIST SRM 93a | NIST | USA | Borosilicate Standard |
| **LGC** | NCS CRM DC61104 | National Testing Co | China | Borosilicate Standard |
| **FGS1** | Float Glass Standard 1 | Bundeskriminalamt | Germany | Soda lime Standard |
| **FGS2** | Float Glass Standard 2 | Bundeskriminalamt | Germany | Soda lime Standard |

**Table 15: Collected samples of glass frictionator, with elements from the primer for each as determined by SEM**

| Sample # | Sample Name | Glass Present & Recovered (yes/no) | Country of Origin (per packaging) | Primer Elements |
|---|---|---|---|---|
| 1 | **Remington** sub-sonic LR N11P1R | Yes | USA | Pb, Ba (Si, Ca, Na, Mg) |
| 2 | **CIL** LR Pistol Match CACU8P9 | Yes | Canada | Pb, Ba (Si, Ca, Na, Mg, Al) |
| 3 | **Federal** Champion LR 2BW667 | Yes | USA | Pb, Ba (Si, Na, Al) |
| 4 | **Sellier Bellot** (unknown) | No | Czechoslovakia | Pb, Ba, Sb (Si) |
| 5 | **CCI** LR Standard Velocity Target MRP8200003 | Yes | USA | Pb, Ba (Si, Na, Al) |
| 6 | **Aguilla** SE Super Extra LR, Remington subsidiary, 31VA | Yes | Mexico (USA subsidiary) | Pb (Si, Na, Mg, Ca, K) |
| 7 | **Eley** Club LR WY6422 | Yes | UK | Pb, Ba (Si, Ca, Na, Al) |
| 8 | **RWS** subsonic 59MFI | Yes | Germany | Pb, Ba (Si, K, Na, Al, Ca) |
| 9 | **Browning** HP LR Winchester subsidiary, EDPK62 | Yes | Australia | Pb, Ba (Si, Na) |
| 10 | **Stirling** High Impact LR for Fuller Firearms, Australia, 091819 | Yes | Philippines (AUS subsidiary) | Pb, Ba (Si, Al, Na, K) |
| 11 | **Winchester** XTRLR Pistol 1DTM62 | Yes | Australia* | Pb, Ba (Si, Na, Al) |
| 12 | **PMC** Zapper 22LR 22-D-446 | Yes | Korea | Pb, Ba (Si, Na, Mg, K, Ca) |
| 13 | **Lapua** Midas M 22LR 2328040 | No | Finland | Pb, Ba, Sb |
| 14 | **Mauser** KK80 22LR 100205 | Yes | Germany | Pb, Ba (Si, Na, Al) |
| 15 | **Fiocchi** Maxac 22LR 0135003 | No | Italy | Pb, Ba (Si) |
| 16 | **Nitron** Naboje 22LR P-714/TLS | No | Poland | Pb, Ba, Sb |
| 17 | **Swartklip** 22LR 231514 | Yes | South Africa | Pb, Ba (Si, Ca, Na, Mg) |
| 18 | **Imperial** (CIC) Hollow Point 22LR | No | Australia | Pb, Ba |
| 19 | **CBC** Super Velox 22LR C-BD AA0116 | Yes | Brazil | Pb, Ba (Si, Ca, Na, Mg) |
| 20 | **Gevelot** 22 Long | Yes | France | Pb, Hg, Sb (Si Al Mg) |
| 21 | **Nicorro** Hollow Point 22LR 10KCCARLIM | No | Germany | Pb, Hg, Sb (Si Al) |
| 22 | **Vostok** Target 22LR <2> M45 | No | USSR | Pb, Ba (Ca, Al) |
| 23 | **Dominion** 22LR | Yes | Canada | Pb, Ba (Si, Ca, Na, Mg, Al) |
| 24 | **Valor** Ultrasonic 22LR | No | Yugoslavia | Pb, Ba (Sb) |
| 25 | **Hornady** 30GR VMAX 22WMR 22MAG A25503 | Yes | USA | Pb, Ba (Si, Ca, Na) |
| 26 | **Winchester** Bushman 22LR ADD1HG7 | Yes | Australia*, | Pb, Ba (Si, Na, Al) |
| 27 | **Winchester** Powerpoint 22LR 1DMH6 Box 1 | Yes | Australia*, | Pb, Ba (Si, Na, Al) |
| 28 | **Winchester** Bushman (2) 22LR ACD1HN1 | Yes | Australia*, | Pb, Ba (Si, Na, Al) |
| 29 | **Winchester** Rapidfire 22LR ADD1VL13 | Yes | Australia* | Pb, Ba (Si, Na, Al) |
| 30 | **Winchester** Powerpoint (2) 22LR 1DMH6 Box 2 | Yes | Australia*, | Pb, Ba (Si, Na, Al) |
| 31 | **Winchester** Powerpoint (3) 22LR ADD1EM31 | Yes | Australia*, | Pb, Ba (Si, Na, Al) |
| 32 | **Winchester** Superspeed 22SHORT ADD1CM61 | Yes | Australia*, | Pb, Ba (Si, Na, Al) |
| 33 | **Winchester** T225 22SHORT AEDICF1 | Yes | Australia*, | Pb, Ba (Si, Na, Al) |
| 34 | **Winchester** Sub-Sonic 22LR 2DAF72 | Yes | Australia*, | Pb, Ba (Si, Na, Al) |
| 35 | **Winchester** Powerpoint (4) 22LR AEDIDN5 Box 2 | Yes | Australia*, | Pb, Ba (Si, Na, Al) |
| 36 | **Winchester** Powerpoint (5) 22LR 1DBA71 (old) | Yes | Australia*, | Pb, Ba (Si, Na, Al) |
| 37 | **Winchester** Powerpoint (6) 22LR 2DWG31 (old) | Yes | Australia*, (old) | Pb, Ba (Si, Na, Al) |

**Although this ammunition is assembled in Australia, the cartridge cases are received ready-primed from the USA.*

**Table 16: Certified concentrations of constituents in CRMs NIST 93a and NCS DC61104, and approximate concentrations of constituents in typical frictionator samples.**

| | % by weight from Certificate of Analysis | | Approximate % by weight* | % by weight from literature ***values in italics are mg/kg of the element (not the oxide)*** | | Approximate % by weight* |
|---|---|---|---|---|---|---|
| Constituent | **NIST SRM 93a †** | **NCS DC61104 [266]** | **Typical Borosilicate Frictionators** | **SRM NIST 612 [268]** | **FGS1 [170]** | **Typical Soda Lime Glass** |
| **$SiO_2$** | 80.8 | 53.98 | 70-75 | **72** | **73.3** | 60-70 |
| **$B_2O_3$** | 12.56 | 8.87 | 8-12 | *32* | Not measured | <0.1 |
| **$Na_2O$** | 3.98 | 0.096 | 2-4 | **14** | **13.9** | 10-14 |
| **MgO** | 0.005 | 4.40 | <0.2 | Not measured | **3.9** | 1-3 |
| **$Al_2O_3$** | 2.28 | 14.50 | 1-3 | **2** | **0.3** | 0.5-3 |
| **$K_2O$** | 0.014 | 0.59 | <0.2 | *64* | **0.1** | <1 |
| **CaO** | 0.01 | 16.54 | <0.2 | **12** | **8.5** | 6-10 |
| **$TiO_2$** | 0.014 | 0.19 | <0.2 | *50.1* | *69* | <LOD |
| **$Fe_2O_3$** | 0.028 (total iron as) | 0.34 | <0.2 | *51 (total Fe)* | *580 (total Fe)* | <LOD |
| **FeO** | 0.016 | Not measured | <LOD | | | |
| **$ZrO_2$** | 0.042 | Not measured | <0.1 | Not measured | *49* | <LOD |
| **F** | Not measured | 0.54 | <0.1 | Not measured | Not measured | <LOD |
| **Cl** | 0.060 | Not measured | <0.1 | Not measured | Not measured | <LOD |
| **Li** | Not measured | Not measured | Not measured | 40 | *6* | Not measured |

**Measured using scanning electron microscopy-energy dispersive X-ray spectrometry*
*† [267]*

## 4.4. Methods

### 4.4.1. Identification of glass in frictionator and gGSR

For identifying glass frictionators from the unfired cartridge, the process of identifying glass particles was relatively simple. Reviews of patents and MSDS documentation from several of the ammunition brands showed that rimfire ammunition, both standard and non-toxic can contain glass as a component. The glass was extracted by removing other primer components using a series of solvent washes (as described in 4.4.3 Frictionator Extraction Process). Glass fragments were examined under a microscope, were found to be colourless, transparent, they showed no birefringence when exposed to polarised light, and when analysed by RI measurements, each particle and particle population, except Gevelot, showed RIs within expected values for glass. Additionally, elemental analyses and mapping showed no heterogeneity within the samples. Using the combination of this evidence, identifying a particle as glass, beyond reasonable doubt, is an achievable challenge, even for the frictionator samples, which are often about 200 μm in diameter.

However, casework samples of glass-containing GSR are usually 5-20 μm in diameter, which is below the range for RI determination by the oil-immersion/temperature-variation methodology offered by commercial instrumentation. For glass-containing GSR, the focus was on comparing elemental profiles of post-firing discharge to the profiles from unfired frictionator samples from the same ammunition and using elemental mapping and birefringence to give an indication of whether the sample is homogeneous and/or demonstrating signs of crystallinity.

In some glass-containing GSR samples, especially where slices were taken, or the encrustation and incorporation of lead (Pb) and barium (Ba) is light, the colourless, transparent nature of the glass can be observed by light microscopy. At the spatial resolution capable by SEM-EDS mapping, the substrate of both the unfired frictionator particles, and the post-discharge gGSR particles appears to be elementally homogeneous, with the exception of various quantities of Pb and Ba incorporation.

### 4.4.2. Isotopic Composition of Li and B in CRMs

#### *4.4.2.1. Sample Preparation*

As discussed above, two glasses (NIST SRM 93a and NCS DC1104) were identified as suitable reference materials for this gunshot residue research. Two samples of NIST SRM 93a were obtained in different years (2014 and 2015), one directly from NIST (National Institute of Standards and Technology, Gaithersburg, USA) and one *via* SPI Supplies (Westchester, USA). A unit of NIST SRM 93a sourced from NIST consists of one disc of glass, 6 mm thick and 32 mm in diameter whereas a unit of NIST SRM 93a sourced from SPI Supplies consisted of 2 cubes, with edge-lengths of approximately 2.5 mm. Documents provided with the latter indicated that it was sourced from NIST despite the difference in presentation. As of the date of this thesis NIST SRM 93a is no longer available from SPI Supplies in this form. NCS DC61104 was sourced from LGC Standards (Teddington, Middlesex, UK) and was delivered as 50 g of small chips/powder (approximately 50-150 µm particle size).

The sample of NIST SRM 93a sourced directly from NIST was placed into a press-seal plastic bag and chips were broken from its periphery over an arc of approximately 55 mm using a small pair of wire side-cutters. Several of the smaller pieces were selected at random from the collection of chips and placed into a polypropylene Eppendorf tube (2 mL capacity). The glass pieces in the tube were reduced to a coarse powder by repeatedly tapping them with the tip of a “spear-point” tungsten carbide electric drill bit (6 mm). Cubes of NIST SRM 93a sourced from SPI Supplies were not sub-sampled further but directly reduced to a coarse powder using the same approach as that used to treat the glass sourced from NIST. For MC-ICP-MS analyses the coarse powders were finely ground in an agate mortar and wet sieved to obtain a homogenous grain-size fraction between 50 and 100 µm. NCS DC61104 was not crushed but used as supplied. For SHRIMP analysis, particles of glass were selected from the coarse powder samples, mounted in rows in an epoxy resin, polished with diamond paste (final polish using 0.3 µm grit) and gold-coated.

#### *4.4.2.2. Boron Isotope Analysis*

**This section is as supplied by Kasemann and Meixner, who undertook the analysis.**

Boron isotope ratios and concentrations of borosilicate glass samples were analysed on a Thermo Scientific NEPTUNE Plus MC-ICP-MS in the Isotope Geochemistry Laboratory at MARUM – Centre for Marine Environmental Sciences, University of Bremen following a method specially set up for high boron concentration samples. Sample dissolution and separation were performed as described previously in Romer et al. [269], Kasemann et al. [260, 262, 263, 270][260, 262, 263, 270][260, 262, 263, 270][260, 262, 263] and Tonarini et al. [271].

Aliquots of up to 6 mg of powdered sample were fused with $K_2CO_3$ (1:200) in Pt-crucibles, rapidly cooled to room temperature, dissolved in $H_2O$ and stored overnight at 50 °C. The sample slurry was completely transferred into a Savillex beaker and tempered for 2 hours at 70 °C. Boron is highly soluble under alkaline conditions, so it can be quantitatively extracted from the slurry by repeated centrifugation and washing of the insoluble residue. All supernatant was collected in a Savillex beaker. The sample solution was homogenised and an aliquot containing about 5 µg of B was used to perform a two-step anion-cation separation procedure. First, approximately 300 µl of cleaned and conditioned B-specific resin (AMBERLITE™ IRA743, 20-50 mesh, Sigma Aldrich) was added to the sample aliquot, which was stirred overnight. The sample-resin mixture was filled in pre-cleaned Bio-Rad Poly-Prep columns. Under basic to neutral conditions, B becomes fixed on the resin. Matrix elements, including K, were washed out with 2 ml $H_2O$ followed by 2 ml 2 M $NH_4OH$ and 4 ml $H_2O$ before B was eluted with 12 ml of 0.5 M HCl. The potential B loss was monitored by collecting an additional 2 ml of eluate ("tail fractions"). The B concentration of 50 µl sample aliquots and of the 2 ml tail fractions were determined using 100 ppb NIST SRM 951 and 0.5 N HCl for standardization. In all cases >99.9 % of the total B was collected in the main fraction.

Mannitol was added to the remaining eluant (B:mannitol=1:40 weight proportion) to avoid B loss during drying. The eluants were dried at <65 °C and immediately dissolved in dilute HCl (1 ml, 0.02 N). Cation separation was performed using 1.9 ml AG50W-X8 resin and Bio-Rad Poly-Prep columns. The B-mannitol complex is stable in acidic conditions below 70 °C and behaves like an anion, so that all cations remain on the resin and B can be eluted with diluted HCl (8 ml, 0.02 N). The samples were dried at <65 °C and dissolved in 5 ml 2% $HNO_3$ for concentration and isotope analyses. The tail fraction (2 mL) was also dried, dissolved in 0.5 ml 2% $HNO_3$ and scanned for B loss. In all main sample fractions, more than 99. 9% of the total B was recovered. Certified reference material boric acid NIST SRM 951 and reference tourmaline IAEA-B-4 were processed with the samples to monitor the precision and

accuracy of the analytical procedure. The procedural blank was <4.2 ng B with a $\delta^{11}B$ of ~-3 ‰ and thus a negligible influence on the isotope composition of samples and reference materials.

Samples and reference materials were matched within 5 % to a 100 ppb NIST SRM 951 reference standard solution and measured repeatedly using the sample-standard bracketing technique. Diluted nitric acid (2 %) was measured directly before and after a sample and standard. The average represents the analytical baseline and was used for correction. Boron isotope compositions are reported relative to NIST SRM 951 primary standard in the conventional $\delta^{11}B$ (‰) notation [$\delta^{11}B$ = **(**[$(^{11}B/^{10}B)_{sample}$/ $(^{11}B/^{10}B)_{NIST\ SRM\ 951}$] −1**)***1000].

The precision of repeatedly analysed reference materials is better than 0.2 ‰ (2 σ) and of B concentrations is better than 6 % (2 σ). Long term $\delta^{11}B$ reproducibility for NIST SRM 951 and IAEA-B4 are -0.1 ± 0.08 ‰ (2 σ, n=11) and -8.95 ± 0.13 ‰ (2 σ, n=6), respectively. During this study, the treated boric acid NIST SRM 951 produced a $\delta^{11}B$ of -0.09 ± 0.1 2‰ (2 σ). Processed tourmaline IAEA-B4 produced a $\delta^{11}B$ value of -8.91 ± 0.08‰ (2 $\sigma_{mean}$), which agrees well with published data **[**-8.97 ± 0.13‰ (2 σ) [272], - 8.86 ± 0.56‰ (2 σ) [273], and -8.71 ± 0.36‰ (2 σ) [274]**]**. All analysed borosilicate samples were fully processed at least twice, each sample solution was repeatedly analysed with an internal and external reproducibility of better than 0.2‰ (2 σ, see Table 20).

#### *4.4.2.3. Lithium Isotope Analysis*

**This section is as supplied by Kasemann and Meixner, who undertook the analysis.**

Lithium concentration and isotope ratios of borosilicate-glass samples were analyzed in the Isotope Geochemistry Laboratory at the MARUM - Center for Marine Environmental Sciences, University of Bremen. Sample digestion, separation and purification of lithium were modified after Moriguti and Nakamura [275] and is described in detail in Hansen, Meixner, Kasemann and Bach [276]. Between 8-12 mg of powdered sample were dissolved at 150 C for 48 hours in 3 ml $HF/HNO_3$ mixture (5:1), dried at 80 °C, repeatedly re-dissolved in 2 ml 2 M $HNO_3$ (at least 3 times) and dried to convert all fluorides into nitrates. The decomposed samples were dissolved in 0.15 M HCl and a sample aliquot of 25 – 290 ng Li was taken to perform a two-step purification procedure using Bio-Rad® AG 50WX8 (200-400 mesh) resin. Lithium must be quantitatively separated from the sample matrix, since the loss of only 1 % of Li during column separation as well as the presence of Na can result in significant shifts in the Li isotope composition [275, 277-279]. The first step removes most matrix elements (e.g. Ca, Mg and rare earth elements) using Bio-Rad® Poly-Prep columns with 1.4 ml of the cation-exchange resin and

0.15 M HCl as reagent. In a second step Na was separated using Bio-Rad® Bio-Spin columns with 1 ml resin and a combination of 0.15 M HCl and 0.5 M HCl both in 50 % ethanol as reagents. The total Li loss during column separation was always < 0.1 % of collected head and the tail fraction and thus did not cause significant offset on the isotopic composition of analyzed materials. Reference materials NIST RM 8545 (LSVEC, Li carbonate standard, Flesch et al. (1973), clay shale ZGI-TB and tourmaline IAEA-B-4 as well as the USGS candidate reference material G-3 (granite) were separated and analyzed together with the samples in order to control the analytical procedure. The Li blank input during the whole analytical procedure was always less than 6 pg Li and had no influence on the isotopic composition of the processed materials.

Lithium concentration and isotope analyses were performed on a MC-ICP-MS Neptune Plus (ThermoFisher Scientific) using the SIS (stable introduction system: low flow PFA nebulizer (50 µl) and a double pass quartz spray chamber) together with a high- efficiency x-cone. Processed samples and reference materials as well as the unprocessed NIST RM 8545 were dissolved in 2% $HNO_3$, closely adjusted to 25 ppb Li content and repeatedly analyzed in the standard-sample bracketing mode using the unprocessed NIST RM 8545 as the standard. The 2% $HNO_3$ used for sample dissolution was measured directly before and after each sample and standard and used as analytical baseline for correction. Isotope compositions are reported as delta-notation (‰) relative to NIST RM 8545 [$\delta^7Li = \left(\left[\left(^7Li/^6Li\right)_{sample} / \left(^7Li/^6Li\right)_{NIST\ RM\ 8545}\right] - 1\right) * 1000$]. The processed NIST RM 8545 shows a $\delta^7Li$ of 0.04 ± 0.02 ‰ (2 σ, n=2) indicating no isotope fractionation during the analytical procedure. Li concentration and $\delta^7Li$ values of ZGI-TB (-3.2 ± 0.3 ‰ (2 σ), 104 µg $g^{-1}$ Li) reproduced published values (-3.3 ± 0.4 ‰, 104 ± 5 µg $g^{-1}$ Li; [269]; 111 µg $g^{-1}$ recommended value, [280]). The USGS G-3 shows $\delta^7Li$ values of 0.6 ± 0.3 ‰ (2 σ) and Li concentration of 31 µg $g^{-1}$ (32 ± 2 µg $g^{-1}$ Li, [281]) and IAEA-B4 615 µg $g^{-1}$ Li with a $\delta^7Li$ of 4.1 ± 0.5 ‰ (Table 21).

#### *4.4.2.4. Notes on interpretation of δ notation of isotope ratio values*

By international convention, stable isotope ratios are generally presented as relative deviation from a standard., and are reported in units of ‰ [193]. They are generally reported relative to an internationally recognised standard that has been designated as 0‰ [261], but may be measured against a different reference material with a known value and then recalibrated to the 0‰ standard value.

When a sample and standard are analysed under the same conditions at the same time, and the results are reported as relative values, there are fewer sources of error to take into account, and a better precision can be reported [193].

Delta notation values can be calculated by the following formula [193], where $R_x$ is the ratio of the heavy to the light isotope measured for x.

$$\delta‰ = \frac{1000(R_{sample} - R_{standard})}{R_{standard}}$$

**Equation 2: Formula for the calculation of delta notations for isotopic ratios**

#### *4.4.2.5. Material Homogeneity*

***This section is as supplied by Magee, who undertook this work with me.***

All SHRIMP analyses were performed on the SHRIMP IIe instrument at Geoscience Australia using positive secondary ions produced by bombardment of the sample with $O_2^-$ ions at an impact energy of 10.68 keV. The primary ions were Köhler projected through a variety of aperture sizes depending on the analytical session, giving sputter crater diameters from 40 to 10 microns. Primary Beam Monitor currents (which measure net sample current and are proportional to primary beam current) varied from 0.5 to 10 nA.

Secondary ions were extracted and focussed through the mass spectrometer into a single collector, with stepping of the analyser magnet used to peak hop between mass stations. The source slit was set to 200 µm and the collector slit was set to 250 µm, giving a nominal mass resolution of approximately 2050 (M/dM).

Helmholtz coils surrounding the source chamber set to 700 mA were used to minimize mass-based secondary beam separation between the sample surface and the source slit caused by ambient magnetic fields. This value was set before the commencement of each analytical session. Six small permanent Nd magnets placed around the mass spectrometer were used to correct for ambient field aberrations beyond the source slit. Magnets were chosen and positioned such that the $^6Li^+$ and $^{238}U^{16}O^+$ ions traversed the mass spectrometer on the same trajectory from the source slit to the mass analyser.

Lithium ions were detected with an electron multiplier. Two backgrounds peaks close to each Li isotope were used to account for a mass-dependent background caused by matrix ions scattered by the flight tube. Boron was measured in the same manner, except that the secondary ions were

collected in an electron-suppressed Faraday Cup. Total secondary beam current was measured using an Australian Scientific Instruments e7600 electrometer. The $^{11}B^{+}$ voltage across a $10^{11}$ Ω resistor was about 1 volt, implying a count rate of approximately 62 million cps.

Data were collected in four, five, or six scans of the analyser magnet. Data were deadtime-corrected in the case of electron multiplier data. The closest background to each mass station was then subtracted, and the mean of the four, five, or six isotopic ratios was determined for each spot. At least 10 spots were collected for each reference material in each session where it was used.

### 4.4.3. Frictionator Extraction Process

The projectile and propellant were removed from each round of ammunition. Glass particles were separated from the other primer components using solvent washes and spin filtration, as adapted from Wallace and McQuillan [119]. Firstly, approximately 1 mL of 2:1 acetone:water was placed with a cartridge into a 5 mL screw-capped glass test tube to soften the gum base.

The tube was left, capped, for at least three hours then its contents were mixed with a vortex mixer for several seconds. The cartridge was removed from the tube and the inside-bottom of the cartridge was scraped using a thin, sharp wire probe with a bent tip that could reach into the rim of the cartridge. This was undertaken while the cartridge was about two-thirds full of the acetone/water mixture.

The cartridge was returned to its tube and a fresh aliquot of solvent (1 mL) was added and used to 'wash' the interior of the cartridge by pumping liquid into its base using a plastic pipette (separate pipettes were used for each round of ammunition).

The tube was allowed to stand for about ten minutes and the plastic pipette was used to draw 1 mL of a liquid and insoluble matter suspension from the bottom of the tube. The suspension was then placed into a spin-filter cup (Costar, 0.45 µm Nylon membrane) and filtered using a centrifuge (Sigma 1-14, at 14,000 rpm for 60 seconds).

This process was repeated until all the liquid and insoluble material in the tube and cartridge had been spin-filtered. After this process, a few mg of glass powder residue was collected in the spin filter cups, and the filtrate was discarded. The residue was washed three times with neat acetone, three times with 5% nitric acid and three times with methanol before being prepared further for analysis. A typical glass frictionator residue is shown in Figure 21.

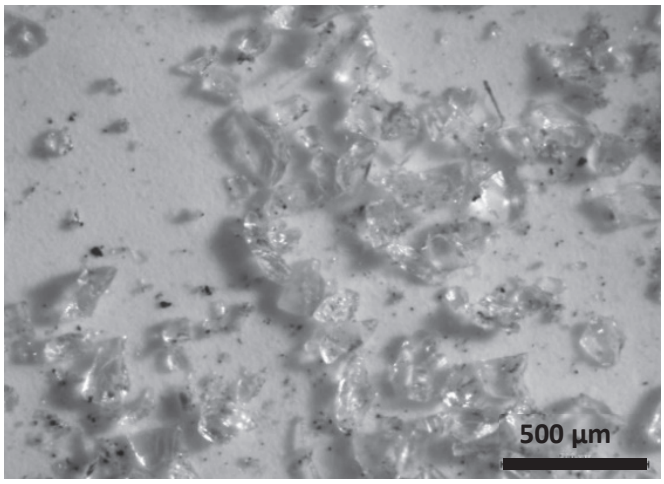


**Figure 21: Typical optical microscopy image (with reflected light) of glass frictionator collected after solvent extraction and spin-filtration, specifically showing residue from Swartklip ammunition. Scale bar represents 500 µm**

One cartridge (sample no. 4, Table 15) initiated during above solvent extraction procedure, ejecting solvent and primer constituents from the cartridge. This occurred frequently (in five of six cartridges attempted for this particular ammunition), and glass was unable to be recovered from sample no. 4 using this method. The different composition of the primer may be responsible for the lack of softening of the gum base and desensitisation of the primer.

Glass samples and reference materials were mounted in an epoxy resin disc and polished according to the method used by Geoscience Australia [282]. Approximately 30 large grains (>50 µm diameter) were mounted per sample (or reference material). After the disc was polished it was coated with 15 nm of gold prior to SHRIMP and ToF-SIMS analysis. For SEM analysis the gold coating was removed by rubbing the disc with a paper tissue moistened with acetone. The disc was then attached to an SEM pin stub, coated with carbon and the surface of the disc was "earthed" to the pin stub using carbon ink (Pasco Scientific Conductive Ink PK–9031).

### 4.4.4. **ToF-SIMS**

#### *4.4.4.1. Analysis*

ToF-SIMS analyses were performed using a Physical Electronics Inc. PHI TRIFT V nanoToF instrument equipped with a pulsed $^{179+}$ Au liquid metal ion gun (LMIG), operating at 30 keV energy. Experiments were performed under a vacuum of $5x10^{-6}$ Pa or better. "Bunched" $Au_1$ settings were used to optimise mass resolution for the collection of positive ion SIMS spectra. The raw frictionator samples were very large (at least 100 by 100 um) compared to the beam size used (10 x 10 um) and glass is generally relatively homogeneous, so it was more important to optimise the mass resolution (allowing differentiation between peaks of the same nominal mass) than the spatial resolution of the spectra collected.

#### *4.4.4.2. Statistical Analysis*

When the data were interrogated offline, 66 ions were identified in the SIMS spectra. These were selected as peaks in WINCadenceN (Software from Physical Electronics (PHI), USA) and the counts were aggregated for all samples. Peaks below 50 counts were not treated, as this represents less than 1 cps, and a signal to noise ratio of less than 3:1, which is insufficient for quantitative, or in this case semi-quantitative analysis. The peaks for Au, In, and Ge were also not treated, as their signal is confounded by sputter coatings, ion guns, and the indium foil which is usually used to mount specimens, leading to a small background value. The remaining 52 peaks were normalised to the $^{28}Si^{+}$ signal as total number of counts per analysis can vary across a sample set, (increasing as vacuum increases) and the counts for artefact peaks (Au etc.) observed can change sample to sample.

For each variable, the mean (from the counts per 100 counts of $^{28}Si^{+}$) with 99% (± 3 standard deviations) confidence intervals were compared between all brand pairs, and individual elemental discrimination powers determined. The ion with the highest discrimination power was determined and the glass samples that could be discriminated by that element were removed from the dataset. Then, for the remaining un-discriminated glass samples, the ion with the next highest discrimination power was determined and all samples discriminated on the basis of that element were removed from the set. This process was continued until no glass samples could be discriminated.

### 4.4.5. **SHRIMP**

#### *4.4.5.1. Analysis*

The SHRIMP IIe at Geoscience Australia was used to determine the relative abundance of the following isotopes in each sample and standard, $^{7}Li^{+}$:$^{6}Li^{+}$, $^{204}Pb^{+}$, $^{206}Pb^{+}$, $^{207}Pb^{+}$, $^{208}Pb^{+}$, $^{232}Th^{+}$ and $^{238}U^{+}$. In addition, the relative concentrations for the major isotopes of $Be^{+}$, $Li^{+}$, $Si^{++}$, $O^{+}$, $Mg^{++}$ and $F^{+}$ ions were determined, presented as per 100 counts of $O^{+}$. $^{11}B$:$^{10}B$ isotopes were also determined for the borosilicate samples only. Each ion in a run required different parameters, and the typical run parameters for each ion are shown in Table 17. Background values were taken and subtracted, as the contributions to the background signal in SIMS techniques can vary according to time, and at different locations within the sample chamber [283].

**Table 17: Typical run parameters for SHRIMP analysis**

| Analytical Run | Isotope | Mass (amu) | Time (s) | Delay (s) |
|---|---|---|---|---|
| 1 | Bkgd1 | 204.02563 | 20 | 1.0 |
| 1 | $^{204}Pb$ | 203.96402 | 20 | 2.0 |
| 1 | $^{206}Pb$ | 205.95599 | 15 | 2.0 |
| 1 | $^{207}Pb$ | 206.95593 | 40 | 2.0 |
| 1 | $^{208}Pb$ | 207.95183 | 5 | 1.0 |
| 1 | $^{248}ThO$ | 248.01283 | 2 | 3.0 |
| 1 | $^{254}UO$ | 254.03274 | 2 | 3.0 |
| 2 | Bkgd2 | 5.52000 | 5 | 5.0 |
| 2 | $^{6}Li$ | 6.00547 | 25 | 3.0 |
| 2 | Bkgd3 | 6.95017 | 5 | 2.0 |
| 2 | $^{7}Li$ | 7.00472 | 2 | 1.0 |
| 3 | Bkgd4 | 5.52000 | 5 | 5.0 |
| 3 | $^{7}Li$ | 6.99597 | 2 | 1.0 |
| 3 | Bkgd5 | 8.89899 | 5 | 2.0 |
| 3 | $^{9}Be$ | 9.00794 | 2 | 2.0 |
| 3 | $^{24}Mg^{++}$ | 11.99508 | 2 | 2.0 |
| 3 | Bkgd6 | 13.84982 | 5 | 2.0 |
| 3 | $^{28}Si^{++}$ | 13.99301 | 2 | 1.0 |
| 3 | $^{16}O$ | 16.01132 | 2 | 2.0 |
| 3 | Bkgd7 | 17.38891 | 5 | 2.0 |
| 3 | $^{19}F$ | 19.01525 | 2 | 2.0 |
| 4 | Bkgd8 | 9.52000 | 5 | 5.0 |
| 4 | $^{10}B$ | 10.01979 | 10 | 1.0 |
| 4 | Bkgd9 | 10.50020 | 5 | 2.0 |
| 4 | $^{11}B$ | 11.01697 | 10 | 1.0 |

Instrumental conditions were mostly the same as described in Section 4.4.2.5 - Material Homogeneity. Additionally, the secondary ions for $^{11}B^+$:$^{10}B^+$ were collected in an electron-suppressed Faraday Cup. Total secondary beam current was measured using an Australian Scientific Instruments e7600 electrometer. The $^{11}B^+$ voltage across a $10^{11}$ Ω resistor was about 1 volt, implying a count rate of approximately 62 million cps. The other ions were detected with an electron multiplier. Two backgrounds peaks close to each isotope were used to account for a mass-dependent background caused by matrix ions scattered by the flight tube.

#### *4.4.5.2. Statistical Analysis*

For the elemental analyses, in each replicate every element signal was normalised to the $^{16}O^+$ signal and presented as 'counts per 100 counts of $^{16}O^+$'. The replicates were then averaged, and the mean ±3σ (99% confidence) was presented for every brand. Brand pairs for which the 99% confidence intervals did not overlap for the element were considered to be discriminated based on the element. The individual element discriminations were successively compiled, from most discriminating to least, to give an overall discrimination factor for the technique.

For the isotopic data, each isotope was considered individually, the mean and standard deviation for each brand was determined, all the brands were compared pair-wise via 95% confidence intervals (±2σ). Any pair combination that did not have overlapping intervals was considered to have been discriminated based on their isotope measurements. The $^{204}Pb^+$, $^{206}Pb^+$, $^{207}Pb^+$, $^{208}Pb^+$, $^{232}Th^+$ and $^{238}U^+$ isotope compositions were not sufficiently variable to allow discrimination based on the ratios and were not used further. SHRIMP isotopic discrimination power was based on B and Li data only.

### 4.4.6. **SEM-EDS**

#### *4.4.6.1. Analysis*

Samples were analysed using a FEI Inspect F50 Scanning Electron Microscope, fitted with an AMETEK EDAX detector, and using the xT microscope and TEAM EDS software. Ten grains of each sample were analysed to ensure that the results were representative of the entire sample. The elements detected were quantified (technique is standard-less and semi-quantitative) using the eZAF method, by oxide ratios. Optimal settings/conditions were determined to be as per Table 18.

**Table 18: Parameters for final SEM-EDS analyses**

| Parameter | Setting |
|---|---|
| Vacuum | ~$10^{-4}$ Pa |
| Working Distance | 10 mm |
| Take off Angle | 34.2° |
| Accelerating Voltage | 15 keV |
| Aperture Size | 20 mm |
| Emission Current | 110 µA |
| Count time | 50 sec |
| Spot size | 6 |
| Dead time | 33-34 % |
| Resolution | 123.1 eV |
| Counts per second | 23000-26000 cps |

#### *4.4.6.2. Statistical Analysis*

The semi-quantitative measurements for the selected elements for the ten particles analysed for each sample of frictionator were averaged and standard deviations and relative standard deviations were determined. The average elemental concentrations were compared to those measured for NIST SRM 93a and NIST SRM 612, which were treated as exemplars of borosilicate and soda lime glass, respectively, to determine the type of glass found in the ammunition. Confidence intervals (±3σ, representing a 99% interval) were determined for every brand of ammunition. The mean ±3σ intervals were compared for each combination of brands pairwise in order to determine the percentage of brands that could be discriminated. This was presented in a pairwise plot, and from that comparison, the discrimination power of the technique for these samples was determined.

#### *4.4.6.3. SEM-EDS for Determination of Primer Components*

A sample of the neat primer was analysed by bulk EDS analysis to determine primer components of the ammunition, to determine whether the additional primer components, other than the glass frictionator, could provide additional discrimination. Spectra were collected using a FEI Inspect F50 Scanning Electron Microscope, fitted with an AMETEK EDAX detector, and using the xT microscope and TEAM EDS software. Spectra were collected as above, except with an accelerating voltage of 30 keV, and the analysis was qualitative only. Results are as per Table 15.

.

### 4.4.7. GRIM

The refractive indices of the frictionator samples were determined to identify whether they had RI values typical of common window soda lime glasses or borosilicate glasses.

#### *4.4.7.1. Analysis*

A Foster and Freeman GRIM 3 instrument, with a Mettler Toledo hotstage model FP82HT and a phase contrast stereomicroscope set up for Köhler illumination was optimised for phase contrast measurements. The GRIM was calibrated using standard methods for the A and B oils (Foster and Freeman). As there are only two calibration standards for the C oil, the RI of NIST SRM 93a was used to verify the adequacy of the two-point calibration. This was achieved by comparing the RI measured for NIST SRM 93a with a separate measurement of the same glass carried out using another GRIM 3 instrument and using different calibration oil (Locke Scientific). As the two RIs matched within ±1 σ (Table 19), it was determined that the calibration was valid. The A oil covers a calibrated range of 1.5521 – 1.5290, the B oil covers a calibrated range of 1.5291 – 1.5023 and the C oil covers a calibrated range of 1.4865 – 1.4641.

Frictionator particles were placed onto slides, covered with B Oil, and the refractive index of each sample was determined, by determining the 'null point', that is, the temperature when the refractive index of the oil reaches that of the glass. Glasses that did not have a null temperature in the B oil were analysed in the C oil, and any that had no null point in either B or C were analysed in A.

**Table 19: Mean null temperature, refractive index and standard deviation of NIST 93a, as measured by two independent GRIM3 systems, identified by location.**

| | Forensic Science SA | Flinders University |
|---|---|---|
| **Number of measurements** | 20 | 8 |
| **Range of temperatures** | 88.47-89.04 | 92.96-93.4 |
| **Mean RI** | 1.47025 | 1.47014 |
| **Standard deviation (σ)** | 0.0000624 | 0.0000638 |
| **Range of RIs** | 1.47019 – 1.47044 | 1.47005 – 1.47024 |
| **Discrepancy** | 1 σ overlaps | 1 σ overlaps |

#### *4.4.7.2. Statistical Analysis*

Samples were compared using 99% confidence intervals, as the quality of edge matches were variable and the relatively large RSDs for some samples made t-tests or ANOVAs of the matches invalid.

## 4.5. Results and Discussion

### 4.5.1. Isotopic Composition of Li and B in CRMs

Table 20 presents the mean B isotope composition for the CRMs examined in this study. As can be observed, the $\delta^{11}B$ (‰) values determined for NIST SRM 951 and IAEA-B-4 are identical to the known reference values, confirming the accuracy of the method used in this study. The NIST SRM 93a samples from the two suppliers were indistinguishable from each other, as was expected (separate samples: 0.02 ± 0.1‰, 0.04 ± 0.04‰). The values recommended for $\delta^{11}B$ for NIST SRM 93a and NCS DC61104 are, therefore, 0.03 ± 0.08‰ and -6.74 ± 0.12‰, respectively, at the 95% confidence level.

**Table 20: Boron reference materials and samples, concentrations and $\delta^{11}B$ (‰), shown for individual solutions, and averaged for each sample Boron concentration and isotope composition for standards reference materials and samples**

| Samples | Description (source) | [B][1] % | Analysis of Each Solution of Samples $\delta^{11}B$ [‰] | | | Overall for each Sample $\delta^{11}B$ [‰] | |
|---|---|---|---|---|---|---|---|
| | | | Mean | 2 σ [‰] | n | Mean of means | 2 σ mean |
| NIST SRM 93a | Borosilicate glass (SPI Supplies) | 3.90 | 0.06 | 0.17 | 5 | 0.02 | 0.12 |
| | | | -0.02 | 0.07 | 5 | | |
| | Borosilicate glass, standard reference material (NIST) | 3.90 | 0.06 | 0.08 | 5 | 0.04 | 0.04 |
| | | | 0.02 | 0.03 | 5 | | |
| | | | 0.04 | 0.03 | 5 | | |
| | | | **TOTAL NIST SRM 93a** | | | **0.03** | **0.06** |
| NCS DC61104 | Borosilicate glass (LGC) | 2.75 | -6.80 | 0.10 | 5 | -6.74 | 0.12 |
| | | | -6.72 | 0.09 | 5 | | |
| | | | -6.78 | 0.10 | 5 | | |
| | | | -6.66 | 0.05 | 5 | | |
| **Reference materials** | **Description (source)** | **Literature Comparison Value** | **Analysis of Each Solution of Samples $\delta^{11}B$ [‰]** | | | **Overall for each Sample $\delta^{11}B$ [‰]** | |
| | | | **Mean** | **2 σ [‰]** | **n** | **Mean of means** | **2 σ [‰]** |
| NIST SRM 951 | Boric acid, standard reference material | $\delta^{11}B$ 0‰[2] | -0.09 | 0.12 | 11 | | |
| IAEA–B-4 | Tourmaline reference material | $\delta^{11}B$ -8.97 ± 0.13‰[3] | -8.88 | 0.06 | 5 | -8.91 | 0.08 |
| | | | -8.93 | 0.05 | 5 | | |
| Blank | Procedural blank [4.8 ng B][4] | | -2.7 | 0.1 | | | |

*[1] These values are derived from the respective samples' certificates of analyses*

*[2] $^{11}B/^{10}B$=4.04362±0.00137 (Catanzaro et al (1970)*

*[3] According to the most recent measurements in [272] M. Kutzschbach, B. Wunder, A. Meixner, R. Wirth, W. Heinrich, G. Franz, Jeremejevite as a precursor for olenitic tourmaline: consequences of non-classical crystallization pathways for composition, textures and B isotope patterns of tourmaline, European Journal of Mineralogy 29(2) (2017) 239-255.*

*[4] The amount of B in the analytical blanks is negligible compared to the amount present in the samples*

Table 21 presents the mean Li concentrations and isotope composition of the standards and reference materials examined by the Isotope Geochemistry Laboratory at University of Bremen in this study. As can be seen, the Li isotope compositions and concentrations determined for the RMs TB and G3, and the $\delta^7$Li value determined for RM TB are consistent with the known reference values.

The concentration for Li in NIST SRM 93a was measured to be 30 ± 3 µg/g with 95% confidence (separate samples: 29 ± 2.1 µg/g, 30.6 ± 0.3 µg/g) and the concentration of Li in NCS DC61104 was measured to be 105.5 ± 0.6 µg/g.

From the calculated averages and uncertainties, the values recommended for $\delta^7$Li for NIST SRM 93a and NCS DC61104 are, therefore, -21.0 ± 0.3‰ and -3.2 ± 0.08‰, respectively at the 95% confidence level. These data are the recommended values for future use.

**Table 21: Lithium isotopic composition and concentrations as determined by Isotope Geochemistry Laboratory at University of Bremen, for both isotopic standards and the samples of borosilicate reference materials.**

| Samples | Description (source) | | Analysis of Each Solution of Samples $\delta^7$Li [‰] | | | Overall for each Sample $\delta^7$Li [‰] | | Concentration Lithium | | |
|---|---|---|---|---|---|---|---|---|---|---|
| | | | Mean | 2 σ [‰] | n | Mean of means | 2 σ mean | Li (ug/g) | Li (ug/g) Mean | 2 σ mean |
| NIST SRM 93a | Borosilicate glass (SPI Supplies) | | -21.24 | 0.23 | 5 | -21.0 | 0.4 | 29.3 | 28.5 | 2.1 |
| | | | -20.97 | 0.26 | 5 | | | 27.3 | | |
| | | | -20.84 | 0.24 | 5 | | | 29.0 | | |
| | Borosilicate glass (NIST) | | -20.91 | 0.28 | 5 | -21.1 | 0.3 | 30.7 | 30.6 | 0.3 |
| | | | -21.18 | 0.24 | 5 | | | 30.4 | | |
| | | | -21.15 | 0.10 | 5 | | | 30.5 | | |
| | | | **TOTAL NIST SRM 93a** | | | **-21.0** | **0.3** | | **30** | **3** |
| NCS DC61104 | Borosilicate glass (LGC) | | -3.22 | 0.21 | 10 | -3.2 | 0.1 | 105.2 | 105.5 | 0.6 |
| | | | -3.16 | 0.17 | 10 | | | 105.7 | | |
| | | | -3.24 | 0.02 | 5/10 [5] | | | 105.6 | | |
| **Reference materials** | **Description (source)** | **Literature Comparison Value[6]** | **Analysis of Each Solution of Samples $\delta^7$Li [‰]** | | | | | | | |
| | | | **Mean** | **2 σ [‰]** | **n** | | | **Li (ug/g)** | | |
| NIST RM 8545 | Lithium Carbonate, reference Material (NIST) LSVEC | $\delta^7$Li 0‰ by definition[7] | -0.05 | 0.24 | 20 | | | | | |
| | | | -0.03 | 0.17 | 10 | | | | | |
| IAEA-B-4 | Tourmaline, quality control (IAEA) | | 4.1 | 0.5 | 5 | | | 615 | | |
| TB | Clay (ZGI), Reference Material | $\delta^7$Li‰ - 3.30±0.34 [Li] 104, 111 ppm | -3.2 | 0.3 | 10 | | | 104 | | |
| G3 | Granite (USGS), Reference Material | [Li] 32 ppm | 0.6 | 0.3 | 10 | | | 30.9 | | |
| Blank | Procedural blank [<6 pg Li] | | | | | | | | | |

[5] two different separations from one sample dissolution

[6] Reference data for TB are from [269] R.L. Romer, A. Meixner, K. Hahne, Lithium and boron isotopic composition of sedimentary rocks — The role of source history and depositional environment: A 250 Ma record from the Cadomian orogeny to the Variscan orogeny, Gondwana Research 26(3–4) (2014) 1093-1110. and [280] K. Govindaraju, 1994 COMPILATION OF WORKING VALUES AND SAMPLE DESCRIPTION FOR 383 GEOSTANDARDS, Geostandards Newsletter 18 (1994) 1-158., and data for G3 from [281] A.J.B. Cotta, J. Enzweiler, Classical and New Procedures of Whole Rock Dissolution for Trace Element Determination by ICP-MS, Geostandards and Geoanalytical Research 36(1) (2012) 27-50.

[7] $\delta^7Li = (({}^7Li/{}^6Li)_{sample}/({}^7Li/{}^6Li)_{L\text{-}SVEC} - 1)*1000$ in ‰. L-SVEC data comes from [284] G.D. Flesch, A.R. Anderson, H.J. Svec, A secondary isotopic standard for 6Li/7Li determinations, International Journal of Mass Spectrometry and Ion Physics 12(3) (1973) 265-272.

Results for repeat inter-fragment B isotope ratio analyses by SHRIMP for glass fragments from NIST SRM 93a and NCS DC61104 are provided in Table 22. For these analyses, no glass CRM with equivalent boron concentration and known homogeneity or a known $\delta^{11}B$ ratio exists. Thus, these CRMs can only be compared to each other. The standard deviation values of the mean ranged between 0.33 and 0.53 ‰ for NIST SRM 93a, and the standard deviation value of the mean for NCS DC61104 fit within this window (0.48 ‰). From these data, it can only be indicated that the CRMs are as homogenous as each other and are unlikely to contain grain-to-grain or cross-grain heterogeneities substantially larger than 1 ‰. As the work detailed later in this chapter is not particularly interested in the exact value for $\delta^{11}B$, rather whether differences in isotopic composition of the frictionators exist, these values were determined to be fit for purpose, although in future, more CRMs should be analysed for absolute heterogeneity to be further assessed.

Results for repeat inter-fragment Li isotope ratio analyses by SHRIMP for glass fragments from NIST SRM 93a, NIST SRM 612 and NCS DC61104 are provided in Table 23. NIST SRM 93a and NIST SRM 612 were analysed in two separate sessions. The standard deviations of the mean for NIST SRM 93a, and for NCS DC61104 were lower than NIST SRM 612 in session 150098, although it should be noted that only NIST SRM 93a from NIST was analysed in this session. Each source of NIST SRM 93a was measured independently in session 150096, and then the two datasets were averaged together to give a combined average. When comparing either or both sources of NIST SRM 93a to NIST SRM 612, NIST SRM 93a had the lower standard deviation of the mean. Therefore, these glasses were considered fit for purpose for Li isotope determination.

Table 22: Summary of SHRIMP measurements showing the homogeneity of the boron isotopic composition of NIST SRM 93a from SPI, NIST SRM 93a from NIST and NCS DC61104.

| Sample | Mean $^{11}B/^{10}B$ (Abs) | 1 $\sigma_{mean}$ [‰] | N | 95% CI (Abs) | 95% CI [‰] | MSWD | Reference value [‰] | Reference ratio | IMF [‰] | IMF ratio |
|---|---|---|---|---|---|---|---|---|---|---|
| **NIST SRM 93a sourced from NIST** | 3.90500 | 0.33 | 4 | 0.0023 | 0.59 | 2.9 | 0.03 | 4.04374 | -34.3 | 0.9657 |
| **NIST SRM 93a sourced from SPI Supplies** | 3.90682 | 0.53 | 17 | 0.00095 | 0.24 | 4.7 | 0.03 | 4.04374 | -33.9 | 0.9661 |
| **NIST SRM 93a combined** | 3.90648 | 0.5 | 21 | 0.00086 | 0.22 | 4.9 | 0.03 | 4.04374 | -33.9 | 0.9661 |
| **NCS DC 61104** | 3.86004 | 0.48 | 9 | 0.00087 | 0.23 | 2.9 | -6.74 | 4.01633 | -38.9 | 0.9611 |

Table 23: Summary of SHRIMP measurements showing the homogeneity of the lithium isotopic composition of NIST SRM 93a from SPI, NIST SRM 93a from NIST, NIST SRM 612 and NCS CRM DC61104.

| Session | Sample | Mean $^{7}Li/^{6}Li$ (Abs) | 1 $\sigma_{mean}$ [‰] | N | 95% CI (Abs) | 95% CI [‰] | MSWD | Reference value [‰] | Reference ratio | IMF [‰] | IMF ratio |
|---|---|---|---|---|---|---|---|---|---|---|---|
| **150096** | NIST SRM 93a sourced from NIST | 11.8830 | 2.7 | 17 | 0.015 | 1.3 | 5.6 | -21 | 11.917367 | -2.9 | -2.3 |
| | NIST SRM 93a sourced from SPI Supplies | 11.9070 | 2.1 | 15 | 0.013 | 1.1 | 3.4 | -21 | 11.917367 | -0.9 | -0.4 |
| | NIST SRM 93a combined | 11.8940 | 2.5 | 32 | 0.011 | 0.89 | 5.4 | -21 | 11.917367 | -2 | -1.4 |
| | NIST SRM 612 | 12.5640 | 3.5 | 23 | 0.019 | 1.5 | 7.4 | 32.1 | 12.5637533 | 0 | 0.9 |
| **150098** | NIST SRM 93a sourced from NIST | 12.0450 | 1.0 | 6 | 0.023 | 1.9 | 0.16 | -21 | 11.917367 | 10.7 | 11.0 |
| | NCS DC 61104 | 12.2160 | 1.8 | 11 | 0.013 | 1.1 | 0.87 | -3.2 | 12.1340464 | 6.8 | 6.7 |
| | NIST SRM 612 | 12.6830 | 1.9 | 6 | 0.025 | 2 | 0.73 | 32.1 | 12.5637533 | 9.5 | 10.7 |

### 4.5.2. **ToF-SIMS Analysis**

The 29 samples of frictionator from 17 brands were analysed *via* ToF-SIMS, along with three soda lime glass standards and two borosilicate glass standards. This technique was able to differentiate easily between samples that were borosilicate and those that were soda lime based on the relative size of the $^{11}B^+$ signal (see Figure 3). Previous work had indicated that the PMC ammunition could contain either borosilicate or soda lime glass frictionator [159]. In this work, the soda lime variant was observed. The RWS sample had a relatively high $^{11}B^+$ concentration compared to the soda lime glasses, indicating that it was likely to be a borosilicate glass, but the high $K^+$, $Ti^+$ and $Zn^+$ in this sample were not typical of the other borosilicate glasses seen, and in analyses by all of the techniques in this study it sat apart.

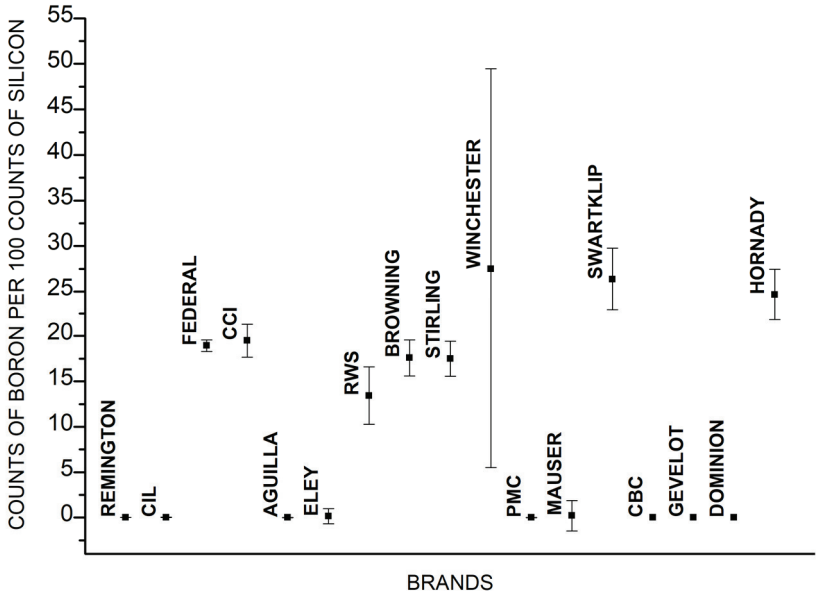


**Figure 22: Mean boron ($^{11}B^+$) signal as a percent of silicon ($^{28}Si^+$) signal for the 17 brands of ammunition examined, with 99% confidence intervals**

Although 13 separate Winchester frictionator samples were analysed from various Winchester brands, most pairs of Winchester samples were not readily distinguishable. Therefore, a single, averaged value of the entire group of samples is presented, and this is the reason for large standard deviations for measurements of Winchester frictionator. The standard deviations achieved for analysis of individual cartridges of Winchester ammunition were generally smaller than presented in this work, which could increase the discrimination powers discussed.

Ion signals were plotted as counts normalised to $^{28}Si^+$ (per 100 counts), as mean ±3σ. 52 of the ions identified were plotted in this way. For example, Figure 23 shows the plot for the ion identified as $^{41}K^+$. The statistical approach used to analyse the data was based on one devised by Trejos et al. [164],

where each pair of samples is compared for every element using ±3σ for each element; if any element does not match within that criterion, then the samples are considered to not match.

From this, a discrimination plot was created for each ion. The discrimination plot for $^{41}K^{+}$ is shown in Figure 24, where 95 pairs out of 136, or 69.9% of the brands can be discriminated by the $^{41}K^{+}$ ion alone. This was the most discriminating ion, followed by boron ($^{11}B^{+}$), and aluminium ($^{26}Al^{+}$). The ions detected in the frictionator set were ranked from most discriminating down, and ions added to the total discrimination plot until no more pairs could be discriminated. The result of this, showing a discrimination power of 94.1% is shown in Figure 25, as is the successive contribution of each ion.

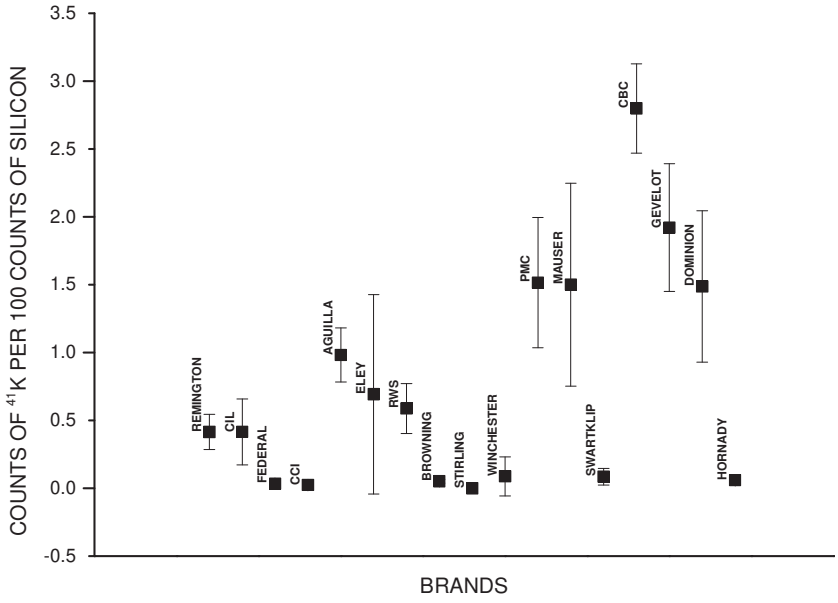


**Figure 23: Plot showing mean counts of $^{41}K^{+}$ per 100 counts of $^{28}Si^{+}$ ±3σ for all brands**

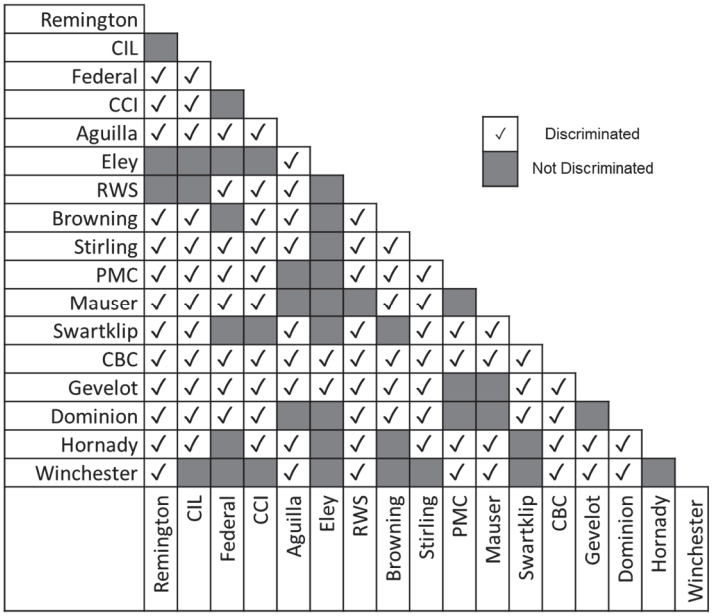


**Figure 24: 99% discrimination plot for ToF-SIMS analysis of the $^{41}K^{+}$ ion**

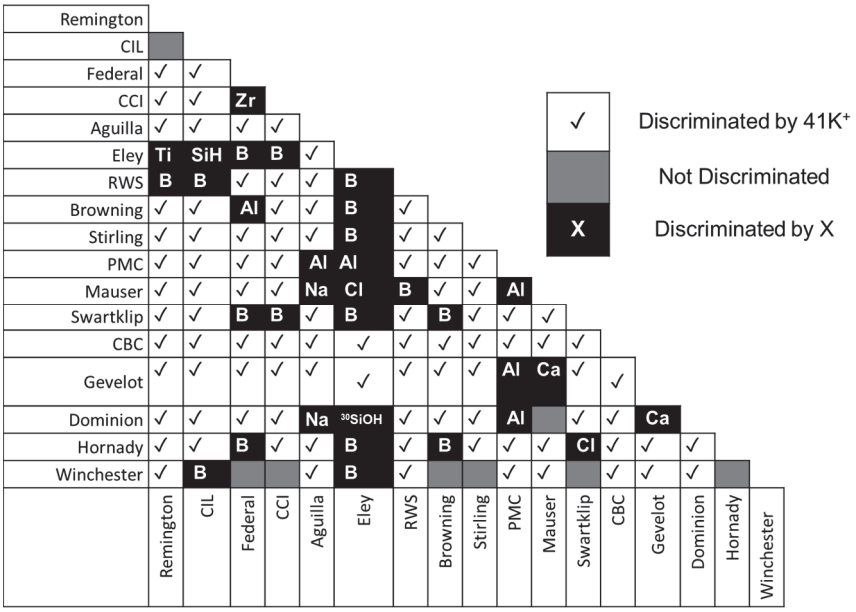


**Figure 25: Discrimination plot of frictionator brands showing successively compiled ToF-SIMS ions**

**Table 24: Successive discrimination pairs of frictionator brands added by ToF-SIMS ions**

| Ions | Added discrimination | Percent discriminated | Cumulative total | Cumulative percent |
|---|---|---|---|---|
| $^{41}K^+$ | 95 | 69.9 | 95 | 69.9 |
| $^{11}B^+$ | 17 | 12.5 | 112 | 82.4 |
| $^{27}Al^+$ | 6 | 4.49 | 118 | 86.8 |
| $^{35}Cl^+$ | 2 | 1.47 | 120 | 88.2 |
| $^{23}Na^+$ | 2 | 1.47 | 122 | 89.7 |
| $^{40}Ca^+$ | 2 | 1.47 | 124 | 91.2 |
| $^{48}Ti^+$ | 1 | 0.74 | 125 | 91.9 |
| $^{91}Zr^+$ | 1 | 0.74 | 126 | 92.6 |
| $^{28}SiH^+$ | 1 | 0.74 | 127 | 93.4 |
| $^{30}SiOH^+$ | 1 | 0.74 | 128 | 94.1 |
| **TOTAL (136)** | | | | |
| **Discriminated** | 128 | 94.1 | | |
| **Un-discriminated** | 8 | 5.9 | | |

After determining the inter-brand discrimination power, the intra-brand discrimination power was also investigated for the 13 Winchester samples. These included several variants, with the details of each sample shown in Table 15. A plot showing the Winchester intra-band discrimination achieved is shown in Figure 26. From this plot, it can be determined that 40/78, or approximately 51% of the pairs could be discriminated. However, when compared to the inter-brand results, the differences examined are far subtler. Whilst most of the pairs that were classed as 'discriminated' in the inter-brand comparison had differences in the abundance of several ions, most 'discriminated' samples of Winchester had only one or two ions with abundances outside the 99% confidence intervals. Additionally, the variation for each element was also significantly smaller. For example, Figure 27, showing the $^{41}K^+$ abundance for the 13 Winchester samples has a range approximately 14x smaller than that of the $^{41}K^+$ abundance for the 17 brands examined earlier (Figure 23). Additionally, it should be noted that from the analysis of the Winchester samples appeared to be no correlation between similarities or combinations that could be discriminated and the Winchester variant or headstamp.

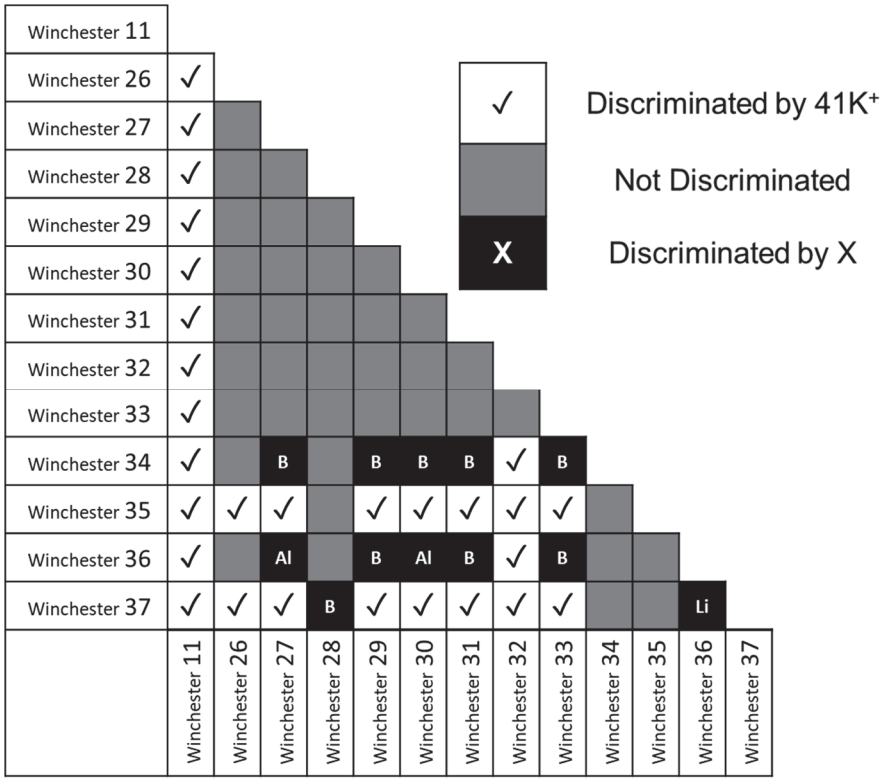


**Figure 26: 99% confidence plot showing pair-wise discrimination of ToF-SIMS for Winchester Samples (by sample number from Table 15)**

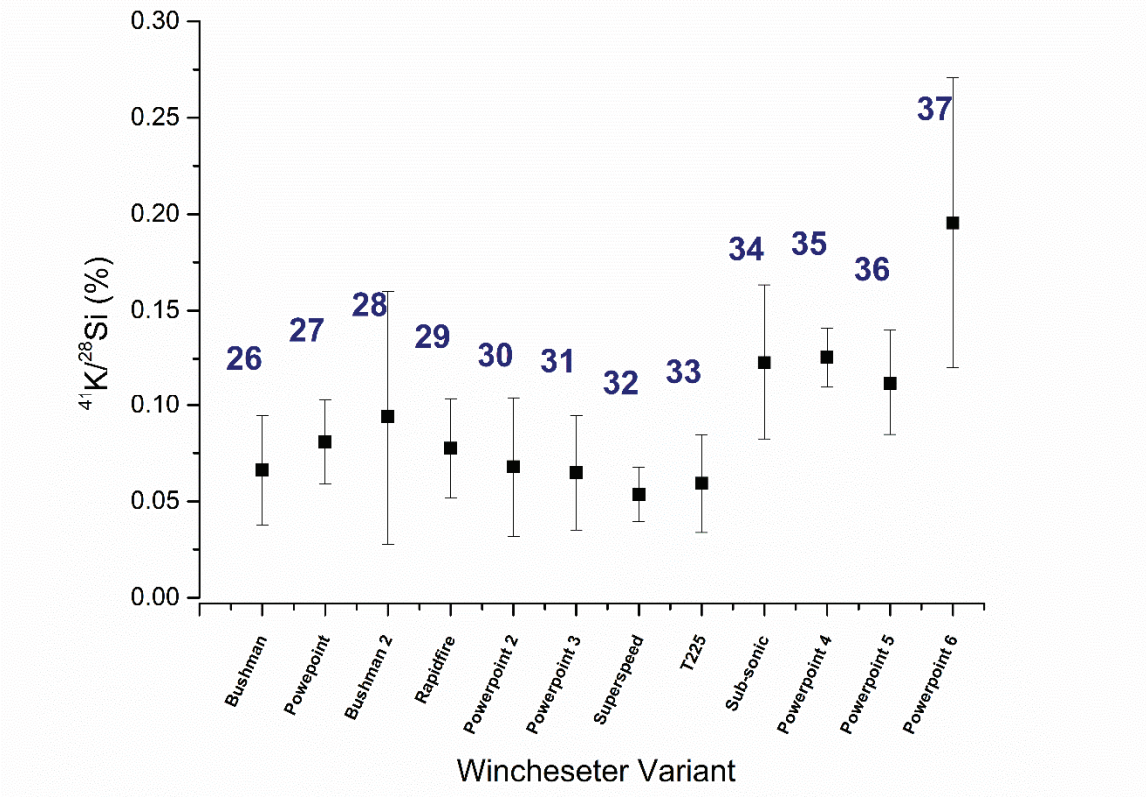


**Figure 27 Mean boron ($^{41}K^+$) signal as a percent of silicon ($^{28}Si^+$) signal for the 13 Winchester items examined, with 99% confidence intervals**

### 4.5.1. SHRIMP Elemental Composition Analysis

The mounted frictionator samples were analysed by SHRIMP for $^{7}Li^{+}$, $^{9}Be^{+}$, $^{19}F^{+}$, $^{28}Si^{++}$, $^{16}O^{+}$ and $^{24}Mg^{++}$ concentrations. The concentrations of these ions, presented in counts relative to $^{16}O^{+}$, were plotted with 99% confidence intervals. The plot for $^{7}Li^{+}$ is seen in Figure 28, which shows that there are some differences that allow differentiation. From the successive layering of these plots, a 99% confidence discrimination plot was created, and as can be seen in Figure 29, 95 out of 136 or 69.9% of pairs of brands could be discriminated by this method.

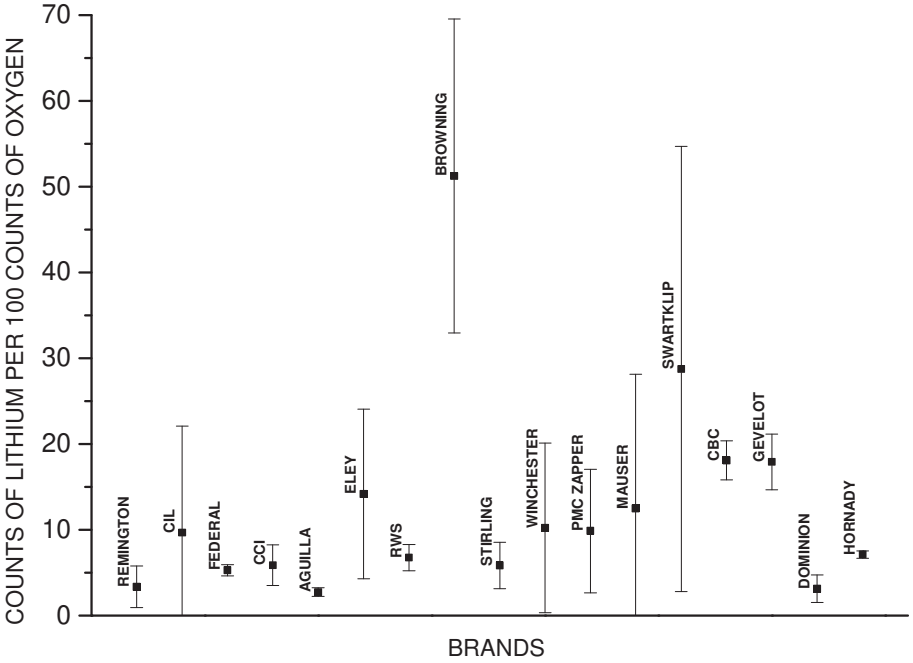


**Figure 28: $^{7}Li^{+}$ elements analysed by SHRIMP, presented as counts relative to oxygen ($^{16}O+$)**

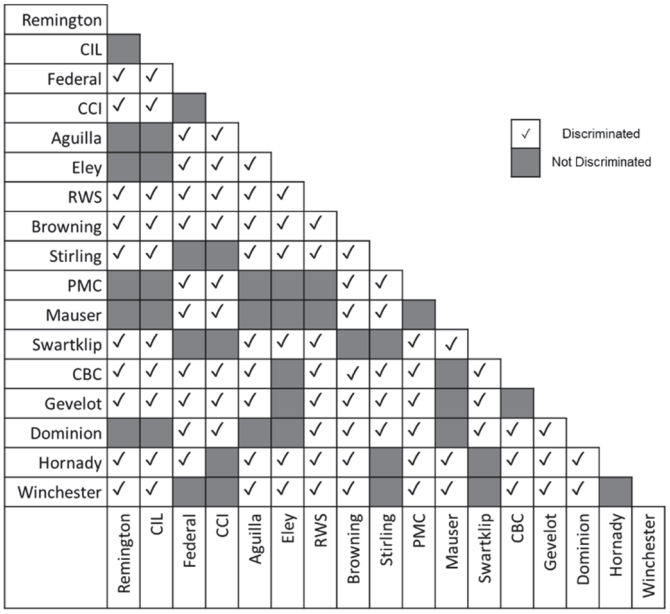


**Figure 29: 99% discrimination plot compiled from SHRIMP elemental composition analyses**

### 4.5.2. SHRIMP Isotope Analysis

In the first instance, the boron isotopic ($\delta^{11}B$) composition was determined for each of the samples where B was a major or minor element. The results, seen in Figure 30, indicate that although SHRIMP is a very powerful technique, and small differences in isotopic composition can be detected through this method, the isotopic variation in the borosilicate glass samples is very small. However, some variation exists, and it was found that 7 out of 28 borosilicate pairs can be distinguished (25%).

The lithium isotopic ($\delta\ ^{7}Li$) composition was also examined. This analysis, shown in Figure 31, also showed that most samples are not distinguishable from each other. The discrimination plot for Li indicated that only 3 out of 120 pairs (2.5%) could be discriminated, leaving 117 pairs that could not. The Swartklip sample was missing from this dataset due to instrumental difficulty.

When the Li and B discrimination factors are compiled, with 95% confidence, 10 out of 136 pairs, or 7.3% can be discriminated. The isotopic compositions of both Li and B were more restricted in the frictionator glasses than had been anticipated. As a result, they were less useful as discriminants for differentiating these particular glass samples. This may indicate glass feedstock sourced from a relatively small number of mineral suppliers.

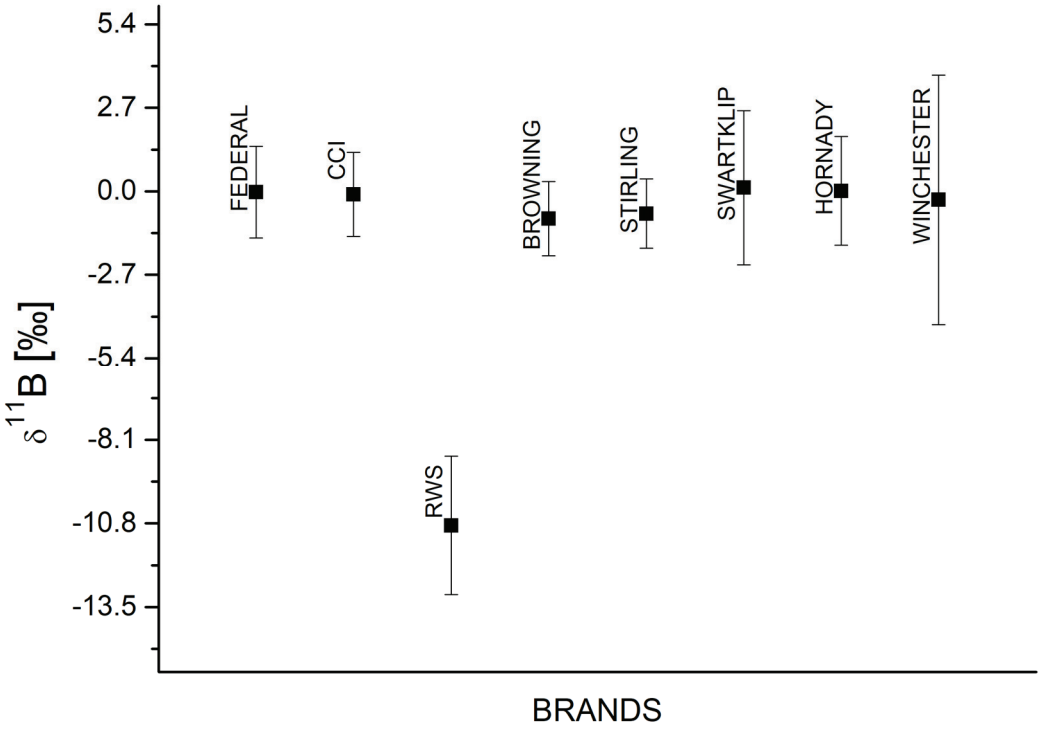


**Figure 30: Average $\delta^{11}B \pm 2\sigma$ for borosilicate glass frictionators (relative to LSVEC)**

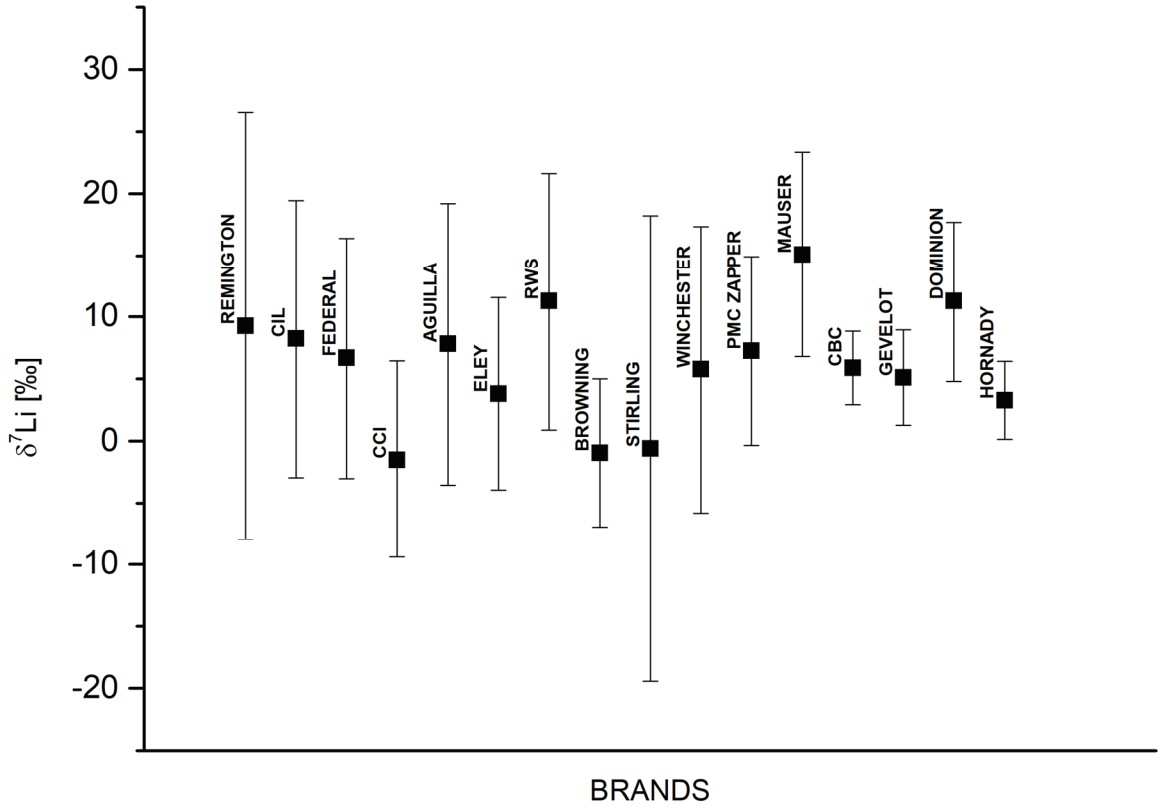


**Figure 31: Average $\delta^7$Li [‰], ± 2σ for glass frictionators (relative to LSVEC)**

$^{204}Pb^+$, $^{206}Pb^+$, $^{207}Pb^+$, $^{208}Pb^+$, $^{232}Th^+$ and $^{238}U^+$ isotopes were additionally analysed *via* SHRIMP. Various ratios were calculated between these isotopes, but the concentrations of these elements were low ppb to ppt range, and therefore the precision of the measurements was low, which lead to the intra-sample variation eclipsing any inter-sample variation. The lead, thorium and uranium isotopic compositions were not considered to have useful discrimination power for these samples.

When the data obtained from SHRIMP elemental analyses are combined with the isotopic composition results, the total discrimination power gained from SHRIMP analyses can be calculated. The isotopic data ($\delta^{11}$B and $\delta^7$Li) were less discriminating than the elemental measurements and did not provide further discrimination compared to the elemental measurements. The final discrimination power for SHRIMP was therefore 69.9%. A consideration when SHRIMP is used is that for each elemental run or isotopic measurement a volume of approximately 30 µm in diameter and 10 µm in depth is ablated from the sample. In casework, the small size of GSR particles could limit the number of analytical replicates per particle, thus diminishing measurement precision.

### 4.5.3. SEM-EDS Analysis

Elements in ten individual grains for each sample were quantified; concentrations and standard deviations were determined. $B_2O_3$ was detected in inflated concentrations compared to the true values. It appeared that the quantification software over-compensated for the instrumental difficulties in detecting $B_2O_3$, and $B_2O_3$ was detected in all standards and samples, regardless of whether it was present in levels detectable by SEM-EDS or not. By comparing the relative 'concentrations' determined by the SEM-EDS to the NIST SRM 612 values where the true concentration B is below the detection limit of EDS analysis, and then to NIST SRM 93a, where the true concentration is above the detection limit of EDS, B was classified as either detected or not detected for each sample. From this, it was possible to re-affirm which of the glasses were borosilicate, and which were soda lime glasses.

The relative concentrations determined for each of the elements appeared to be both consistent and effective as a means of classification; as such semi-quantitative results are presented in Table 25.

For each element, the mean and 99% confidence intervals (±3σ) were plotted for all brands, in the manner seen in Figure 32. From this, a discrimination plot for each element (99% confidence) was created to show whether each pair could or could not be discriminated by the element. Concentration and discrimination plots were created for $Na_2O$, $B_2O_3$, MgO, $Al_2O_3$, $K_2O$, and CaO. The individual element discrimination plots were layered, so that in the final plot (Figure 33) tiles with ticks show pairs that can be discriminated by one or more elements and grey tiles show pairs that cannot be discriminated by any element. After the consideration of all the elements, 108 of the 136 pairs (79.4%) could be discriminated.

When this work was extended to intra-brand analysis of samples from Winchester ammunition, it was found that none of the Winchester frictionator samples could be discriminated from any other using SEM-EDS analysis.

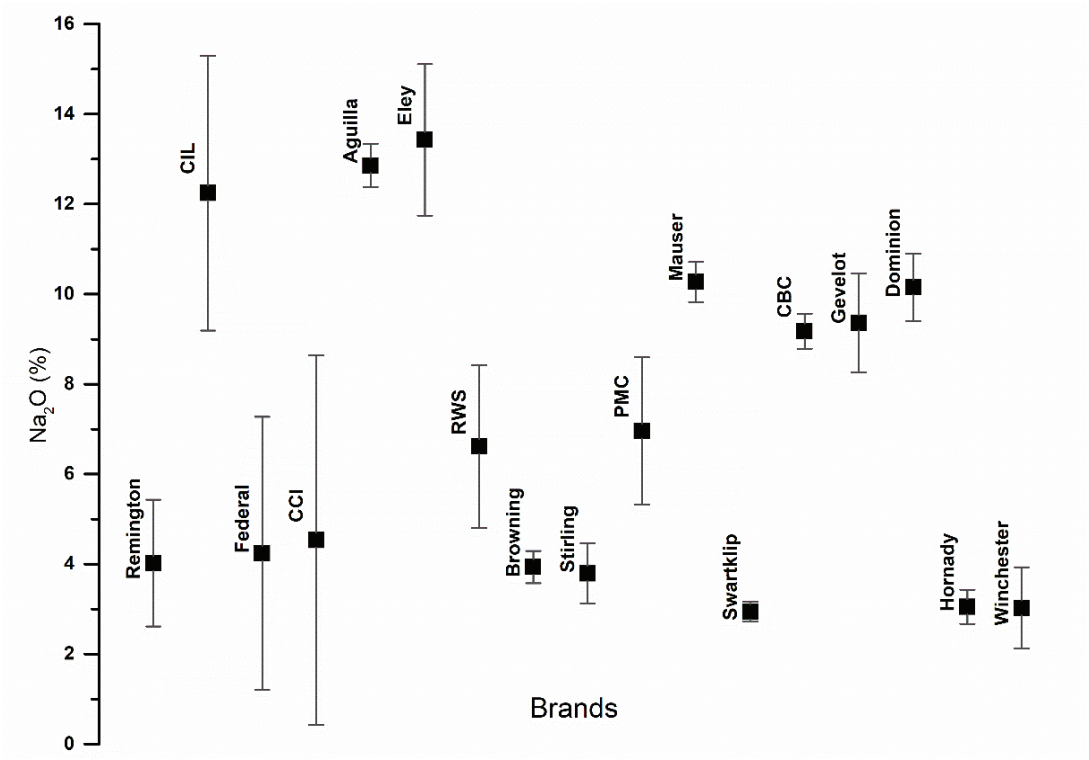


**Figure 32: Mean $Na_2O$ concentrations with 99% confidence intervals showing which pairs can be discriminated by $Na_2O$ concentration**

Table 25: SEM-EDS (weight %) quantification results for the analysis of 29 samples of frictionator by brand, and 3 reference materials, shown as average ± 3σ.

| Sample | $B_2O_3$ | $Na_2O$ | MgO | $Al_2O_3$ | $SiO_2$ | $K_2O$ | CaO |
|---|---|---|---|---|---|---|---|
| **NCS CRM DC 61104** | detected | 0.03 ± 0.04 | 3.7 ± 0.2 | 11.5 ± 0.3 | 38.2 ± 1 | 0.55 ± 0.1 | 13.5 ± 0.5 |
| **NIST SRM 93a** | detected | 3.2 ± 1 . | 0.21 ± 0.1 | 2.5 ± 0.8 | 61.1 ± 21 | 0.18± 0.1 | 0.11± 0.09 |
| **NIST SRM 612** | not detected | 11.6 ± 1 . | 0.13 ± 0.1 | 2.1 ± 0.6 | 54.9 ± 17 | 0.13 ± 0.1 | 10.0 ± 3 |
| **Remington** | not detected | 4.0 ± 2 | 3.6 ± 1 | 0.74 ± 0.5 | 72.5 ± 2 | 0.16 ± 0.3 | 8.6 ± 2 |
| **CIL** | not detected | 12.2 ± 3 | 3.2 ± 2 | 1.5 ± 1 | 59.6 ± 16 | 0.36 ± 0.7 | 7.8 ± 4 |
| **Federal** | detected | 4.2 ± 3 | 0.23 ± 0.07 | 3.2 ± 3 | 70.1 ± 12 | 0.29 ± 0.4 | 0.16 ± 0.4 |
| **CCI** | detected | 4.5 ± 4 | 0.24 ± 0.09 | 3.6 ± 4 | 69.5 ± 6 | 0.38 ± 0.9 | 0.21 ± 0.5 |
| **Aguilla** | not detected | 12.9 ± 0.5 | 3.4 ± 2 | 0.60 ± 0.2 | 61.5 ± 2 | 0.11 ± 0.1 | 8.4 ± 2 |
| **Eley** | not detected | 13.4 ± 2 | 0.75 ± 1 | 2.0 ± 1 | 62.2 ± 3 | 0.62 ± 1 | 9.2 ± 2 |
| **RWS** | detected | 6.6 ± 2 | 0.34 ± 1 | 5.0 ± 2 | 58.3 ± 6 | 5.90 ± 5 | 0.67 ± 3 |
| **Browning** | detected | 3.9 ± 0.4 | 0.23± 0.07 | 3.0 ± 0.4 | 71.0 ± 9 | 0.20 ± 0.09 | 0.13 ± 0.1 |
| **Stirling** | detected | 3.8 ± 0.7 | 0.23 ± 0.2 | 2.8± 0.8 | 69.8 ± 16 | 0.21 ± 0.2 | 0.12 ± 0.09 |
| **PMC** | not detected | 7.0 ± 2 | 0.97 ± 0.2 | 2.8 ± 0.4 | 45.4 ± 4 | 5.5 ± 3 | 1.6 ± 0.2 |
| **Mauser** | not detected | 10.3 ± 0.5 | 1.7 ± 4 | 1.5 ± 1 | 50.0 ± 2 | 0.38 ± 0.3 | 7.9 ± 2 |
| **Swartklip** | detected | 2.9 ± 0.2 | 0.22 ± 0.1 | 2.3 ± 0.2 | 56.6 ± 2 | 0.17 ± 0.08 | 0.10 ± 0.05 |
| **CBC** | not detected | 9.2 ± 0.4 | 2.9 ± 0.09 | 1.5 ± 0.05 | 50.5 ± 2 | 0.65 ± 0.07 | 6.5 ± 0.3 |
| **Gevelot** | not detected | 9.4 ± 1 | 2.9 ± 0.2 | 1.5 ± 0.2 | 50.8 ± 2 | 0.65 ± 0.1 | 6.5 ± 0.64 |
| **Dominion** | not detected | 10.2 ± 0.7 | 2.9 ± 0.2 | 0.90± 1.0 | 50.0 ± 2 | 0.20 ± 0.3 | 6.5 ± 0.3 |
| **Hornady** | detected | 3.1 ± 0.4 | 0.20 ± 0.1 | 2.2 ± 0.1 | 56.2 ± 2 | 0.16 ± 0.1 | 0.08 ± 0.06 |
| **Winchester** | detected | 3.0 ± 0.9 | 0.22 ± 0.1 | 2.3 ± 0.5 | 57.2 ± 13 | 0.17 ± 0.1 | 0.10 ± 0.07 |

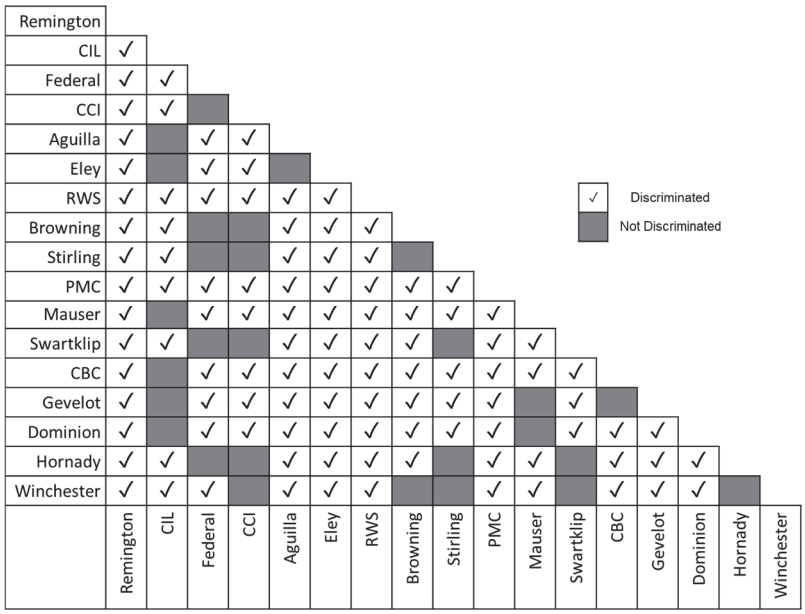


**Figure 33: 99% discrimination plot for SEM-EDS analysis created by successively layering individual discrimination factors**

### 4.5.4. Comparison and Contrast of Techniques.

The techniques applied to the analysis of frictionators shows that there is variance in the glass used across the ammunition market. However, the variation was not as large as expected and even stable isotope analyses using SHRIMP, a technique expected to provide significant further discrimination between frictionators, was not as powerful as anticipated. A summary of the discrimination power of each technique is shown in Table 26.

ToF-SIMS has the highest individual discrimination power, measures the widest range of elements, measures all elements simultaneously, has very low detection limits (low ppm) and affects only the top tens of angstroms of the sample's surface. It is thus a very effective approach even when used without combination with another technique.

SHRIMP features a high-resolution mass analyser, which can resolve peaks that would interfere on most mass spectrometers. It can measure isotope ratios and it has the lowest detection limit of all the techniques (less than ppb for some elements, in optimum setup [190]). However, it can only measure a few ions in a limited mass range at any time, and is the most time-consuming technique, especially regarding locating GSR particles on SEM stubs. This technique is also more destructive than ToF-SIMS and is possibly unsuitable for analysis of typical small particles encountered in casework. Furthermore, the precision observed for measurement of B and Li isotope ratios was relatively low, so much so that discrimination between samples difficult, even when 95% confidence intervals were applied.

Comparatively, SEM-EDS has a high limit of detection (~0.1%), has relatively low elemental resolution (especially regarding resolution of B from C) and it cannot easily detect elements with low atomic number. However, it also is the fastest and cheapest technique examined and the one most widely available to forensic laboratories. As a stand-alone technique for the analysis of frictionators it achieved a discrimination power of over 79%, which was surprising as only seven oxides were used for the discrimination.

The discrimination power within the dataset examined could be increased by combining two or more of these techniques. For example, SEM-EDS and SHRIMP results each discriminated one pair that ToF-SIMS did not, and SHRIMP results discriminated eight pairs that SEM-EDS did not. The discrimination power for all combinations is shown in Table 27, which shows that the use of all 3 techniques provides the highest discrimination power, however the combination of ToF-SIMS and SEM-EDS would most likely be the most efficient use of resources in casework. It would allow an independent analysis *via* two techniques, one of which is a standard technique that most likely would have already been applied in a typical GSR examination. The approach would preserve the sample for re-examination and these techniques are quicker and require less sample preparation than SHRIMP. Although both SHRIMP and ToF-SIMS are specialized techniques, ToF-SIMS is more widely available.

LA-ICP-MS, although a commonly used technique in the forensic analysis of glass, was not used in this survey. This was because the particle sizes for extracted frictionator were barely large enough for effective LA-ICP-MS analysis and for the analysis of genuine glass-containing GSR, the particles are even smaller, and the technique would therefore not be suitable.

**Table 26: Summary of discrimination power of each analytical technique**

| Techniques | Pairs Discriminated | Discrimination Power |
|---|---|---|
| **ToF-SIMS** | 128/136 | 94.1% |
| **SEM-EDS** | 108/136 | 79.4% |
| **SHRIMP** | 95/136 | 69.9% |

**Table 27: Discrimination power of various combinations of the techniques used in this study, compared to ToF-SIMS**

| Techniques | Pairs Discriminated | Discrimination Power |
|---|---|---|
| **ToF-SIMS** | 128/136 | 94.1% |
| **ToF-SIMS & SHRIMP** | 129/136 | 94.9% |
| **ToF-SIMS & SEM-EDS** | 129/136 | 94.9% |
| **SEM-EDS & SHRIMP** | 116/136 | 85.3% |
| **Total (3 techniques)** | 130/136 | 95.6% |

### 4.5.5. Refractive Index Measurement

Refractive index measurements were carried out to characterise the frictionator samples further. Frictionator samples that had a refractive index null point in the B oil are shown in Figure 34, and those that had a refractive index null point in the C oil are shown in Figure 36. The glass standard reference materials and 29 frictionator samples were measured by GRIM analysis. NIST SRM 93a had a null point in oil C and NIST SRM 612 had a null point in oil B, which is to be expected for borosilicate and soda lime glasses, respectively [285]. One frictionator sample, which was extracted from Gevelot ammunition (no. 20), did not have a RI matching in any of the oils, despite its elemental profile suggesting that it is made from soda lime glass. Frictionator extracted from Swartklip ammunition (no. 17) had many different null points at across the RI range of the B Oil, and an average RI or range of RIs was unable to be determined. Frictionator from RWS and PMC Zapper ammunition were quite interesting in that they achieved the highest RI of all the samples tested, which would indicate that they were made from soda lime glass, but each contained low levels of Ca and Na. Conversely, glass from Mauser ammunition returned an RI value consistent with borosilicate glass yet it also contained high-levels of Ca and Na. The pertinent figures summarising the refractive index measurements are found in Table 28.

It was observed that the frictionator grains from most samples were already in the correct size domain for GRIM analysis, and if they were to be crushed to produce clean, sharp edges they would be too small for analysis. Due to this, there were few edges of high enough quality to allow the measurement at the level of precision typical for forensic examination of glass evidence.

ANOVA was the first, logical choice considered for the comparison of RI values, and the data obtained were evaluated for analysis by ANOVA. The validity of results from any statistical test depends on whether the dataset meets the assumptions that underlie that test. The assumptions about a dataset used for ANOVA are: independence of cases, normality of the population and homoscedasticity of the population. As the differences in standard deviations between samples was large, with some samples having a much higher intrasample variability than others, statistical comparison analyses via ANOVA was not possible for the frictionator samples. Therefore, frictionator samples were analysed by comparing 99% confidence intervals instead.

The GRIM results from this survey indicate that for most ammunition products examined, the glass frictionator present has low intra-sample variability, with Swartklip ammunition being a notable exception. The use of borosilicate glass or soda lime glass, and the narrow range of RIs in both the borosilicate and soda lime glass samples is a curiosity, as controlling the glass in ammunition would

not be the cheapest option for ammunition manufacturers. Prior to research it was expected that a wide range of soda lime glass, possibly obtained from glass recycled from many sources, may have been used as a frictionator, but this does not seem to be borne-out in this study.

The data acquired regarding Winchester frictionator is particularly interesting. Although ammunition from twelve different batches produced over many decades was examined (as indicated by the head stamps logos of the cartridges, known to have been used during different eras) all the frictionators examined were of the borosilicate type and for practical purposes exhibited identical RI, elemental and isotopic composition. As an example, Figure 35 shows that the refractive indices of the Winchester samples are very similar. The consistent nature of the borosilicate glass observed within and across brands may indicate some control or optimisation of the glass used as frictionators in 0.22 calibre rimfire ammunitions.

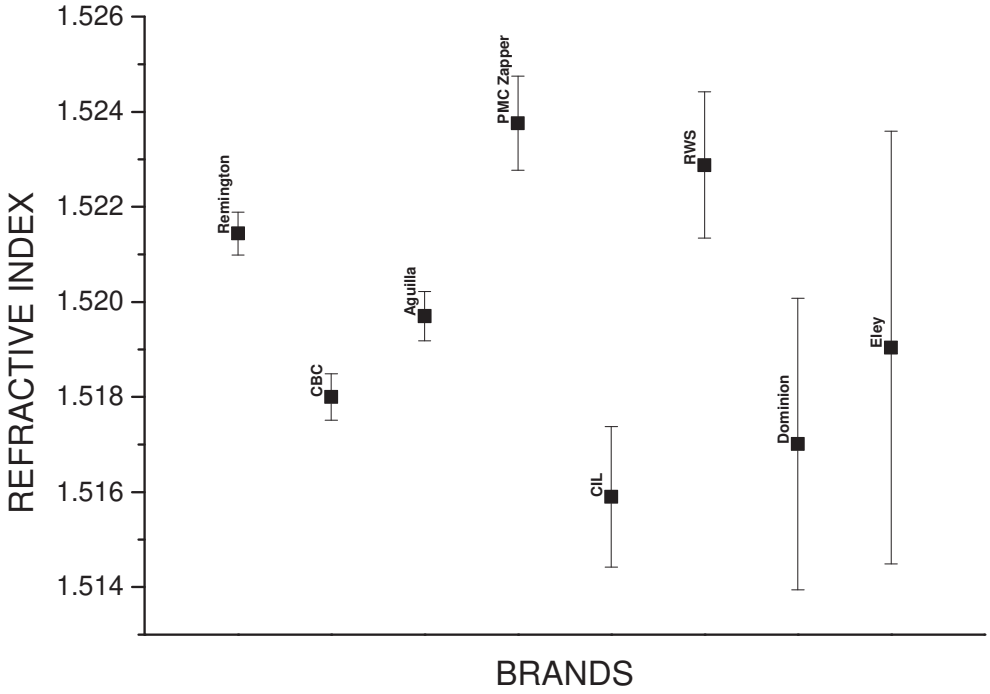


**Figure 34: Mean refractive indices ±3σ of frictionator samples which had a null temperature in the B oil**

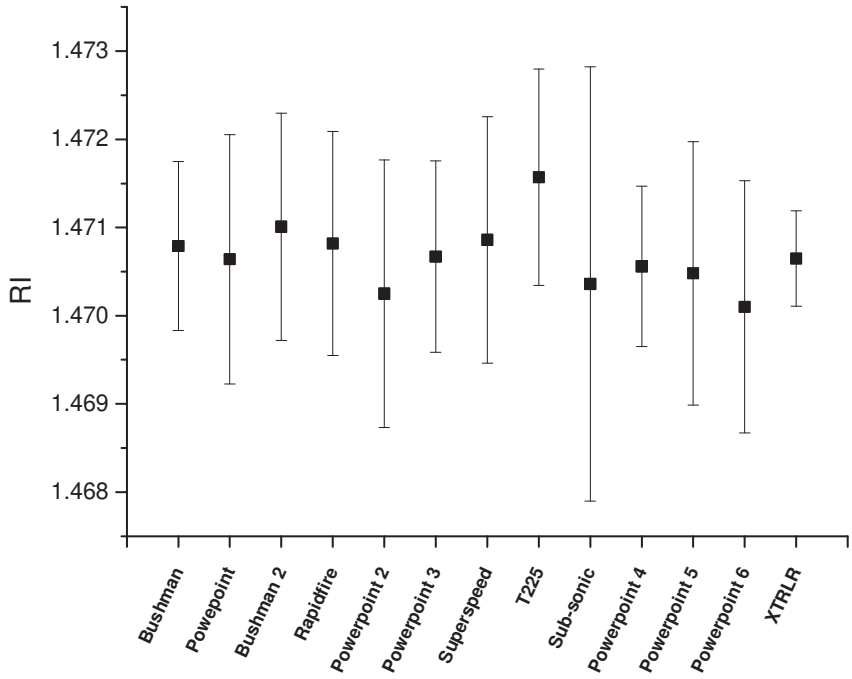


**Figure 35: RI Values for the 13 Winchester samples, including 7 different 0.22 variants**

Table 28: Results of GRIM analysis for frictionator samples successfully extracted from cartridges or 0.22 calibre rimfire ammunitions.

| # | Sample | N | Oil of null point | Mean Temperature of null point | Mean RI | σ (RI) | 3 σ | Range of RIs |
|---|---|---|---|---|---|---|---|---|
| | **NIST 93a** | 8 | C | 93.19 | 1.47014 | 0.0000638 | 0.0001914 | 1.47005-1.47024 |
| | **LGC** | 4 | None | none | n/a | n/a | n/a | n/a |
| | **NIST 612** | 10 | B | 59.07 | 1.52191 | 0.0000288 | 0.0000864 | 1.52188-1.52196 |
| **1** | **Remington** | 8 | B | 60.37 | 1.52144 | 0.0001502 | 0.0004506 | 1.52132-1.52176 |
| **2** | **CIL** | 10 | B | 75.49 | 1.51590 | 0.0004925 | 0.0014775 | 1.51498-1.51661 |
| **3** | **Federal Champion** | 10 | C | 91.35 | 1.47092 | 0.0002218 | 0.0006654 | 1.47065-1.47141 |
| **5** | **CCI** | 10 | C | 91.42 | 1.47089 | 0.0004446 | 0.0013338 | 1.47024-1.47168 |
| **6** | **Aguilla** | 8 | B | 65.13 | 1.51970 | 0.0001714 | 0.0005142 | 1.51943-1.51993 |
| **7** | **Eley** | 11 | B | 66.93 | 1.51904 | 0.0015168 | 0.0045504 | 1.51640-1.52066 |
| **8** | **RWS** | 8 | B | 56.43 | 1.52288 | 0.0005131 | 0.0015393 | 1.52215-1.52362 |
| **9** | **Browning** | 12 | C | 91.41 | 1.47089 | 0.0004855 | 0.0014565 | 1.46995-1.47152 |
| **10** | **Stirling** | 11 | C | 91.19 | 1.47098 | 0.0004162 | 0.0012486 | 1.47038-1.47164 |
| **11** | **Winchester** | 12 | C | 91.99 | 1.47065 | 0.0003188 | 0.0009564 | 1.47010-1.47117 |
| **12** | **PMC Zapper** | 9 | B | 54.02 | 1.52376 | 0.0003293 | 0.0009879 | 1.52322-1.52408 |
| **14** | **Mauser** | 11 | C | 90.63 | 1.47122 | 0.0006724 | 0.0020172 | 1.47048-1.47233 |
| **17** | **Swartklip** | n/a | B | N/a | N/a | N/a | N/a | N/a |
| **19** | **CBC** | 10 | B | 69.76 | 1.51800 | 0.0001658 | 0.0004884 | 1.51770-1.51822 |
| **20** | **Gevelot** | 4 | None | None | n/a | n/a | n/a | n/a |
| **23** | **Dominion** | 7 | B | 72.46 | 1.51701 | 0.0010215 | 0.0030645 | 1.51573-1.51862 |
| **25** | **Hornady** | 10 | C | 92.34 | 1.47050 | 0.0002083 | 0.0006249 | 1.47018-1.47081 |
| **26** | **Winchester Bushman** | 11 | C | 91.64 | 1.47079 | 0.0004716 | 0.0014148 | 1.47012-1.47173 |
| **27** | **Winchester Powerpoint** | 12 | C | 92.02 | 1.47064 | 0.0004291 | 0.0012873 | 1.46990-1.47122 |
| **28** | **Winchester Bushman (2)** | 11 | C | 91.12 | 1.47101 | 0.0004236 | 0.0012708 | 1.47041-1.47182 |
| **29** | **Winchester Rapidfire** | 11 | C | 91.57 | 1.47082 | 0.0005054 | 0.0015162 | 1.46989-1.47150 |
| **30** | **Winchester Powerpoint (2)** | 12 | C | 92.93 | 1.47025 | 0.0003615 | 0.0010845 | 1.46972-1.47109 |
| **31** | **Winchester Powerpoint (3)** | 12 | C | 91.93 | 1.47067 | 0.0004655 | 0.0013965 | 1.46997-1.47144 |
| **32** | **Winchester Superspeed** | 13 | C | 91.48 | 1.47086 | 0.0004084 | 0.0012252 | 1.47017-1.47149 |
| **33** | **Winchester T225** | 13 | C | 89.80 | 1.47157 | 0.0008208 | 0.0024624 | 1.47027-1.47304 |
| **34** | **Winchester Sub-Sonic** | 11 | C | 92.67 | 1.47036 | 0.0003025 | 0.0009075 | 1.46993-1.47096 |
| **35** | **Winchester Powerpoint (4)** | 12 | C | 92.21 | 1.47056 | 0.0004975 | 0.0014925 | 1.46967-1.47141 |
| **36** | **Winchester Powerpoint (5)** | 12 | C | 92.39 | 1.47048 | 0.0004767 | 0.0014301 | 1.46980-1.47134 |
| **37** | **Winchester Powerpoint (6)** | 12 | C | 93.27 | 1.47010 | 0.0001800 | 0.0005400 | 1.46984-1.47051 |

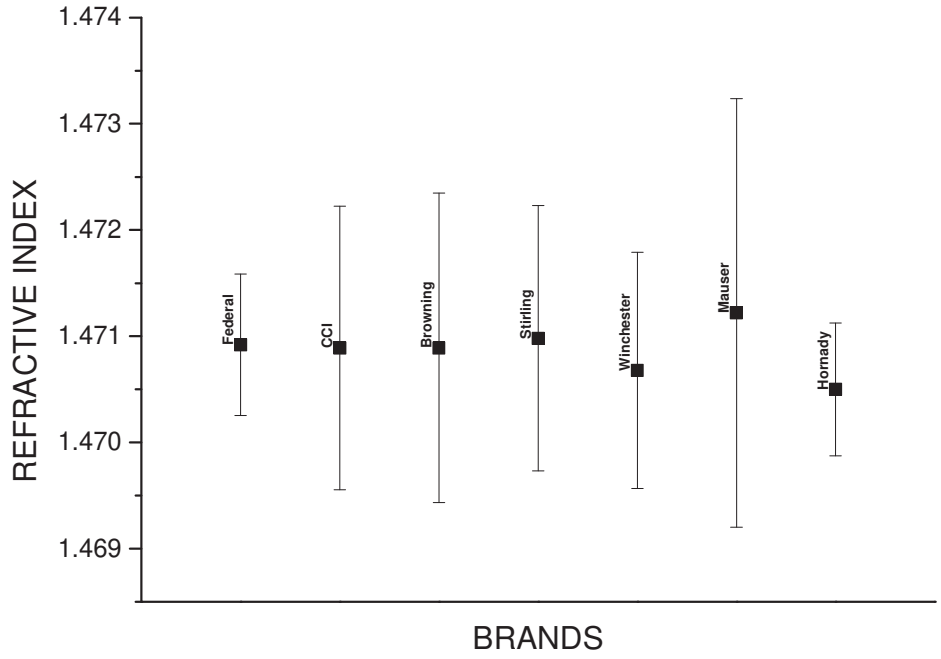


**Figure 36: Mean refractive indices ±3σ of frictionator samples (by brand) which had a null temperature in the C oil. The Winchester value indicates an average of all the samples measured**

## 4.6. Comparison to Previous Results

In the previous work conducted by ChemCentre and Coumbaros [159], various glass-containing GSR (gGSR) samples from 11 brands of ammunition were identified as two or three-component primers, and for the presence and identity of any glass. From this study, they found 2/11 brands to not contain glass, 1/9 glass containing brands to contain solely soda lime glass, 2/9 containing a mix of borosilicate and soda lime glass, and 6/9 brands to contain only borosilicate glass. Of the ammunition primers that did not contain glass, one contained a three-component Pb/Ba/Sb primer, and one contained only a two-component primer (Pb/Ba). Most of the glass-containing samples contained only a two-component primer, except for 2 of the 6 Federal variants, and the Stirling Sample.

In this work, 25 brands of ammunition, and 13 exhibits from Winchester were studied. Of those brands 8 brands contained borosilicate glass, and 9 brands appeared to contain soda lime glass, with a further brand (no. 4 Sellier Bellot) containing glass of unknown identity, and 7 brands appearing not to contain glass.

At first glance, this would seem to disagree with the previous work, with most brands not containing borosilicate glass. However, the samples used in this study were collected from the South Australia Police ammunition library, representing ammunitions that have been of interest in at least one case in the past – and it should be noted that the SA Police have been operating 180 years – but not

necessarily everything on the ammunition market. It should also be noted that the existence of the 25 brands in no way implies an equal likelihood of observing samples using each of their brands, or that these brands represent all ammunition possibilities in Australia.

A survey of ammunitions from 10 Australian-based online retailers (see Table 29) showed that Winchester (8), CCI (8) and Federal (7) are the brands most commonly offered on the market in 2018. Of the brands that were available on the market, only 2 were not looked at in this study- SK and Norma are additionally available from 5 and 3 retailers, respectively. SK is owned and manufactured by the same company as Lapua, which did not contain glass. However, the SDS for SK does indicate that the primer includes ground glass, so future work should incorporate this brand. Norma is owned by Ruag (the manufacturers of RWS), and its 0.22 LR SDS indicates that it contains both antimony sulfide and calcium silicide, both of which are known to act as frictionators, and so it is unlikely that this formulation contains glass.

**Table 29: Ammunitions available from nine online retailers based in Australia**

| Brand\Retailer | 1 | 2 | 3* | 4 | 5 | 6+ | 7 | 8 | 9 | 10 | Total |
|---|---|---|---|---|---|---|---|---|---|---|---|
| **Browning** | | X | X | X | | | | | | | 3 |
| **CCI** | X | | X | X | X | | X | X | X | X | 8 |
| **Eley** | X | | X | X | | | X | X | | | 5 |
| **Federal** | X | | X | X | | | X | X | X | X | 7 |
| **Fiocchi** | | X | | X | | | X | | | | 3 |
| **Highland** | | | X | | | X | | | X | | 3 |
| **Hornady** | X | | X | X | | | | | X | X | 5 |
| **Lapua** | | | X | X | | | X | X | | | 4 |
| **Remington** | | | X | X | X | X | | | X | | 5 |
| **RWS** | X | | X | X | | | X | | | | 4 |
| **S&B** | | | X | X | | | | | | X | 3 |
| **Winchester** | X | X | X | X | | X | X | | X | X | 8 |
| **Others** | SK Norma | Norma | Norma | SK Norma | | | SK Norma | SK | | SK | SK 5 Norma 3 |

*This brand additionally sold several other ammunitions that weren't available anywhere else
+this is a site for 2nd hand sales

In the Coumbaros work, a combination of glass identity and other primer residues was investigated. It was considered, that in examinations of gGSR, as will be discussed in Chapter 5, that examining the primer residues and the glass identity could potentially improve the power of discrimination provided by this analysis. When the discrimination power provided by the elemental composition of the glasses

were supplemented by the primer composition information, 2 extra pairs (added 1.5%, or a total of ~95.6%) were added to the ToF-SIMS discrimination power, bringing the total discrimination power of this study to 97.0%. When extending this work to genuine gGSR samples, incorporating analysis of primer elements could be helpful.

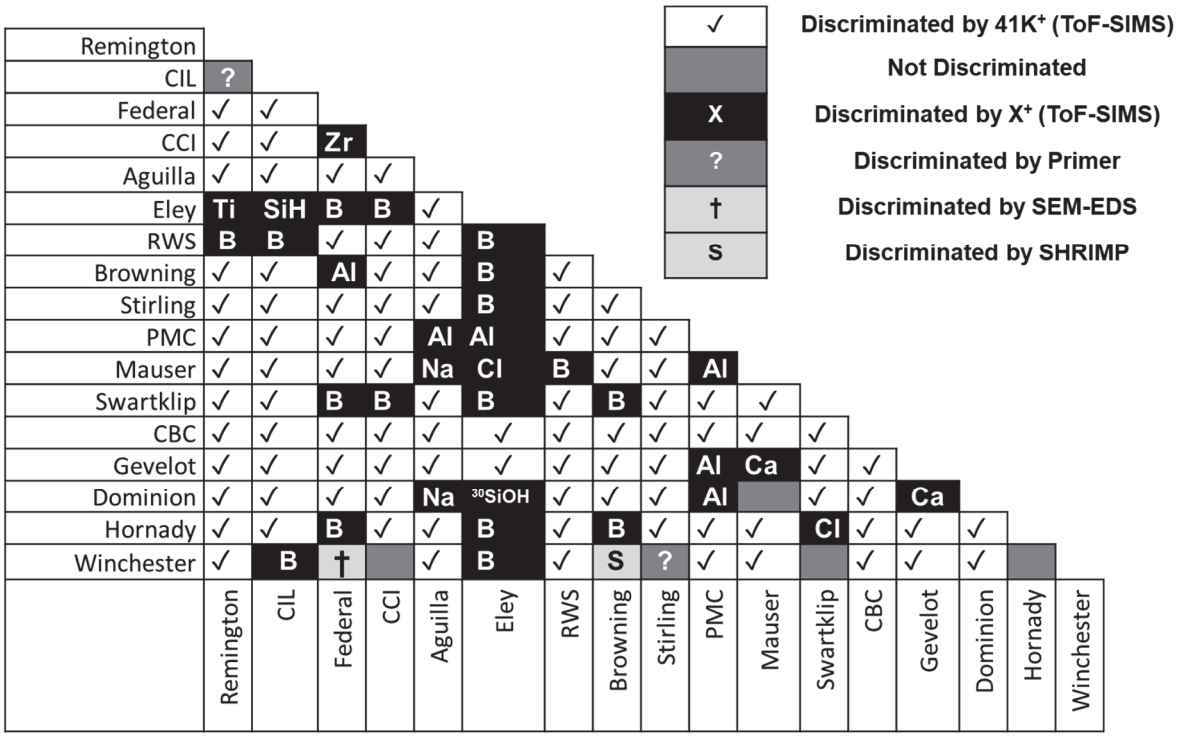


**Figure 37: Total power of discrimination including macro-characteristics of primer (i.e. one-, two-, or three-component, or Hg-based) as an added variable**

## 4.7. Summary and Conclusions

The B and Li isotopic compositions of two standard borosilicate glasses were investigated to be used as reference materials isotopic composition for SHRIMP analyses. Recommended B isotope values of borosilicate standards NIST SRM 93a and NCS DC61104 have been determined *via* MC-ICP-MS to be 0.03 ± 0.08‰ and -6.74 ± 0.12‰ (2σ) respectively. Recommended Li isotope ratios for the same glasses were determined to be -21.05 ± 0.32‰ and -3.22 ± 0.25‰ respectively, also *via* MC-ICP-MS.

The Li distribution within the two glasses, as assessed using SHRIMP, appears at least as homogenous as the Li distribution within NIST SRM 612. There was no CRM available that was a borosilicate glass that had previously been assessed for homogeneity for B, but when assessed by SHRIMP NIST SRM 93a and NCS DC61104 appear to be approximately as homogenous as each other.

A survey of the elemental and isotopic composition of frictionator samples taken from 0.22 calibre ammunition from a wide range of manufacturers has been conducted using the analytical techniques SEM-EDS, ToF-SIMS, and SHRIMP. No survey like this study has been undertaken previously on glass frictionator samples, and the information generated by this work represents an original contribution to forensic science. It was found that the elemental variation across the population examined is sufficient to allow discrimination between frictionators from most of the manufacturers.

More than 95% of samples could be discriminated using ToF-SIMS alone, or at least 83% using SEM-EDS could be discriminated when using the macro primer composition (i.e. one, two or three components, or Hg-based) as another variable. Together, these two techniques could discriminate 96.3% of the population studied (including primer composition). This technique is not currently used in casework in South Australia, but is available at universities in both South Australia and Western Australia. Some Australian operational forensic laboratories already have agreements with universities to use instruments for casework (such as LA-ICPMS for glass analysis) and similar arrangements could potentially be organised in the future to allow use of techniques such as ToF-SIMS (or other relevant techniques) for frictionator analysis.

Although most rounds of ammunition studied were drawn from single boxes, the Winchester ammunition sampled covered many batches and covered a wide time span of production. Thus, some data with regards to inter-batch variation were collected and this variation was small, which may indicate some control exerted by Winchester over the glass' properties. More work should be conducted in future to look at intra-batch variation of other brands.

SHRIMP was evaluated as a technique for analysis of frictionators because it offers the capability for carrying out measurement of stable isotope ratios of elements in particles of 20 µm or less. However, it was found that the isotopes of B, Li, Pb, U and Th exhibited very little variation across the frictionator samples examined, even that sourced from the numerous batches of Winchester ammunition. Although SHRIMP can also be used to measure trace element concentrations as well as stable isotope ratios, the precision of the analytical results in this case was not high enough, due to the low amounts of isotopic variation observed. There would also be difficulties accessing an instrument for many laboratories undertaking GSR casework. Although it was not a useful technique for the samples used in this study, it could be considered for use on other samples of forensic interest in future.

Refractive index measurements, supported by elemental analysis of frictionator samples was undertaken, confirming that borosilicate and soda lime glasses are used as frictionators. These analyses also indicated that the glass frictionators have a low intra-sample variability.

The elemental variation between frictionators suggests that there is scope for frictionator analysis to add value to forensic casework examinations by linking GSR to unfired ammunition or in demonstrating similarity (or difference) between GSR samples. Therefore, in the next chapter research is presented that evaluates the extension of SEM-EDS and ToF-SIMS from the analysis of raw frictionator to the analysis of frictionator present in typical GSR. Glass has been observed in GSR arising from other ammunition calibres, and thus a wider survey of ammunition is warranted.

# 5. Methods for Analysis of Glass in Glass-Containing Gunshot Residue (gGSR) Particles

## 5.1. Preface

This chapter represents the third and final strand of research contributing to the development of new capabilities for GSR analysis through the incorporation of gGSR particles. This chapter presents an investigation into original methodologies for the sectioning and remounting of gGSR particles for subsequent analysis, and the comparison of gGSR particles to their unfired frictionator counterparts. This method is unlike any other that has been considered for the analysis of gGSR, and supports the research presented in Chapters 3 and 4, providing a promising proof of concept for the incorporation of the analysis of gGSR into casework.

This chapter is substantially the same as a paper published in Forensic Science International [286].

## 5.2. Chapter Summary

When lead (Pb), barium (Ba) and antimony (Sb), or Pb, Ba, calcium (Ca), silicon (Si) and tin (Sn) are found together in particles associated with a shooting investigation they are considered characteristic of gunshot residue (GSR). Antimony and tin are often absent from the primer of many low calibre rimfire ammunitions, which are the type most commonly used in Australia. Therefore, the likelihood of characteristic particles forming during the firing process of such rimfire ammunition is significantly less than the likelihood of these particles arising from higher calibre ammunition. This means that it can be more difficult to positively identify or interpret GSR from these lower calibre rimfire ammunitions. The majority of rimfire ammunition examined in this research contains ground glass in the primer, which functions as a frictionator. These ammunitions produce a small number of gunshot residue particles containing glass coated with other primer components, which we refer to as glass-containing GSR (gGSR). If these particles are observed in an investigation, they have the potential to add a new dimension to gunshot residue analysis because they are not common in the environment. Furthermore, the composition of glass frictionator is stable during firing, which raises the possibility that chemical testing of the glass in gGSR may be used to identify the ammunition from which the residue was derived or to link deposits of GSR.

This chapter examines the application of scanning electron microscopy – energy dispersive X-ray spectrometry (SEM-EDS), focussed ion beam (FIB) techniques and time of flight–secondary ion mass spectrometry (ToF-SIMS) to the semi-quantitative analysis of gGSR and frictionator extracted from unfired cartridges. SEM-EDS is effective for comparing gGSR with unfired frictionator, but the use of FIB to expose clean glass from the centre of gGSR followed by ToF-SIMS, or ToF-SIMS using ion sputtering to expose clean glass, offers more power for glass discrimination.

## 5.3. Introduction

There are approximately three million legally owned firearms in Australia, and a further 260 thousand suspected to be owned illegally [5]. Of these, small calibre long rifles and shotguns are subject to the least regulation, and make up a large majority of the firearms in the country, even on the illicit market [5]. Small calibre long rifles and shotguns are also the most commonly associated with crime and death in Australia [9]. This represents a significant difference to other jurisdictions, such as the UK or USA, where handguns and other types of weapons are much more commonly associated with crime and/or deaths [6, 7, 10]. This regional divergence is noteworthy, because while many centrefire ammunition primers contain lead styphnate, barium nitrate, and antimony trisulfide as the major ingredients (Table 1) [17, 156], the majority of rimfire ammunitions (including those available in Australia) do not contain any antimony compounds in their primer formulation [8, 158]. Therefore in typical Australian shooting investigations the majority of particles present in gunshot residues (GSR), and on occasions the only type of particles present, have a composition that only allows them to be classified as 'consistent' with firearm origin under the ASTM guidelines [32]. This terminology is intended to indicate that the residue is of comparatively low probative value compared to residues containing lead (Pb), barium (Ba), and antimony (Sb), which are classified as 'characteristic' of firearm origin. As all rimfire ammunition available in Australia is either fully imported or assembled using imported, ready-primed cartridge cases, the comments above are relevant overseas as well. This situation led us to seek new attributes of rimfire residues that may be used enhance the relatively low significance currently attached to them.

In the majority of rimfire ammunition, ground glass is used as a frictionator, instead of the more traditional antimony sulfide or calcium silicide [158] present in high calibre ammunition. In early work [158] a combination of SEM-EDS and time of flight – secondary ion mass spectrometry (ToF-SIMS) demonstrated the presence of glass particles with Pb and Ba fused to the surface in GSR residues from 0.22-calibre rimfire ammunition. Further research has indicated that other primers, including those for larger calibre and heavy metal free ammunitions can also contain glass as a frictionator [23, 24, 29-31, 243, 287].

**Table 30: Inorganic compounds associated with primer GSR and their functions, with compounds in bold being reported as the most common for 0.22 calibre [17, 35]**

| Function | Compound | |
|---|---|---|
| **Oxidizer** | Barium nitrate | Barium peroxide |
| | Lead nitrate | Lead peroxide |
| **Initiator** | Lead styphnate | Lead azide* |
| | Mercury fulminate* | |
| **Fuel** | Calcium silicide | Lead thiocyanate |
| | Powdered zirconium | Powdered aluminium |
| | Antimony sulfide# | |
| **Sensitisers** | Tetrazene | Pentaerythritol tetranitrate |
| | Trinitrotoluene | |
| **Frictionator** | Antimony sulfide | Calcium silicide |
| | Ground glass | |

**historical # common for ammunitions other than 0.22*

It was proposed that this glass-containing gunshot residue (gGSR) may have a higher probative value than the usual rimfire GSR evidence if it can be established that particles of this nature do not originate from industrial or non-firearm sources. Additionally, if it could be shown that glass frictionators are elementally stable during firearm discharge, and that glass frictionators are elementally variable between manufactures or samples, glass analysis could be used to associate GSR with a putative source ammunition or spent cartridge case, allow discrimination between GSR deposits, or to show associations between GSR deposits. Chapters 3 and 4 have shown that frictionator composition varies across different ammunition sources and that particles resembling gGSR are rare in the community. However, in order to advance the field, robust methodology for analysing glass in gGSR particles and comparing it to unfired frictionator or glass in other gGSR is required; the present article deals with the development of such methodology.

As gGSR is usually encrusted with residues arising from the other primer components, the biggest operational hurdle to exploiting the value of these particles is finding or exposing a clean surface of glass to analyse. A dual beam SEM-EDS with a focussed ion beam (FIB) system allows particles of gGSR to be dissected, revealing their interior morphology and composition.

A focussed ion beam (FIB) system is similar to an SEM system, except that instead of, or in addition to an electron source, it has a liquid metal ion source (LMIS), often using a $Ga^+$ beam. The benefits and

mechanics of this system have been described elsewhere [186, 187, 288, 289] as this technique is routinely used by the semi-conductor industry, for TEM sample preparation, and for nano-etching. However, this technique has undergone rapid improvement and expansion of applications in the last two decades. The LMIS makes highly site-specific ion sputtering possible, which allows sectioning of 'casework-size' GSR particles [186]. The instrument used for this investigation was a dual beam instrument, equipped with a platinum gas injection system (GIS) and a nano-manipulation system, which allowed *in situ* lift out (INLO) of slices of glass.

FIB has only occasionally been utilised for forensic applications. In 1999, Niewöhner and Wenz [141] used a FIB instrument to ablate the edges of GSR particles from ammunitions of different composition, focussing on heavy metal free (HMF) brands, and assessing their internal morphologies. They examined one type of 3-component primer, and three different HMF brands with differing formulations. Their investigation focussed on particle morphology, and in attempts to look at composition, they noted a limitation in that the instrument they used for SEM-EDS mapping could not 'resolve' or perceive elemental differences in the separate phases visible in the backscatter images. Sarvas *et al.* and *W*uhrer *et al.* [142, 143] also used FIB to investigate internal particle morphologies and composition, and to examine possible distinguishing features of GSR compared to environmental particles.

A similar assessment of sub-surface morphology was attempted by Basu [22] by using a microtome to section particles prior to analysis. However, the morphologies observed by Basu were quite different to what was observed by Niewöhner and Wenz [141], and many of the particles had a scratched interior morphology, which were potentially artefacts of the microtome process used to section the particles. An advantage of using FIB for this application is that the ion milling process is "essentially stress free" [187] and does not usually affect the morphology of the exposed surface, meaning that it potentially gives a much clearer picture of the true internal morphology of the particle [187, 289].

Another approach is to use an ion beam in a ToF-SIMS to sputter away the encrustation on gGSR prior to analysis of the exposed glass. This approach was used in the initial exploration of the utility of gGSR [159] and was re-examined in the work described here and compared to methods involving FIB sectioning of particles.

## 5.4. Materials and Methods

### 5.4.1. Sample Collection

#### *5.4.1.1. Sample Collection of gGSR Particles using Manual Discharge of Cartridge Cases*

Exemplar ammunition cartridges were collected from commercially obtained 0.22 Winchester Powerpoint (batch 1DMH6) and PMC Zapper (batch 22-D-446) rimfire ammunition. Projectiles were removed from cartridge case with pliers. The propellant was decanted. The cartridges containing only primer were then placed into a machined aluminium holder. When placed in the holder, the cartridge extended through a hole leading down onto the bench, but 'legs' on the holder ensured that the mouth the cartridge was held just above the bench, which was covered with a piece of clean waterproof parchment paper. The primer was then manually discharged using a punch and mallet. Residues were collected off the paper with a GSR stub. A diagram of the holder is shown in Figure 38, together with a photomicrograph showing typical particles collected using this approach. Glass-containing gunshot residue particles (gGSR) were located using BSE SEM imaging to find Pb- or Ba-containing particles and then EDS analysis was used to determine whether any of these particles

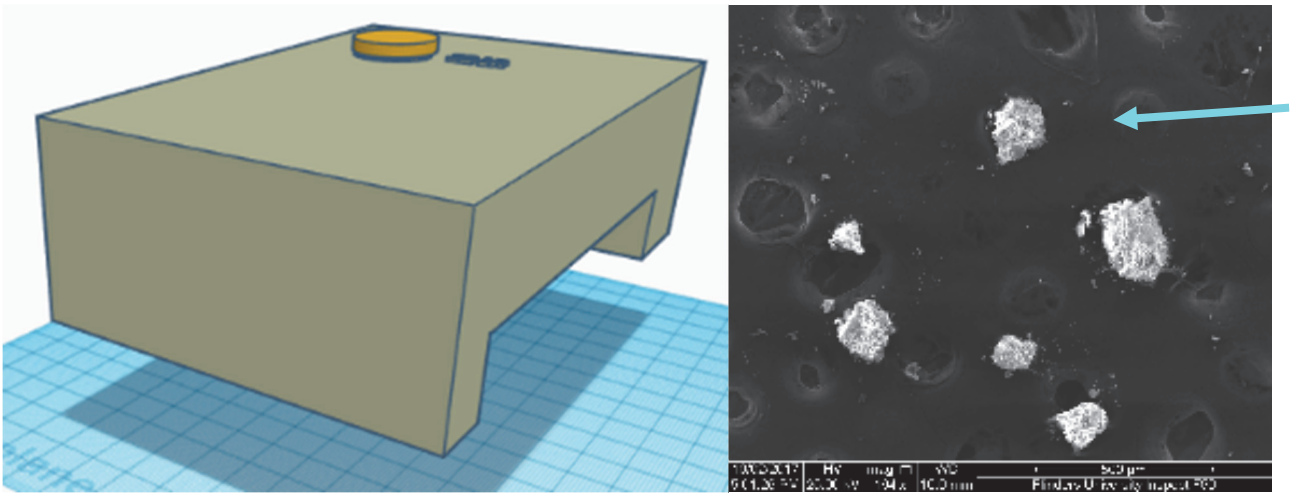

**Figure 38: Left. Diagram of the aluminium holder designed to safely discharge disassembled ammunition cartridges, with a cartridge placed in the holder. The diameter of the hole through which the cartridge is place is smaller than the diameter of the cartridge case base but sufficient to allow cases to be inserted easily and removed after discharge. Right. Typical particles of Winchester Powerpoint GSR, the arrow indicates a particle that was later sectioned using the FIB.**

displayed co-located Si, Na, Al and O signals, which indicates the presence of glass.

#### *5.4.1.2. PMC Zapper gGSR Particles using Muzzle-Discharge Collection*

A model 10/22 Ruger firearm was cleaned, conditioned with 20 rounds, and then fired once through a PET catcher, following the method described in Seyfang *et al.* [195], and Chapter 3. The inside of the catcher was stubbed with a GSR stub. The samples were analysed, and gGSR particles were located using BSE-SEM and SEM-EDS as described above; images of typical particles collected using this method are provided in Figure 39.

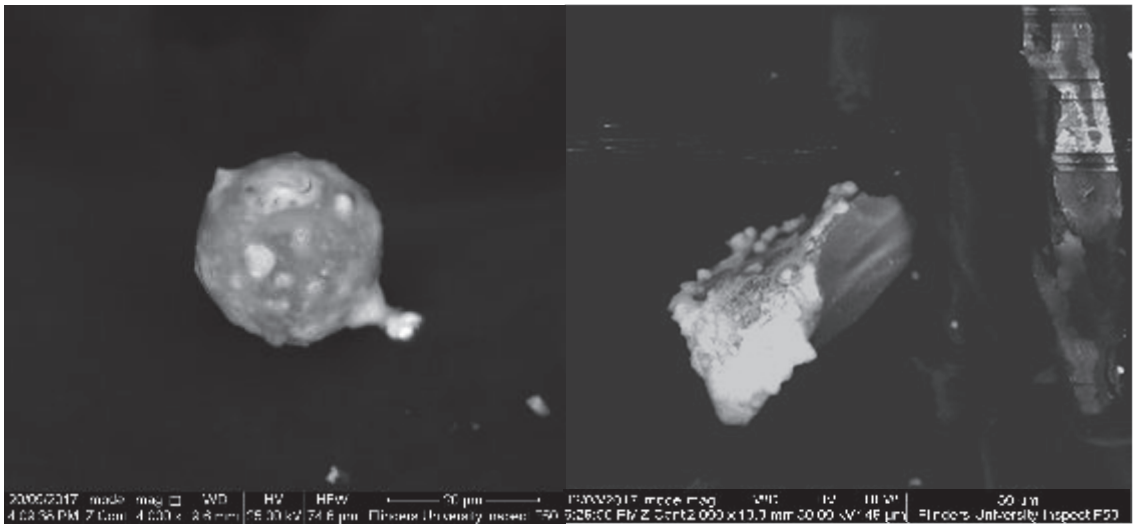

**Figure 39: Particles collected from PMC Zapper ammunition that were chosen for sectioning by FIB, intended for further analysis. The left particle is the one for which analytical results are presented in this chapter.**

#### *5.4.1.3. Collection and Preparation of Unfired (Rimfire) Frictionator Samples for Comparison*

For the comparison between Winchester gGSR and unfired frictionator, a cartridge taken from a Winchester Powerpoint rimfire ammunition (batch 1DMH6, not the same box as above) was disassembled and emptied as described above. The cartridge was filled with a mixture of 3:1 acetone: water and left overnight. A fine, curved metal probe was used to dislodge primer particles from within the rim of the cartridge, and the acetone: water solution was emptied into the cup of a spin filter using a disposable plastic pipette. The spin filter was centrifuged at 13 krpm for one minute to remove any solvent. The filtrate was discarded, and the cartridge was then rinsed a further two times with acetone: water, with each rinse transferred into the spin filter and centrifuged. The spin filter was then rinsed with acetone three times - each time the tube was half-filled, agitated with a vortex mixer for ten seconds, and centrifuged for one minute. The residues were then rinsed three times with nitric acid (5%) and then three final times with methanol.

For the PMC Zapper samples, each cartridge was dismantled and manually discharged onto parchment paper as described above. The residues were transferred from the paper into a spin filter, any residues left inside the cartridge were rinsed with acetone and added to the spin filter. After centrifugation the contents of the spin filter were washed with nitric acid and methanol, as described above. A cartridge from one of the PMC Zapper samples was also prepared by the first method (sample Korean batch 22-D-446 (1) in Figure 52) and analysed against the samples prepared by the second method, to discern whether the two methods appeared to clean the glass for analysis equally. Both methods removed traces of Pb and Ba to below the detection limit of SEM-EDS, and the frictionator from the other cartridge appeared to have an elemental profile that was indistinguishable by SEM-EDS.

#### *5.4.1.4. Collection of Federal (centrefire) Premium Particles using Hand-Stubbing*

A volunteer SAPOL officer's hands were washed and blank hand stubs were collected from the backs of hands, trigger finger and webbing between thumb and forefinger using GSR stubs, stubbing approximately 50 times or until stubs were no longer sticky. The officer fired 20 shots of .40 Smith and Wesson (centrefire) Federal Premium Law Enforcement HST Ammunition from a Smith and Wesson Military and Police (M&P) .40 Semi-automatic pistol over a 30-minute period of drills. Immediately after the end of the session, the officer's hands were stubbed again. The collected stubs were analysed and gGSR particles were located using BSE-SEM and EDS analyses, as above. This ammunition was used because it has been found by us to contain glass frictionator within the primer mixture.

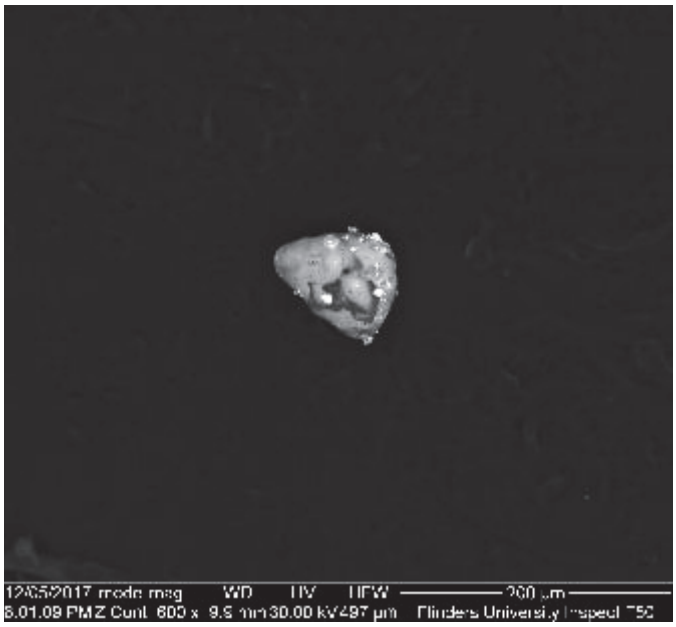

**Figure 40: gGSR particle collected from Federal Premium (centrefire) particle from hands that was sectioned by FIB for further analysis**

Compared to rimfire ammunition the .40 calibre ammunition would subject GSR particles to higher temperatures and pressures within the cartridge and chamber during the firing process. The aim of this exercise was to recover gGSR particles consistent with what would be encountered in firearms casework, albeit a relatively extreme example, and consistent with particles on hands, as distinct from those collected *via* manual discharge or muzzle discharge. The particle selected for further analysis is shown in Figure 40.

### 5.4.2. SEM EDS Identification of GSR particles

All GSR samples collected in this study were collected using an aluminium pin stub covered in carbon adhesive (Tri-Tech Forensics Inc. North Carolina, USA.)

SEM EDS analysis of all samples was completed using a FEI Inspect F50 SEM-EDS system (FEI Inc., Oregon, USA), operating in Backscattered Electron Mode (BSE).

Particles were initially identified using GSR Magnum particle analysis system (FEI Inc., Oregon, USA). Exemplar spectra and elemental maps collected using TEAM Analysis Software (EDAX Inc., New Jersey, USA). Pre-FIB and post-FIB elemental and phase maps were collected using an accelerating voltage of 20 keV, a 30 µm aperture, a spot size of 6, an emission current of approximately 110 µA and a resolution of 128 eV. Analyses of regions of interest or 'spots' were initially undertaken on all samples; the samples were also mapped to check whether the glassy areas were reasonably homogeneous.

### 5.4.3. Sample Preparation by Focussed Ion Beam (FIB)

The instrument used for FIB was a FEI Helios Dual beam Nanolab 600. Particles previously identified using the Inspect SEM were found using the SE or BSE SEM functionality on the Helios microscope. A backscattered electron top-down view (Figure 42, left), and a secondary electron view from a 52° stage tilt (Figure 42, right) is shown of a particle collected from the PMC Zapper ammunition in Figure 41. It should be noted that the particle is shown from two angles here.

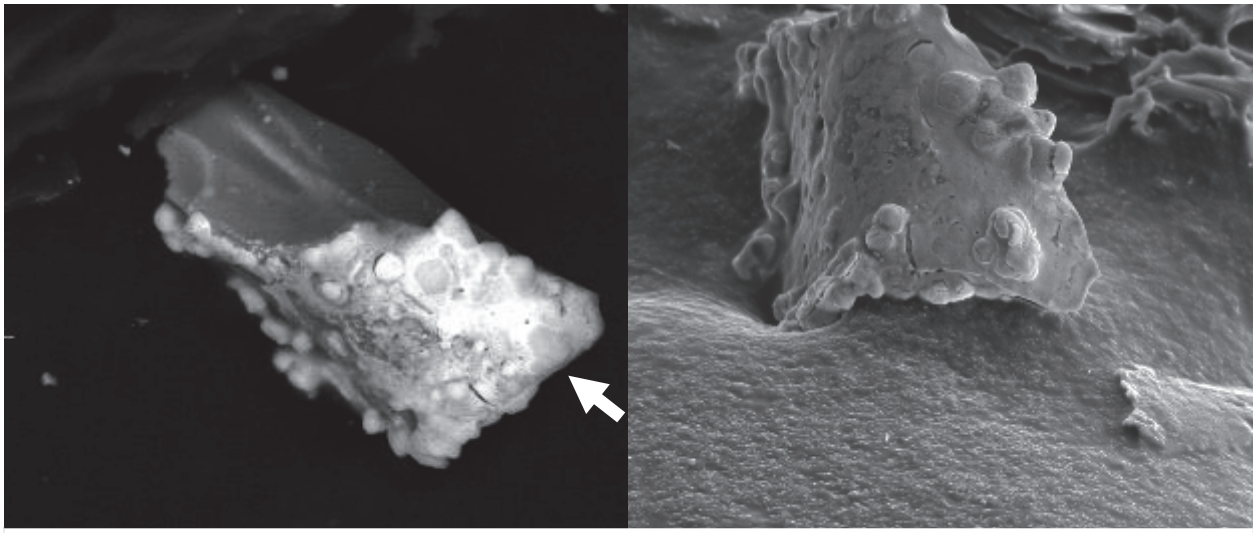

**Figure 41: Top-down view (left) of gGSR particle from PMC Zapper taken using BSE-SEM-EDS on the FEI F50 instrument (note the typical glass choncoidal fracture evident), and an SE-SEM-EDS (right) image of the same particle taken at a 52° stage tilt and a clockwise rotation of about 45° on the FEI helios dualbeam nanolab 600 instrument. n.b. The white arrow on the BSE image (Left) indicates the viewpoint for the SE image (Right). The view of the exposed glass is obscured by the bulk of the particle in the view on the right**

A 2 µm thick layer of platinum was deposited over the region where the FIB was to operate with a platinum GIS. This serves to protect the sample, provide a conductive layer close to the milled area in order to minimise the 'theatre curtain' or 'waterfall' effect, which is a known FIB artefact, and it also provides a surface to which a probe can be welded for subsequent *in situ* manipulation [186]. After the platinum was deposited, troughs were sputtered around three sides of the region of interest using a $Ga^+$ LMIS at a beam current of up to 21 nA. An example of the troughs is shown in Figure 42.

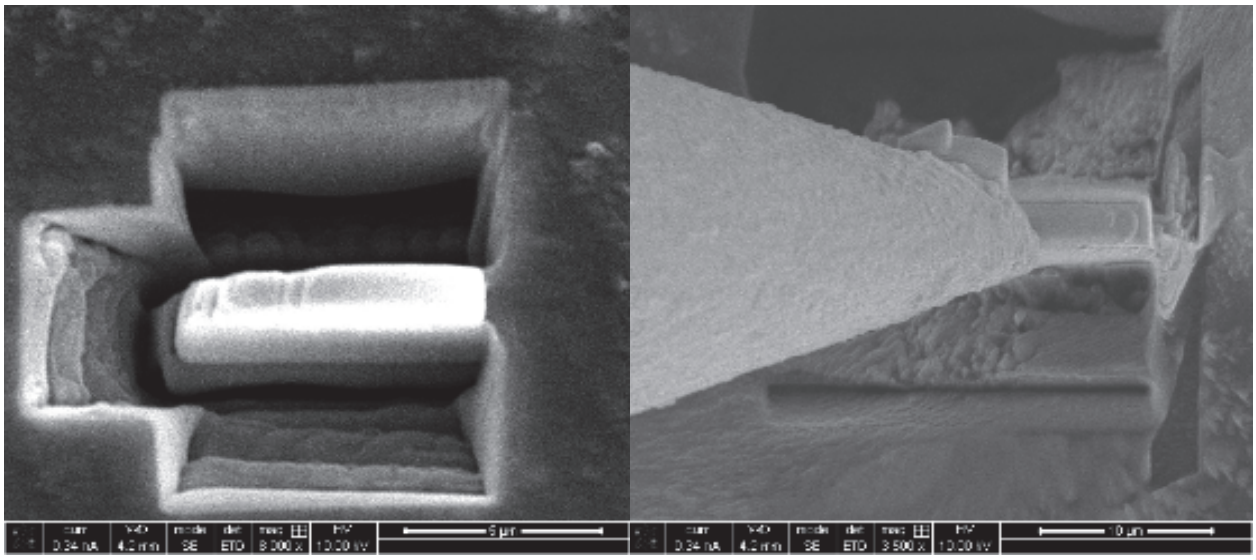

**Figure 42: Troughs milled around the slice in the region of interest in a PMC Zapper gGSR particle (left) and needle from the nanomanipulator welded to top of the slice, to allow *in situ* transfer of it to a holder (right)**

Following this initial sputtering, lower current beams of 6.5 nA and then 2.8 nA were used to clean the surface of the slice. The bottom of the slice was milled in the same way, but at a 7° stage tilt, so that the milling was almost directly across the base.

The next step of the process involved welding a tungsten needle to the slice using the platinum GIS and a Kleindiek Nanotechnik Nano-manipulator. This was accomplished by aligning the tungsten needle with the slice, controlled by the nano-manipulator, using the two angles (ion image and SE image), and moving it into position so that it barely touched the deposited platinum layer on top of the slice. The GIS was then used to deposit a 1.5 µm thick layer joining the needle to the platinum layer. Finally, the last side of the slice (right side of slices in Figure 42, left) was sputtered, freeing the slice from rest of the particle. The slice was reviewed to verify that all sides had been milled clear, and then the stage was moved away from the needle. The slice was then welded to a copper holder, and the platinum attaching the needle to the slice was removed by sputtering with the GIS. The slice can be seen welded to the copper holder in Figure 43. When the specimen was placed under a transmitted light microscope it was possible to see through the central part of the thin slice that was excised, as is expected if it is a glass frictionator residue. For each slice prepared, optical microscopy was used to confirm that the particles were retained on the copper holder and had not been dislodged during the venting of the vacuum chamber or the inter-institutional travel.

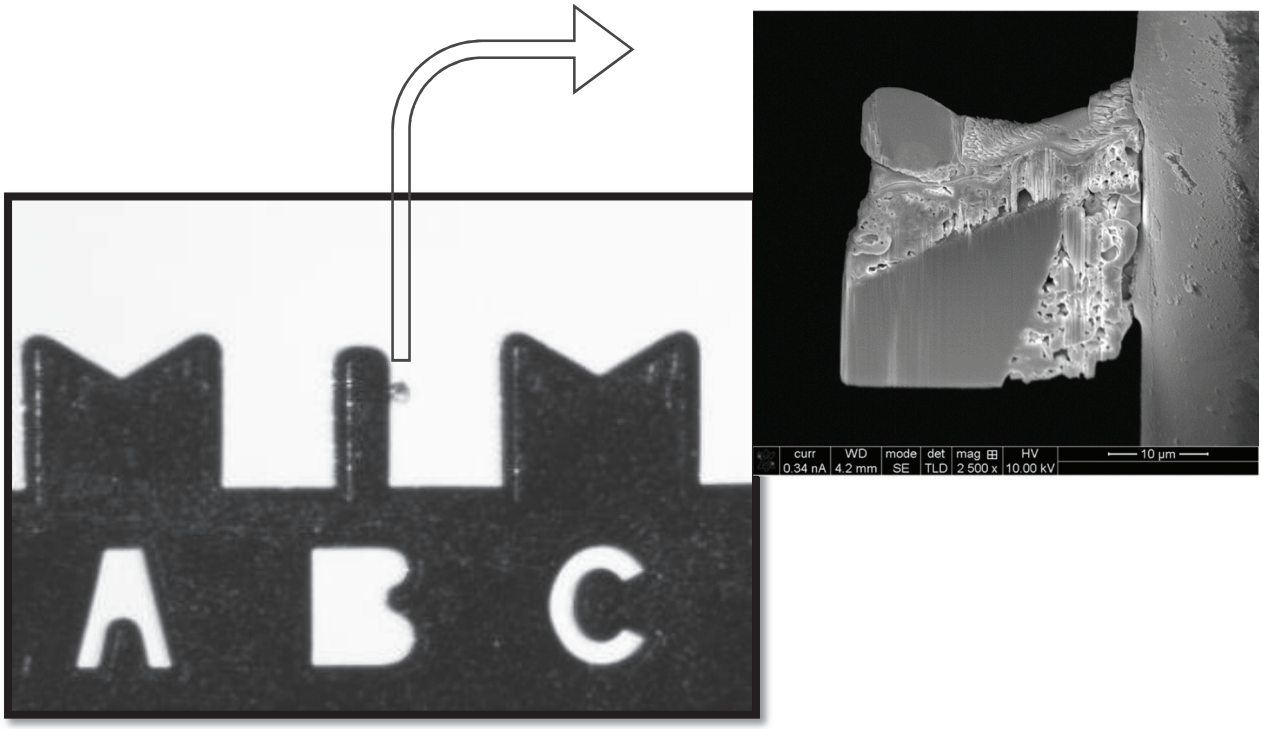


**Figure 43: A slice of GSR welded to the copper peg (above the "B") of a sample holder. Inset is an electron photomicrograph image of the slice at 2,500 x magnification. Note that the specimen on the right is rotated about its vertical axis compared to the one on the left.**

### 5.4.4. Preparation for X-ray Spot Analyses and Mapping and SEM-EDS Analysis of FIB Slices

After optical examination using a light microscope, samples were prepared for further analysis by attaching the slice-holder to bare aluminium pin stubs using conductive carbon ink (Pasco Scientific Conductive Ink Dispenser PK–9031). Post-FIB SEM-EDS analyses were undertaken using the FEI Inspect F50 as detailed above.

The FIB-prepared particles were analysed by semi-quantitative EDS analysis and the results were compared to analysis of particles which had been prepared by solvent washes and mounting as described in [202].

A key question for research is whether the approach involving FIB sectioning of particles followed by elemental analysis is fit and practical for the forensic comparison purpose. In order to explore this question, glass frictionator fragments extracted from two cartridges taken from one box of Mexican Zapper and from 4 cartridges taken from three boxes of South Korean Zapper cartridges covering 3 batches (a duplicate selection was taken from one box chosen at random) were compared using SEM-EDX to a FIB-prepared slice of a gGSR fragment from a sample of PMC Zapper ammunition of origin unknown to the analyst.

### 5.4.5. ToF-SIMS Analysis of FIB-prepared slices of gGSR

ToF–SIMS experiments were performed using a Physical Electronics Inc. PHI TRIFT V nanoToF instrument equipped with a pulsed liquid metal $^{79}Au^{+}$ primary ion gun (LMIG), operating at 30 keV energy. Experiments were performed under a vacuum of $5 \times 10^{-6}$ Pa or better. 'Bunched' $Au_1$ settings were used to optimise mass resolution for the collection of SIMS spectra. 'Un-bunched' $Au_1$ settings were used were used to optimise the collection of image resolution.

The sample surface was sputtered for one minute, where required, to help dislodge surface contamination, and mass spectra were collected for two minutes.

ToF-SIMS was used to semi-quantitatively analyse the glassy region of each of the FIB-prepared slices of gGSR and extracted, polished frictionator specimens. Several measurements of each specimen were made, rastering 5 x 5 µm areas.

## 5.5. Results and Discussion

### 5.5.1. SEM-EDS analysis of FIB Slice – X-ray Spot Analyses and Mapping

SEM-EDS analysis was undertaken for all of the slices collected. Figure 44 shows a SE image of the particle from Winchester Power Point ammunition, and the regions that were analysed using EDS. From this figure, several distinct regions can be observed. On the left of each region is the copper holder to which the particle is attached (incorporating selected area 8), and then a platinum welding region which attaches the particle to the holder and protects the top of the slice (incorporating selected area 7, and the layer above area 2). A Pb and Ba crust from the outside of the particle is shown in selected areas 6, 2 and 3, and the glassy region is represented in areas 1, 4 and 5. The spectra generated in the regions were collated into Table 31, which shows that the different regions have specific compositions. Of particular note, is that calcium is not detected in the glass region, which suggests that it is a borosilicate.

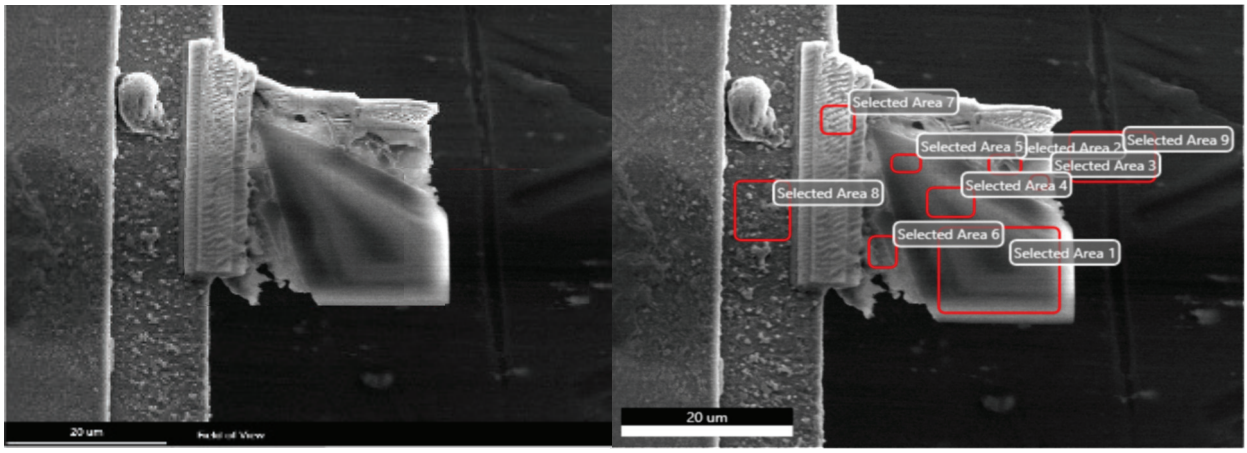


**Figure 44: SE-SEM Image of a sliced Winchester Powerpoint particle showing clearly the glassy interior, and crusted exterior (left), and the 9 selected regions analysed by electron dispersive X-ray spectroscopy (right).**

Following this, SEM-EDS mapping of the specimen was undertaken. The map (Figure 45) shows that the elemental composition of the glassy region was homogeneous, with neither Si, O, Al nor Na traces showing areas of varied intensity across the slice. Some elements observed in the slices are present due to the FIB process, and would not have been present in the original particle: Ga is an artefact from implantation from the LMIS; Pt was deposited to protect the particle and allow manipulation within the vacuum chamber; Cu was from the holder to which the particle is welded; and Al in regions 2, 3, 6 and 9 arises from the stub to which the holder is attached.

**Table 31: Elements present in a Winchester Powerpoint ammunition slice, by region, organised by intensity.**

| Region | Elements Present (in approximately descending order of intensity) |
|---|---|
| **1. Glass Region (1)** | Si O Al Na |
| **2. Crust** | Al Pt Si Pb O Ga Ba |
| **3. Thin Crust Region** | Al Pb Ba O Si Cu |
| **4. Glass Region (2)** | Si O Al Na |
| **5. Glass Region (3)** | Si O Al Na |
| **6. Crust-Glass Interface** | Al Pb Si Pt O Ga Ba Cu |
| **7. Platinum Cap** | Pt Ga Cu (trace) |
| **8. Sample Holder** | Cu |
| **9. Background (Al pin stub)** | Al Cu (trace) |

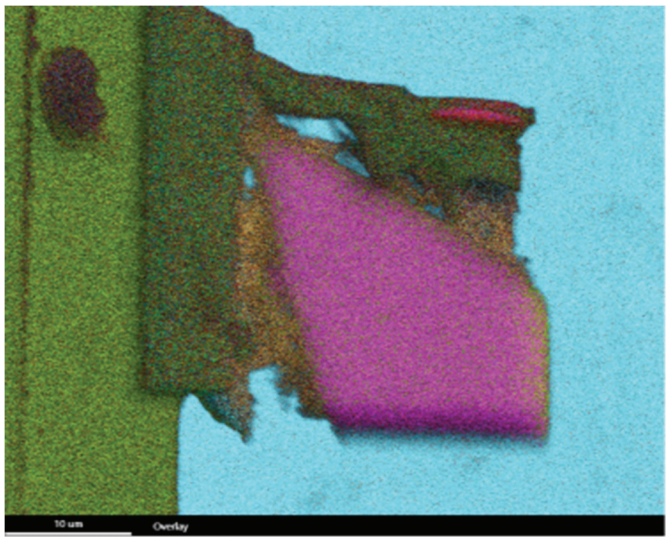


**Figure 45: SEM-EDS mapping of particle sliced with a FIB. Overlay of elements showing Cu (lightest green, sample holder), Pt (dark green, weld and coating), Pb (brown-yellow, primer residue) and Si (pink, glass, area also contained significant O, Na), and Al (blue, stub surface)**

Two particles of PMC Zapper ammunition were similarly prepared from the PMC Zapper sample for which the country of origin was unknown to the researcher. The left panel of Figure 46 shows the BSE-SEM image of one of the slices, and the right panel shows the regions analysed.

The elements identified in each of these regions are shown in Table 32; the detection of calcium in the glass suggests that it is of the soda lime type. The BSE image (Figure 46) shows variation in the glassy region of the particle slice, and this was largely supported by the observed elemental intensities. Unlike the previously sectioned particle, this example has a number of voids visible.

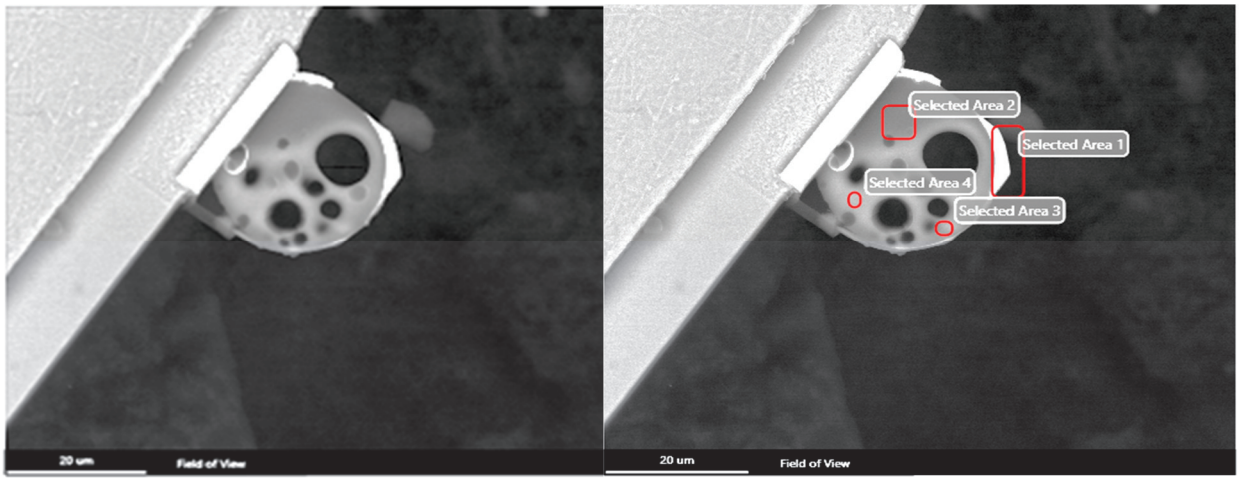


**Figure 46: Left BSE image showing the various regions and voids in the PMC Zapper particle, and right, the regions examined via EDS analysis.**

Table 32: Elements present in the particle of PMC Zapper ammunition, divided by region and then ordered approximately in decreasing intensity

| Regions | Elements Present (in approximate order of decreasing intensity) |
|---|---|
| **1. Platinum Cap** | Al Pt Ga |
| **2. Glassy region (1)** | Si O Al Na K Ba Cu Ca Mg |
| **3. Glassy region (2)** | Si Al O Na Ba K Ca Cu Mg Pb |
| **4. Glassy region (3)** | Si O Ba Al Na K Pb Ca Mg Cu |

This particle was mapped using EDS to further investigate the homogeneity and composition of the particle interior. The map is seen in Figure 47, and shows various regions of compositional heterogeneity, including in the glassy region. There are two distinct phases visible in the glass structure via BSE, which was confirmed by the mapping. The lighter regions by BSE imaging, which corresponded to the pink phase in the map in Figure 47, indicate a higher incorporation of the heavy elements Pb and Ba. Similarly, the darker regions, which correspond with the blue phase, indicate a lower level of Pb and Ba incorporation (see Figure 48).

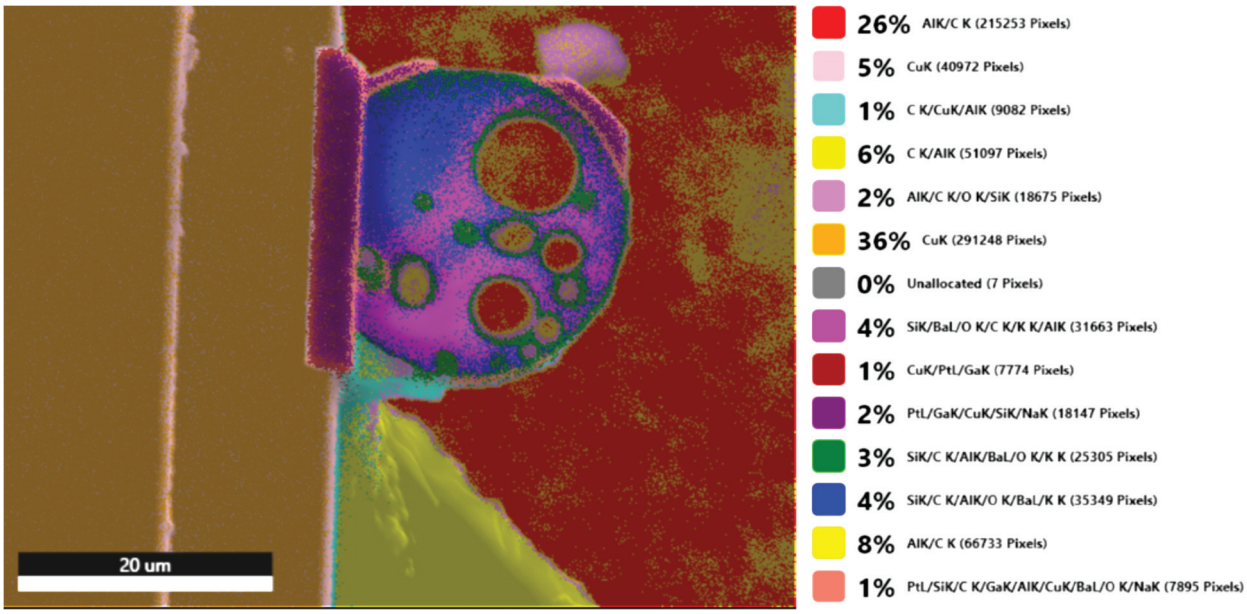


Figure 47: Map showing overlay of phases found by SEM-EDS mapping of a particle of PMC Zapper sliced open using FIB

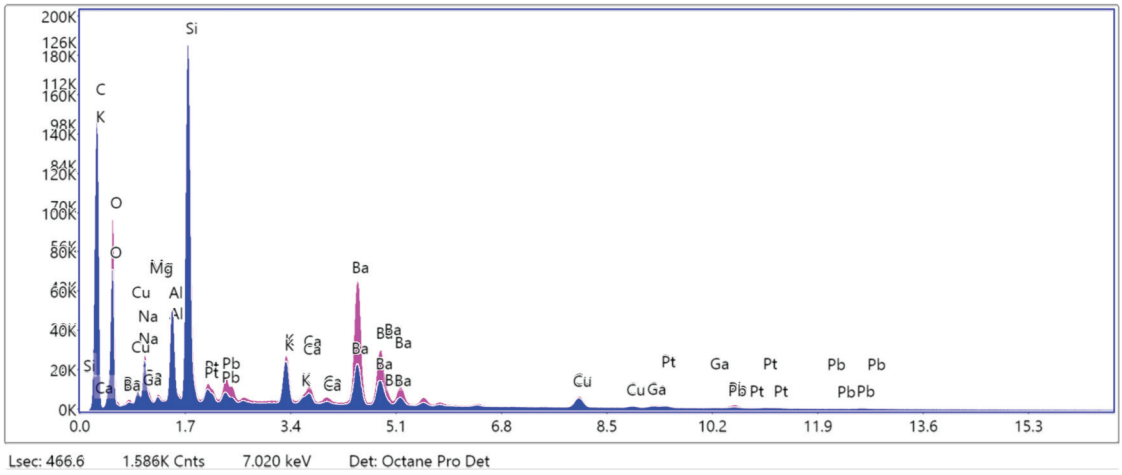


**Figure 48: EDS spectra of the 2 glassy phases from the slice of PMC Zapper, the blue region showing less incorporation of Pb and barium, and the pink region showing a greater incorporation of Pb and Ba into the glass**

Finally, Figure 49 shows a SE image and a BSE image of the slice of the particle from Federal Premium centrefire ammunition (top-left and top-right). Of note is a particle embedded in the glassy region visible by both SE- and BSE-SEM. Three other phases are also clearly visible in the BSE image.

The elements present in each region, in approximate order of decreasing intensity, are shown in Table 33**.** The darkest region (Figure 49 - region 1) contained the glass elements Si O Al Na (which are indicative of borosilicate glass) and contained a small Cu-rich inclusion. The other regions contained Pb and Ba, with the Ba having higher intensities in region 3, and Pb having higher intensities in regions 2 and 4.

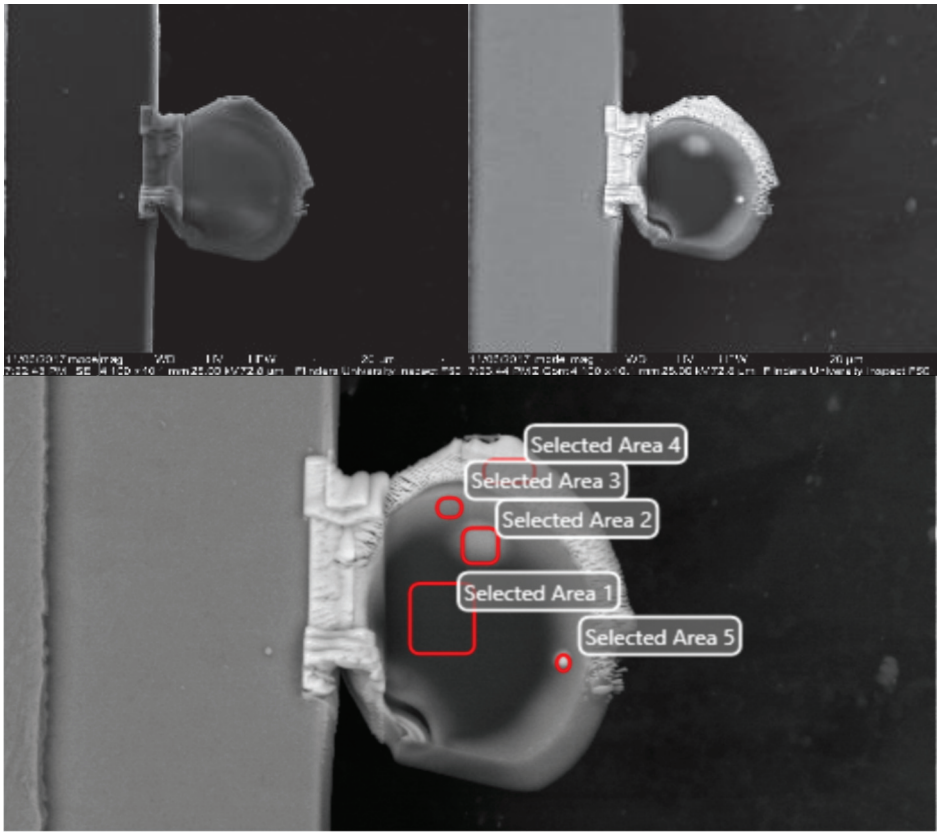


**Figure 49: SE-SEM image showing the sliced particle from the Federal Premium (centrefire) particle (top left), showing two regions, a core and a crust. BSE image (top right) showing four distinct regions in the core, and an outer rim with Pb and Ba incorporated, Diagram (bottom) labelling the various regions of the particle examined corresponding to the compositions listed in Table 33.**

**Table 33: Elements present in the various regions of the particle slice from Federal Premium centrefire ammunition**

| Regions | Elements Present (in approximate order of decreasing intensity) |
|---|---|
| **1. Glassy region (1)** | Al Si O Cu Na |
| **2. Glassy region (2)** | Al Si O Pb Cu Ba Na |
| **3. Glassy region (3)** | Al Si O Ba Pb Cu Na |
| **4. Platinum Cap** | Pt Al Ga Cu |
| **5. White spot in glassy region 2** | Al Si O Pb Ba Cu Na |

The single element maps shown in Figure 50 indicate that the particle is mainly glass, with a Pb/Ba enriched outer zone. It also shows that the silicon signal is fairly consistent across the core. The two inclusions observed in the glass from the BSE image exhibit higher concentrations of Pb, and the outer region of the glass shows that the Pb and Ba in the outer zone has implanted approximately 3-4 µm

from every angle. The phase diagram shown in Figure 51, although not clearly showing the Pb nodules, does appear to highlight the homogeneity of the glass matrix in the particle.

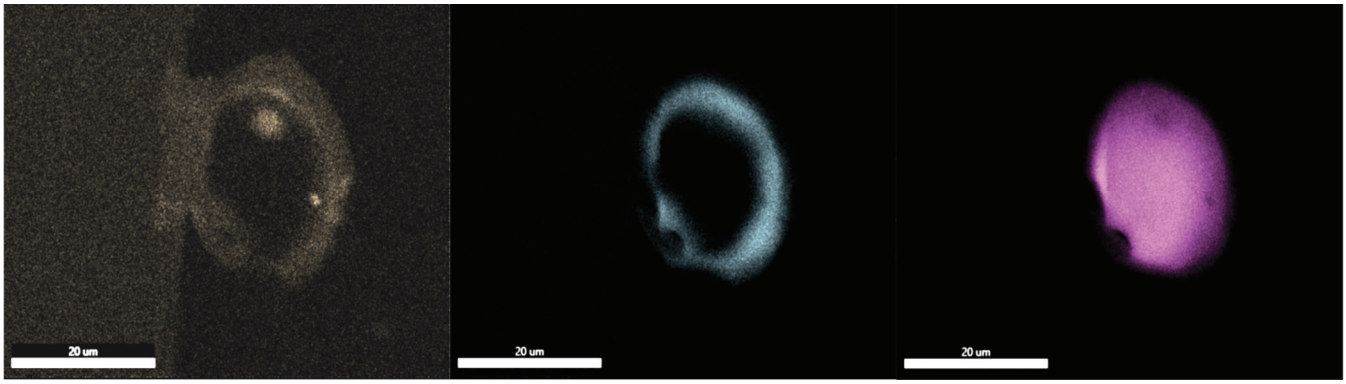


**Figure 50: Single element maps of particle of Federal Premium (centrefire), showing a silicon containing glassy core (right), with incorporated Pb nodules (left), and a Pb/Ba incorporation on the outer rim of the particle (Ba, centre).**

It can be observed that in the first particle (the Winchester rimfire), only a very minor rim of the glass has had element (Pb/Ba) migration, in the Federal Premium (centrefire) particle, there has been migration of elements up to 2-3 µm into the glass, and in the PMC Zapper (rimfire) particle the migration has progressed into the centre of the particle. We hypothesise that during firing, the glass particles are present in a solid or semi-solid state while the other elements from the primer coalesce and cool around their outside to form gGSR. As the pressures generated during discharge may be very

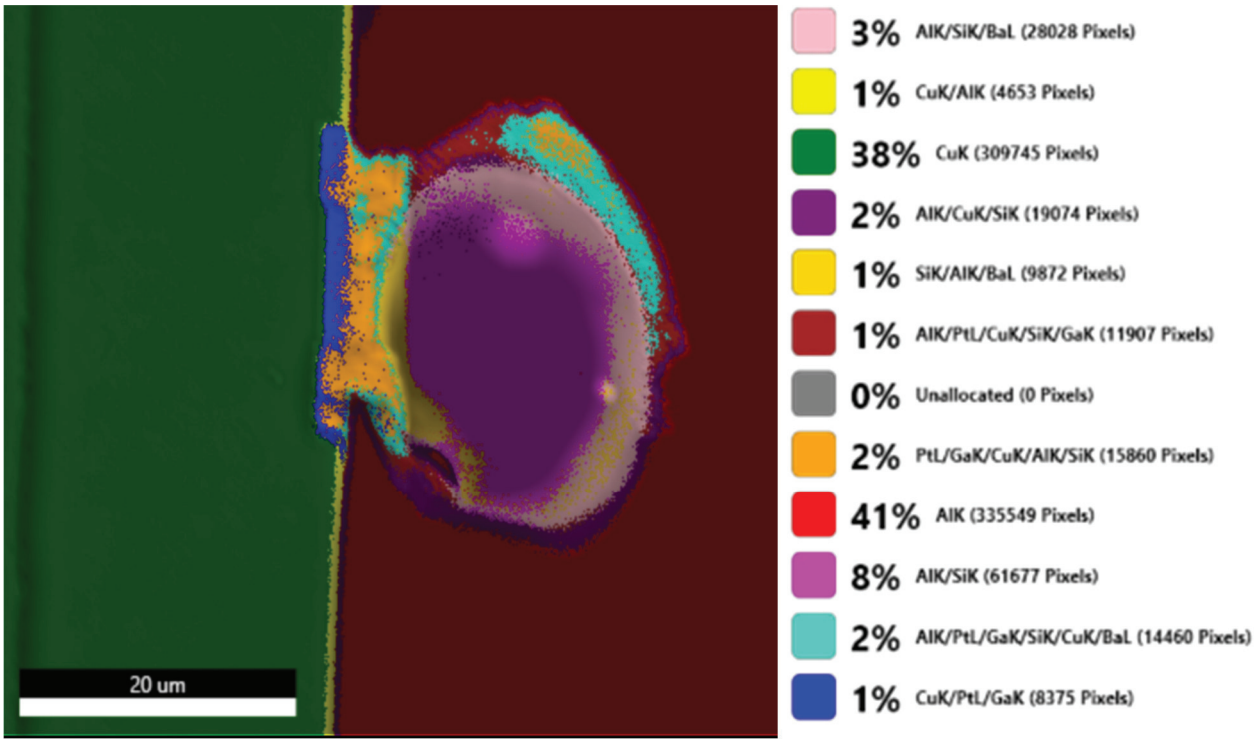


**Figure 51: Phase overlay diagram of SEM-EDS map of Federal Premium centrefire ammunition sliced open using FIB**

high (estimated to be approximately 35,000 psig for .40 Smith and Wesson cartridges [290]and approximately 24,000 psig for 0.22 calibre cartridges [291] ) it is not surprising that migration of heavy metal primer residues into frictionator fragments takes place.

Particles showing these morphological/chemical characteristics are not likely to be produced by common environmental or industrial processes [158]. If such sources are rare then the detection of these particles could provide a valuable new capability for GSR examination, especially in shootings involving rimfire ammunition or when a residue collected involves a small number of particles that do not include the three key elements. Further work has been carried out in Chapter 3 to identify whether non-cartridge sources can produce particles resembling gGSR, and no such sources have been identified as yet.

### 5.5.2. Comparison of gGSR to extracted frictionator using SEM-EDS

After characterising these particles by SEM-EDS, it was of interest to investigate whether the pre- and post- firing residues could be linked, and whether particles from different sources could be differentiated. In Chapter 4, it was noted that frictionator particles from different brands of ammunition could be differentiated based on their elemental composition, but surprisingly, differentiation within the Winchester brand was not possible despite a large time-span (decades) in the manufacturing date of the cartridges sampled.

Unlike Winchester ammunition, PMC Zapper has previously been identified as having frictionator compositional variance within the brand [159], even to the extent that some batches contained borosilicate glass whereas other contained soda lime glass. Therefore, there is the potential to demonstrate a link, or not, between gGSR and a putative source ammunition or between two deposits of gGSR, for example between deposits at two crime scenes or between deposits on a victim and deposits on a suspect.

The newer (Mexican) cartridges had at least two glass fragment populations within the individual cartridge (Figure 52), but as only one box was available it was not possible to determine the generality of this finding. Only one frictionator composition was observed within each cartridge of the South Korean variant and these compositions could not be distinguished using SEM-EDS (Figure 52). For this comparison, the mean ±3σ are presented and at least 10 gGSR particles per stub were analysed.

This Figure also displays the composition of the glass present in the FIB-prepared Zapper gGSR sample (the country of origin for which was not known to the researchers at the time) and it can be seen that its composition is different from both populations present in the Mexican examples of PMC Zapper.

This difference can be established from the sodium, magnesium, potassium, calcium and tin concentrations.

However, the FIB-prepared sample could not be distinguished from any of the South Korean samples using SEM-EDS, indicating that it may have been made in South Korea. After testing was complete, the origin of the FIB-prepared sample was revealed as South Korea, thus confirming the test indications. From the limited number of cartridges examined it appears to be the case that the composition of frictionator from the Mexican Zapper cartridges has greater variety than the frictionator from South Korean Zapper.

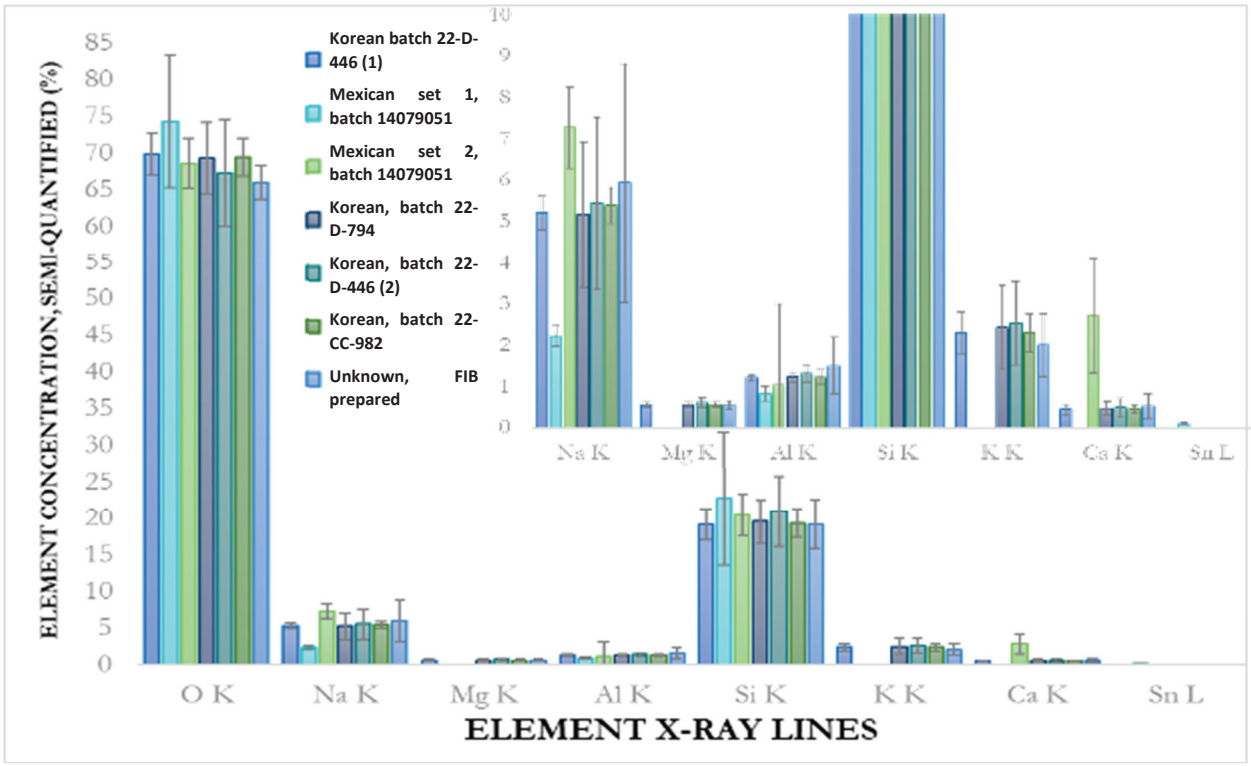


**Figure 52: SEM-EDS comparison of glass frictionator fragment populations from PMC Zapper samples of various manufacture and a gGSR particle from a PMC Zapper particle of unknown manufacture. It is important to note that the two populations of Mexican frictionator present originated from one cartridge, where all other samples represent separate cartridges. Inset: a close-up of the low concentration elements. X-axis shows the X-ray lines for each element used for quantitation.**

### 5.5.3. Comparison of gGSR to extracted frictionator using ToF-SIMS

The comparison of composition between gGSR collected from muzzle discharge and extracted frictionator samples for Winchester and PMC Zapper using ToF-SIMS are shown in Figure 53 and Figure 54, respectively. Figure 53 shows that the 99% confidence intervals for the relative intensities of the extracted and the FIB-prepared gGSR from Winchester ammunition overlap for every element, with the exception of Pb, which is present only in the FIB-prepared sample, indicating that it was most likely not incorporated during the firing process. Glass from Winchester ammunition has previously been

observed to exhibit no significant variation between different batches, factories and ammunition types over the past several decades [159, 202]. The relatively low abundance of K and Ca indicate that the glass is of the borosilicate type.

Figure 54 shows a comparison of the compositions (mean ±3σ) of the PMC Zapper gGSR slice and one of the South Korean PMC Zapper samples that were shown to be indistinguishable by SEM-EDS. The higher analytical power of ToF-SIMS allowed minor differences (assessed by 99% confidence intervals not overlapping) between the two glass samples to be observed with regards to Mg, Al, K and Na concentrations. Differences between the samples with regards to Cu and Pb were also observed, but these elements were only detected in the FIB-section. As this phenomenon was also noted in the Winchester FIB slice, the abundance of these elements is most likely connected to the deposition of other primer components onto the surface of the glass during discharge and/or FIB process and these elements were not used as a basis for discrimination.

Our previous work indicated that ToF-SIMS had a greater power of discrimination than SEM-EDS for comparing clean, extracted frictionator samples [202]. The results presented here support the relative powers regarding comparing sectioned gGSR particles with frictionator extracted from putative source ammunition.

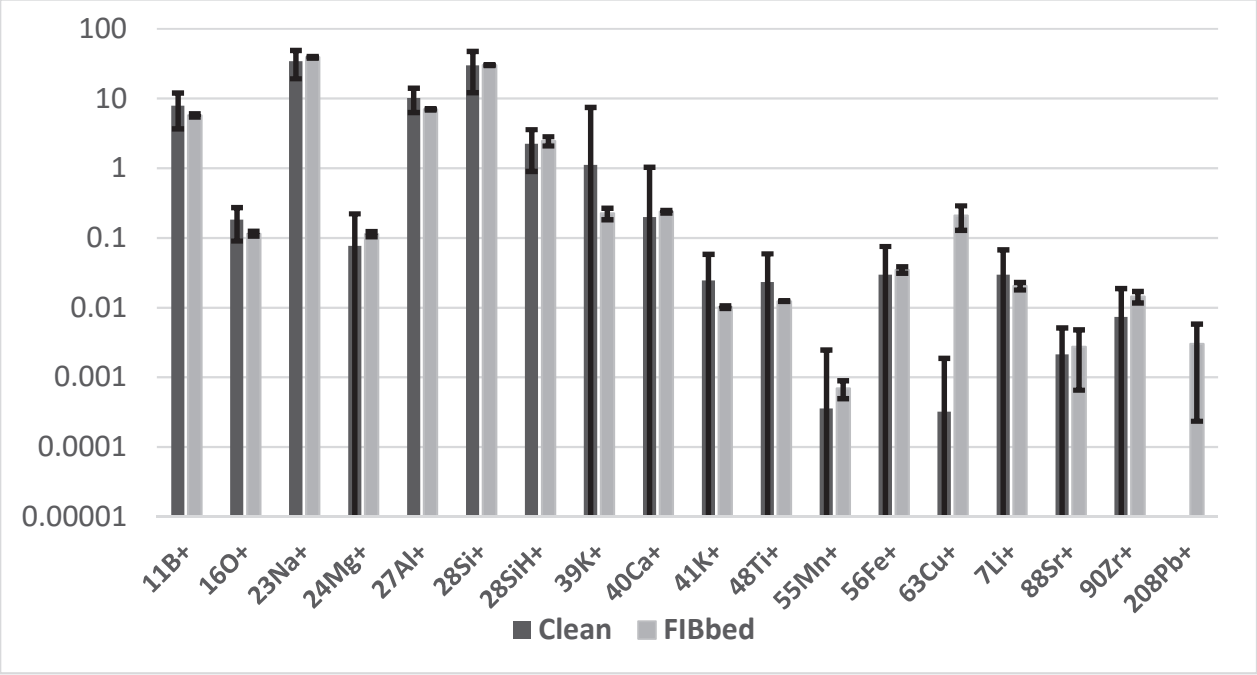


**Figure 53: Mean intensities of fragments ±3σ, as a percentage of total counts of, comparing extracted frictionator and FIB-prepared gGSR samples from Winchester**

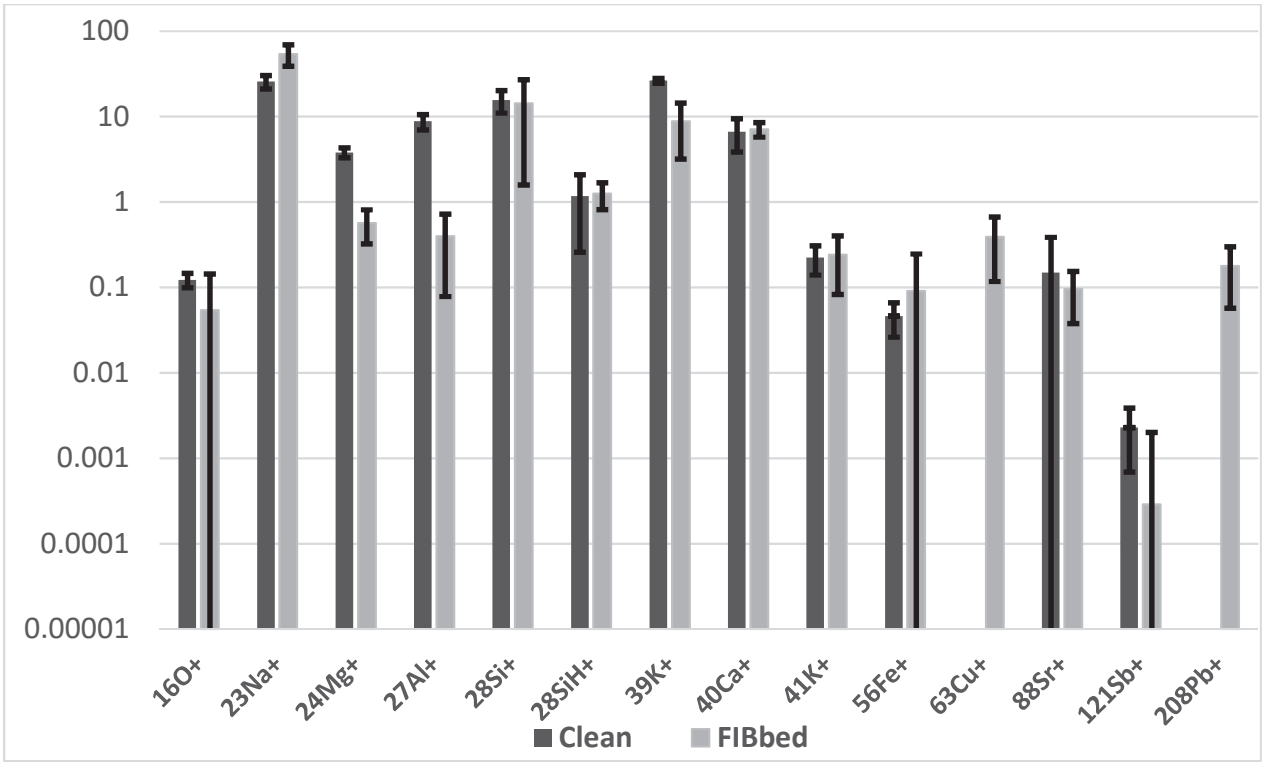


**Figure 54: Mean intensities of fragments ±3σ, as a percentage of total counts, comparing extracted frictionator and FIB-prepared gGSR samples from PMC Zapper**

## 5.6. Conclusions

gGSR particles are fragments of glass frictionator partially or completely covered with a heavy-metal crust derived mainly from other components of the primer. In other studies, we have not been able to find environmental sources of particles resembling gGSR. Therefore, the detection of gGSR in a case is potentially valuable evidence, especially in shootings involving 0.22 rimfire ammunition, which frequently contains glass frictionator but does not contain residues of antimony trisulfide. The purpose of the investigation described here was to explore methodologies for obtaining elemental profiles of the glass in gGSR as a means of associating particles with putative source ammunition or with other deposits of GSR (such as those arising from a different shooting). This chapter shows that it is feasible to obtain such profiles and thus presents an insight into the possibilities for a new forensic capability.

In order to obtain pristine samples of the frictionator core of gGSR particles for analysis, the particles were sectioned using a focussed ion beam (FIB) to expose a clean glass surface for examination. ToF-SIMS and SEM-EDS were used to generate semi-quantitative elemental profiles of glass from FIB-prepared slices for comparison with profiles generated from frictionator particles extracted from unfired cartridges. The particles examined in this study were larger than particles generally encountered in case work, and were chosen for convenience for re-locating the particles, for trialling the methodologies used and to allow replicate elemental analyses on non-overlapping points of the sample, but the techniques used, FIB, SEM-EDS and ToF-SIMS are capable of analysing case-sized particles, and sectioning particles using FIB is faster and simpler for smaller particles.

The elemental profile of a FIB-sectioned gGSR particle from Winchester ammunition was found to be similar to previously obtained profiles for Winchester frictionator. This demonstrates the concept that gGSR can be compared to frictionator extracted from unfired ammunition.

An additional demonstration of the concept was carried out using PMC Zapper ammunition, using both FIB-prepared samples and particles with exposed glass. Even across a few ammunition samples, it was noted that frictionator from PMC Zapper ammunition manufactured in Korea showed more variation than that from Winchester, but Mexican PMC frictionator showed more variation than the Korean PMC Zapper. SEM-EDS was easily capable of discriminating elemental compositions of frictionator and genuine particles obtained from Winchester and PMC ammunitions and between Mexican PMC and Korean PMC. Using SEM-EDS the elemental profile of a FIB-section of a Zapper gGSR particle (not known to be of South Korean origin at the time of analysis) was found to resemble closely the profiles of frictionator extracted from a small population of South Korean PMC frictionator

samples. ToF-SIMS was capable of achieving discrimination amongst all the extracted South Korean Frictionator samples and the section of gGSR, which supports the earlier finding (Chapter 4) that ToF-SIMS exhibits a higher discrimination power than SEM-EDS with regards to analysis of frictionator.

Processing of gGSR using a FIB is straightforward, if not a little slow, and as the unit is usually an accessory in an SEM; finding particles already detected by a traditional GSR search is quite simple. However, the equipment is not commonly available in forensic laboratories. The earlier works [158] used the ion beam in the ToF-SIMS to expose the glass core of particles by sputtering away primer encrustations prior to glass elemental profiling. Finding GSR particles using ToF-SIMS is more difficult than in a FIB-SEM, the ToF-SIM beam sputtered more slowly through the glass than using the FIB preparation method, and it did not allow particles to be lifted off of the stub. However, it was capable of sputtering sufficiently to obtain mass spectra of the glass without major Pb and Ba contamination so as to be comparable to pre-fired samples and could be used in casework.

Hundreds of glass-containing gunshot residue particles have now been observed and it has been noticed that a considerable proportion of particles have only a small fraction of their surface encrusted with heavy metal deposits. In particles such as these it is possible to acquire an elemental profile of the glass present very simply using SEM-EDS. Even though ToF-SIMS offers better discrimination than SEM-EDS, the latter can achieve a discrimination power of about 79%, which suggests that SEM-EDS may be the best initial test for rapid evaluation of whether a sample of gGSR may be associated with a particular source of ammunition or another deposit of gGSR.

SEM-EDS X-ray mapping was used to investigate elemental homogeneity within slices of gGSR and to determine whether primer-derived heavy metals migrate into the glassy matrix during firing. It was found that the frictionator samples can be compositionally stable during firing, but it was also found that elements from the primer can migrate into the glass core of gGSR particles, which could affect the elemental profiles, but also be an indicator of the route of formation. This may indicate some mixing between molten metals, and glass during discharge of a firearm. Other than through the discharge of primer from a firearm or cartridge tool, such as a cartridge-operated nail gun, it is expected that sources of gGSR particles would be rare.

Although HMF ammunition was not specifically examined in this study, gGSR has been observed originating from a few brands in related work. Therefore, a separate study is needed to determine whether there are environmental sources of glass-containing particles that resemble gGSR from HMF ammunition, such as glass with strontium-containing deposits on their surface, and whether there is compositional variance amongst the glass frictionators used in various brands of HMF ammunition.

This chapter has assessed and compared several methods of analysing gGSR particles in order to add new information and capabilities to GSR analysis in forensic casework, and to further the fundamental understanding about the presence, formation, morphology and composition, and the potential use of these particles.

# 6. Conclusions and Future Works

The research described in this thesis has investigated gunshot residue particles that include glass cores derived from frictionators. It has been conducted as part of a larger collaboration aimed at transforming the analysis and interpretation of GSR evidence, with a specific emphasis placed on the relatively unusual casework conditions present in Australia and locally in South Australia.

In the first stream of the project, glass-containing residues, such as Pb/glass, Ba/glass or Pb/Ba/glass, were assessed to determine whether they have the ability to add value to forensic GSR investigation. GSR, including glass-containing GSR, has been compared to other sources of particulate matter in order to determine whether automotive sources, fireworks, matches or nail guns could produce residues similar to glass-containing GSR or residues characteristic of GSR.

The second element of the project investigated prevalence of frictionators in 0.22 rimfire cartridges, the variation of elemental composition of the glass frictionators across different brands on the market, and the possibility of using SEM-EDS and SIMS techniques for differentiation between frictionators from different sources.

In the third stream, glass-containing gunshot residues were examined to investigate whether the elemental composition and variation seen in the frictionators was preserved through discharge of the ammunition in a firearm. Methods were then investigated to locate, section, analyse and compare the morphological and compositional characteristics of glass-containing GSR particles.

These projects were undertaken in order to investigate whether glass-containing GSR particles could be exploited to enhance GSR analyses in casework. The results of the above projects will be explored here to address that question.

### 6.1.1. Occupational residue sources and gunshot residues

Several sources of particles that had the potential to produce particles resembling GSR, or have previously been reported to do so, were examined. This survey included particles collected from fireworks, matches, nail guns and brake pads. None of these sources were found to be a source of particles characteristic of GSR, but nail guns produced 2-component particles and glass containing particles similar to those from a firearm discharge.

A key result presented in this thesis is that only two sources – firearm cartridges and cartridge-actuated nail gun cartridges (such as those produced by Hilti) – were found to be capable of producing residues containing glass mixed with Pb, Ba or Sb or any combination of these elements.

### 6.1.2. Concluding comments concerning Glass-containing residues

It is described in this thesis and a published article arising therefrom that consistent GSR particles, glass, and particles similar to gGSR, have also been observed from nail gun discharge. Therefore, they could potentially appear similar to residues from ammunitions that do not contain antimony. In a further complication, it was found that the piston design of the nail gun, where the charge doesn't directly contact the nail, seemed to prevent the formation of the Zn- and Fe-containing particles that have been previously reported [224] to disqualify a residue as GSR, making it very similar to GSR from 2-component primers.

Although there was no reason to exclude the known nail gun residues as being consistent with GSR using the classification system as per the ASTM guidelines, one difference was noted between the nail gun particle population and that of the GSR. In GSR from hands and surfaces, the ratio of Pb : Pb/Ba was found to be between 5:1 and 10:1, but in nail gun residues, the ratio was roughly reversed, with a 5-10 times excess of Pb/Ba particles. It is unclear whether this was a product of the temperature and pressure differences between the nail gun and the firearm, or whether it was a function of the composition used in the cartridges. More research may illuminate whether this trend tends to be true from other cartridges (both for nail guns and firearms), and if this ratio persists, the Pb : Pb/Ba ratio may be a way to differentiate firearm residues from nail gun residues.

Additionally, the popularity of battery-powered and/or pneumatic nail guns has meant that cartridge-actuated nail guns are no longer widely available to buy or rent in South Australia and may soon be rare in the community. Therefore, if considered as a possible source of a residue, on a case-by-case scenario, nail guns are not likely to impact the interpretation of GSR in casework, as very few people would be exposed to nail guns on a regular basis.

It is also possible, that by examining the glass composition, that nail gun and GSR residues could be distinguished in many cases in the future. The nail gun cartridges examined in this study contained

only borosilicate glass, meaning that some brands of ammunition, containing soda-lime glass, would be easily distinguished. A technique with a higher discrimination power than SEM-EDS, such as ToF-SIMS, could be applied to detect smaller differences in elemental composition of the glass.

Although they did not produce particles containing glass, fireworks produced small amounts of Pb, Ba or Sb particles (0.3-3.5%), and Pb/Ba or other 'consistent' particles at up to 1% of the total particle population collected. Although Sb, Ba and Pb can all be present in fireworks, and despite international evidence suggesting that characteristic particles can be produced by fireworks, none was detected in the particles collected from fireworks in this study. This may indicate that the different elements (Pb, Ba, Sb) were kept separate by location or timing in the fireworks used in this study, which may minimise mixing potential. Numerous K/Cl and Fe containing particles, in addition to Sr and Zr, were observed from firework samples, the presence of which allows differentiation between GSR and firework particles.

Matches create particles with morphologies typical of GSR, but do not contain glass or any elements that are considered to characteristic to either traditional or HMF ammunitions. Similar to fireworks, a number of elongated, K/Cl particles were observed, probably originating from potassium perchlorate, as well as Zr, and Ti/Zn and Zn in some match variants. Matches contained some silicon-containing particles, but these appear to be from a silicate such as $SiO_2$, or similar.

### 6.1.3. Concluding comments regarding particles characteristic of GSR

Particles from brake pads, mechanics' hands, and other automotive sources were considered for their potential to provide evidence that would be indistinguishable from GSR. One false-positive 3 component particle was observed, but no true characteristic particles and no particles containing glass were observed out of over 148 000 particles.

From the analysis of approximately 98 000 particles from nail guns, one three-component Pb/Ba/Sb particle was observed. Only four of the other particles found on hands, from three different individuals, contained Sb and these particles do not appear to be sourced from the nail, primer mix, or the nail gun assembly. It is possible that the Sb incorporated into the observed Pb/Ba/Sb particle is not relevant to the nail gun but was incorporated into the particle from hands from a secondary or background source. A similarly low level of Sb-containing particles was found when hands were stubbed after being used to strike matches; 0.3% of particles collected were found to contain Sb. Matches do not contain Sb according to their safety data sheets or according to any of the previous literature. Furthermore, when matches were struck over surfaces, residues showed no Sb. A study by

Lucas *et al.* [198] into GSR on the random population indicated that approximately one-third (32%) of subjects sampled had Sb on their hands, and could have between one and seventy particles thereof. Therefore, the possibility that this three-component particle, was created by the mixing of components from multiple sources and is a highly unlikely outcome from the discharge of a nail gun must be considered.

Although brake pads, fireworks and match samples do not appear likely to cause a trained GSR analyst to incorrectly designate a sample as GSR, high numbers of particles sourced from brake pads or fireworks could conceivably mask a small GSR population.

## 6.2. Analysis of Glass Frictionators

To determine whether glass frictionators could provide information to connect GSR deposits from the same source, several requirements must be met. Firstly, the glass from within a singular source, i.e. a cartridge case, or two cartridge cases from the same box, needs to match. Secondly, the glass from pre-fired cartridges needs to be able to be linked to post-fired particles. And finally, sufficient variation needs to exist between samples – i.e. brands, types of ammunition, batches, etc., to allow discrimination between samples from different sources.

In order to examine whether linking deposits is feasible, and to settle on an appropriate analysis method for glass particles which may be incorporated in GSR residues, several analytical techniques which are capable of chemical profiling of glass particles smaller than ~50 μm in diameter were examined. The techniques examined were SEM-EDS, ToF-SIMS, and SHRIMP.

SHRIMP was chosen although it may not be capable of examining casework-size samples (<20 μm diameter) and it is technique that is not widely available. However, it has the capability to provide information about elemental composition and isotopic composition and it was felt that the latter capability offered the promise of extremely high specificity. The elemental analysis provided 69.9% inter-brand discrimination (assessed by comparing brands mean ± 3 σ pairwise). It was found that there was not sufficient isotopic variation to differentiate between different brands of frictionator using B, Li, or Pb, Th and U isotopes. The isotopic analyses did not add the further discrimination expected, therefore SHRIMP was not used in further work.

SEM-EDS was selected as it is fast, inexpensive and widely available to forensic scientists. In casework involving genuine GSR samples, the frictionator-containing particles would be initially detected and identified by SEM-EDS. This technique had a pairwise brand power of discrimination of approximately

79%, using the seven oxides that were detected in most samples. Using SEM-EDS boron could be detected but could not be quantified.

The final technique chosen, and the one with the highest pairwise brand power of discrimination was ToF-SIMS. This technique was used because it has high sensitivity, high spatial resolution and has the capability for depth-profiling. Data for more than fifty ions can be collected from glass down to a 5 x 5 µm region, and the power of discrimination for this technique was determined to be 94.1%, based on frictionator composition.

From this work, it was found that there are elemental composition differences between brands of manufacture that can be exploited. It was demonstrated that different brands of frictionator, could be discerned with more than 99% confidence approximately 94% of the time using ToF-SIMS, or that with 99% confidence, non-matching samples could be discriminated by SEM-EDS with approximately 80% power of discrimination. These results show that any intra-source variation, such as within a cartridge or box, or, in the case of Winchester, within the brand, tends to be smaller than the inter-source variation, such as between samples. This means that differentiation of gunshot residues using glass from frictionators in casework samples is theoretically possible.

## 6.3. Glass-Containing Gunshot Residues

After showing that the possibility exists to tie two exhibits of GSR together, or potentially a fired and unfired sample, it was necessary to show empirical evidence that pre-fired and post-fired samples could be linked. Genuine GSR samples were collected from 0.22 rimfire ammunitions from Winchester and PMC Zapper, as was a sample of 0.40 calibre police ammunition.

SEM-EDS mapping was used to show that the glass structure was relatively homogenous, even after firing. It showed that there were different levels of metal encrustation and incorporation into the glass structure in different particles. One of the particles had mostly encrustation, and less than 1 µm of migration of the metals into the glass structure. A second particle had some metal incorporation, with the lead and barium migrating 2-3 µm into the glass matrix. Another particle showed that the incorporation had proceeded into the bulk glass matrix proper and had created a glass-GSR conglomerate. The crusted coating onto, or the incorporation of lead and barium into the glass matrix, especially in a heterogeneous manner could be considered a highly probative indicator of association with a firearm or cartridge discharge source, as the occurrence of molten glass, lead and barium has not been found from any other source.

The particle from Winchester, which had only a small depth of metal incorporation, was able to be linked using ToF-SIMS to unfired Winchester frictionator particles. The PMC Zapper particle, which showed more metal incorporation, did not appear to match unfired PMC Zapper frictionator particles. However, unfired frictionators from the same box were unable to be obtained, and this ammunition has previously been reported to have intra-brand variance. It was also considered that the incorporation of the lead and barium may have caused matrix effects. It was unclear why the larger glass particle from PMC Zapper had much more metal penetration than the smaller Winchester particle. It could be due to random effects or may be because the PMC Zapper particle is soda-lime, as soda lime glasses tend to soften at a lower temperature than borosilicate glasses.

During this work, it was noted that gGSR particles observed from ammunition tended to be smaller and have more lead and barium incorporation than those seen from the nail gun experiments discussed previously. The nail gun particles tended to have more angular morphology and more regions of exposed glass than the gGSR particles, which may indicate that the pressure inside the nail gun was lower than would be expected in a firearm. However, as only a single nail gun and brand of cartridge was used, this may not be representative of all nail gun particles.

## 6.4. Recommendations and Future Works

From the work that has been discussed in this thesis, there are a number of recommendations to be made.

Pb/Ba/Si, Pb/Si and Ba/Si should be incorporated into particle searching lists for GSR analysis, to allow detection of gGSR. If Pb/Ba/Si particles are detected and are shown to contain ratios of Na and Al to Si consistent with glass, this would indicate the presence of glass, and that the likelihood of the source of the sample being firearm related is very high, although the possibility that nail guns could also be the source should be considered during evidence interpretation.

A comprehensive ‘random man’ study should be conducted, or existing data reviewed, to determine the probability that someone who has not recently had contact with a firearm would have Pb/Ba/glass particles on their hands. If that value is found to be sufficiently low, that finding together with the targeted study of firework and match particles would demonstrate that particles containing Pb, Ba and glass should be considered for inclusion into the ASTM guidelines for particles that are

characteristic of firearms origin rather than consistent with firearms origin. This would have the greatest impact in cases where rimfire ammunition is involved.

The last recommendation from this study is that any forensic laboratories interested in developing the capability to use elemental composition of gGSR particles to distinguish between samples from different sources should develop internal casework-based databases of gGSR and frictionator compositions.

There were several other avenues for future work arising from the research undertaken. In some critical cases, using a technique such as ToF-SIMS may be beneficial to compare residues which contain gGSR particles, to determine whether two residues match or to suggest a brand. More research would be required to determine whether this could be extended to other ammunition calibres. However, in the course of this project preliminary research was undertaken indicating that Federal Premium 0.40 centrefire ammunition and several .308 ammunitions may be glass-containing, and therefore it is probable that glass frictionator is used in other, similar ammunitions, which should be further investigated.

In reviewing patent literature concerning glass frictionators, it was found that several low toxicity/heavy metal free (HMF) primer formulation patents include glass as a frictionator, either alone, or in addition to boron particles or calcium silicide [24, 29-31, 243, 287]. In continuing work in this field, research into the possibility to use glass to enhance the probative value of HMF ammunitions should be considered, and a survey could be undertaken to examine if, and how many, HMF formulations include glass as a frictionator. If a number of formulations include glass, there is the possibility that particles such as glass/Sr/Al, or glass/Ti/Zn may be discovered, and these may be found to have a high probative value.

During analysis of the gGSR, it was noted that there were different levels of incorporation of Pb and Ba into the glass structure in different particles. It was initially assumed that the incorporation would be higher in smaller particles, as they would melt faster, but evidence was found that this may not be the case. The three particles that were examined were each between 20 -60 µm in diameter, with the particle having the most encrustation, and least permeation of Pb and Ba, being the largest of the particles, and borosilicate. The slice from the smaller particle of borosilicate had a greater permeation depth of Pb and Ba than the larger particle. The particle that had the most incorporation, where the metals permeated into the centre of the particle, was the particle from PMC Zapper, which notably, was the only soda-lime glass containing ammunition examined and was the mid-sized particle. Further research may illuminate the main influences for lead and barium incorporation and whether particle

size, glass composition, external or environmental (pressure and temperature) factors within the firearm during discharge are the most important factors in determining the degree of metal incorporation.

However, other explanations for the differing levels of metal incorporation into the particles could be due to the metals themselves. SEM-EDS alone is not able to determine the form of the elements detected. In the literature review it was discussed that in the primer, the Pb, Ba and Sb are usually present as salts, such as lead styphnate, barium nitrate and antimony sulfide. However, there are other salts used, such as lead nitrate and lead or barium peroxide, and it is possible that the identity of the salt used has an effect on GSR or gGSR morphology. Additionally, projectiles are made of metallic alloys, usually including Pb and Sb metals. It is possible that these metals could also be incorporated in gGSR particles, and that the inclusion of metallic Pb may have an effect on morphology and composition, and this area is worthy of further investigation.

FIB, as was used in Chapter 5 to expose clean glass surfaces for SEM-EDS and ToF-SIMS analysis, is a technique commonly used for TEM sample preparation, and could be used to further thin the slices of particles for analysis using TEM. Further investigation into the formation of gGSR, and the differences in morphologies observed could therefore be undertaken using FIB and TEM and is an avenue worth exploration in future.

Further, this combination of FIB and TEM could be used to investigate other GSR particles. Investigation into the forms of metals in other GSR particles could contribute positively to the current conversation about the formation of three-component particles from two-component primers. This may help to inform the current discussion regarding the relative magnitude of the effects from weapon memory or projectile inclusion.

Another technique that may be of interest for future work is μ-XRF. Although μ-XRF was not available for this project, it has many attributes that could make it a preferred technique in future. Many operational forensic laboratories have access to μ-XRF, it has lower limits of detection than EDS analysis, it can be used for quantitative or semi-quantitative analysis, and it can be used for elemental mapping. Additionally, μ-XRF is sometimes found as a secondary beam on an SEM-EDS instrument, which would be very convenient for incorporation of gGSR analysis into current processes. Current commercially available μ-XRF instruments can use spot sizes below 20 μm in diameter, and therefore may be suitable for case-sized particles [292]. Some newer instruments can analyse elements down to carbon (Z=6) [292] and synchrotron source μ-XRF can use sub-micron spot sizes [293]. An important forensic consideration is admissibility in court. SEM-EDS and μ-XRF are already well accepted in the

courtroom as established scientific techniques (XRF for other evidence types), and because they are non-destructive to the samples, any sample analysed by SEM-EDS or μ-XRF can be re-analysed in future, which makes the results obtained easier to defend, because they could be independently verified.

## 6.5. Impacts of this Research

The impacts of this research could be far-reaching if they are successfully transitioned into capabilities for casework. The research described in this thesis addressed several areas of original contribution. The first assessed the probative value of glass-containing GSR particles, to determine whether the presence of these particles could improve GSR identification or interpretation.

It was the first survey to investigate glass-containing particles, and the results of this survey indicate that sources thought to have the potential to produce particles 'similar to GSR' do not produce particles similar to gGSR, with the exception of explosive nail gun cartridges. Consequently, this indicates that detection of particles such as Pb/Ba/glass or Pb/Ba/Sb/glass could improve the probative value of GSR evidence.

For example, the detection of gGSR particles would strongly support a hypothesis that a firearm was the source of the particles. This could be important in casework, as it may allow greater certainty that a firearm was involved in case, especially when there are no, or limited amounts of primer-sourced antimony contributing to the GSR deposit, such as may be the case when many 0.22 rimfire variants are used, which is of great relevance in South Australia and Australia in general.

This research also involved an attempt to develop a novel capability in forensic GSR analysis; the ability to discriminate between two or more samples of GSR from different source ammunition. This aim was investigated by exploiting gGSR particles, showing that glass appears to be elementally stable during firing, even though it shows evidence of melting and re-forming. The particles were characterised using FIB, SEM-EDS and ToF-SIMS, which had not previously been attempted on glass-containing GSR, and very rarely applied to any form of GSR. ToF-SIMS and SEM-EDS both showed a promising ability to be able to link samples from a single-source and discriminate samples from different sources, in both unfired and fired samples.

This new capability could help to connect residues more specifically then possible using current techniques, thereby increasing the evidentiary value of a positive result, and excluding samples from alternate sources.

# 7. References


[1] A. Biedermann, S. Bozza, F. Taroni, Probabilistic evidential assessment of gunshot residue particle evidence (Part I): Likelihood ratio calculation and case pre-assessment using Bayesian networks, Forensic Science International 191(1) (2009) 24-35.

[2] N. Lucas, M. Cook, K.P. Kirkbride, H.J. Kobus, A framework for the assessment of gunshot residue (GSR) evidence: transfer, contamination, and preservation., American Academy of Forensic Sciences 70th Annual Meeting, Seattle, Washington, 2018.

[3] D.L. McGuire, The controversy concerning gunshot residues examinations, Forensic Magazine, 2008.

[4] Australian Bureau of Statistics, Weapon use in violent crime, by victims per year (n) 1995-2012, in: A.I.o. Criminology (Ed.) Facts & Figures online data tool, Canberra, Australia, 2013.

[5] Australian Criminal Intelligence Commission, Illicit Firearms in Australia, Canberra, Australia, 2016.

[6] Centers for Disease Control and Prevention, National Center for Health Statistics, Underlying Cause of Death 1999-2015 on CDC WONDER Online Database, released December, 2016. Data are from the Multiple Cause of Death Files, 1999-2015, as compiled from data provided by the 57 vital statistics jurisdictions through the Vital Statistics Cooperative Program. Accessed at http://wonder.cdc.gov/ucd-icd10.html on May 31, 2017 1:13:31 AM (EDT). 2016.

[7] Office for National Statistics, Offences involving the use of weapons: data tables, year ending March 2018, https://www.ons.gov.uk/peoplepopulationandcommunity/crimeandjustice/datasets/offencesinvolvingtheuseofweaponsdatatables, access date 9 Nov 2019.

[8] J.S. Wallace, Chemical Analysis of Firearms, Ammunition, and Gunshot Residue, CRC Press,2008.

[9] ABS, *Causes of Death Australia, 2006-2015* 'Table 13.1 Underlying cause of death, All causes, Year of Occurrence, Australia 2005-2015', data cube: Excel spreadsheet, cat. no. 3303.0, viewed 26 May 2017, www.abs.gov.au/AUSSTATS/abs@.nsf/DetailsPAge/3303.02015?OpenDocument, 2016.

[10] Office for National Statistics, Mortality statistics - underlying cause, sex and age, 2013-2018, in: a.N. nomis https://www.nomisweb.co.uk/query/construct/summary.asp?mode=construct&version=0&dataset=161 (Ed.).

[11] C. Haw, L. Sutton, S. Simkin, D. Gunnell, N. Kapur, M. Nowers, Suicide by gunshot in the United Kingdom: a review of the literature, Med., Sci. Law 44 (2004) 295–310.

[12] Y.Y. Avissar, A.E. Sagiv, D. Mandler, J. Almog, Identification of firearms holders by the [Fe(PDT)3](+2) complex. Quantitative determination of iron transfer to the hand and its dependence on palmar moisture levels, Journal of Forensic Sciences 49(6) (2004) 1215-1219.

[13] F.S. Romolo, Overview, Analysis, and Interpretation, in: M.M. Houck, J.A. Siegel, P.J. Saukko (Eds.), Encyclopedia of Forensic Sciences, Academic Press, Waltham, 2013, pp. 195-201.

[14] J. Andrasko, S. Pettersson, A simple method for collection of gunshot residues from clothing, Journal of the Forensic Science Society 31(3) (1991) 321-330.

[15] I. Aleksandar, Is there a way to precisely identify that the suspect fired from the firearm?, Forensic Science International, ELSEVIER SCI IRELAND LTD CUSTOMER RELATIONS MANAGER, BAY 15, SHANNON …, 2003, pp. 158-159.

[16] Z. Brozek-Mucha, Comparison of cartridge case and airborne GSR - A study of the elemental composition and morphology by means of SEM-EDX, X-Ray Spectrometry 36(6) (2007) 398-407.

[17] H.H. Meng, B. Caddy, Gunshot residue analysis - A review, Journal of Forensic Sciences 42(4) (1997) 553-570.

[18] J. Coumbaros, K.P. Kirkbride, G. Klass, W. Skinner, Characterisation of 0.22 caliber rimfire gunshot residues by time-of-flight secondary ion mass spectrometry (TOF-SIMS): a preliminary study, Forensic Science International 119(1) (2001) 72-81.
[19] F. Saverio Romolo, P. Margot, Identification of gunshot residue: a critical review, Forensic Science International 119(2) (2001) 195-211.
[20] A. Zeichner, Recent developments in methods of chemical analysis in investigations of firearm-related events, Analytical and Bioanalytical Chemistry 376(8) (2003) 1178-1191.
[21] K.H. Chang, P.T. Jayaprakash, C.H. Yew, A.F.L. Abdullah, Gunshot residue analysis and its evidential values: A review, Australian Journal of Forensic Sciences 45(1) (2013) 3-23.
[22] S. Basu, Formation of gunshot residues, Journal of Forensic Sciences 27(1) (1982) 72-91.
[23] L.A. Burrows, W. Brun, Ammunition priming mixture, Google Patents, 1944.
[24] L. Guindon, Low toxicity primer compositions for reduced energy ammunition, Google Patents, 2009.
[25] I.J. Fisher, D.J. Pain, V.G. Thomas, A review of lead poisoning from ammunition sources in terrestrial birds, Biological conservation 131(3) (2006) 421-432.
[26] J.M. Arnemo, O. Andersen, S. Stokke, V.G. Thomas, O. Krone, D.J. Pain, R. Mateo, Health and Environmental Risks from Lead-based Ammunition: Science Versus Socio-Politics, EcoHealth 13(4) (2016) 618-622.
[27] D.C. Bellinger, A. Bradman, J. Burger, T.J. Cade, D.A. Cory-Slechta, D. Doak, M. Finkelstein, A.R. Flegal, M. Fry, R.E. Green, H. Hu, D.E. Jacobs, C. Johnson, T. Kelly, M. Kosnett, P.J. Landrigan, B. Lanphear, H.W. Mielke, I. Newton, M.A. Pokras, R.H. Poppenga, P.T. Redig, B.A. Rideout, R.W. Risebrough, T. Scheuhammer, E. Silbergeld, D.R. Smith, B. Strupp, V.G. Thomas, R. Wright, Health Risks from Lead-Based Ammunition in the Environment - A Consensus Statement of Scientists, UC Santa Cruz: Microbiology and Environmental Toxicology Retrieved from https://escholarship.org/uc/item/6dq3h64x (2013).
[28] R.K. Bjerke, J.P. Ward, D.O. Ells, K.P. Kees, Improved primer composition, Google Patents, 1991.
[29] G.B. Carter, Primer composition, Google Patents, 2000.
[30] J.R. Duguet, Rimfire primer and process for the manufacture thereof, Google Patents, 1996.
[31] F.G. Lopata, G.C. Mei, Non-toxic, non-corrosive rimfire cartridge, Google Patents, 1987.
[32] ASTM, E1588-17, Standard Practice for Gunshot Residue Analysis by Scanning Electron Microscopy/Energy Dispersive X-Ray Spectrometry, www.astm.org, West Conshohocken, PA, 2017.
[33] M. Morelato, A. Beavis, P. Kirkbride, C. Roux, Forensic applications of desorption electrospray ionisation mass spectrometry (DESI-MS), Forensic Science International 226(1-3) (2013) 10-21.
[34] E.E. Hodge, Current Methods in Forensic Gunshot Residue Analysis, Journal of Forensic Identification 50(6) (2000) 597-599.
[35] O. Dalby, D. Butler, J.W. Birkett, Analysis of Gunshot Residue and Associated Materials—A Review, Journal of Forensic Sciences 55(4) (2010) 924-943.
[36] A.J. Bandodkar, A.M. O'Mahony, J. Ramirez, I.A. Samek, S.M. Anderson, J.R. Windmiller, J. Wang, Solid-state Forensic Finger sensor for integrated sampling and detection of gunshot residue and explosives: towards 'Lab-on-a-finger', Analyst (Cambridge UK) 138(18) (2013) 5288-5295.
[37] J. Bueno, V. Sikirzhytski, I.K. Lednev, Raman Spectroscopic Analysis of Gunshot Residue Offering Great Potential for Caliber Differentiation, Analytical Chemistry 84(10) (1975) 4334-4339.
[38] J. Bueno, I. Lednev, Raman microspectroscopic chemical mapping and chemometric classification for the identification of gunshot residue on adhesive tape, Analytical and Bioanalytical Chemistry 406(19) (2014) 4595-4599.
[39] Z. Abrego, N. Grijalba, N. Unceta, M. Maguregui, A. Sanchez, A. Fernandez-Isla, M.A. Goicolea, R.J. Barrio, A novel method for the identification of inorganic and organic gunshot residue particles of lead-free ammunitions from the hands of shooters using scanning laser ablation-ICPMS and Raman micro-spectroscopy, Analyst 139(23) (2014) 6232-6241.

[40] S.P. Sharma, S.C. Lahiri, A preliminary investigation into the use of FTIR microscopy as a probe for the identification of bullet entrance holes and the distance of firing, Science & Justice 49(3) (2009) 197-204.
[41] L.S. Leggett, P.F. Lott, Gunshot residue analysis via organic stabilizers and nitrocellulose, Microchemical Journal 39(1) (1989) 76-85.
[42] C.K. Muro, K.C. Doty, J. Bueno, L. Halámková, I.K. Lednev, Vibrational Spectroscopy: Recent Developments to Revolutionize Forensic Science, Analytical Chemistry 87(1) (2015) 306-327.
[43] M. López-López, J.J. Delgado, C. García-Ruiz, Analysis of macroscopic gunshot residues by Raman spectroscopy to assess the weapon memory effect, Forensic Science International 231(1–3) (2013) 1-5.
[44] M. López-López, J.L. Ferrando, C. García-Ruiz, Comparative analysis of smokeless gunpowders by Fourier transform infrared and Raman spectroscopy, Analytica Chimica Acta 717(0) (2012) 92-99.
[45] O. Dalby, J.W. Birkett, The evaluation of solid phase micro-extraction fibre types for the analysis of organic components in unburned propellant powders, Journal of Chromatography A 1217(46) (2010) 7183-7188.
[46] J.M.F. Douse, Dynamic headspace method for the improved clean-up of gunshot residues prior to the detection of nitroglycerine by capillary column gas chromatography with thermal energy analysis detection, Journal of Chromatography A 464(0) (1991) 178-185.
[47] A. Tarifa, J.R. Almirall, Fast detection and characterization of organic and inorganic gunshot residues on the hands of suspects by CMV-GC–MS and LIBS, Science & Justice (0) (2015).
[48] A. Zeichner, B. Eldar, B. Glattstein, A. Koffman, T. Tamiri, D. Muller, Vacuum collection of gunpowder residues from clothing worn by shooting suspects, and their analysis by GC/TEA, IMS, and GC/MS, Journal of forensic sciences 48(5) (2003) 961-972.
[49] D. Muller, A. Levy, A. Vinokurov, M. Ravreby, R. Shelef, E. Wolf, B. Eldar, B. Glattstein, A Novel Method for the Analysis of Discharged Smokeless Powder Residues, Journal of Forensic Sciences 52(1) (2007) 75-78.
[50] C. Weyermann, V. Belaud, F. Riva, F.S. Romolo, Analysis of organic volatile residues in 9 mm spent cartridges, Forensic Science International 186(1–3) (2009) 29-35.
[51] S.J. Speers, K. Doolan, J. McQuillan, J.S. Wallace, Evaluation of improved methods for the recovery and detection of organic and inorganic cartridge discharge residues, Journal of Chromatography A 674(1-2) (1994) 319-327.
[52] M. Morelato, A. Beavis, A. Ogle, P. Doble, P. Kirkbride, C. Roux, Screening of gunshot residues using desorption electrospray ionisation-mass spectrometry (DESI-MS), Forensic Science International 217(1-3) (2012) 101-106.
[53] M. Zhao, S. Zhang, C. Yang, Y. Xu, Y. Wen, L. Sun, X. Zhang, Desorption Electrospray Tandem MS (DESI-MSMS) Analysis of Methyl Centralite and Ethyl Centralite as Gunshot Residues on Skin and Other Surfaces, Journal of Forensic Sciences 53(4) (2008) 807-811.
[54] M. Maitre, K.P. Kirkbride, M. Horder, C. Roux, A. Beavis, Current perspectives in the interpretation of gunshot residues in forensic science: A review, Forensic Science International 270 (2017) 1-11.
[55] D. Laza, B. Nys, J. De Kinder, A. Kirsch-De Mesmaeker, C. Moucheron, Development of a quantitative LC-MS/MS method for the analysis of common propellant powder stabilizers in gunshot residue, Journal of Forensic Sciences 52(4) (2007) 842-850.
[56] R.V. Taudte, C. Roux, L. Blanes, M. Horder, K.P. Kirkbride, A. Beavis, The development and comparison of collection techniques for inorganic and organic gunshot residues, Analytical and Bioanalytical Chemistry 408(10) (2016) 2567-2576.
[57] L. Gandy, K. Najjar, M. Terry, C. Bridge, A Novel Protocol for the Combined Detection of Organic, Inorganic Gunshot Residue, Forensic Chemistry 8 (2018) 1-10.

[58] Z. Brożek-Mucha, A study of gunshot residue distribution for close-range shots with a silenced gun using optical and scanning electron microscopy, X-ray microanalysis and infrared spectroscopy, Science & Justice 57(2) (2017) 87-94.
[59] A. Brandone, F. De Ferrari, P. Pelizza, M. Signori, The labelling of gunpowder: An approach to improve gunshot residues determination, Forensic Science International 47(3) (1990) 289-295.
[60] I.T. Weber, A.J.G. de Melo, M.A.d.M. Lucena, M.O. Rodrigues, S. Alves, High Photoluminescent Metal–Organic Frameworks as Optical Markers for the Identification of Gunshot Residues, Analytical Chemistry 83(12) (1975) 4720-4723.
[61] I.T. Weber, A.J.G. Melo, M.A.M. Lucena, E.F. Consoli, M.O. Rodrigues, G.F. de Sá, A.O. Maldaner, M. Talhavini, S. Alves, Use of luminescent gunshot residues markers in forensic context, Forensic Science International 244 (2014) 276-84.
[62] C.A. Destefani, L.C. Motta, G. Vanini, L.M. Souza, J.F.A. Filho, C.J. Macrino, E.M. Silva, S.J. Greco, D.C. Endringer, W. Romao, Europium-organic complex as luminescent marker for the visual identification of gunshot residue and characterization by electrospray ionization FT-ICR mass spectrometry, Microchemical Journal 116 (2014) 216-224.
[63] N.G.R. Hearns, D.N. Laflèche, M.L. Sandercock, Preparation of a Ytterbium-tagged Gunshot Residue Standard for Quality Control in the Forensic Analysis of GSR, Journal of Forensic Sciences 60(3) (2015) 737-742.
[64] L. Niewoehner, N. Buchholz, J. Merkel, New ammunitions for the German police, Proceedings of SCANNING, FAMS, Inc., Monterey, CA., 2005 p. 69.
[65] P. Griess, On a New Series of Bodies in Which Nitrogen is Substituted for Hydrogen, Philosophical Transactions of the Royal Society of London 154 (1864) 667-731.
[66] P. Griess, Bemerkungen zu der Abhandlung der HH. Weselsky und Benedikt "Ueber einige Azoverbindungen", Berichte der deutschen chemischen Gesellschaft 12(1) (1879) 426-428.
[67] M.G. Haag, L.C. Haag, Chapter 6 - Distance and Orientation Derived from Gunshot Residue Patterns, in: M.G. Haag, L.C. Haag (Eds.), Shooting Incident Reconstruction (Second Edition), Academic Press, San Diego, 2011, pp. 87-103.
[68] N. Petraco, M. Yander, J. Sardone, A method for the quantitative determination of nitrites in gunshot residue cases, Forensic Science International 18(1) (1981) 85-92.
[69] I. Castellanos, La Puela de Parafina. Tomo I. Seria Cubana de Criminalistica, Biblioteca Juridica de Autores Cubanos y Extranjeros 119 (1948).
[70] H.L. Schlesinger, I. Golf General Atomic, Special Report on Gunshot Residues Measured by Neutron Activation Analysis, Gulf General Atomic Incorporated,1970.
[71] T.A. Gonzales, Wounds by firearms in civil life, The American Journal of Surgery 26(1) (1934) 43-52.
[72] F. Feigl, Beiträge zur qualitativen Mikroanalyse. II, Mikrochemie 2(11-12) (1924) 186-188.
[73] H.C. Harrison, R. Gilroy, Firearms discharge residues, Journal of Forensic Sciences 4(2) (1959) 184-199.
[74] G. Price, Firearms discharge residues on hands, Journal of the Forensic Science Society 5(4) (1965) 199-200.
[75] V.J.M. DiMaio, Gunshot Wounds: Practical Aspects of Firearms, Ballistics, and Forensic Techniques, Second Edition, CRC Press, 2002.
[76] V.P. Guinn, Recent Developments in the Application of Neutron Activation Analysis Techniques to Forensic Problems, Journal of the Forensic Science Society 4(4) (1964) 184-191.
[77] R.R. Ruch, J.D. Buchanan, V.P. Guinn, S.C. Bellanca, R.H. Pinker, Neutron Activation Analysis in Scientific Crime Detection - Some Recent Developments, Journal of Forensic Sciences 9 (1964) 119-33.
[78] M.E. Cowan, P.L. Purdon, C.M. Hoffman, R. Brunelle, S.R. Gerber, M. Pro, Barium and antimony levels on hands significance as indicator of gunfire residue, J. Radioanal. Chem. 15(1) (1973) 203-218.

[79] S.S. Krishnan, R.E. Jervis, Characterization of shotgun pellets and gunshot residues by trace element concentration patterns by neutron activation analysis using the SLOWPOKE reactor, Journal of the Canadian Society of Forensic Science 17(4) (1984) 167-81.
[80] S.S. Krishnan, Detection of gunshot residues on the hands by trace element analysis, Journal of Forensic Sciences 22(2) (1977) 304-24.
[81] S.S. Krishnan, Trace element analysis by atomic absorption spectrometry and neutron activation analysis in the investigation of shooting cases, Journal of the Canadian Society of Forensic Science 6(2) (1973) 55-77.
[82] G. Capannesi, C. Ciavola, A.F. Sedda, Determination of firing distance and firing angle by neutron activation analysis in a case involving gunshot wounds, Forensic Science International 61(2-3) (1993) 75-84.
[83] G. Capannesi, A.F. Sedda, Bullet identification: A case of a fatal hunting accident resolved by comparison of lead shot using instrumental neutron activation analysis, Journal of Forensic Sciences 37(2) (1992) 657-662.
[84] M. Jauhari, T. Singh, S.M. Chatterji, Characterization of firearm discharge residue of ammunition of Indian origin by neutron activation analysis, Forensic Science International 22(2-3) (1983) 117-121.
[85] M. Jauhari, T. Singh, S.M. Chatterji, Primer residue analysis of ammunition of Indian origin by Neutron Activation Analysis, Forensic Science International 19(3) (1982) 253-258.
[86] R. Cornelis, Truth Has Many Facets: The Neutron Activation Analysis Story, Journal of the Forensic Science Society 20(2) (1980) 93-98.
[87] J.L. Booker, D.D. Schroeder, J.H. Propp, A note on the variability of barium and antimony levels in cartridge primers and its implication for gunshot residue identification, Journal of the Forensic Science Society 24(2) (1984) 81-84.
[88] S.S. Krishnan, K.A. Gillespie, E.J. Anderson, Rapid detection of firearm discharge residues by atomic absorption and neutron activation analysis, Journal of Forensic Sciences 16(2) (1971) 144-151.
[89] I.C. Stone Jr, C.S. Petty, Examination of gunshot residues, Journal of Forensic Sciences 19(4) (1974) 784-788.
[90] D.G. Havekost, C.A. Peters, R.D. Koons, Barium and antimony distributions on the hands of nonshooters, Journal of Forensic Sciences 35(5) (1990) 1096-114.
[91] W.D. Kinard, D.R. Lundy, A Comparison of Neutron Activation Analysis and Atomic Absorption Spectroscopy on Gunshot Residue, Forensic Science, American Chemical Society1975, pp. 97-107.
[92] E. Rudzitis, Analysis of the Results of Gunshot Residue Detection in Case Work, Journal of Forensic Sciences 25(4) (1980) 839-846.
[93] J.H. Liu, W.F. Lin, J.D. Nicol, The application of anodic stripping voltammetry to forensic science. II. Anodic stripping voltammetric analysis of gunshot residues, Forensic Science International 16(1) (1980) 53-62.
[94] R.C. Briner, S. Chouchoiy, R.W. Webster, R.E. Popham, Anodic stripping voltammetric determination of antimony in gunshot residue, Analytica Chimica Acta 172(C) (1985) 31-37.
[95] C.A. Woolever, D.E. Starkey, H.D. Dewald, Differential pulse anodic stripping voltammetry of lead and antimony in gunshot residues, Forensic Science International 102(1) (1999) 45-50.
[96] D.M. Northrop, Gunshot residue analysis by micellar electrokinetic capillary electrophoresis: assessment for application to casework. Part I, Journal of Forensic Sciences 46(3) (2001) 549-559.
[97] C.A. Woolever, H.D. Dewald, Differential pulse anodic stripping voltammetry of barium and lead in gunshot residues, Forensic Science International 117(3) (2001) 185-190.
[98] S. Erden, Z. Durmus, E. Kiliç, Simultaneous Determination of Antimony and Lead in Gunshot Residue by Cathodic Adsorptive Stripping Voltammetric Methods, Electroanalysis 23(8) (2011) 1967-1974.

[99] X. Cetó, A.M. O'Mahony, I.A. Samek, J.R. Windmiller, M. del Valle, J. Wang, Rapid Field Identification of Subjects Involved in Firearm-Related Crimes Based on Electroanalysis Coupled with Advanced Chemometric Data Treatment, Analytical Chemistry 84(23) (2012) 10306-10314.
[100] Z. Abrego, A. Ugarte, N. Unceta, A. Fernandez-Isla, M.A. Goicolea, R.J. Barrio, Unambiguous Characterization of Gunshot Residue Particles Using Scanning Laser Ablation and Inductively Coupled Plasma-Mass Spectrometry, Analytical Chemistry 84(5) (2012) 2402-2409.
[101] E. Diaz, J.E. Souza Sarkis, S. Viebig, P. Saldiva, Measurement of airborne gunshot particles in a ballistics laboratory by sector field inductively coupled plasma mass spectrometry, Forensic Science International 214(1) (2012) 44-47.
[102] J.E.S. Sarkis, O.N. Neto, S. Viebig, S.F. Durrant, Measurements of gunshot residues by sector field inductively coupled plasma mass spectrometry—Further studies with pistols, Forensic Science International 172(1) (2007) 63-66.
[103] A. Zeichner, S. Ehrlich, E. Shoshani, L. Halicz, Application of lead isotope analysis in shooting incident investigations, Forensic Science International 158(1) (2006) 52-64.
[104] R.D. Koons, Analysis of gunshot primer residue collection swabs by inductively coupled plasma-mass spectrometry, Journal of Forensic Sciences 43(4) (1998) 748-754.
[105] R. Keto, Analysis and comparison of bullet leads by inductively-coupled plasma mass spectrometry, Journal of Forensic Sciences 44(5) (1999) 1020-1026.
[106] S. Steffen, M. Otto, L. Niewoehner, M. Barth, Z. Brozek-Mucha, J. Biegstraaten, R. Horváth, Chemometric classification of gunshot residues based on energy dispersive X-ray microanalysis and inductively coupled plasma analysis with mass-spectrometric detection, Spectrochimica Acta - Part B Atomic Spectroscopy 62(9) (2007) 1028-1036.
[107] R.D. Koons, D.G. Havekost, Determination Of Barium In Gunshot Residue Collection Swabs Using Inductively Coupled Plasma-Atomic Emission Spectometry, Journal of Forensic Sciences 33(1) (1988) 35-41.
[108] E. Turillazzi, G.n.P. Di Peri, A. Nieddu, S. Bello, F. Monaci, M. Neri, C. Pomara, R. Rabozzi, I. Riezzo, V. Fineschi, Analytical and quantitative concentration of gunshot residues (Pb, Sb, Ba) to estimate entrance hole and shooting-distance using confocal laser microscopy and inductively coupled plasma atomic emission spectrometer analysis: An experimental study, Forensic Science International 231(1) (2013) 142-9.
[109] G. Vanini, C.A. Destefani, B.B. Merlo, M.T.W.D. Carneiro, P.R. Filgueiras, R.J. Poppi, W. Romão, Forensic ballistics by inductively coupled plasma-optical emission spectroscopy: Quantification of gunshot residues and prediction of the number of shots using different firearms, Microchemical Journal 118(0) (2015) 19-25.
[110] G. Vanini, M.O. Souza, M.T.W.D. Carneiro, P.R. Filgueiras, R.E. Bruns, W. Romao, Multivariate optimisation of ICP OES instrumental parameters for Pb/Ba/Sb measurement in gunshot residues, Microchemical Journal 120 (2015) 58-63.
[111] G. Vanini, R.M. Souza, C.A. Destefani, B.B. Merlo, T.M. Piorotti, E.V.R. de Castro, M.T.W.D. Carneiro, W. Romão, Analysis of gunshot residues produced by .38 caliber handguns using inductively coupled plasma-optical emission spectroscopy (ICP OES), Microchemical Journal 115(0) (2014) 106-112.
[112] R.D. Koons, D.G. Havekost, Analysis Of Gunshot Primer Residue Collection Swabs Using Flameless Atomic Absorption Spectrophotometry And Inductively Coupled Plasma-Atomic Emission Spectrometry: Effects Of A Modified Extraction Procedure And Storage Of Standards, Journal of Forensic Sciences 34(1) (1989) 218-221.
[113] Ç. Aksoy, T. Bora, N. Şenocak, F. Aydin, A new method to reduce false positives due to antimony in detection of gunshot residues, Forensic Science International 250 (2015) 87-90.
[114] R.S. Nesbitt, J.E. Wessel, P.F. Jones, Detection of gunshot residue by use of the scanning electron microscope, Journal of Forensic Sciences 21(3) (1976) 595-610.

[115] G.M. Wolten, R.S. Nesbitt, A.R. Calloway, G.L. Loper, P.F. Jones, Final Report on Particle Analysis for Gunshot Residue Detection, in: T.A.C. Law Enforcement Development Group (Ed.) National Institute of Law Enforcement and Criminal Justice, Law Enforcement Assistance Administration, U.S. Department of Justice, Washington, D. C. 20024, 1977.
[116] G.M. Wolten, R.S. Nesbitt, A.R. Calloway, G.L. Loper, P.F. Jones, Particle Analysis for the Detection of Gunshot Residue. I: Scanning Electron Microscopy/Energy Dispersive X-Ray Characterization of Hand Deposits from Firing, Journal of Forensic Sciences 24(2) (1979) 409-422.
[117] G.M. Wolten, R.S. Nesbitt, A.R. Calloway, G.L. Loper, Particle Analysis for the Detection of Gunshot Residue. II: Occupational and Environmental Particles, Journal of Forensic Sciences 24(2) (1979) 423-430.
[118] G.M. Wolten, R.S. Nesbitt, A.R. Calloway, Particle analysis for the detection of gunshot residue: III: The case record, Journal of Forensic Sciences 24(4) (1979) 864-869.
[119] J.S. Wallace, J. McQuillan, Discharge Residues from Cartridge-operated Industrial Tools, Journal of the Forensic Science Society 24(5) (1984) 495-508.
[120] A. Zeichner, N. Levin, More on the Uniqueness of Gunshot Residue (GSR) Particles, Journal of Forensic Sciences 42(6) (1997) 1027-1028.
[121] L. Garofano, M. Capra, F. Ferrari, G.P. Bizzaro, D. Di Tullio, M. Dell'Olio, A. Ghitti, Gunshot residue: Further studies on particles of environmental and occupational origin, Forensic Science International 103(1) (1999) 1-21.
[122] S.A. Phillips, Pyrotechnic residues analysis – detection and analysis of characteristic particles by scanning electron microscopy/energy dispersive spectroscopy, Science & Justice 41(2) (2001) 73-80.
[123] C. Torre, G. Mattutino, V. Vasino, C. Robino, Brake linings: A source of non-GSR particles containing lead, barium, and antimony, Journal of Forensic Sciences 47(3) (2002) 494-504.
[124] K.L. Kosanke, R.C. Dujay, B. Kosanke, Characterization of pyrotechnic reaction residue particles by SEM/EDS, Journal of Forensic Sciences 48(3) (2003) 531-537.
[125] K.L. Kosanke, R.C. Dujay, B.J. Kosanke, Pyrotechnic Reaction Residue Particle Analysis, Journal of Forensic Sciences 51(2) (2006) 296-302.
[126] M. Grima, M. Butler, R. Hanson, A. Mohameden, Firework displays as sources of particles similar to gunshot residue, Science & Justice 52(1) (2012) 49-57.
[127] R.S. White, A.D. Owens, Automation of gunshot residue detection and analysis by scanning electron microscopy/energy dispersive X-ray analysis (SEM/EDX), Journal of Forensic Sciences 32(6) (1987) 1595-1603.
[128] W.L. Tillman, Automated Gunshot Residue Particle Search And Characterization, Journal of Forensic Sciences 32(1) (1987) 62-71.
[129] J. Lebiedzik, D.L. Johnson, Rapid search and quantitative analysis of gunshot residue particles in the SEM, Journal of Forensic Sciences 45(1) (2000) 83-92.
[130] A. Zeichner, N. Levin, E. Springer, Gunshot residue particles formed by using different types of ammunition in the same firearm, Journal of Forensic Sciences 36(4) (1991) 1020-1026.
[131] S. Charles, B. Nys, N. Geusens, Primer composition and memory effect of weapons—Some trends from a systematic approach in casework, Forensic Science International 212(1–3) (2011) 22-26.
[132] O. Israelsohn-Azulay, Y. Zidon, T. Tsach, A mixed composition particle highlights the formation mechanism of the weapon memory effect phenomenon, Forensic Science International 286 (2018) 18-22.
[133] Z. Oommen, S.M. Pierce, Lead-free primer residues: A qualitative characterization of Winchester WinClean™, Remington/UMC LeadLess™, Federal BallistiClean™, and Speer Lawman CleanFire™ handgun ammunition, Journal of Forensic Sciences 51(3) (2006) 509-519.
[134] Z. Brozek-Mucha, G. Zadora, Grouping of ammunition types by means of frequencies of occurrence of GSR, Forensic Science International 135(2) (2003) 97-104.

[135] Z. Brozek-Mucha, A. Jankowicz, Evaluation of the possibility of differentiation between various types of ammunition by means of GSR examination with SEM–EDX method, Forensic Science International 123(1) (2001) 39-47.
[136] Z. Brozek-Mucha, G. Zadora, Frequency of occurrence of certain chemical classes of GSR from various ammunition types, Z Zagadnien Nauk Sadowych 46 (2001) 281-287.
[137] P. Sen, N. Panigrahi, Application Of Proton-Induced X-Ray Emission Technique To Gunshot Residue Analyses, Journal of Forensic Sciences 27(2) (1982) 330-339.
[138] M.J. Bailey, K.J. Kirkby, C. Jeynes, Trace element profiling of gunshot residues by PIXE and SEM-EDS: a feasibility study, X-Ray Spectrometry 38(3) (2009) 190-194.
[139] F.S. Romolo, M.E. Christopher, M. Donghi, L. Ripani, C. Jeynes, R.P. Webb, N.I. Ward, K.J. Kirkby, M.J. Bailey, Integrated Ion Beam Analysis (IBA) in Gunshot Residue (GSR) characterisation, Forensic Science International 231(1–3) (2013) 219-228.
[140] M.E. Christopher, J.-W. Warmenhoeven, F.S. Romolo, M. Donghi, R.P. Webb, C. Jeynes, N.I. Ward, K.J. Kirkby, M.J. Bailey, A new quantitative method for gunshot residue analysis by ion beam analysis, Analyst 138(16) (2013) 4649-4655.
[141] L. Niewöhner, H.W. Wenz, Applications of focused ion beam systems in gunshot residue investigation, Journal of Forensic Sciences 44(1) (1999) 105-109.
[142] I. Sarvas, H. Kobus, L. Green, P.G. Kotula, R. Wuhrer, Gun Shot Residue Analysis and Distinguishing the Formation of GSR from Environmental Particles, Microscopy and Microanalysis 15(S2) (2009) 64-65.
[143] R. Wuhrer, I. Sarvas, L. Green, R. Lam, V. Spikmans, H. Kobus, Investigations of gunshot residue and environmental particles through use of focused ion beam and other characterisation techniques, 18th International Microscopy Congress, Prague, Czech Republic, 7-12 September, 2014: Proceedings, 2014.
[144] G. Hellmiss, W. Lichtenberg, M. Weiss, Investigation of gunshot residues by means of Auger electron spectroscopy, Journal of Forensic Sciences 32(3) (1987) 747-760.
[145] B. Charpentier, C. Desrochers, Analysis of primer residue from lead free ammunition by X-ray microfluorescence, Journal of Forensic Sciences 45(2) (2000) 447-52.
[146] A. Berendes, D. Neimke, R. Schumacher, M. Barth, A Versatile Technique for the Investigation of Gunshot Residue Patterns on Fabrics and Other Surfaces: m-XRF, Journal of Forensic Sciences 51(5) (2006) 1085-1090.
[147] R. Schumacher, M. Barth, D. Neimke, L. Niewöhner, Investigation of gunshot residue patterns using milli-XRF-techniques: First experiences in casework, Proceedings of SPIE - The International Society for Optical Engineering, 2010.
[148] J. Flynn, M. Stoilovic, C. Lennard, I. Prior, H. Kobus, Evaluation of X-ray microfluorescence spectrometry for the elemental analysis of firearm discharge residues, Forensic Science International 97(1) (1998) 21-36.
[149] S. Latzel, D. Neimke, R. Schumacher, M. Barth, L. Niewoehner, Shooting distance determination by m-XRF-Examples on spectra interpretation and range estimation, Forensic Science International 223(1-3) (2012) 273-278.
[150] C.R. Dockery, S.R. Goode, Laser-induced breakdown spectroscopy for the detection of gunshot residues on the hands of a shooter, Applied Optics 42(30) (2003) 6153-6158.
[151] M.B. Rosenberg, C.R. Dockery, Determining the Lifetime of Detectable Amounts of Gunshot Residue on the Hands of a Shooter Using Laser-Induced Breakdown Spectroscopy, Applied Spectroscopy 62(11) (2008) 1238-1241.
[152] A. Tarifa, J.R. Almirall, Fast detection and characterization of organic and inorganic gunshot residues on the hands of suspects by CMV-GC-MS and LIBS, Science and Justice (2015).

[153] M. López-López, C. Alvarez-Llamas, J. Pisonero, C. García-Ruiz, N. Bordel, An exploratory study of the potential of LIBS for visualizing gunshot residue patterns, Forensic science international 273 (2017) 124-131.
[154] T. Trejos, C. Vander Pyl, K. Menking-Hoggatt, A.L. Alvarado, L.E. Arroyo, Fast identification of inorganic and organic gunshot residues by LIBS and electrochemical methods, Forensic Chemistry 8 (2018) 146-156.
[155] A. Doña-Fernández, I. de Andres-Gimeno, P. Santiago-Toribio, E. Valtuille-Fernández, F. Aller-Sanchez, A. Heras-González, Real-time detection of GSR particles from crime scene: A comparative study of SEM/EDX and portable LIBS system, Forensic Science International 292 (2018) 167-175.
[156] L.G.A. Melo, A. Martiny, A.L. Pinto, Nano characterization of gunshot residues from Brazilian ammunition, Forensic Science International 240 (2014) 69-79.
[157] J. Coumbaros, K.P. Kirkbride, H. Kobus, I. Sarvas, Distribution of lead and barium in gunshot residue particles derived from 0.22 Caliber rimfire ammunition, Journal of Forensic Sciences 46(6) (2001) 1352-1357.
[158] P. Collins, J. Coumbaros, G. Horsley, B. Lynch, K.P. Kirkbride, W. Skinner, G. Klass, Glass-containing gunshot residue particles: A new type of highly characteristic particle?, Journal of Forensic Sciences 48(3) (2003) 538-553.
[159] J. Coumbaros, New frontiers for mass spectrometry in forensic science: Applications of time of flight secondary ion mass spectrometry, University of South Australia, 2002, p. 333.
[160] W.R. Henderson, The Analysis of Glass Frictionators from 0.22 Calibre Ammunition by ICP-AES, School of Chemistry, University of Tasmania, Australia, 2011.
[161] A. Martiny, A.P.C. Campos, M.S. Sader, M.A.L. Pinto, SEM/EDS analysis and characterization of gunshot residues from Brazilian lead-free ammunition, Forensic Science International 177(1) (2008) e9-e17.
[162] G. Zadora, Glass analysis for forensic purposes—a comparison of classification methods, Journal of Chemometrics: A Journal of the Chemometrics Society 21(5-6) (2007) 174-186.
[163] R. Winstanley, C. Rydeard, Concepts of annealing applied to small glass fragments, Forensic Science International 29(1-2) (1985) 1-10.
[164] T. Trejos, S. Montero, J. Almirall, Analysis and comparison of glass fragments by laser ablation inductively coupled plasma mass spectrometry (LA-ICP-MS) and ICP-MS, Analytical and Bioanalytical Chemistry 376(8) (2003) 1255-1264.
[165] T. Trejos, R. Koons, P. Weis, S. Becker, T. Berman, C. Dalpe, M. Duecking, J. Buscaglia, T. Eckert-Lumsdon, T. Ernst, C. Hanlon, A. Heydon, K. Mooney, R. Nelson, K. Olsson, E. Schenk, C. Palenik, E.C. Pollock, D. Rudell, S. Ryland, A. Tarifa, M. Valadez, A. van Es, V. Zdanowicz, J. Almirall, Forensic analysis of glass by μ-XRF, SN-ICP-MS, LA-ICP-MS and LA-ICP-OES: evaluation of the performance of different criteria for comparing elemental composition, Journal of Analytical Atomic Spectrometry 28(8) (2013) 1270-1282.
[166] Y. Suzuki, M. Kasamatsu, S. Suzuki, T. NAKANISHI, M. TAKATSU, S. MURATSU, O. SHIMODA, S. WATANABE, Y. NISHIWAKI, N. MIYAMOTO, Forensic discrimination of sheet glass by a refractive-index measurement and elemental analysis with synchrotron radiation X-ray fluorescence spectrometry, Analytical sciences 21(7) (2005) 855-859.
[167] Y. Nishiwaki, T. Nakanishi, Y. Terada, T. Ninomiya, I. Nakai, Nondestructive discrimination of small glass fragments for forensic examination using high energy synchrotron radiation x-ray fluorescence spectrometry, X-Ray Spectrometry: An International Journal 35(3) (2006) 195-199.
[168] B.E. Naes, S. Umpierrez, S. Ryland, C. Barnett, J.R. Almirall, A comparison of laser ablation inductively coupled plasma mass spectrometry, micro X-ray fluorescence spectroscopy, and laser induced breakdown spectroscopy for the discrimination of automotive glass, Spectrochimica Acta Part B: Atomic Spectroscopy 63(10) (2008) 1145-1150.

[169] J. Locke, M. Underhill, Automatic refractive index measurement of glass particles, Forensic Science International 27(4) (1985) 247-260.
[170] C. Latkoczy, S. Becker, M. Ducking, D. Gunther, J.A. Hoogewerff, J.R. Almirall, J. Buscaglia, A. Dobney, R.D. Koons, S. Montero, G.J. van der Peijl, W.R. Stoecklein, T. Trejos, J.R. Watling, V.S. Zdanowicz, Development and evaluation of a standard method for the quantitative determination of elements in float glass samples by LA-ICP-MS, Journal of Forensic Sciences 50(6) (2005) 1327-41.
[171] R.D. Koons, J. Buscaglia, The forensic significance of glass composition and refractive index measurements, Journal of Forensic Sciences 44(3) (1999) 496-503.
[172] T. Hicks, F. Monard Sermier, T. Goldmann, A. Brunelle, C. Champod, P. Margot, The classification and discrimination of glass fragments using non destructive energy dispersive X-ray µfluorescence, Forensic Science International 137(2–3) (2003) 107-118.
[173] D.C. Duckworth, S.J. Morton, C.K. Bayne, R.D. Koons, S. Montero, J.R. Almirall, Forensic glass analysis by ICP-MS: a multi-element assessment of discriminating power via analysis of variance and pairwise comparisons, Journal of Analytical Atomic Spectrometry 17(7) (2002) 662-668.
[174] J. Coumbaros, J. Denman, K.P. Kirkbride, G.S. Walker, W. Skinner, An Investigation into the Spatial Elemental Distribution Within a Pane of Glass by Time of Flight Secondary Ion Mass Spectrometry, Journal of Forensic Sciences 53(2) (2008) 312-320.
[175] S. Berends-Montero, W. Wiarda, P. de Joode, G. van der Peijl, Forensic analysis of float glass using laser ablation inductively coupled plasma mass spectrometry (LA-ICP-MS): validation of a method, Journal of Analytical Atomic Spectrometry 21(11) (2006) 1185-1193.
[176] J. Almirall, B. Nayes, E. Cahoon, T. Trejos, Elemental Analysis of Glass by SEM-EDS, µXRF, LIBS and LA-ICP-MS, Department of Chemistry and Biochemistry and International Forensic Research Institute Florida International University, NCJRS, 2012.
[177] T. Hoffman, R. Corzo, P. Weis, E. Pollock, A. van Es, W. Wiarda, A. Stryjnik, H. Dorn, A. Heydon, E. Hoise, S. Le Franc, X. Huifang, B. Pena, T. Scholz, J. Gonzalez, J. Almirall, An inter-laboratory evaluation of LA-ICP-MS analysis of glass and the use of a database for the interpretation of glass evidence, Forensic Chemistry 11 (2018) 65-76.
[178] H. Dorn, D.E. Ruddell, A. Heydon, B.D. Burton, Discrimination of float glass by LA-ICP-MS: assessment of exclusion criteria using casework samples, Canadian Society of Forensic Science Journal 48(2) (2015) 85-96.
[179] R. Corzo, T. Hoffman, P. Weis, J. Franco-Pedroso, D. Ramos, J. Almirall, The use of LA-ICP-MS databases to calculate likelihood ratios for the forensic analysis of glass evidence, Talanta 186 (2018) 655-661.
[180] ASTM, E2927 − 16 Standard Test Method for Determination of Trace Elements in Soda-Lime Glass Samples Using Laser Ablation Inductively Coupled Plasma Mass Spectrometry for Forensic Comparisons, ASTM International, West Conshohocken, PA., 2016.
[181] J. Locke, H.V. Locke, Refractive Index Standards for the Forensic Scientist.
[182] Foster and Freeman, Grim3 Overview, 2007.
[183] Microscopy Australia, Scanning Electron Microscopy. <https://myscope.training/#/SEMlevel_3_1>, 2019 (accessed 11 Nov 2019.).
[184] J.I. Goldstein, D.E. Newbury, J.R. Michael, N.W. Ritchie, J.H.J. Scott, D.C. Joy, Scanning electron microscopy and X-ray microanalysis, Third Edition ed., Springer2003.
[185] TESCAN, Secondary Ion TESCAN Detector (SITD). 2019 (accessed 11 Nov 2019.).
[186] L.A. Giannuzzi, Introduction to Focused Ion Beams: Instrumentation, Theory, Techniques and Practice, Springer Science & Business Media2004.
[187] A.T. Ampere, Recent developments in micromilling using focused ion beam technology, Journal of Micromechanics and Microengineering 14(4) (2004) R15.
[188] S. Fearn, An Introduction to Time-of-Flight Secondary Ion Mass Spectrometry (ToF-SIMS) and its Application to Materials Science, Morgan & Claypool Publishers, 2015.

[189] A. Schnieders, Time-of-Flight Secondary Ion Mass Spectrometry, Microscopy Today 19(2) (2011) 30-33.
[190] Australian Scientific Instruments asi, SHRIMP IIe: Reliable, Productive Ion Microprobe, https://asi-pl.com.au/wp/wp-content/uploads/2018/04/SHRIMP-IIe-brochure-2015.pdf 2015.
[191] D. Beauchemin, Inductively Coupled Plasma Mass Spectrometry, Analytical Chemistry 82(12) (2010) 4786-4810.
[192] T. Scientific™, Neptune™ Series High Resolution Multicollector ICP-MS. <https://www.thermofisher.com/order/catalog/product/IQLAAEGAASFADOMAJL#/IQLAAEGAASFADOMAJL>, 2019 (accessed 9 Nov 2019.).
[193] S. Benson, C. Lennard, P. Maynard, C. Roux, Forensic applications of isotope ratio mass spectrometry—A review, Forensic Science International 157(1) (2006) 1-22.
[194] W. Tucker, N. Lucas, K.E. Seyfang, K.P. Kirkbride, R.S. Popelka-Filcoff, Gunshot residue and brakepads: Compositional and morphological considerations for forensic casework, Forensic Science International 270 (2017) 76-82.
[195] K.E. Seyfang, N. Lucas, K.E. Redman, R.S. Popelka-Filcoff, H.J. Kobus, K.P. Kirkbride, Glass-containing gunshot residues and particles of industrial and occupational origins: Considerations for evaluating GSR traces, Forensic Science International 298 (2019) 284-297.
[196] ASTM, E1588-17 Standard practice for gunshot residue analysis by scanning electron microscopy/energy dispersive X-ray spectrometry, ASTM International, West Conshohocken, PA., 2017.
[197] Z. Brozek-Mucha, On the prevalence of gunshot residue in selected populations - An empirical study performed with SEM-EDX analysis, Forensic Science International 237 (2014) 46-52.
[198] N. Lucas, H. Brown, M. Cook, K. Redman, T. Condon, H. Wrobel, K.P. Kirkbride, H. Kobus, A study into the distribution of gunshot residue particles in the random population, Forensic Science International 262 (2016) 150-155.
[199] Z. Brozek-Mucha, Chemical and physical characterisation of welding fume particles for distinguishing from gunshot residue, Forensic Science International 254 (2015) 51-58.
[200] R.E. Berk, Automated SEM/EDS Analysis of Airbag Residue. II: Airbag Residue as a Source of Percussion Primer Residue Particles, Journal of Forensic Sciences 54(1) (2009) 69.
[201] D.J.N. Laflèche, S.J.J. Brière, N.F. Faragher, N.G.R. Hearns, Gunshot residue and airbags: Part I. Assessing the risk of deployed automotive airbags to produce particles similar to gunshot residue, Canadian Society of Forensic Science Journal (2018) 1-10.
[202] K.E. Seyfang, H.J. Kobus, R.S. Popelka-Filcoff, A. Plummer, C.W. Magee, K.E. Redman, K.P. Kirkbride, Analysis of elemental and isotopic variation in glass frictionators from 0.22 rimfire primers, Forensic Science International 293 (2018) 47-62.
[203] M. Kumar, R.K. Singh, V. Murari, A.K. Singh, R.S. Singh, T. Banerjee, Fireworks induced particle pollution: A spatio-temporal analysis, Atmospheric Research 180 (2016) 78-91.
[204] H.-H. Tsai, L.-H. Chien, C.-S. Yuan, Y.-C. Lin, Y.-H. Jen, I.-R. Ie, Influences of fireworks on chemical characteristics of atmospheric fine and coarse particles during Taiwan's Lantern Festival, Atmospheric Environment 62 (2012) 256-264.
[205] J.A. Licudine, H. Yee, W.L. Chang, A.C. Whelen, Hazardous Metals in Ambient Air Due to New Year Fireworks During 2004–2011 Celebrations in Pearl City, Hawaii, Public Health Reports 127(4) (2012) 440-450.
[206] J. Feng, P. Sun, X. Hu, W. Zhao, M. Wu, J. Fu, The chemical composition and sources of PM2.5 during the 2009 Chinese New Year's holiday in Shanghai, Atmospheric Research 118 (2012) 435-444.
[207] J. Crespo, E. Yubero, J.F. Nicolás, F. Lucarelli, S. Nava, M. Chiari, G. Calzolai, High-time resolution and size-segregated elemental composition in high-intensity pyrotechnic exposures, Journal of Hazardous Materials 241–242 (2012) 82-91.

[208] T. Moreno, X. Querol, A. Alastuey, F. Amato, J. Pey, M. Pandolfi, N. Kuenzli, L. Bouso, M. Rivera, W. Gibbons, Effect of fireworks events on urban background trace metal aerosol concentrations: Is the cocktail worth the show?, Journal of Hazardous Materials 183(1–3) (2010) 945-949.
[209] R. Vecchi, V. Bernardoni, D. Cricchio, A. D'Alessandro, P. Fermo, F. Lucarelli, S. Nava, A. Piazzalunga, G. Valli, The impact of fireworks on airborne particles, Atmospheric Environment 42(6) (2008) 1121-1132.
[210] Y. Wang, G. Zhuang, C. Xu, Z. An, The air pollution caused by the burning of fireworks during the lantern festival in Beijing, Atmospheric Environment 41(2) (2007) 417-431.
[211] T. Moreno, X. Querol, A. Alastuey, M. Cruz Minguillón, J. Pey, S. Rodriguez, J. Vicente Miró, C. Felis, W. Gibbons, Recreational atmospheric pollution episodes: Inhalable metalliferous particles from firework displays, Atmospheric Environment 41(5) (2007) 913-922.
[212] S.C. Barman, R. Singh, M.P.S. Negi, S.K. Bhargava, Ambient air quality of Lucknow City (India) during use of fireworks on Diwali Festival, Environmental Monitoring and Assessment 137(1) (2008) 495-504.
[213] S.F. Kong, L. Li, X.X. Li, Y. Yin, K. Chen, D.T. Liu, L. Yuan, Y.J. Zhang, Y.P. Shan, Y.Q. Ji, The impacts of firework burning at the Chinese Spring Festival on air quality: insights of tracers, source evolution and aging processes, Atmos. Chem. Phys. 15(4) (2015) 2167-2184.
[214] U.C. Kulshrestha, T. Nageswara Rao, S. Azhaguvel, M.J. Kulshrestha, Emissions and accumulation of metals in the atmosphere due to crackers and sparkles during Diwali festival in India, Atmospheric Environment 38(27) (2004) 4421-4425.
[215] B. Thakur, S. Chakraborty, A. Debsarkar, S. Chakrabarty, R.C. Srivastava, Air pollution from fireworks during festival of lights (Deepawali) in Howrah, India - a case study, Atmósfera 23(4) (2010).
[216] A. Chatterjee, C. Sarkar, A. Adak, U. Mukherjee, S.K. Ghosh, S. Raha, Ambient air quality during diwali festival over Kolkata - A mega-city in India, Aerosol and Air Quality Research 13(3) (2013) 1133-1144.
[217] H. Jing, Y.-F. Li, J. Zhao, B. Li, J. Sun, R. Chen, Y. Gao, C. Chen, Wide-range particle characterization and elemental concentration in Beijing aerosol during the 2013 Spring Festival, Environmental Pollution 192 (2014) 204-211.
[218] K.J. Godri, D.C. Green, G.W. Fuller, M. Dall'osto, D.C. Beddows, F.J. Kelly, R.M. Harrison, I.S. Mudway, Particulate oxidative burden associated with Firework activity, Environmental Science and Technology 44(21) (2010) 8295-8301.
[219] P.V. Mosher, M.J. McVicar, E.D. Randall, E.H. Sild, Gunshot Residue-Similar Particles Produced by Fireworks, Canadian Society of Forensic Science Journal 31(3) (1998) 157-168.
[220] M. Grima, R. Hanson, H. Tidy, An assessment of firework particle persistence on the hands and related police force practices in relation to GSR evidence, Forensic Science International 239(0) (2014) 19-26.
[221] M.A. Trimpe, Analysis of Fireworks for Particles of the Type Found in Primer Residue (GSR), International Association of Microanalysis Newsletter 4(1) (2003) 1-4.
[222] M. Kasamatsu, Y. Suzuki, R. Sugita, S. Suzuki, Forensic discrimination of match heads by elemental analysis with inductively coupled plasma-atomic emission spectrometry, Journal of Forensic Sciences 50(4) (2005) 883-6.
[223] J. Andrasko, Identification of Burnt Matches by Scanning Electron Microscopy, Journal of Forensic Sciences 23(4) (1978) 637-642.
[224] B. Cardinetti, C. Ciampini, C. D'Onofrio, G. Orlando, L. Gravina, F. Ferrari, D. Di Tullio, L. Torresi, X-ray mapping technique: a preliminary study in discriminating gunshot residue particles from aggregates of environmental occupational origin, Forensic Science International 143(1) (2004) 1-19.
[225] R. Meija, Why we cannot rely on firearm forensics, New Scientist 188(2527) (2005).

[226] E. Gilchrist, F. Jongekrijg, L. Harvey, N. Smith, L. Barron, Characterisation of gunshot residue from three ammunition types using suppressed anion exchange chromatography, Forensic Science International 221(1–3) (2012) 50-56.
[227] D. Chan, G.W. Stachowiak, Review of automotive brake friction materials, Proceedings of the Institution of Mechanical Engineers, Part D: Journal of Automobile Engineering 218(9) (2004) 953-966.
[228] Clean Air Act Ammendments of 1977, in 42 U.S.C. 7524 1977, US Code, Chapter 85— Air Pollution Prevention And Control, Subchapter II—Emission Standards For Moving Sources, Part A—Motor Vehicle Emission and Fuel Standards, Section 7545. Regulation of Fuels: United States of America.
[229] European Parliament Council of the European Union, Directive 98/70/EC of the European Parliament and of the Council of 13 October 1998 relating to the quality of petrol and diesel fuels and amending Council Directive 93/12/EEC, in Directive 98/70/EC, T.E., Union, Editor. 1998, Official Journal of the European Communities. p. 58–68.
[230] Secretary of State for the Environment, Transport and the Regions, The Motor Fuel (Composition and Content) Regulations 1999, in 1999 No. 3107, E.A.W. PUBLIC HEALTH, S. Public Health, and N.I. Public Health, Editors. 1999, UK Government: UK Government.
[231] Environment, Fuel Quality Standards Act 2000, in Act No.153, 2000, Australian Government, Editor. 2000, Australian Government: Canberra, Australia.
[232] Management Committee of the Special Programme on the Control of Chemical, Declaration on Risk Reduction for Lead, in 20 February 1996—C (96)42/FINAL, The United Nations, Editor. 1996, Decisions, Recommendations and other Instruments of the Organisation for Economic Co-Operation and Development.
[233] N. Lucas, M. Cook, J. Wallace, K.P. Kirkbride, H. Kobus, Quantifying gunshot residues in cases of suicide: Implications for evaluation of suicides and criminal shootings, Forensic Science International 266 (2016) 289-298.
[234] E.K. Wilson, What's in fireworks, and what produces those colorful explosions, Chemical & Engineering News, American Chemical Society, 2017, pp. 24-25.
[235] N. Lucas, M. Cook, J. Wallace, K.P. Kirkbride, H. Kobus, Author's response—Letter to the Editor (FSI-D-16-00737), Forensic Science International 270 (2017) e28-e29.
[236] M.R. Rijnders, A. Stamouli, A. Bolck, Comparison of GSR Composition Occurring at Different Locations Around the Firing Position, Journal of Forensic Sciences 55(3) (2010) 616-623.
[237] B. Burnett, Observations on the composition of breech gunshot residue from a. 22 pistol, International Association for MicroAnalysis 4(1) (2003) 12-15.
[238] G.C. Rangel, Match and Striker Method and Apparatus, Google Patents, 2012.
[239] A.F. Emery, P. Kumar, J.C. Firey, Experimental Study of Automotive Brake System Temperatures, 1997.
[240] G. Steinhauser, J.H. Sterba, M. Foster, F. Grass, M. Bichler, Heavy metals from pyrotechnics in New Years Eve snow, Atmospheric Environment 42(37) (2008) 8616-8622.
[241] E.A. Staba, Ammunition priming composition of dry particulate ingredients with karaya gum binder, Google Patents, 1969.
[242] E.A. Staba, Priming composition containing carbon which exhibits conchoidal fracture, Google Patents, 1967.
[243] L. Guindon, D. Allard, Low toxicity primer composition, Google Patents, 1995.
[244] L. Guindon, D. Lepage, J.P. Drolet, Non-toxic primers for small caliber ammunition, Google Patents, 2006.
[245] A. Zeichner, B. Schecter, R. Brener, Antimony enrichment on the bullets' surfaces and the possibility of finding it in gunshot residue (GSR) of the ammunition having antimony-free primers, Journal of Forensic Sciences 43(3) (1998) 493-501.

[246] Z. Brozek-Mucha, Scanning Electron Microscopy and X-Ray Microanalysis for Chemical and Morphological Characterisation of the Inorganic Component of Gunshot Residue: Selected Problems, BioMed Research International (2014).
[247] J. Yañez, M. Paz Farías, V. Zúñiga, C. Soto, D. Contreras, E. Pereira, H.D. Mansilla, R. Saavedra, R. Castillo, P. Sáez, Differentiation of two main ammunition brands in Chile by Regularized Discriminant Analysis (RDA) of metals in gunshot residues, Microchemical Journal 101(0) (2012) 43-48.
[248] C.M. Mahoney, G. Gillen, A.J. Fahey, Characterization of gunpowder samples using time-of-flight secondary ion mass spectrometry (TOF-SIMS), Forensic Science International 158(1) (2006) 39-51.
[249] K. Lund, J.N. Aleinikoff, K.V. Evans, C.M. Fanning, SHRIMP U-Pb geochronology of Neoproterozoic Windermere Supergroup, central Idaho: Implications for rifting of western Laurentia and synchroneity of Sturtian glacial deposits, Bulletin of the Geological Society of America 115(3) (2003) 349-372.
[250] J.M. McLelland, M.E. Bickford, B.M. Hill, C.C. Clechenko, J.W. Valley, M.A. Hamilton, Direct dating of Adirondack massif anorthosite by U-Pb SHRIMP analysis of igneous zircon: Implications for AMCG complexes, Bulletin of the Geological Society of America 116(11) (2004) 1299-1317.
[251] T.R. Riley, I.L. Millar, M.K. Watkeys, M.L. Curtis, et al., U-Pb zircon (SHRIMP) ages for the Lebombo rhyolites, South Africa: refining the duration of Karoo volcanism, Journal of the Geological Society 161 (2004) 547-550.
[252] L.P. Beranek, P. Karl Link, C.M. Fanning, Miocene to Holocene landscape evolution of the western Snake River Plain region, Idaho: Using the SHRIMP detrital zircon provenance record to track eastward migration of the Yellowstone hotspot, Bulletin of the Geological Society of America 118(9) (2006) 1027-1050.
[253] C.J. Gregory, D. Rubatto, C.M. Allen, I.S. Williams, J. Hermann, T. Ireland, Allanite micro-geochronology: A LA-ICP-MS and SHRIMP U-Th-Pb study, Chemical Geology 245(3-4) (2007) 162-182.
[254] C.S. Siddoway, C. Fanning, Paleozoic tectonism on the East Gondwana margin: Evidence from SHRIMP U-Pb zircon geochronology of a migmatite-granite complex in West Antarctica, Tectonophysics 477(3-4) (2009) 262-277.
[255] M. Drobe, M.L. de Luchi, A. Steenken, K. Wemmer, R. Naumann, R. Frei, S. Siegesmund, Geodynamic evolution of the Eastern Sierras Pampeanas (Central Argentina) based on geochemical, Sm-Nd, Pb-Pb and SHRIMP data, International Journal of Earth Sciences: Geologische Rundschau 100(2-3) (2011) 631-657.
[256] P.L. Tikhomirov, M.V. Luchitskaya, A.L. Shats, Age of granitoid plutons, North Chukotka: Problem formulation and new SHRIMP U-Pb zircon datings, Doklady Earth Sciences 440(2) (2011) 1363-1366.
[257] X. Ma, B. Chen, J. Chen, X. Niu, Zircon SHRIMP U-Pb age, geochemical, Sr-Nd isotopic, and in-situ Hf isotopic data of the Late Carboniferous-Early Permian plutons in the northern margin of the North China Craton, Science China. Earth Sciences 56(1) (2013) 126-144.
[258] R. Stern, A Time Machine for Geoscience Australia, AUSGEO News, Geoscience Australia, Australian Government, Canberra, 2006, p. 3.
[259] G.H. Swihart, P.B. Moore, E.L. Callis, Boron isotopic composition of marine and nonmarine evaporite borates, Geochimica et Cosmochimica Acta 50(6) (1986) 1297-1301.
[260] S.A. Kasemann, A. Meixner, J. Erzinger, J.G. Viramonte, R.N. Alonso, G. Franz, Boron isotope composition of geothermal fluids and borate minerals from salar deposits (central Andes/NW Argentina), Journal of South American Earth Sciences 16(8) (2004) 685-697.
[261] W. Brand, A., T. Coplen, B., J. Vogl, M. Rosner, T. Prohaska, Assessment of international reference materials for isotope-ratio analysis (IUPAC Technical Report), Pure and Applied Chemistry, 2014, p. 425.
[262] S.A. Kasemann, A.B. Jeffcoate, T. Elliott, Lithium Isotope Composition of Basalt Glass Reference Material, Analytical Chemistry 77(16) (2005) 5251-5257.

[263] S. Kasemann, A. Meixner, A. Rocholl, T. Vennemann, M. Rosner, A.K. Schmitt, M. Wiedenbeck, Boron and Oxygen Isotope Composition of Certified Reference Materials NIST SRM 610/612 and Reference Materials JB-2 and JR-2, Geostandards Newsletter 25(2-3) (2001) 405-416.
[264] Y. Nishio, S.i. Nakai, T. Ishii, Y. Sano, Isotope systematics of Li, Sr, Nd, and volatiles in Indian Ocean MORBs of the Rodrigues Triple Junction: Constraints on the origin of the DUPAL anomaly, Geochimica et Cosmochimica Acta 71(3) (2007) 745-759.
[265] K.P. Jochum, B. Stoll, K. Herwig, M. Willbold, A.W. Hofmann, M. Amini, S. Aarburg, W. Abouchami, E. Hellebrand, B. Mocek, I. Raczek, A. Stracke, O. Alard, C. Bouman, S. Becker, M. Dücking, H. Brätz, R. Klemd, D. de Bruin, D. Canil, D. Cornell, C.-J. de Hoog, C. Dalpé, L. Danyushevsky, A. Eisenhauer, Y. Gao, J.E. Snow, N. Groschopf, D. Günther, C. Latkoczy, M. Guillong, E.H. Hauri, H.E. Höfer, Y. Lahaye, K. Horz, D.E. Jacob, S.A. Kasemann, A.J.R. Kent, T. Ludwig, T. Zack, P.R.D. Mason, A. Meixner, M. Rosner, K. Misawa, B.P. Nash, J. Pfänder, W.R. Premo, W.D. Sun, M. Tiepolo, R. Vannucci, T. Vennemann, D. Wayne, J.D. Woodhead, MPI-DING reference glasses for in situ microanalysis: New reference values for element concentrations and isotope ratios, Geochemistry, Geophysics, Geosystems 7(2) (2006) Q02008.
[266] LGC Standards, NCS DC61104 - Borosilicate glass - Constituents (NIM-GBW03132), 2016.
[267] National Institute of Standards & Technology NIST, Standard Reference Material 93a Borosilicate Glass (12.5% B2O3), Department of Commerce, United States of America, Gaithersburg, MD 20899, 1991 (originally 1973).
[268] National Institute of Standards & Technology NIST, Standard Reference Material 612 Trace Elements in Glass, Department of Commerce, United States of America, Gaithersburg, MD 20899, 2012.
[269] R.L. Romer, A. Meixner, K. Hahne, Lithium and boron isotopic composition of sedimentary rocks — The role of source history and depositional environment: A 250 Ma record from the Cadomian orogeny to the Variscan orogeny, Gondwana Research 26(3–4) (2014) 1093-1110.
[270] R. Gy, Ion exchange for glass strengthening, Materials Science and Engineering: B 149(2) (2008) 159-165.
[271] S. Tonarini, M. Pennisi, W.P. Leeman, Precise boron isotopic analysis of complex silicate (rock) samples using alkali carbonate fusion and ion-exchange separation, Chemical Geology 142(1) (1997) 129-137.
[272] M. Kutzschbach, B. Wunder, A. Meixner, R. Wirth, W. Heinrich, G. Franz, Jeremejevite as a precursor for olenitic tourmaline: consequences of non-classical crystallization pathways for composition, textures and B isotope patterns of tourmaline, European Journal of Mineralogy 29(2) (2017) 239-255.
[273] C. Meyer, B. Wunder, A. Meixner, R.L. Romer, W. Heinrich, Boron-isotope fractionation between tourmaline and fluid: an experimental re-investigation, Contributions to Mineralogy and Petrology 156(2) (2008) 259-267.
[274] R. Gonfiantini, S. Tonarini, M. Gröning, A. Adorni-Braccesi, A.S. Al-Ammar, M. Astner, S. Bächler, R.M. Barnes, R.L. Bassett, A. Cocherie, A. Deyhle, A. Dini, G. Ferrara, J. Gaillardet, J. Grimm, C. Guerrot, U. Krähenbühl, G. Layne, D. Lemarchand, A. Meixner, D.J. Northington, M. Pennisi, E. Reitznerová, I. Rodushkin, N. Sugiura, R. Surberg, S. Tonn, M. Wiedenbeck, S. Wunderli, Y. Xiao, T. Zack, Intercomparison of Boron Isotope and Concentration Measurements. Part II: Evaluation of Results, Geostandards Newsletter 27(1) (2003) 41-57.
[275] T. Moriguti, E. Nakamura, High-yield lithium separation and the precise isotopic analysis for natural rock and aqueous samples, Chemical Geology 145(1) (1998) 91-104.
[276] C.T. Hansen, A. Meixner, S.A. Kasemann, W. Bach, New insight on Li and B isotope fractionation during serpentinization derived from batch reaction investigations, Geochimica et Cosmochimica Acta 217 (2017) 51-79.

[277] Y. Nishio, S.i. Nakai, Accurate and precise lithium isotopic determinations of igneous rock samples using multi-collector inductively coupled plasma mass spectrometry, Analytica Chimica Acta 456(2) (2002) 271-281.
[278] A.B. Jeffcoate, T. Elliott, A. Thomas, C. Bouman, Precise/ Small Sample Size Determinations of Lithium Isotopic Compositions of Geological Reference Materials and Modern Seawater by MC-ICP-MS, Geostandards and Geoanalytical Research 28(1) (2004) 161-172.
[279] R.H. James, M.R. Palmer, The lithium isotope composition of international rock standards, Chemical Geology 166(3–4) (2000) 319-326.
[280] K. Govindaraju, 1994 COMPILATION OF WORKING VALUES AND SAMPLE DESCRIPTION FOR 383 GEOSTANDARDS, Geostandards Newsletter 18 (1994) 1-158.
[281] A.J.B. Cotta, J. Enzweiler, Classical and New Procedures of Whole Rock Dissolution for Trace Element Determination by ICP-MS, Geostandards and Geoanalytical Research 36(1) (2012) 27-50.
[282] E.I. Chisholm, K.N. Sircombe, D.L. DiBugnara, Handbook of Geochronology Mineral Separation Laboratory Techniques, Geoscience Australia, Canberra, 2014.
[283] R.S. Hockett, High Purity Silicon VI: Proceedings of the Sixth International Symposium, Electrochemical Society2000.
[284] G.D. Flesch, A.R. Anderson, H.J. Svec, A secondary isotopic standard for 6Li/7Li determinations, International Journal of Mass Spectrometry and Ion Physics 12(3) (1973) 265-272.
[285] K.E. Seyfang, K.E. Redman, R.S. Popelka-Filcoff, K.P. Kirkbride, Glass fragments from portable electronic devices: Implications for forensic examinations, Forensic Science International 257(Supplement C) (2015) 442-452.
[286] K.E. Seyfang, N. Lucas, R.S. Popelka-Filcoff, H.J. Kobus, K.E. Redman, K.P. Kirkbride, Methods for analysis of glass in glass-containing gunshot residue (gGSR) particles, Forensic Science International 298 (2019) 359-371.
[287] J.A. Erickson, J.M. Melberg, Lead-free primer mix for centerfire cartridges, Google Patents, 1998.
[288] M. Hiscock, C. Lang, P. Statham, F. Bauer, C. Hartfield, Enhancing Materials and Device Analysis Capability in the SEM and FIB-SEM by using a Nanomanipulator, Microscopy and Microanalysis 22(S3) (2016) 16-17.
[289] R. Steve, P. Robert, A review of focused ion beam applications in microsystem technology, Journal of Micromechanics and Microengineering 11(4) (2001) 287.
[290] Sporting Arms and Ammunition Manufacturers' Institute, inc. (SAAMI), ANSI/SAAMI Z299, ANSI/SAAMI Z299.3 - American National Standard Voluntary Industry Performance Standards for Pressure and Velocity of Centerfire Pistol and Revolver Ammunition for the Use of Commercial Manufacturers, American National Standards Institute (ANSI), 2015.
[291] Sporting Arms and Ammunition Manufacturers' Institute, inc. (SAAMI), ANSI/SAAMI Z299, Z299.1 - American National Standard Voluntary Industry Performance Standards for Pressure and Velocity of Rimfire Sporting Ammunition for the Use of Commercial Manufacturers, American National Standards Institute (ANSI), 2015.
[292] BRUKER, Micro-XRF and TXRF. <https://www.bruker.com/products/x-ray-diffraction-and-elemental-analysis/micro-xrf-and-txrf.html>, 2019 (accessed 24 Nov 2019.2019).
[293] Australian Synchrotron, Microspectroscopy - XFM. <https://archive.synchrotron.org.au/images/stories/beamline/factsheets/synchrotron-fact-sheet-microspec-sept08.pdf>, 2009 (accessed 24 Nov 2019.2019).

# 8. Appendices

The following pages contain data summaries that may be read for further information, and which support the assertions made in this thesis, but are not essential reading, copies of published manuscripts upon which several chapters in this are based and plots of data that would be too numerous to include in the body of the thesis, but which support certain chapters.

## 8.1. Plots of ToF-SIMS data with Average Abundance and 99% Confidence Intervals

| | SAMPLE | | 10B | 17O | 18O | 25Mg | 26Mg | 29Si | 29SiH | 29SiOH | 29SiO2H | 29SiO | 29SiO2 |
|---|---|---|---|---|---|---|---|---|---|---|---|---|---|
| 1 | REMINGTO | Average | 0 | 0.119194 | 0.023596 | 4.589399 | 3.964435 | 5.50022 | 2.810551 | 0.916654 | 0.102151 | 0.188516 | 0.059072 |
| 2 | CIL | Average | 0 | 0.127726 | 0.022116 | 4.442511 | 3.84437 | 5.883341 | 3.011262 | 0.913443 | 0.097075 | 0.241547 | 0.060933 |
| 3 | FEDERAL | Average | 4.942121 | 0.091524 | 0.019039 | 0.055639 | 0.02794 | 5.829706 | 3.020064 | 0.553698 | 0.015284 | 0.18498 | 0.013523 |
| 5 | CCI | Average | 5.13888 | 0.106539 | 0.017905 | 0.061025 | 0.028643 | 6.133535 | 3.222643 | 0.546106 | 0.013802 | 0.215639 | 0.012519 |
| 6 | AGUILLA | Average | 0 | 0.142239 | 0.027021 | 8.515811 | 7.661501 | 5.182713 | 2.483226 | 1.784628 | 0.28041 | 0.302816 | 0.12003 |
| 7 | ELEY | Average | 0.018983 | 0.14146 | 0.022276 | 1.682437 | 1.357068 | 5.095822 | 2.66963 | 1.374871 | 0.20041 | 0.384777 | 0.127445 |
| 8 | RWS | Average | 3.509857 | 0.134333 | 0.018722 | 0.195364 | 0.071142 | 5.829726 | 2.407291 | 0.96667 | 0.092694 | 0.406028 | 0.013126 |
| 9 | BROWNIN( | Average | 4.588899 | 0.11235 | 0.021361 | 0.060722 | 0 | 5.447989 | 2.777907 | 0.559343 | 0 | 0.324162 | 0.016008 |
| 10 | STIRLING | Average | 4.543892 | 0.10459 | 0.01793 | 0.065508 | 0 | 5.378381 | 2.416652 | 0.508443 | 0 | 0.403935 | 0.019059 |
| 11 | 11 | Average | 4.476073 | 0.068383 | 0 | 0.043012 | 0 | 5.083018 | 1.669894 | 0.100692 | 0 | 0.332586 | 0 |
| 12 | PMC | Average | 0 | 0.229259 | 0.031143 | 4.896365 | 4.327694 | 7.100234 | 3.500127 | 1.571688 | 0.274316 | 0.341068 | 0.057217 |
| 14 | MAUSER | Average | 0.055904 | 0.210321 | 0.037471 | 6.22824 | 5.404779 | 6.923109 | 3.596167 | 2.498408 | 0.4178 | 0.547544 | 0.195634 |
| 17 | SWARTKLIF | Average | 7.491785 | 0.184629 | 0.032093 | 0.125524 | 0.042025 | 7.943121 | 4.178369 | 0.981526 | 0.048715 | 2.520696 | 0.056011 |
| 19 | CBC | Average | 0 | 0.035298 | 0 | 18.82196 | 15.38371 | 1.627022 | 0.659628 | 0.216509 | 0.149033 | 0.051492 | 0.126297 |
| 20 | GEVELOT | Average | 0 | 0.037655 | 0 | 14.1769 | 11.66082 | 1.795442 | 0.772997 | 0.347121 | 0.099936 | 0.072959 | 0.214307 |
| 23 | DOMINION | Average | 0 | 0.194546 | 0.03539 | 12.2312 | 11.11598 | 7.026802 | 3.413081 | 2.691353 | 0.462394 | 0.255696 | 0.170389 |
| 25 | HORNADY | Average | 6.998552 | 0.1166 | 0.020863 | 0.136419 | 0.052773 | 6.098154 | 2.924981 | 0.691601 | 0.039933 | 2.557338 | 0.039672 |
| 26 | 26 | Average | 6.671875 | 0.126563 | 0.021633 | 0.12425 | 0.04418 | 7.55752 | 3.25387 | 0.712724 | 0.026139 | 1.035607 | 0.027261 |
| 27 | 27 | Average | 7.199425 | 0.156321 | 0.026526 | 0.109742 | 0.047296 | 7.274475 | 4.234825 | 0.856613 | 0.041245 | 0.599278 | 0.038701 |
| 28 | 28 | Average | 7.562728 | 0.163451 | 0.027389 | 0.1439 | 0.077388 | 7.605325 | 4.235497 | 0.911685 | 0.045007 | 0.972277 | 0.040053 |
| 29 | 29 | Average | 6.505757 | 0.138045 | 0.023974 | 0.122335 | 0.068183 | 6.872165 | 3.912999 | 0.78641 | 0.036991 | 0.404997 | 0.030393 |
| 30 | 30 | Average | 6.591197 | 0.136375 | 0.022559 | 0.10955 | 0.057599 | 6.828546 | 3.786769 | 0.76853 | 0.032716 | 0.575115 | 0.030505 |
| 31 | 31 | Average | 6.063198 | 0.126882 | 0.021425 | 0.138718 | 0.07802 | 6.278085 | 3.596328 | 0.710064 | 0.031044 | 0.457814 | 0.032351 |
| 32 | 32 | Average | 5.687375 | 0.112441 | 0.019247 | 0.121767 | 0.071579 | 5.526929 | 3.083144 | 0.676432 | 0.036629 | 1.603005 | 0.038231 |
| 33 | 33 | Average | 6.054122 | 0.114449 | 0.018921 | 0.154177 | 0.102683 | 5.591461 | 3.101782 | 0.685685 | 0.040219 | 1.540867 | 0.036736 |
| 34 | 34 | Average | 10.78542 | 0.217755 | 0.03739 | 0.197316 | 0.116691 | 10.31932 | 5.959929 | 1.215483 | 0.046561 | 0.371262 | 0.041205 |
| 35 | 35 | Average | 9.986947 | 0.184501 | 0.034054 | 0.26393 | 0.175033 | 9.955355 | 5.476732 | 1.100181 | 0.043162 | 0.312785 | 0.030449 |
| 36 | 36 | Average | 9.591531 | 0.184361 | 0.02955 | 0.216718 | 0.102806 | 9.670933 | 5.446931 | 1.061206 | 0.047234 | 0.308147 | 0.033539 |
| 37 | 37 | Average | 12.71775 | 0.321516 | 0.054434 | 0.259258 | 0.118859 | 12.96915 | 7.144241 | 1.627653 | 0.058608 | 0.458863 | 0.049947 |

| | SAMPLE | | 29SiOH | 30Si | 30SiH | 30SiOH | 30SiO2H | 30SiO | 30SiO2 | 37Cl | 41K | 42Ca | 43Ca |
|---|---|---|---|---|---|---|---|---|---|---|---|---|---|
| 1 | REMINGTO | Average | 0.750539 | 0.238907 | 0.222768 | 0.397409 | 0.013579 | 0.079756 | 0 | 0 | 0.414561 | 0.420593 | 0.08614 |
| 2 | CIL | Average | 0.74975 | 0.249923 | 0.237967 | 0.411284 | 0.01699 | 0.082143 | 0 | 0 | 0.416049 | 0.47225 | 0.100328 |
| 3 | FEDERAL | Average | 0.437319 | 0.244227 | 0.231416 | 0.338649 | 0 | 0.077572 | 0 | 0 | 0.033995 | 0 | 0 |
| 5 | CCI | Average | 0.416598 | 0.24126 | 0.258686 | 0.348893 | 0 | 0.082214 | 0 | 0 | 0.025141 | 0 | 0 |
| 6 | AGUILLA | Average | 1.507887 | 0.2153 | 0.162177 | 0.494841 | 0.059669 | 0.107084 | 0 | 0 | 0.982485 | 1.011366 | 0.214885 |
| 7 | ELEY | Average | 1.136987 | 0.223977 | 0.171701 | 0.371881 | 0.039595 | 0.092471 | 0 | 0 | 0.693109 | 1.106851 | 0.236635 |
| 8 | RWS | Average | 0.680052 | 0.203294 | 0.19045 | 0.80799 | 0.049688 | 0.390503 | 0 | 0 | 0.587655 | 0 | 0 |
| 9 | BROWNIN( | Average | 0.430171 | 0.231348 | 0.191332 | 0.333444 | 0 | 0.080417 | 0 | 0 | 0.052014 | 0 | 0 |
| 10 | STIRLING | Average | 0.384296 | 0.239567 | 0.180759 | 0.325232 | 0 | 0.083103 | 0 | 0 | 0 | 0 | 0 |
| 11 | 11 | Average | 0.060546 | 0.236151 | 0.122985 | 0.061654 | 0 | 0.051675 | 0 | 0 | 0 | 0 | 0 |
| 12 | PMC | Average | 1.301043 | 0.350365 | 0.249957 | 0.592218 | 0.027928 | 0.116477 | 0.224387 | 0 | 1.514947 | 0.362487 | 0.094367 |
| 14 | MAUSER | Average | 2.136581 | 0.359727 | 0.267998 | 0.654987 | 0.091262 | 0.16434 | 0.052867 | 0 | 1.499878 | 1.765388 | 0.369326 |
| 17 | SWARTKLIF | Average | 0.709848 | 0.514879 | 0.342091 | 0.616429 | 0.011501 | 0.240499 | 0 | 0 | 0.08575 | 0 | 0 |
| 19 | CBC | Average | 0.106723 | 0.839221 | 0.073885 | 0.354357 | 0.510522 | 0.025632 | 0.025722 | 0 | 2.798496 | 0.421005 | 0.061259 |
| 20 | GEVELOT | Average | 0.117878 | 0.625102 | 0.097576 | 0.435716 | 0.333464 | 0.024877 | 0.046239 | 0 | 1.920305 | 0.602329 | 0.081651 |
| 23 | DOMINION | Average | 2.312989 | 0.310868 | 0.248341 | 0.755935 | 0.085745 | 0.135571 | 0.027797 | 0 | 1.487338 | 1.443247 | 0.302099 |
| 25 | HORNADY | Average | 0.457582 | 0.478805 | 0.219257 | 0.433998 | 0.010515 | 0.224539 | 0.015262 | 0 | 0.05914 | 0.004127 | 0 |
| 26 | 26 | Average | 0.520972 | 0.396732 | 0.245972 | 0.448354 | 0 | 0.15744 | 0 | 0 | 0.06612 | 0.003089 | 0 |
| 27 | 27 | Average | 0.674103 | 0.417792 | 0.282995 | 0.490451 | 0.005275 | 0.129363 | 0 | 0 | 0.08082 | 0.004677 | 0 |
| 28 | 28 | Average | 0.707197 | 0.450092 | 0.300188 | 0.53531 | 0.006889 | 0.156714 | 0 | 0.00716 | 0.093951 | 0.008447 | 0 |
| 29 | 29 | Average | 0.62116 | 0.374264 | 0.249693 | 0.437236 | 0 | 0.112253 | 0 | 0.007529 | 0.077397 | 0.007187 | 0 |
| 30 | 30 | Average | 0.596629 | 0.384005 | 0.254944 | 0.448825 | 0 | 0.118966 | 0 | 0.006001 | 0.067825 | 0.006794 | 0 |
| 31 | 31 | Average | 0.561095 | 0.348668 | 0.232728 | 0.405063 | 0 | 0.110261 | 0 | 0.008488 | 0.064857 | 0.007629 | 0 |
| 32 | 32 | Average | 0.493938 | 0.365763 | 0.213566 | 0.395725 | 0 | 0.157323 | 0 | 0.008534 | 0.053509 | 0.008623 | 0 |
| 33 | 33 | Average | 0.496005 | 0.364949 | 0.216825 | 0.399226 | 0 | 0.14672 | 0 | 0.017761 | 0.059162 | 0.014026 | 0 |
| 34 | 34 | Average | 0.942368 | 0.543519 | 0.391116 | 0.683218 | 0 | 0.177952 | 0 | 0.019991 | 0.122831 | 0.013153 | 0.01156 |
| 35 | 35 | Average | 0.858945 | 0.48491 | 0.343876 | 0.618475 | 0 | 0.167385 | 0 | 0.028564 | 0.125703 | 0.020282 | 0.015558 |
| 36 | 36 | Average | 0.824454 | 0.465127 | 0.326005 | 0.589621 | 0 | 0.161488 | 0 | 0.012824 | 0.112358 | 0.01229 | 0 |
| 37 | 37 | Average | 1.282439 | 0.61123 | 0.577562 | 0.973029 | 0 | 0.194792 | 0 | 0.018355 | 0.195497 | 0.012471 | 0 |

| | SAMPLE | | 44Ca | 48Ca | 6Li | Al | Ba | C | CHSiO | CH2 | CN | Ca | Cl |
|---|---|---|---|---|---|---|---|---|---|---|---|---|---|
| 1 | REMINGTO | Average | 0 | 0.149436 | 0 | 7.020498 | 0 | 0.066738 | 5.774584 | 0.062611 | 0.203641 | 58.32554 | 0 |
| 2 | CIL | Average | 0 | 0.182894 | 0 | 8.946406 | 0 | 0.080142 | 6.202805 | 0.067399 | 0.201197 | 62.25639 | 0 |
| 3 | FEDERAL | Average | 0 | 0.03443 | 0 | 19.28098 | 0 | 0.077027 | 0.064443 | 0.080498 | 0 | 0.338162 | 0 |
| 5 | CCI | Average | 0 | 0.037536 | 0 | 19.89506 | 0 | 0.088498 | 0.062202 | 0.082242 | 0 | 0.327264 | 0 |
| 6 | AGUILLA | Average | 0 | 0.252071 | 0 | 2.331626 | 0 | 0.046943 | 14.84193 | 0.033852 | 0.429297 | 132.5983 | 0 |
| 7 | ELEY | Average | 0 | 0.414258 | 0.001234 | 17.8983 | 0.126577 | 0.073845 | 14.63246 | 0.049295 | 0.082654 | 136.5226 | 0 |
| 8 | RWS | Average | 0 | 10.07316 | 0 | 59.40134 | 0.002535 | 0.098367 | 0.255653 | 0.070275 | 0 | 1.534249 | 0 |
| 9 | BROWNINC | Average | 0 | 0 | 0.025152 | 25.36767 | 0 | 0.039591 | 0.059402 | 0.037003 | 0 | 0.35039 | 0 |
| 10 | STIRLING | Average | 0 | 0 | 0 | 22.05706 | 0 | 0.058248 | 0.075195 | 0.043622 | 0 | 0.496666 | 0 |
| 11 | 11 | Average | 0 | 0 | 0 | 17.57198 | 0 | 0.084229 | 0 | 0 | 0 | 0.281552 | 0 |
| 12 | PMC | Average | 0.015493 | 0.407404 | 0.025897 | 57.37251 | 15.51942 | 0.068999 | 5.685352 | 0.057138 | 0.265996 | 45.5769 | 0.00813 |
| 14 | MAUSER | Average | 0.048703 | 0.537735 | 0.163831 | 27.36472 | 0.036799 | 0.058963 | 25.41008 | 0.056498 | 0.319895 | 129.0775 | 0.004775 |
| 17 | SWARTKLIF | Average | 0 | 0.050853 | 0.036324 | 36.36632 | 0 | 0.069322 | 0.085618 | 0.07929 | 0.009082 | 0.349705 | 0 |
| 19 | CBC | Average | 0.011646 | 0.054554 | 0 | 16.90058 | 0.099984 | 0.065091 | 26.94924 | 0 | 2.082075 | 61.48508 | 0.012029 |
| 20 | GEVELOT | Average | 0.014006 | 0.077343 | 0 | 18.8126 | 0.158247 | 0.05338 | 20.09973 | 0.007869 | 1.209725 | 85.85385 | 0.013077 |
| 23 | DOMINION | Average | 0.037037 | 0.39422 | 0 | 14.73272 | 0 | 0.073088 | 21.03041 | 0.049498 | 0.620564 | 122.7429 | 0.007631 |
| 25 | HORNADY | Average | 0 | 0.057584 | 0 | 31.02939 | 0 | 0.043127 | 0.0619 | 0.047869 | 0.011341 | 0.218131 | 0.009565 |
| 26 | 26 | Average | 0 | 0.063641 | 0 | 32.48441 | 0 | 0.101898 | 0.079111 | 0.061074 | 0.009789 | 0.377956 | 0 |
| 27 | 27 | Average | 0 | 0.063262 | 0 | 34.51453 | 0 | 0.051865 | 0.079274 | 0.06874 | 0.009159 | 0.366019 | 0.007321 |
| 28 | 28 | Average | 0 | 0.085341 | 0.014403 | 36.67334 | 0 | 0.057571 | 0.10289 | 0.068998 | 0.01274 | 0.544089 | 0.013132 |
| 29 | 29 | Average | 0 | 0.039133 | 0.015918 | 33.40132 | 0.021529 | 0.049311 | 0.083694 | 0.062054 | 0.010477 | 0.434016 | 0.012401 |
| 30 | 30 | Average | 0 | 0.064519 | 0.01134 | 32.48619 | 0 | 0.092331 | 0.076851 | 0.069381 | 0.010007 | 0.392878 | 0.008905 |
| 31 | 31 | Average | 0 | 0.061698 | 0.013461 | 31.66408 | 0 | 0.051412 | 0.087439 | 0.062126 | 0.011253 | 0.519717 | 0.013147 |
| 32 | 32 | Average | 0 | 0.044674 | 0.013232 | 29.42563 | 0 | 0.048711 | 0.092934 | 0.065577 | 0.011994 | 0.440665 | 0.013519 |
| 33 | 33 | Average | 0 | 0.044533 | 0.021016 | 29.60125 | 0 | 0.041444 | 0.08099 | 0.05334 | 0.016626 | 0.441921 | 0.026881 |
| 34 | 34 | Average | 0 | 0.083712 | 0.016365 | 45.56462 | 0 | 0.05391 | 0.110057 | 0.064552 | 0.018543 | 0.44917 | 0.029296 |
| 35 | 35 | Average | 0 | 0.093853 | 0.024125 | 44.08324 | 0 | 0.050439 | 0.158129 | 0.056223 | 0.023002 | 0.943045 | 0.044562 |
| 36 | 36 | Average | 0 | 0.06528 | 0.016072 | 43.08753 | 0 | 0.051112 | 0.124485 | 0.058163 | 0.014898 | 0.537072 | 0.022244 |
| 37 | 37 | Average | 0 | 0.092355 | 0.022017 | 51.80602 | 0.009942 | 0.145139 | 0.118014 | 0.176801 | 0.021167 | 0.332654 | 0.028692 |

| | SAMPLE | | K | Li | Mg | Na | O | OH | P | Sb | Si | SiH | SiOH |
|---|---|---|---|---|---|---|---|---|---|---|---|---|---|
| 1 | REMINGTO | Average | 6.026792 | 0.019721 | 24.91901 | 222.9628 | 0.349085 | 0.131272 | 0.2538 | 0 | 100 | 6.292397 | 7.904522 |
| 2 | CIL | Average | 8.805208 | 0.029273 | 23.78434 | 194.2926 | 0.368414 | 0.140012 | 0.272218 | 0 | 100 | 6.748408 | 8.303979 |
| 3 | FEDERAL | Average | 1.475829 | 0.017506 | 0.125941 | 71.02538 | 0.282824 | 0.100905 | 0.261251 | 0 | 100 | 6.630601 | 8.165072 |
| 5 | CCI | Average | 1.426599 | 0.019374 | 0.121489 | 66.03919 | 0.285784 | 0.117658 | 0.295206 | 0 | 100 | 7.141957 | 8.144763 |
| 6 | AGUILLA | Average | 2.026792 | 0.038796 | 47.46441 | 404.057 | 0.489013 | 0.159096 | 0.195934 | 0 | 100 | 4.909868 | 7.295468 |
| 7 | ELEY | Average | 30.53593 | 0.118677 | 8.62957 | 306.8827 | 0.460447 | 0.154983 | 0.200142 | 0 | 100 | 5.273045 | 7.336561 |
| 8 | RWS | Average | 249.5657 | 0.067079 | 0.476435 | 245.9313 | 0.446965 | 0.153755 | 0.232143 | 0 | 100 | 5.334574 | 7.164067 |
| 9 | BROWNIN( | Average | 0.869453 | 0.269058 | 0.104781 | 115.5735 | 0.339594 | 0.124049 | 0.220841 | 0 | 100 | 5.577104 | 7.858453 |
| 10 | STIRLING | Average | 1.32734 | 0.031517 | 0.151032 | 104.7337 | 0.336803 | 0.119526 | 0.214033 | 0 | 100 | 5.382455 | 7.608351 |
| 11 | 11 | Average | 0.422784 | 0 | 0.085716 | 47.04211 | 0.437316 | 0.090644 | 0.18159 | 0 | 100 | 3.487249 | 1.112435 |
| 12 | PMC | Average | 174.9412 | 0.265004 | 25.31347 | 172.2741 | 0.79836 | 0.256003 | 0.302405 | 0.01443 | 100 | 7.1328 | 11.26864 |
| 14 | MAUSER | Average | 30.43209 | 1.903057 | 29.13534 | 167.748 | 0.739598 | 0.235591 | 0.310689 | 0 | 100 | 7.434376 | 11.56856 |
| 17 | SWARTKLIF | Average | 0.681962 | 0.425721 | 0.197065 | 116.2701 | 0.655898 | 0.210249 | 0.406872 | 0 | 100 | 9.088426 | 12.59761 |
| 19 | CBC | Average | 9.723434 | 0.048618 | 77.98494 | 207.3209 | 1.125321 | 0.055809 | 0.182873 | 0 | 100 | 5.044732 | 0.578357 |
| 20 | GEVELOT | Average | 19.33318 | 0.08049 | 62.27793 | 259.4961 | 0.856212 | 0.062741 | 0.211657 | 0 | 100 | 5.343736 | 1.129726 |
| 23 | DOMINION | Average | 14.71468 | 0.04495 | 58.53322 | 177.805 | 0.712661 | 0.217837 | 0.291867 | 0 | 100 | 7.024117 | 11.04217 |
| 25 | HORNADY | Average | 0.991481 | 0.068026 | 0.153454 | 122.4916 | 0.583201 | 0.141701 | 0.284292 | 0 | 100 | 6.61911 | 8.352351 |
| 26 | 26 | Average | 1.670462 | 0.099035 | 0.195326 | 125.4158 | 0.550397 | 0.150053 | 0.314009 | 0 | 100 | 6.820547 | 9.36143 |
| 27 | 27 | Average | 0.914735 | 0.09869 | 0.176326 | 121.9641 | 0.583454 | 0.173033 | 0.319811 | 0 | 100 | 8.149088 | 11.34664 |
| 28 | 28 | Average | 1.75762 | 0.116488 | 0.284712 | 122.0306 | 0.659577 | 0.182693 | 0.350492 | 0 | 100 | 8.177968 | 12.02167 |
| 29 | 29 | Average | 1.283508 | 0.130567 | 0.229834 | 127.5497 | 0.558106 | 0.151931 | 0.286787 | 0 | 100 | 7.085553 | 10.29913 |
| 30 | 30 | Average | 1.489806 | 0.079463 | 0.203273 | 125.405 | 0.558859 | 0.151154 | 0.293839 | 0 | 100 | 7.297614 | 10.29126 |
| 31 | 31 | Average | 1.433576 | 0.107805 | 0.276857 | 126.9662 | 0.509675 | 0.139496 | 0.266191 | 0 | 100 | 6.77971 | 9.424876 |
| 32 | 32 | Average | 1.132434 | 0.108202 | 0.243592 | 128.7598 | 0.510413 | 0.126696 | 0.252462 | 0 | 100 | 6.186146 | 8.771357 |
| 33 | 33 | Average | 0.912321 | 0.116855 | 0.220648 | 127.582 | 0.520063 | 0.130617 | 0.262901 | 0 | 100 | 6.216064 | 8.702173 |
| 34 | 34 | Average | 1.773309 | 0.096098 | 0.25139 | 115.806 | 0.829438 | 0.239718 | 0.454674 | 0 | 100 | 10.39702 | 15.43376 |
| 35 | 35 | Average | 2.390129 | 0.172662 | 0.517352 | 120.2111 | 0.767553 | 0.209297 | 0.408646 | 0 | 100 | 9.064296 | 13.81121 |
| 36 | 36 | Average | 2.578476 | 0.079034 | 0.290162 | 118.4945 | 0.75378 | 0.205749 | 0.381396 | 0 | 100 | 9.088747 | 13.19566 |
| 37 | 37 | Average | 5.157072 | 0.151829 | 0.319012 | 117.417 | 0.987961 | 0.356929 | 0.6728 | 0 | 100 | 14.04934 | 21.15675 |

| | SAMPLE | | SiO3 | Sr | Ti | Zn | Zr | Ag | Au | B | CH | CH3 | Cr |
|---|---|---|---|---|---|---|---|---|---|---|---|---|---|
| 1 | REMINGTO | Average | 0 | 0 | 0.175808 | 0 | 0 | 0 | 0.130212 | 0.022415 | 0.046135 | 0.080879 | 0.020061 |
| 2 | CIL | Average | 0 | 0 | 0.21711 | 0 | 0 | 0 | 0.183854 | 0.024393 | 0.057675 | 0.088469 | 0.02068 |
| 3 | FEDERAL | Average | 0 | 0 | 0.046986 | 0 | 0 | 0 | 0.215365 | 18.93713 | 0.059047 | 0.120914 | 0.017632 |
| 5 | CCI | Average | 0 | 0 | 0.050747 | 0 | 0.010516 | 0 | 0.274185 | 19.49841 | 0.062396 | 0.108107 | 0.018028 |
| 6 | AGUILLA | Average | 0 | 0 | 0.283918 | 0 | 0 | 0 | 0.220278 | 0.002605 | 0.028327 | 0.032343 | 0 |
| 7 | ELEY | Average | 0 | 0 | 0.506508 | 0 | 0 | 0 | 0.250463 | 0.144549 | 0.053431 | 0.053834 | 0.017948 |
| 8 | RWS | Average | 0 | 0 | 16.13782 | 0.520202 | 0 | 0 | 0.271096 | 13.42769 | 0.062491 | 0.075502 | 0.035088 |
| 9 | BROWNIN( | Average | 0 | 0 | 0.038255 | 0 | 0 | 0 | 0.435769 | 17.58442 | 0.02389 | 0.053656 | 0.00355 |
| 10 | STIRLING | Average | 0 | 0 | 0.03736 | 0 | 0 | 0 | 0.276282 | 17.4852 | 0.034168 | 0.056989 | 0 |
| 11 | 11 | Average | 0 | 0 | 0 | 0 | 0 | 0 | 0.109641 | 17.89744 | 0.021767 | 0 | 0 |
| 12 | PMC | Average | 0.017492 | 1.106437 | 0.529312 | 0 | 0.01005 | 0.006348 | 0.265571 | 0.007035 | 0.035289 | 0.084452 | 0.003713 |
| 14 | MAUSER | Average | 0.015748 | 0.071657 | 0.624217 | 0 | 0.008736 | 0 | 0.297877 | 0.216134 | 0.032512 | 0.088879 | 0.317992 |
| 17 | SWARTKLIF | Average | 0.027479 | 0.011894 | 0.069377 | 0 | 0.04798 | 0.009922 | 0.604412 | 26.34749 | 0.041355 | 0.139368 | 0 |
| 19 | CBC | Average | 0.033057 | 0.01857 | 0.068691 | 0 | 0 | 0 | 0.040878 | 0 | 0 | 0 | 0 |
| 20 | GEVELOT | Average | 0.02107 | 0.028391 | 0.093674 | 0 | 0 | 0 | 0.060163 | 0 | 0.008145 | 0 | 0 |
| 23 | DOMINION | Average | 0.015613 | 0.059329 | 0.448126 | 0 | 0.006781 | 0 | 0.287912 | 0 | 0.032394 | 0.08142 | 0.003231 |
| 25 | HORNADY | Average | 0.028192 | 0.008291 | 0.08674 | 0.005569 | 0.02652 | 0.004556 | 0.306059 | 24.65353 | 0.02328 | 0.086056 | 0.00149 |
| 26 | 26 | Average | 0.025135 | 0.007888 | 0.089735 | 0 | 0.020643 | 0 | 0.458568 | 25.83479 | 0.032385 | 0.112144 | 0 |
| 27 | 27 | Average | 0.022589 | 0.006447 | 0.081393 | 0 | 0.026781 | 0.005834 | 0.628772 | 25.85534 | 0.033599 | 0.130476 | 0 |
| 28 | 28 | Average | 0.025144 | 0.011339 | 0.115291 | 0 | 0.026439 | 0.006451 | 0.551864 | 26.94 | 0.033767 | 0.134722 | 0 |
| 29 | 29 | Average | 0.020358 | 0.009597 | 0.050949 | 0 | 0.021333 | 0.0053 | 0.525223 | 23.83434 | 0.030596 | 0.121401 | 0 |
| 30 | 30 | Average | 0.019868 | 0.005407 | 0.08261 | 0 | 0.021095 | 0.004947 | 0.527252 | 23.96337 | 0.03567 | 0.137165 | 0 |
| 31 | 31 | Average | 0.017587 | 0.005307 | 0.079128 | 0 | 0.021843 | 0 | 0.567352 | 22.19493 | 0.030979 | 0.126446 | 0 |
| 32 | 32 | Average | 0.017918 | 0.008946 | 0.063573 | 0 | 0.022841 | 0 | 0.318944 | 20.76762 | 0.030971 | 0.138309 | 0 |
| 33 | 33 | Average | 0.019614 | 0.008943 | 0.06271 | 0 | 0.02649 | 0 | 0.345394 | 21.95266 | 0.026544 | 0.107625 | 0 |
| 34 | 34 | Average | 0.034233 | 0.007188 | 0.105562 | 0 | 0.039325 | 0.012152 | 1.007429 | 36.66161 | 0.032302 | 0.113473 | 0.006056 |
| 35 | 35 | Average | 0.032705 | 0.007286 | 0.12282 | 0 | 0.033273 | 0.011032 | 0.871362 | 34.62954 | 0.028266 | 0.105766 | 0.008339 |
| 36 | 36 | Average | 0.03386 | 0.007596 | 0.083233 | 0 | 0.051412 | 0.015931 | 1.04209 | 33.27793 | 0.029115 | 0.107173 | 0.005019 |
| 37 | 37 | Average | 0.046718 | 0.008468 | 0.119784 | 0 | 0.036257 | 0.01147 | 1.570497 | 42.506 | 0.104729 | 0.279384 | 0.006189 |

| | SAMPLE | | Cu | Fe | Ge | In | Mn | OH2 | Pd | SiNa | SiO | SiOH | SiO2 |
|---|---|---|---|---|---|---|---|---|---|---|---|---|---|
| 1 | REMINGTO | Average | 0 | 0.560069 | 0.478648 | 0 | 0 | 0.026033 | 0 | 0.104132 | 2.076716 | 6.44455 | 0.025698 |
| 2 | CIL | Average | 0 | 0.22186 | 0.586146 | 0 | 0 | 0.025185 | 0 | 0.108735 | 2.216393 | 6.973685 | 0.025147 |
| 3 | FEDERAL | Average | 0 | 0.081344 | 0.633393 | 0 | 0 | 0.021335 | 0 | 0.024541 | 2.081331 | 7.0465 | 0.014611 |
| 5 | CCI | Average | 0 | 0.078925 | 0.661786 | 0 | 0 | 0.021058 | 0.006703 | 0.022525 | 2.021326 | 6.624092 | 0.013158 |
| 6 | AGUILLA | Average | 0 | 0.795438 | 0.411815 | 0 | 0 | 0.030803 | 0 | 0.20412 | 2.108995 | 6.033148 | 0.042039 |
| 7 | ELEY | Average | 0 | 0.500442 | 0.511349 | 0 | 0.092921 | 0.025664 | 0 | 0.159732 | 2.164644 | 6.281149 | 0.042193 |
| 8 | RWS | Average | 0 | 0.185565 | 0.437907 | 0 | 0 | 0.023217 | 0 | 0.077395 | 1.494855 | 5.812975 | 0.005945 |
| 9 | BROWNIN( | Average | 0 | 0.0572 | 0.609075 | 0 | 0 | 0.024575 | 0.006425 | 0.04036 | 1.937748 | 6.496981 | 0.014377 |
| 10 | STIRLING | Average | 0 | 0.063879 | 0.446891 | 0 | 0 | 0.021948 | 0 | 0.028917 | 1.760931 | 6.196056 | 0 |
| 11 | 11 | Average | 0 | 0.040068 | 0.194457 | 0 | 0 | 0 | 0 | 0 | 0.521581 | 0.783731 | 0 |
| 12 | PMC | Average | 0 | 0.313996 | 0.639996 | 0.002931 | 0.017945 | 0.036937 | 0.00658 | 0.176069 | 2.443585 | 9.475603 | 0.027073 |
| 14 | MAUSER | Average | 0 | 0.475597 | 0.708309 | 0.00465 | 0.190766 | 0.044205 | 0.003167 | 0.289642 | 3.158475 | 9.798649 | 0.073295 |
| 17 | SWARTKLIF | Average | 0 | 0.085792 | 1.040207 | 0 | 0 | 0.039738 | 0.024536 | 0.060212 | 2.822866 | 10.06406 | 0.022201 |
| 19 | CBC | Average | 0 | 0.067919 | 0.102994 | 0 | 0 | 0 | 0 | 0.01262 | 4.901339 | 0.266695 | 0.197091 |
| 20 | GEVELOT | Average | 0 | 0.081904 | 0.131037 | 0 | 0 | 0.009125 | 0 | 0.016116 | 3.210862 | 0.299981 | 0.158949 |
| 23 | DOMINION | Average | 0 | 0.546399 | 0.707813 | 0.005348 | 0.029003 | 0.041808 | 0.002712 | 0.312157 | 3.019206 | 9.465136 | 0.065147 |
| 25 | HORNADY | Average | 0.000365 | 0.050351 | 0.67734 | 0 | 0 | 0.027341 | 0.010274 | 0.046191 | 2.012709 | 6.160311 | 0.017893 |
| 26 | 26 | Average | 0 | 0.103995 | 0.787324 | 0 | 0 | 0.027271 | 0.011817 | 0.045725 | 2.253216 | 7.454783 | 0.016448 |
| 27 | 27 | Average | 0 | 0.094677 | 1.209154 | 0 | 0 | 0.031404 | 0.014315 | 0.073863 | 2.988929 | 9.826433 | 0.025224 |
| 28 | 28 | Average | 0 | 0.117926 | 1.221033 | 0 | 0 | 0.033083 | 0.014576 | 0.076052 | 3.110204 | 10.20754 | 0.023786 |
| 29 | 29 | Average | 0 | 0.074832 | 1.130665 | 0 | 0 | 0.028394 | 0.011488 | 0.073864 | 2.852383 | 8.969951 | 0.022783 |
| 30 | 30 | Average | 0.00012 | 0.08914 | 1.077472 | 0 | 0 | 0.026914 | 0.011382 | 0.066064 | 2.724998 | 8.896719 | 0.021889 |
| 31 | 31 | Average | 0 | 0.09123 | 1.092504 | 0 | 0 | 0.025123 | 0.011984 | 0.065392 | 2.659909 | 8.239435 | 0.020987 |
| 32 | 32 | Average | 0 | 0.077709 | 0.79394 | 0 | 0 | 0.023613 | 0.009268 | 0.05507 | 2.265731 | 7.030322 | 0.019644 |
| 33 | 33 | Average | 0 | 0.076107 | 0.80659 | 0 | 0 | 0.023097 | 0.010625 | 0.05444 | 2.301077 | 7.029735 | 0.019693 |
| 34 | 34 | Average | 0.004189 | 0.108579 | 1.878934 | 0 | 0 | 0.044493 | 0.027521 | 0.109036 | 4.434105 | 13.13659 | 0.036977 |
| 35 | 35 | Average | 0.003789 | 0.151987 | 1.707643 | 0.003318 | 0.007871 | 0.039807 | 0.021816 | 0.108598 | 4.1196 | 11.67759 | 0.036016 |
| 36 | 36 | Average | 0.003421 | 0.118371 | 1.800864 | 0.003766 | 0.004976 | 0.03583 | 0.038429 | 0.1112 | 4.023948 | 11.1206 | 0.030591 |
| 37 | 37 | Average | 0.005725 | 0.129646 | 2.44565 | 0 | 0.005039 | 0.064595 | 0.025674 | 0.134788 | 5.025096 | 18.41829 | 0.037863 |

| | SAMPLE | | SiO2H | SiO2H2 | Si2 | Sn |
|---|---|---|---|---|---|---|
| 1 | REMINGTO | Average | 0.039757 | 0.089075 | 1.807009 | 0 |
| 2 | CIL | Average | 0.046918 | 0.079892 | 1.979729 | 0 |
| 3 | FEDERAL | Average | 0.038307 | 0.033599 | 0.121902 | 0 |
| 5 | CCI | Average | 0.033004 | 0.030726 | 0.121746 | 0 |
| 6 | AGUILLA | Average | 0.06398 | 0.195297 | 4.074493 | 0 |
| 7 | ELEY | Average | 0.066044 | 0.142522 | 4.58193 | 0 |
| 8 | RWS | Average | 0.02723 | 0.074932 | 0.116744 | 0 |
| 9 | BROWNIN( | Average | 0.039705 | 0.036235 | 0.100995 | 0 |
| 10 | STIRLING | Average | 0.036015 | 0.034341 | 0.085404 | 0 |
| 11 | 11 | Average | 0 | 0.002557 | 0.045832 | 0 |
| 12 | PMC | Average | 0.055034 | 0.167582 | 1.466754 | 0 |
| 14 | MAUSER | Average | 0.098254 | 0.192117 | 7.295085 | 0 |
| 17 | SWARTKLIF | Average | 0.070893 | 0.050706 | 0.151817 | 0 |
| 19 | CBC | Average | 0.415373 | 0.078826 | 0.544543 | 0 |
| 20 | GEVELOT | Average | 0.340519 | 0.094318 | 0.423679 | 0 |
| 23 | DOMINION | Average | 0.086178 | 0.230393 | 5.848779 | 0 |
| 25 | HORNADY | Average | 0.045161 | 0.031701 | 0.107412 | 0 |
| 26 | 26 | Average | 0.045267 | 0.041919 | 0.130535 | 0 |
| 27 | 27 | Average | 0.057431 | 0.054583 | 0.170259 | 0 |
| 28 | 28 | Average | 0.063594 | 0.057776 | 0.177944 | 0 |
| 29 | 29 | Average | 0.05219 | 0.0516 | 0.158868 | 0 |
| 30 | 30 | Average | 0.053908 | 0.050291 | 0.151387 | 0 |
| 31 | 31 | Average | 0.051824 | 0.045771 | 0.155431 | 0 |
| 32 | 32 | Average | 0.045393 | 0.034493 | 0.12975 | 0 |
| 33 | 33 | Average | 0.043847 | 0.035905 | 0.127714 | 0 |
| 34 | 34 | Average | 0.084535 | 0.077966 | 0.245827 | 0 |
| 35 | 35 | Average | 0.072012 | 0.073057 | 0.24821 | 0 |
| 36 | 36 | Average | 0.067897 | 0.068179 | 0.232372 | 0 |
| 37 | 37 | Average | 0.119759 | 0.119161 | 0.271044 | 0 |

| | SAMPLE | | 10B | 17O | 18O | 25Mg | 26Mg | 29Si | 29SiH | 29SiOH | 29SiO2H | 29SiO | 29SiO2 |
|---|---|---|---|---|---|---|---|---|---|---|---|---|---|
| 1 | REMINGTO | 3s | 0 | 0.017775 | 0.009258 | 1.00714 | 0.985653 | 0.433608 | 0.309638 | 0.16419 | 0.045695 | 0.126266 | 0.015761 |
| 2 | CIL | 3s | 0 | 0.020097 | 0.007911 | 2.258239 | 2.125274 | 0.796987 | 0.306284 | 0.256681 | 0.069956 | 0.10892 | 0.038263 |
| 3 | FEDERAL | 3s | 0.311443 | 0.015371 | 0.003438 | 0.025663 | 0.024845 | 0.367575 | 0.188171 | 0.083096 | 0.009178 | 0.079346 | 0.005327 |
| 5 | CCI | 3s | 0.439045 | 0.025899 | 0.009809 | 0.030001 | 0.01303 | 1.39267 | 0.569961 | 0.085392 | 0.006994 | 0.19321 | 0.016535 |
| 6 | AGUILLA | 3s | 0 | 0.021756 | 0.010738 | 4.426665 | 4.149021 | 0.846214 | 0.167356 | 0.34201 | 0.09939 | 0.297469 | 0.061198 |
| 7 | ELEY | 3s | 0.180088 | 0.021726 | 0.009878 | 6.565951 | 5.859942 | 0.911585 | 0.381277 | 1.908166 | 0.413414 | 0.441913 | 0.076162 |
| 8 | RWS | 3s | 0.702291 | 0.063141 | 0.010411 | 0.109691 | 0.08409 | 1.011855 | 0.440994 | 0.167839 | 0.058134 | 0.249242 | 0.022257 |
| 9 | BROWNINC | 3s | 0.58848 | 0.036611 | 0.007719 | 0.024247 | 0 | 0.76615 | 0.482453 | 0.099641 | 0 | 0.183632 | 0.005797 |
| 10 | STIRLING | 3s | 0.519932 | 0.032647 | 0.009787 | 0.057711 | 0 | 0.838471 | 0.395043 | 0.086625 | 0 | 0.252723 | 0.013164 |
| 11 | 11 | 3s | 0.865344 | 0.032472 | 0 | 0.036411 | 0 | 0.734402 | 0.516929 | 0.124586 | 0 | 0.462834 | 0 |
| 12 | PMC | 3s | 0 | 0.047599 | 0.015124 | 1.040948 | 0.888527 | 1.977966 | 0.768296 | 0.871592 | 0.320564 | 0.669643 | 0.011441 |
| 14 | MAUSER | 3s | 0.438594 | 0.053916 | 0.007791 | 17.16831 | 15.67808 | 1.589661 | 0.641852 | 1.383252 | 0.320642 | 1.197886 | 0.080427 |
| 17 | SWARTKLIF | 3s | 0.942383 | 0.052327 | 0.009401 | 0.057119 | 0.02059 | 1.264392 | 1.685252 | 0.231916 | 0.027851 | 4.919111 | 0.021285 |
| 19 | CBC | 3s | 0 | 0.012663 | 0 | 1.753828 | 1.153448 | 0.677421 | 0.239198 | 0.152393 | 0.012835 | 0.07368 | 0.062187 |
| 20 | GEVELOT | 3s | 0 | 0.011216 | 0 | 1.172175 | 1.426476 | 1.14854 | 0.39949 | 0.149397 | 0.047235 | 0.073534 | 0.060083 |
| 23 | DOMINION | 3s | 0 | 0.029051 | 0.007698 | 5.207102 | 4.767171 | 1.02075 | 0.497022 | 0.798993 | 0.255946 | 0.104035 | 0.040933 |
| 25 | HORNADY | 3s | 0.851317 | 0.046487 | 0.006597 | 0.032212 | 0.018569 | 2.008818 | 0.376332 | 0.137714 | 0.012637 | 2.071072 | 0.021932 |
| 26 | 26 | 3s | 2.879057 | 0.042709 | 0.009001 | 0.145129 | 0.066544 | 3.847833 | 1.042187 | 0.316918 | 0.018585 | 2.727085 | 0.020254 |
| 27 | 27 | 3s | 0.787262 | 0.018905 | 0.006333 | 0.033942 | 0.027674 | 1.127318 | 0.584475 | 0.125127 | 0.007085 | 0.472135 | 0.008308 |
| 28 | 28 | 3s | 1.65138 | 0.056393 | 0.008491 | 0.082095 | 0.050909 | 2.614307 | 1.697475 | 0.260184 | 0.020421 | 2.565329 | 0.025621 |
| 29 | 29 | 3s | 0.765465 | 0.019547 | 0.007756 | 0.028316 | 0.013136 | 0.941594 | 0.357921 | 0.104477 | 0.015302 | 0.515224 | 0.017563 |
| 30 | 30 | 3s | 1.575578 | 0.057876 | 0.011674 | 0.029957 | 0.034753 | 2.005589 | 1.303275 | 0.271622 | 0.012898 | 1.88982 | 0.024053 |
| 31 | 31 | 3s | 0.382228 | 0.021177 | 0.006255 | 0.03938 | 0.020806 | 0.650822 | 0.40019 | 0.06664 | 0.00777 | 0.908365 | 0.017619 |
| 32 | 32 | 3s | 0.701203 | 0.02687 | 0.00774 | 0.036986 | 0.027434 | 0.82258 | 0.730299 | 0.076066 | 0.005437 | 1.685354 | 0.011084 |
| 33 | 33 | 3s | 0.67137 | 0.038989 | 0.010291 | 0.078036 | 0.107635 | 0.830137 | 0.857037 | 0.083182 | 0.008506 | 1.932786 | 0.010806 |
| 34 | 34 | 3s | 2.117142 | 0.03738 | 0.009969 | 0.084947 | 0.055489 | 1.325448 | 0.730449 | 0.130585 | 0.019868 | 0.440871 | 0.02236 |
| 35 | 35 | 3s | 1.440144 | 0.029527 | 0.008079 | 0.133536 | 0.105626 | 1.047777 | 0.391751 | 0.115383 | 0.015641 | 0.16584 | 0.015385 |
| 36 | 36 | 3s | 1.69436 | 0.012683 | 0.003058 | 0.080497 | 0.03729 | 1.775274 | 0.558299 | 0.085671 | 0.017926 | 0.183398 | 0.025655 |
| 37 | 37 | 3s | 2.795997 | 0.067238 | 0.016142 | 0.126772 | 0.087526 | 2.950055 | 1.012339 | 0.403335 | 0.014815 | 0.247028 | 0.020809 |

| | SAMPLE | | 29SiOH | 30Si | 30SiH | 30SiOH | 30SiO2H | 30SiO | 30SiO2 | 37Cl | 41K | 42Ca | 43Ca |
|---|---|---|---|---|---|---|---|---|---|---|---|---|---|
| 1 | REMINGTO | 3s | 0.172018 | 0.05138 | 0.055689 | 0.047371 | 0.006378 | 0.022833 | 0 | 0 | 0.129838 | 0.102747 | 0.022695 |
| 2 | CIL | 3s | 0.215201 | 0.036674 | 0.03014 | 0.051549 | 0.008516 | 0.021119 | 0 | 0 | 0.243739 | 0.392398 | 0.064885 |
| 3 | FEDERAL | 3s | 0.058243 | 0.025837 | 0.041735 | 0.025488 | 0 | 0.021442 | 0 | 0 | 0.010352 | 0 | 0 |
| 5 | CCI | 3s | 0.11007 | 0.058342 | 0.037777 | 0.042585 | 0 | 0.019902 | 0 | 0 | 0.007112 | 0 | 0 |
| 6 | AGUILLA | 3s | 0.314754 | 0.047449 | 0.024795 | 0.110302 | 0.02998 | 0.062275 | 0 | 0 | 0.200756 | 0.410719 | 0.10414 |
| 7 | ELEY | 3s | 1.608679 | 0.013212 | 0.039982 | 0.145304 | 0.06542 | 0.039308 | 0 | 0 | 0.733611 | 0.684807 | 0.153983 |
| 8 | RWS | 3s | 0.095445 | 0.026282 | 0.171364 | 0.143573 | 0.033533 | 0.165543 | 0 | 0 | 0.183536 | 0 | 0 |
| 9 | BROWNIN( | 3s | 0.083616 | 0.042915 | 0.046302 | 0.063891 | 0 | 0.011194 | 0 | 0 | 0.013607 | 0 | 0 |
| 10 | STIRLING | 3s | 0.069386 | 0.044825 | 0.044449 | 0.057321 | 0 | 0.035664 | 0 | 0 | 0 | 0 | 0 |
| 11 | 11 | 3s | 0.081553 | 0.100694 | 0.052048 | 0.0774 | 0 | 0.064651 | 0 | 0 | 0 | 0 | 0 |
| 12 | PMC | 3s | 0.819651 | 0.130424 | 0.076267 | 0.120577 | 0.027128 | 0.057621 | 0.195657 | 0 | 0.478711 | 0.177072 | 0.035269 |
| 14 | MAUSER | 3s | 1.24792 | 0.148749 | 0.102619 | 0.385439 | 0.059063 | 0.136778 | 0.071611 | 0 | 0.74672 | 0.703729 | 0.14775 |
| 17 | SWARTKLIF | 3s | 0.329389 | 0.062262 | 0.065931 | 0.105078 | 0.017881 | 0.285762 | 0 | 0 | 0.061624 | 0 | 0 |
| 19 | CBC | 3s | 0.06959 | 0.24158 | 0.016313 | 0.077384 | 0.052832 | 0.025048 | 0.013126 | 0 | 0.32861 | 0.150212 | 0.04052 |
| 20 | GEVELOT | 3s | 0.09605 | 0.043432 | 0.008189 | 0.063223 | 0.098559 | 0.042178 | 0.024634 | 0 | 0.470422 | 0.084884 | 0.035862 |
| 23 | DOMINION | 3s | 0.751767 | 0.056319 | 0.049485 | 0.115661 | 0.042233 | 0.036793 | 0.017306 | 0 | 0.558265 | 0.262613 | 0.064382 |
| 25 | HORNADY | 3s | 0.130206 | 0.034666 | 0.089657 | 0.105483 | 0.015828 | 0.199983 | 0.024533 | 0 | 0.02414 | 0.001685 | 0 |
| 26 | 26 | 3s | 0.22505 | 0.137758 | 0.113619 | 0.266585 | 0 | 0.297419 | 0 | 0 | 0.028457 | 0.006394 | 0 |
| 27 | 27 | 3s | 0.098536 | 0.026183 | 0.060822 | 0.056078 | 0.002183 | 0.031548 | 0 | 0 | 0.021881 | 0.00258 | 0 |
| 28 | 28 | 3s | 0.324147 | 0.075259 | 0.125926 | 0.141856 | 0.009435 | 0.126417 | 0 | 0.006926 | 0.066104 | 0.003981 | 0 |
| 29 | 29 | 3s | 0.074769 | 0.05942 | 0.039846 | 0.061822 | 0 | 0.032171 | 0 | 0.003312 | 0.025785 | 0.004699 | 0 |
| 30 | 30 | 3s | 0.241314 | 0.124337 | 0.138282 | 0.171106 | 0 | 0.059201 | 0 | 0.003724 | 0.035981 | 0.002457 | 0 |
| 31 | 31 | 3s | 0.076461 | 0.049681 | 0.070282 | 0.035746 | 0 | 0.035338 | 0 | 0.003449 | 0.029765 | 0.00335 | 0 |
| 32 | 32 | 3s | 0.103682 | 0.050982 | 0.072476 | 0.072685 | 0 | 0.077413 | 0 | 0.006963 | 0.014064 | 0.003861 | 0 |
| 33 | 33 | 3s | 0.134024 | 0.058459 | 0.055792 | 0.043336 | 0 | 0.080902 | 0 | 0.025877 | 0.025346 | 0.01701 | 0 |
| 34 | 34 | 3s | 0.132305 | 0.08297 | 0.088936 | 0.0943 | 0 | 0.018714 | 0 | 0.018658 | 0.040486 | 0.008226 | 0.009455 |
| 35 | 35 | 3s | 0.083781 | 0.071003 | 0.060607 | 0.079484 | 0 | 0.017781 | 0 | 0.015619 | 0.015203 | 0.010672 | 0.004555 |
| 36 | 36 | 3s | 0.059197 | 0.076405 | 0.054818 | 0.050598 | 0 | 0.027553 | 0 | 0.003347 | 0.027664 | 0.008705 | 0 |
| 37 | 37 | 3s | 0.294604 | 0.173084 | 0.143043 | 0.278134 | 0 | 0.031794 | 0 | 0.014655 | 0.075211 | 0.006878 | 0 |

| | SAMPLE | | 44Ca | 48Ca | 6Li | Al | Ba | C | CHSiO | CH2 | CN | Ca | Cl |
|---|---|---|---|---|---|---|---|---|---|---|---|---|---|
| 1 | REMINGTO | 3s | 0 | 0.038496 | 0 | 16.90321 | 0 | 0.037238 | 1.049224 | 0.034183 | 0.05777 | 12.50194 | 0 |
| 2 | CIL | 3s | 0 | 0.179693 | 0 | 15.60184 | 0 | 0.020488 | 4.381782 | 0.024515 | 0.108127 | 41.56355 | 0 |
| 3 | FEDERAL | 3s | 0 | 0.015599 | 0 | 1.635646 | 0 | 0.039386 | 0.027852 | 0.06642 | 0 | 0.355252 | 0 |
| 5 | CCI | 3s | 0 | 0.017717 | 0 | 4.382822 | 0 | 0.043075 | 0.018799 | 0.059265 | 0 | 0.157578 | 0 |
| 6 | AGUILLA | 3s | 0 | 0.10723 | 0 | 7.367157 | 0 | 0.044572 | 5.927739 | 0.029712 | 0.219579 | 39.30493 | 0 |
| 7 | ELEY | 3s | 0 | 0.16812 | 0.011702 | 21.01661 | 0.65019 | 0.114107 | 8.471865 | 0.053082 | 0.392049 | 74.12634 | 0 |
| 8 | RWS | 3s | 0 | 5.260292 | 0 | 15.15839 | 0.02012 | 0.229204 | 0.311363 | 0.162491 | 0 | 3.135935 | 0 |
| 9 | BROWNIN( | 3s | 0 | 0 | 0.007385 | 3.359737 | 0 | 0.017095 | 0.01605 | 0.014898 | 0 | 0.086988 | 0 |
| 10 | STIRLING | 3s | 0 | 0 | 0 | 1.492035 | 0 | 0.064332 | 0.125979 | 0.035313 | 0 | 1.188986 | 0 |
| 11 | 11 | 3s | 0 | 0 | 0 | 3.063529 | 0 | 0.055705 | 0 | 0 | 0 | 0.254817 | 0 |
| 12 | PMC | 3s | 0.020386 | 0.173701 | 0.05724 | 6.74145 | 20.11079 | 0.049963 | 1.934463 | 0.040087 | 0.060574 | 18.4836 | 0.004376 |
| 14 | MAUSER | 3s | 0.142298 | 0.314157 | 1.044854 | 30.65634 | 0.100086 | 0.0422 | 9.583213 | 0.051938 | 0.908001 | 29.16387 | 0.004313 |
| 17 | SWARTKLIF | 3s | 0 | 0.030764 | 0.066938 | 3.902194 | 0 | 0.031768 | 0.019874 | 0.03412 | 0.003783 | 0.151364 | 0 |
| 19 | CBC | 3s | 0.013586 | 0.026518 | 0 | 1.986692 | 0.060751 | 0.01545 | 1.799987 | 0 | 0.50904 | 15.4436 | 0.013286 |
| 20 | GEVELOT | 3s | 0.017141 | 0.042809 | 0 | 0.313592 | 0.069759 | 0.010119 | 3.686582 | 0.003332 | 0.287399 | 10.0591 | 0.00727 |
| 23 | DOMINION | 3s | 0.097224 | 0.052443 | 0 | 25.93329 | 0 | 0.068049 | 3.178977 | 0.02301 | 0.275481 | 16.21692 | 0.009037 |
| 25 | HORNADY | 3s | 0 | 0.01386 | 0 | 3.90172 | 0 | 0.035764 | 0.013938 | 0.051789 | 0.005315 | 0.086182 | 0.00456 |
| 26 | 26 | 3s | 0 | 0.092705 | 0 | 14.0475 | 0 | 0.212407 | 0.038759 | 0.058201 | 0.015913 | 0.326905 | 0 |
| 27 | 27 | 3s | 0 | 0.020719 | 0 | 3.047438 | 0 | 0.024112 | 0.030134 | 0.040346 | 0.004884 | 0.257975 | 0.005441 |
| 28 | 28 | 3s | 0 | 0.1075 | 0.005185 | 6.842342 | 0 | 0.036666 | 0.077673 | 0.044364 | 0.006238 | 0.750371 | 0.013785 |
| 29 | 29 | 3s | 0 | 0.039382 | 0.006871 | 4.337873 | 0.023572 | 0.022663 | 0.014501 | 0.035463 | 0.001869 | 0.046254 | 0.00675 |
| 30 | 30 | 3s | 0 | 0.098067 | 0.004178 | 6.313764 | 0 | 0.319727 | 0.044837 | 0.062892 | 0.006273 | 0.393404 | 0.007434 |
| 31 | 31 | 3s | 0 | 0.042774 | 0.005182 | 2.854702 | 0 | 0.092492 | 0.02516 | 0.062761 | 0.004424 | 0.228535 | 0.006473 |
| 32 | 32 | 3s | 0 | 0.067892 | 0.002966 | 1.460162 | 0 | 0.078166 | 0.134888 | 0.106925 | 0.004081 | 0.140053 | 0.006898 |
| 33 | 33 | 3s | 0 | 0.062582 | 0.020287 | 3.495981 | 0 | 0.021608 | 0.042692 | 0.021998 | 0.014271 | 0.340984 | 0.034253 |
| 34 | 34 | 3s | 0 | 0.095232 | 0.011096 | 6.124975 | 0 | 0.018962 | 0.038022 | 0.033286 | 0.006249 | 0.41673 | 0.024471 |
| 35 | 35 | 3s | 0 | 0.114932 | 0.013376 | 5.704738 | 0 | 0.017952 | 0.095673 | 0.028831 | 0.010418 | 0.930375 | 0.021004 |
| 36 | 36 | 3s | 0 | 0.077284 | 0.005179 | 3.88141 | 0 | 0.018209 | 0.126482 | 0.022048 | 0.006374 | 0.626559 | 0.008325 |
| 37 | 37 | 3s | 0 | 0.067265 | 0.009184 | 8.656354 | 0.018847 | 0.085748 | 0.025793 | 0.088616 | 0.01075 | 0.097635 | 0.020605 |

| | SAMPLE | | K | Li | Mg | Na | O | OH | P | Sb | Si | SiH | SiOH |
|---|---|---|---|---|---|---|---|---|---|---|---|---|---|
| 1 | REMINGTO | 3s | 13.73282 | 0.027166 | 6.199748 | 100.8479 | 0.042266 | 0.019467 | 0.058659 | 0 | 0 | 0.767385 | 1.297423 |
| 2 | CIL | 3s | 25.13479 | 0.050092 | 12.28949 | 56.35363 | 0.050645 | 0.017158 | 0.027846 | 0 | 0 | 0.376834 | 0.91649 |
| 3 | FEDERAL | 3s | 0.787161 | 0.010408 | 0.135362 | 5.912078 | 0.037577 | 0.02029 | 0.033021 | 0 | 0 | 0.844101 | 0.523808 |
| 5 | CCI | 3s | 0.825934 | 0.025544 | 0.085824 | 5.675397 | 0.027915 | 0.021842 | 0.037792 | 0 | 0 | 1.083396 | 1.250447 |
| 6 | AGUILLA | 3s | 4.080704 | 0.045607 | 24.91962 | 70.73408 | 0.070423 | 0.030526 | 0.040903 | 0 | 0 | 0.485011 | 0.733579 |
| 7 | ELEY | 3s | 58.70777 | 0.109494 | 35.66847 | 331.5953 | 0.154527 | 0.024449 | 0.049671 | 0 | 0 | 0.764319 | 2.2233 |
| 8 | RWS | 3s | 26.83776 | 0.035662 | 0.574588 | 66.55259 | 0.046876 | 0.07037 | 0.204635 | 0 | 0 | 2.769795 | 2.80084 |
| 9 | BROWNIN( | 3s | 0.661556 | 0.092854 | 0.07435 | 21.39657 | 0.051433 | 0.03462 | 0.05045 | 0 | 0 | 1.135929 | 1.725622 |
| 10 | STIRLING | 3s | 1.606422 | 0.022981 | 0.249899 | 46.03237 | 0.037817 | 0.033484 | 0.041482 | 0 | 0 | 0.759641 | 1.459227 |
| 11 | 11 | 3s | 0.570786 | 0 | 0.10225 | 35.38996 | 0.108573 | 0.038678 | 0.051612 | 0 | 0 | 1.51856 | 1.59074 |
| 12 | PMC | 3s | 39.82009 | 0.684683 | 5.504323 | 55.10005 | 0.091528 | 0.047752 | 0.104783 | 0.009992 | 0 | 1.649542 | 4.057332 |
| 14 | MAUSER | 3s | 48.70183 | 12.1676 | 79.77226 | 35.34343 | 0.060428 | 0.051319 | 0.109992 | 0 | 0 | 2.598559 | 3.746923 |
| 17 | SWARTKLIF | 3s | 0.185372 | 0.771925 | 0.065597 | 3.684838 | 0.072615 | 0.047303 | 0.055553 | 0 | 0 | 1.940944 | 5.199229 |
| 19 | CBC | 3s | 5.715738 | 0.042432 | 3.129742 | 37.93526 | 0.131542 | 0.023098 | 0.024854 | 0 | 0 | 0.296278 | 0.54877 |
| 20 | GEVELOT | 3s | 5.588773 | 0.017344 | 5.695263 | 15.12369 | 0.056292 | 0.02656 | 0.009205 | 0 | 0 | 0.31168 | 0.669251 |
| 23 | DOMINION | 3s | 27.57048 | 0.029847 | 22.31852 | 28.24577 | 0.048297 | 0.025444 | 0.059968 | 0 | 0 | 0.974392 | 2.373532 |
| 25 | HORNADY | 3s | 0.449138 | 0.025994 | 0.037246 | 4.550196 | 0.070362 | 0.064067 | 0.137173 | 0 | 0 | 0.93548 | 2.501162 |
| 26 | 26 | 3s | 1.877639 | 0.085034 | 0.183007 | 49.50464 | 0.275153 | 0.059842 | 0.162841 | 0 | 0 | 2.718112 | 5.048488 |
| 27 | 27 | 3s | 0.935443 | 0.017998 | 0.165612 | 2.796985 | 0.072803 | 0.025284 | 0.067276 | 0 | 0 | 1.490427 | 1.477953 |
| 28 | 28 | 3s | 1.525131 | 0.034798 | 0.342587 | 9.143471 | 0.119684 | 0.056774 | 0.13053 | 0 | 0 | 2.956689 | 3.907352 |
| 29 | 29 | 3s | 0.325418 | 0.046394 | 0.041594 | 7.19074 | 0.051661 | 0.022995 | 0.047083 | 0 | 0 | 1.131532 | 1.144178 |
| 30 | 30 | 3s | 2.958677 | 0.069725 | 0.209455 | 27.06475 | 0.146809 | 0.06417 | 0.144792 | 0 | 0 | 2.841733 | 3.900388 |
| 31 | 31 | 3s | 0.704742 | 0.096855 | 0.108143 | 3.3389 | 0.042577 | 0.02045 | 0.073591 | 0 | 0 | 0.868278 | 1.045216 |
| 32 | 32 | 3s | 0.63256 | 0.042384 | 0.145105 | 9.225816 | 0.045505 | 0.023334 | 0.074325 | 0 | 0 | 1.369118 | 1.510293 |
| 33 | 33 | 3s | 1.134078 | 0.117069 | 0.116415 | 4.54245 | 0.032788 | 0.032567 | 0.060818 | 0 | 0 | 0.593046 | 1.849116 |
| 34 | 34 | 3s | 1.980337 | 0.058987 | 0.191144 | 4.850064 | 0.08252 | 0.03908 | 0.090987 | 0 | 0 | 1.433744 | 2.192169 |
| 35 | 35 | 3s | 1.778154 | 0.119273 | 0.484307 | 4.73146 | 0.03686 | 0.031049 | 0.075022 | 0 | 0 | 0.876363 | 1.215498 |
| 36 | 36 | 3s | 2.559913 | 0.022807 | 0.159829 | 6.674915 | 0.052465 | 0.015335 | 0.067031 | 0 | 0 | 1.169746 | 1.020871 |
| 37 | 37 | 3s | 6.390317 | 0.029585 | 0.312209 | 4.879269 | 0.205165 | 0.080248 | 0.170169 | 0 | 0 | 2.867468 | 5.169294 |

| | SAMPLE | | SiO3 | Sr | Ti | Zn | Zr | Ag | Au | B | CH | CH3 | Cr |
|---|---|---|---|---|---|---|---|---|---|---|---|---|---|
| 1 | REMINGTO | 3s | 0 | 0 | 0.046521 | 0 | 0 | 0 | 0.038676 | 0.009965 | 0.025441 | 0.028997 | 0.008731 |
| 2 | CIL | 3s | 0 | 0 | 0.25013 | 0 | 0 | 0 | 0.135352 | 0.017644 | 0.011664 | 0.019163 | 0.00607 |
| 3 | FEDERAL | 3s | 0 | 0 | 0.018812 | 0 | 0 | 0 | 0.096068 | 0.64569 | 0.048942 | 0.100903 | 0.008173 |
| 5 | CCI | 3s | 0 | 0 | 0.018018 | 0 | 0.005786 | 0 | 0.175769 | 1.821568 | 0.041957 | 0.074555 | 0.005953 |
| 6 | AGUILLA | 3s | 0 | 0 | 0.121898 | 0 | 0 | 0 | 0.073396 | 0.022104 | 0.028109 | 0.024454 | 0 |
| 7 | ELEY | 3s | 0 | 0 | 0.17638 | 0 | 0 | 0 | 0.20808 | 0.826814 | 0.078922 | 0.073132 | 0.051363 |
| 8 | RWS | 3s | 0 | 0 | 8.666429 | 0.380731 | 0 | 0 | 0.283888 | 3.157704 | 0.124324 | 0.109892 | 0.200502 |
| 9 | BROWNIN( | 3s | 0 | 0 | 0.018184 | 0 | 0 | 0 | 0.168624 | 1.974013 | 0.016058 | 0.022802 | 0.01138 |
| 10 | STIRLING | 3s | 0 | 0 | 0.051471 | 0 | 0 | 0 | 0.237848 | 1.929065 | 0.036734 | 0.03597 | 0 |
| 11 | 11 | 3s | 0 | 0 | 0 | 0 | 0 | 0 | 0.08067 | 3.773001 | 0.063659 | 0 | 0 |
| 12 | PMC | 3s | 0.007865 | 1.414098 | 0.175143 | 0 | 0.008544 | 0.005924 | 0.129817 | 0.01196 | 0.022474 | 0.046115 | 0.006684 |
| 14 | MAUSER | 3s | 0.00622 | 0.165462 | 0.416379 | 0 | 0.010806 | 0 | 0.232067 | 1.670192 | 0.035559 | 0.08578 | 1.372168 |
| 17 | SWARTKLIF | 3s | 0.010978 | 0.005736 | 0.033345 | 0 | 0.051265 | 0.015355 | 0.60356 | 3.429915 | 0.02059 | 0.086318 | 0 |
| 19 | CBC | 3s | 0.01213 | 0.016942 | 0.029965 | 0 | 0 | 0 | 0.015095 | 0 | 0 | 0 | 0 |
| 20 | GEVELOT | 3s | 0.008081 | 0.00995 | 0.055179 | 0 | 0 | 0 | 0.045705 | 0 | 0.004443 | 0 | 0 |
| 23 | DOMINION | 3s | 0.006776 | 0.293794 | 0.076234 | 0 | 0.006015 | 0 | 0.243017 | 0 | 0.020148 | 0.034058 | 0.006971 |
| 25 | HORNADY | 3s | 0.008233 | 0.004506 | 0.022427 | 0.004913 | 0.020744 | 0.003513 | 0.125303 | 2.818262 | 0.028223 | 0.083033 | 0.005853 |
| 26 | 26 | 3s | 0.029677 | 0.015319 | 0.110619 | 0 | 0.016428 | 0 | 0.341067 | 16.82591 | 0.025723 | 0.123217 | 0 |
| 27 | 27 | 3s | 0.007392 | 0.005129 | 0.024151 | 0 | 0.029205 | 0.008029 | 0.283665 | 2.626277 | 0.022458 | 0.075499 | 0 |
| 28 | 28 | 3s | 0.007812 | 0.009826 | 0.139175 | 0 | 0.026205 | 0.012713 | 0.437755 | 5.478574 | 0.023145 | 0.081595 | 0 |
| 29 | 29 | 3s | 0.00708 | 0.007525 | 0.057933 | 0 | 0.00734 | 0.003483 | 0.196015 | 2.60945 | 0.017431 | 0.070434 | 0 |
| 30 | 30 | 3s | 0.007794 | 0.004405 | 0.120091 | 0 | 0.016061 | 0.006438 | 0.44062 | 5.140303 | 0.03363 | 0.11011 | 0 |
| 31 | 31 | 3s | 0.00554 | 0.003609 | 0.054639 | 0 | 0.007389 | 0 | 0.175449 | 1.335603 | 0.044021 | 0.135651 | 0 |
| 32 | 32 | 3s | 0.006081 | 0.003448 | 0.101176 | 0 | 0.013429 | 0 | 0.180773 | 2.790477 | 0.05903 | 0.25942 | 0 |
| 33 | 33 | 3s | 0.007057 | 0.002808 | 0.088144 | 0 | 0.021616 | 0 | 0.225906 | 2.728516 | 0.014539 | 0.054024 | 0 |
| 34 | 34 | 3s | 0.00782 | 0.006395 | 0.117329 | 0 | 0.050594 | 0.020657 | 0.645933 | 6.44015 | 0.016563 | 0.053192 | 0.005366 |
| 35 | 35 | 3s | 0.00887 | 0.003962 | 0.146345 | 0 | 0.020068 | 0.009826 | 0.404572 | 4.804589 | 0.014916 | 0.056236 | 0.005766 |
| 36 | 36 | 3s | 0.00521 | 0.006492 | 0.099222 | 0 | 0.081728 | 0.027655 | 0.401844 | 5.781756 | 0.011008 | 0.05292 | 0.002461 |
| 37 | 37 | 3s | 0.012895 | 0.002873 | 0.087264 | 0 | 0.014353 | 0.004222 | 0.562032 | 8.232682 | 0.060877 | 0.131212 | 0.00324 |

| | SAMPLE | | Cu | Fe | Ge | In | Mn | OH2 | Pd | SiNa | SiO | SiOH | SiO2 |
|---|---|---|---|---|---|---|---|---|---|---|---|---|---|
| 1 | REMINGTO | 3s | 0 | 0.708802 | 0.09735 | 0 | 0 | 0.009278 | 0 | 0.038344 | 0.240017 | 1.244017 | 0.006476 |
| 2 | CIL | 3s | 0 | 0.171883 | 0.284247 | 0 | 0 | 0.007632 | 0 | 0.052349 | 0.199506 | 0.709192 | 0.010961 |
| 3 | FEDERAL | 3s | 0 | 0.031939 | 0.064352 | 0 | 0 | 0.00385 | 0 | 0.007173 | 0.104987 | 0.72971 | 0.007157 |
| 5 | CCI | 3s | 0 | 0.027421 | 0.178582 | 0 | 0 | 0.006761 | 0.004274 | 0.010702 | 0.414246 | 1.80919 | 0.004718 |
| 6 | AGUILLA | 3s | 0 | 1.332852 | 0.10287 | 0 | 0 | 0.014644 | 0 | 0.072314 | 0.180668 | 0.599797 | 0.018962 |
| 7 | ELEY | 3s | 0 | 0.379464 | 0.148245 | 0 | 0.311255 | 0.010857 | 0 | 0.218844 | 0.446731 | 1.980396 | 0.016037 |
| 8 | RWS | 3s | 0 | 0.85413 | 0.295833 | 0 | 0 | 0.013478 | 0 | 0.044175 | 0.215512 | 2.199644 | 0.022327 |
| 9 | BROWNIN( | 3s | 0 | 0.020445 | 0.220971 | 0 | 0 | 0.006887 | 0.013786 | 0.019773 | 0.352139 | 1.592408 | 0.008263 |
| 10 | STIRLING | 3s | 0 | 0.092382 | 0.247712 | 0 | 0 | 0.013288 | 0 | 0.01682 | 0.303949 | 1.340849 | 0 |
| 11 | 11 | 3s | 0 | 0.023656 | 0.115543 | 0 | 0 | 0 | 0 | 0 | 0.460012 | 1.241176 | 0 |
| 12 | PMC | 3s | 0 | 0.16192 | 0.252339 | 0.00871 | 0.020927 | 0.016595 | 0.005861 | 0.165242 | 0.491744 | 3.299918 | 0.004973 |
| 14 | MAUSER | 3s | 0 | 1.169318 | 0.217119 | 0.002626 | 0.794869 | 0.009352 | 0.010752 | 0.15077 | 0.611244 | 3.328684 | 0.036534 |
| 17 | SWARTKLIF | 3s | 0 | 0.057861 | 0.776762 | 0 | 0 | 0.006522 | 0.029333 | 0.046123 | 1.453579 | 6.370192 | 0.008489 |
| 19 | CBC | 3s | 0 | 0.087669 | 0.060885 | 0 | 0 | 0 | 0 | 0.01381 | 0.403046 | 0.245235 | 0.027995 |
| 20 | GEVELOT | 3s | 0 | 0.102081 | 0.05643 | 0 | 0 | 0.006614 | 0 | 0.015832 | 0.533885 | 0.36428 | 0.036752 |
| 23 | DOMINION | 3s | 0 | 1.177499 | 0.187809 | 0.002251 | 0.044547 | 0.008253 | 0.007405 | 0.12236 | 0.522892 | 1.835825 | 0.020452 |
| 25 | HORNADY | 3s | 0.003466 | 0.033775 | 0.249365 | 0 | 0 | 0.01035 | 0.007131 | 0.025059 | 0.550944 | 1.980109 | 0.003924 |
| 26 | 26 | 3s | 0 | 0.029356 | 0.515755 | 0 | 0 | 0.011863 | 0.011477 | 0.03159 | 0.872195 | 4.390483 | 0.007947 |
| 27 | 27 | 3s | 0 | 0.042612 | 0.211663 | 0 | 0 | 0.004691 | 0.024883 | 0.016615 | 0.298298 | 1.426597 | 0.005853 |
| 28 | 28 | 3s | 0 | 0.070315 | 0.680089 | 0 | 0 | 0.008886 | 0.020198 | 0.039292 | 1.330449 | 4.722889 | 0.008464 |
| 29 | 29 | 3s | 0 | 0.027256 | 0.236406 | 0 | 0 | 0.009738 | 0.005751 | 0.014566 | 0.340642 | 1.036968 | 0.008114 |
| 30 | 30 | 3s | 0.001134 | 0.066977 | 0.510142 | 0 | 0 | 0.012762 | 0.009236 | 0.032363 | 0.842939 | 4.299959 | 0.006165 |
| 31 | 31 | 3s | 0 | 0.021403 | 0.287756 | 0 | 0 | 0.006395 | 0.010553 | 0.021071 | 0.407445 | 1.546467 | 0.005352 |
| 32 | 32 | 3s | 0 | 0.046519 | 0.29953 | 0 | 0 | 0.007059 | 0.009467 | 0.020464 | 0.432731 | 1.56145 | 0.005186 |
| 33 | 33 | 3s | 0 | 0.049794 | 0.326398 | 0 | 0 | 0.008726 | 0.011796 | 0.02667 | 0.761881 | 3.07735 | 0.008857 |
| 34 | 34 | 3s | 0.002993 | 0.032936 | 0.45389 | 0 | 0 | 0.008695 | 0.045544 | 0.040996 | 0.523005 | 1.92459 | 0.008117 |
| 35 | 35 | 3s | 0.002808 | 0.040131 | 0.172925 | 0.001662 | 0.005053 | 0.008458 | 0.022364 | 0.016034 | 0.241924 | 1.017631 | 0.005088 |
| 36 | 36 | 3s | 0.001663 | 0.031818 | 0.407522 | 0.001937 | 0.004868 | 0.003995 | 0.071028 | 0.01668 | 0.313182 | 0.958784 | 0.004907 |
| 37 | 37 | 3s | 0.002866 | 0.05477 | 0.385167 | 0 | 0.003816 | 0.019291 | 0.008534 | 0.022706 | 0.830236 | 4.960636 | 0.007819 |

| | SAMPLE | | SiO2H | SiO2H2 | Si2 | Sn |
|---|---|---|---|---|---|---|
| 1 | REMINGTO | 3s | 0.016384 | 0.033733 | 0.345325 | 0 |
| 2 | CIL | 3s | 0.017323 | 0.046461 | 1.398683 | 0 |
| 3 | FEDERAL | 3s | 0.013348 | 0.01004 | 0.018001 | 0 |
| 5 | CCI | 3s | 0.022297 | 0.015592 | 0.019179 | 0 |
| 6 | AGUILLA | 3s | 0.027007 | 0.100103 | 1.386394 | 0 |
| 7 | ELEY | 3s | 0.021888 | 0.250284 | 2.945223 | 0 |
| 8 | RWS | 3s | 0.01728 | 0.035824 | 0.195258 | 0 |
| 9 | BROWNIN( | 3s | 0.013677 | 0.020929 | 0.020365 | 0 |
| 10 | STIRLING | 3s | 0.025606 | 0.020323 | 0.033774 | 0 |
| 11 | 11 | 3s | 0 | 0.009466 | 0.030907 | 0 |
| 12 | PMC | 3s | 0.029385 | 0.137658 | 0.620445 | 0 |
| 14 | MAUSER | 3s | 0.046813 | 0.200237 | 2.216308 | 0 |
| 17 | SWARTKLIF | 3s | 0.027841 | 0.049181 | 0.075609 | 0 |
| 19 | CBC | 3s | 0.061426 | 0.027699 | 0.220146 | 0 |
| 20 | GEVELOT | 3s | 0.074888 | 0.03796 | 0.400362 | 0 |
| 23 | DOMINION | 3s | 0.027159 | 0.105464 | 0.971378 | 0 |
| 25 | HORNADY | 3s | 0.011082 | 0.012886 | 0.023712 | 0 |
| 26 | 26 | 3s | 0.028617 | 0.020299 | 0.045761 | 0 |
| 27 | 27 | 3s | 0.013745 | 0.010513 | 0.030926 | 0 |
| 28 | 28 | 3s | 0.022714 | 0.034101 | 0.080185 | 0 |
| 29 | 29 | 3s | 0.008965 | 0.013431 | 0.021912 | 0 |
| 30 | 30 | 3s | 0.025272 | 0.030747 | 0.073285 | 0 |
| 31 | 31 | 3s | 0.01789 | 0.014746 | 0.026841 | 0 |
| 32 | 32 | 3s | 0.014532 | 0.01386 | 0.047469 | 0 |
| 33 | 33 | 3s | 0.009567 | 0.026382 | 0.047016 | 0 |
| 34 | 34 | 3s | 0.018178 | 0.019869 | 0.044101 | 0 |
| 35 | 35 | 3s | 0.008695 | 0.012002 | 0.034206 | 0 |
| 36 | 36 | 3s | 0.011289 | 0.014044 | 0.031039 | 0 |
| 37 | 37 | 3s | 0.036349 | 0.027945 | 0.056563 | 0 |

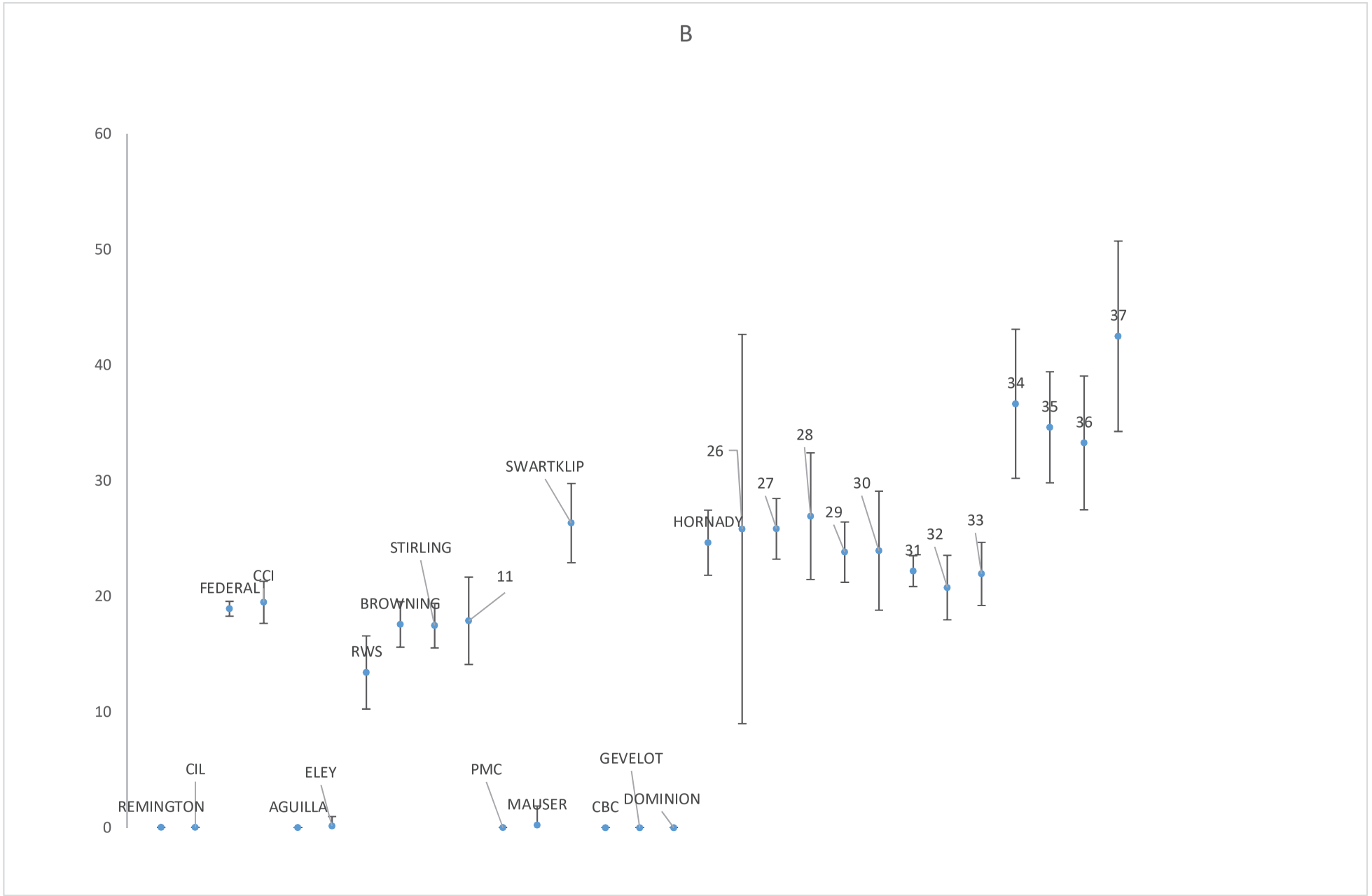
B
60
50
40
30
20
10
0
REMINGTON
CIL
FEDERAL
CCI
AGUILLA
ELEY
RWS
BROWNING
STIRLING
11
SWARTKLIP
PMC
MAUSER
CBC
GEVELOT
DOMINION
HORNADY
26
27
28
29
30
31
32
33
34
35
36
37

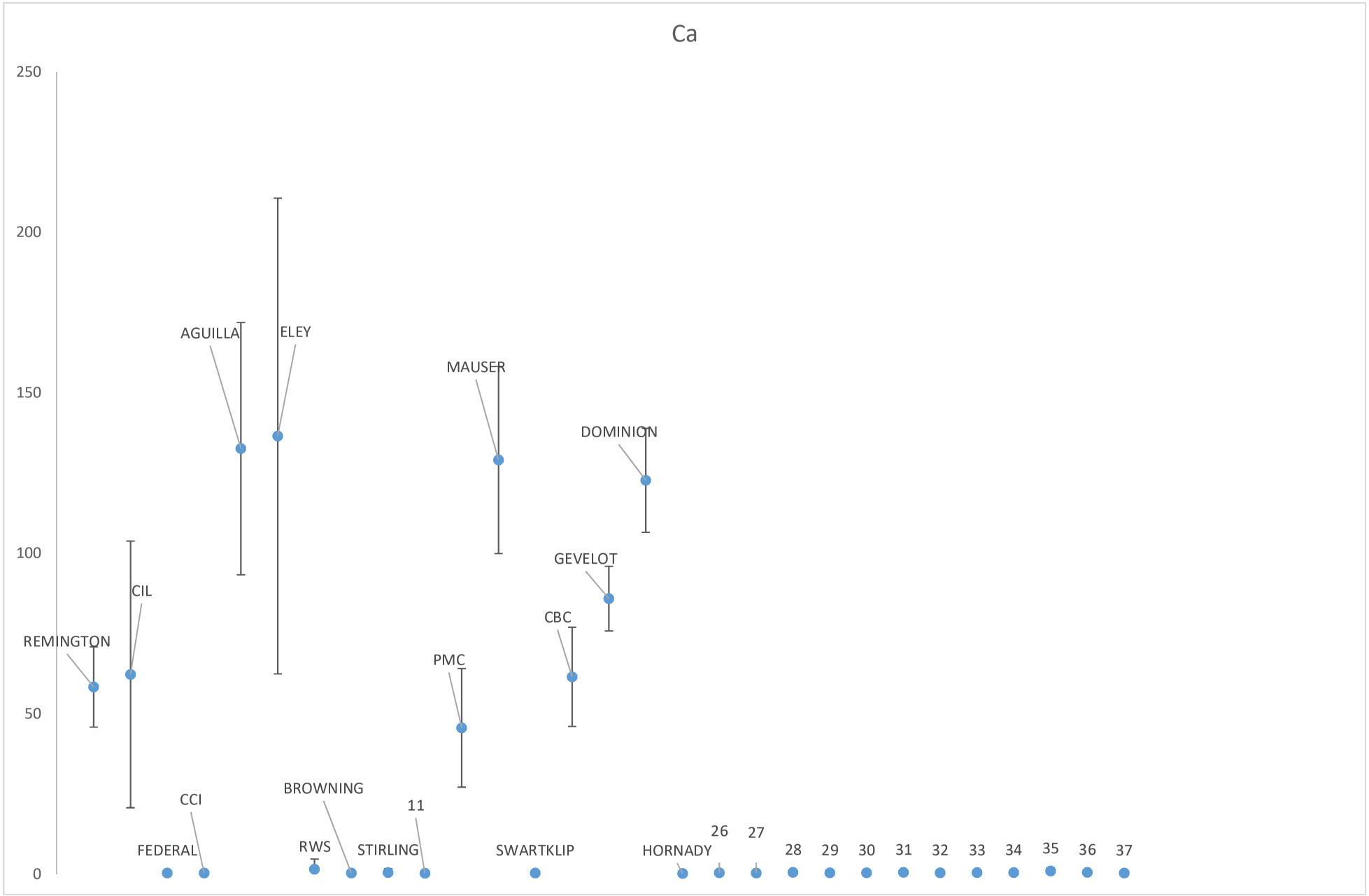
Ca
250
200
150
100
50
0
AGUILLA
ELEY
MAUSER
DOMINION
GEVELOT
CBC
CIL
REMINGTON
PMC
CCI
BROWNING
11
FEDERAL
RWS
STIRLING
SWARTKLIP
HORNADY
26
27
28
29
30
31
32
33
34
35
36
37

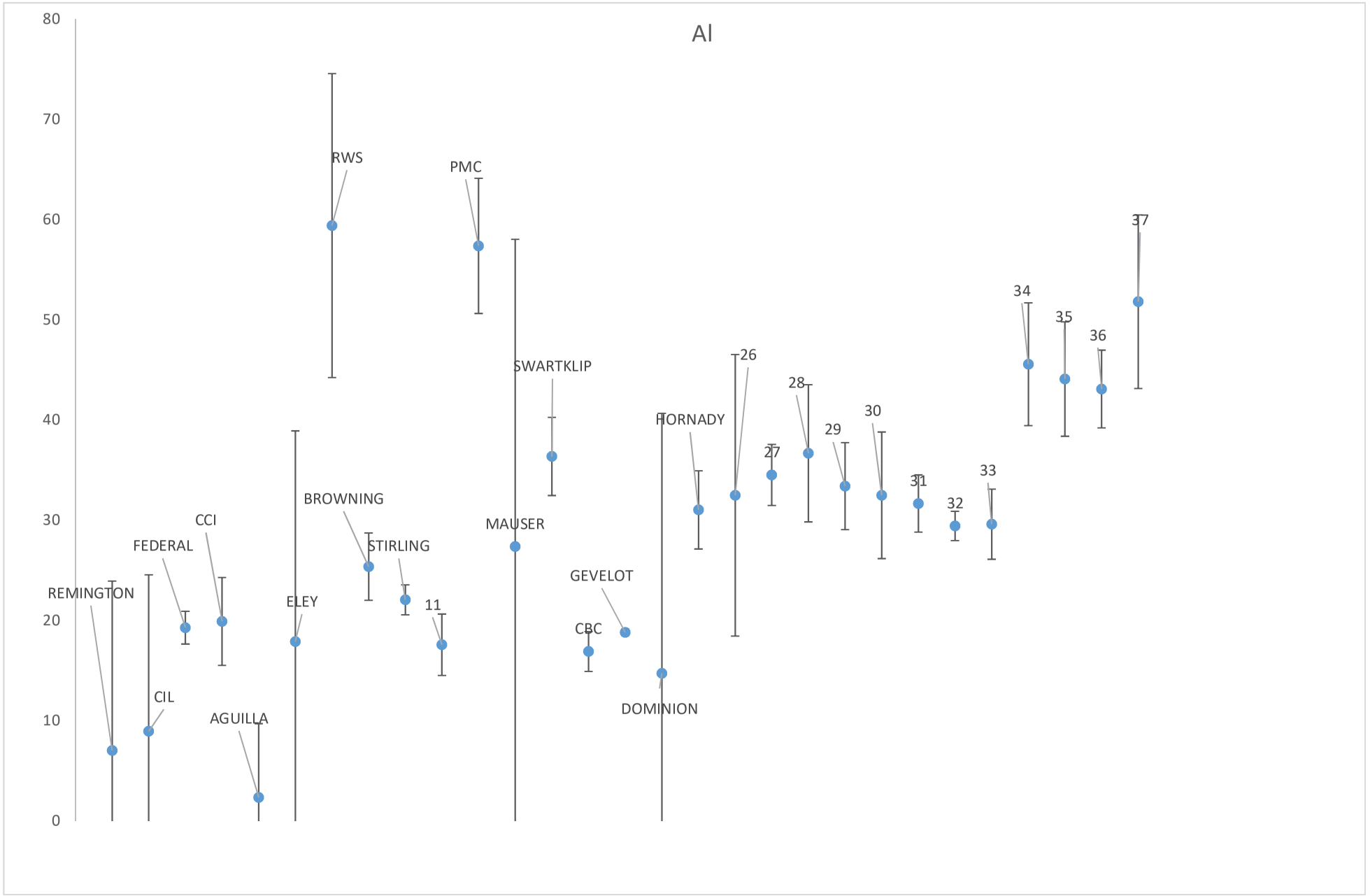
Al
80
70
60
50
40
30
20
10
0
REMINGTON
FEDERAL
CCI
CIL
AGUILLA
ELEY
BROWNING
STIRLING
11
RWS
PMC
MAUSER
SWARTKLIP
GEVELOT
CBC
DOMINION
HORNADY
26
27
28
29
30
31
32
33
34
35
36
37

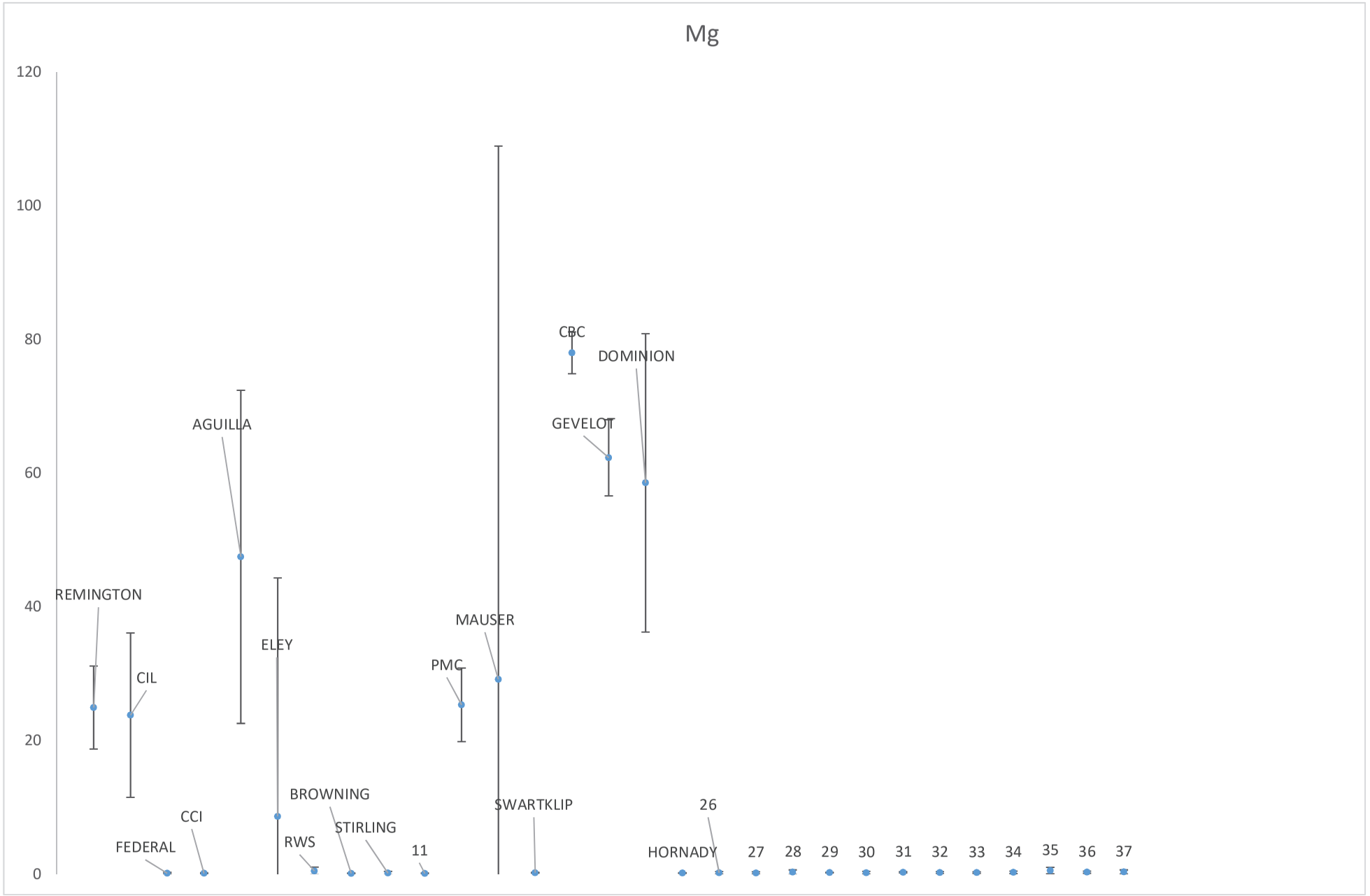
Mg
120
100
80
60
40
20
0
REMINGTON
CIL
FEDERAL
CCI
AGUILLA
ELEY
RWS
BROWNING
STIRLING
11
PMC
MAUSER
SWARTKLIP
CBC
DOMINION
GEVELOT
HORNADY
26
27
28
29
30
31
32
33
34
35
36
37

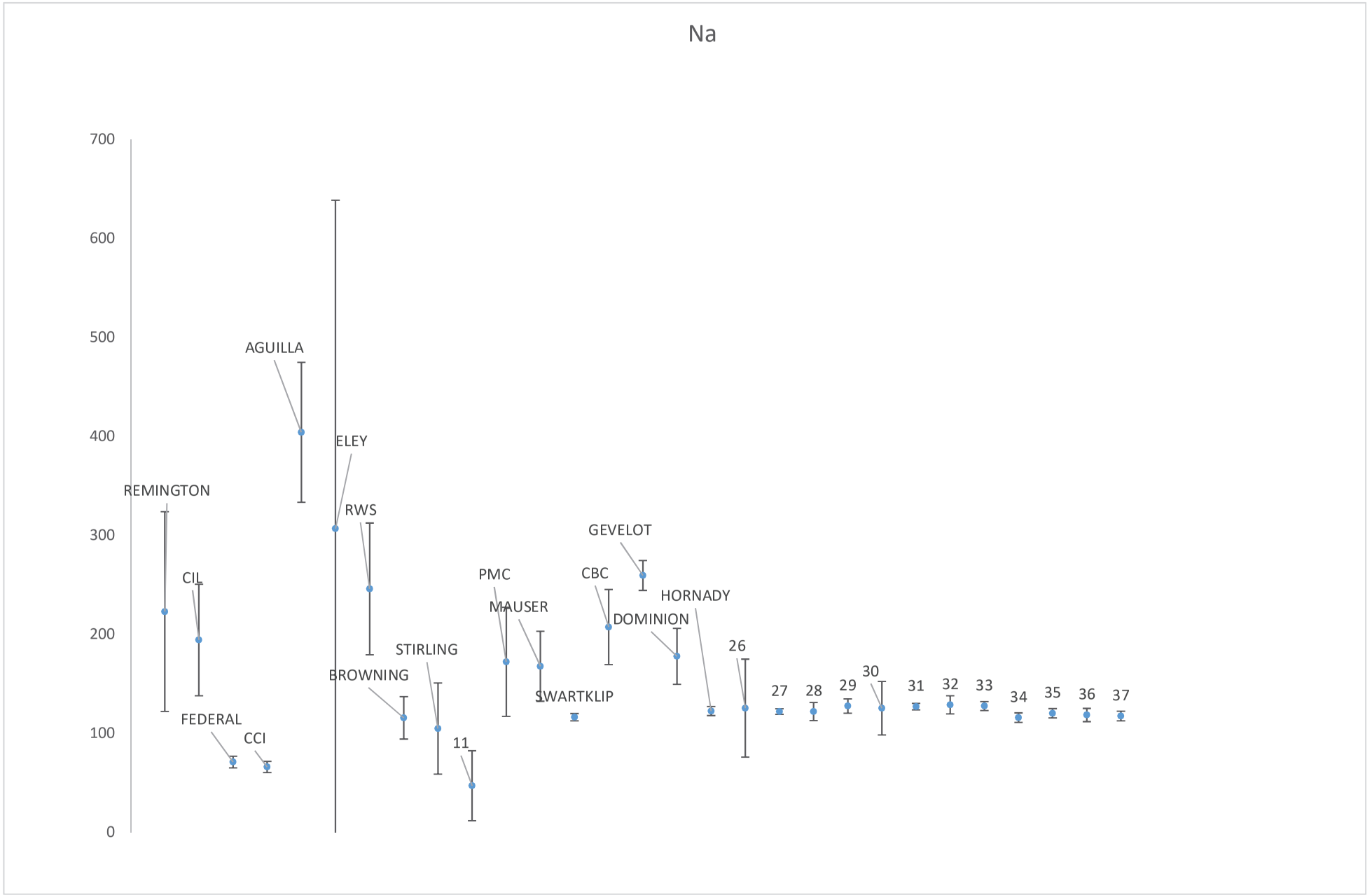
Na
700
600
500
400
300
200
100
0
REMINGTON
CIL
FEDERAL
CCI
AGUILLA
ELEY
RWS
BROWNING
STIRLING
11
PMC
MAUSER
SWARTKLIP
GEVELOT
CBC
DOMINION
HORNADY
26
27
28
29
30
31
32
33
34
35
36
37

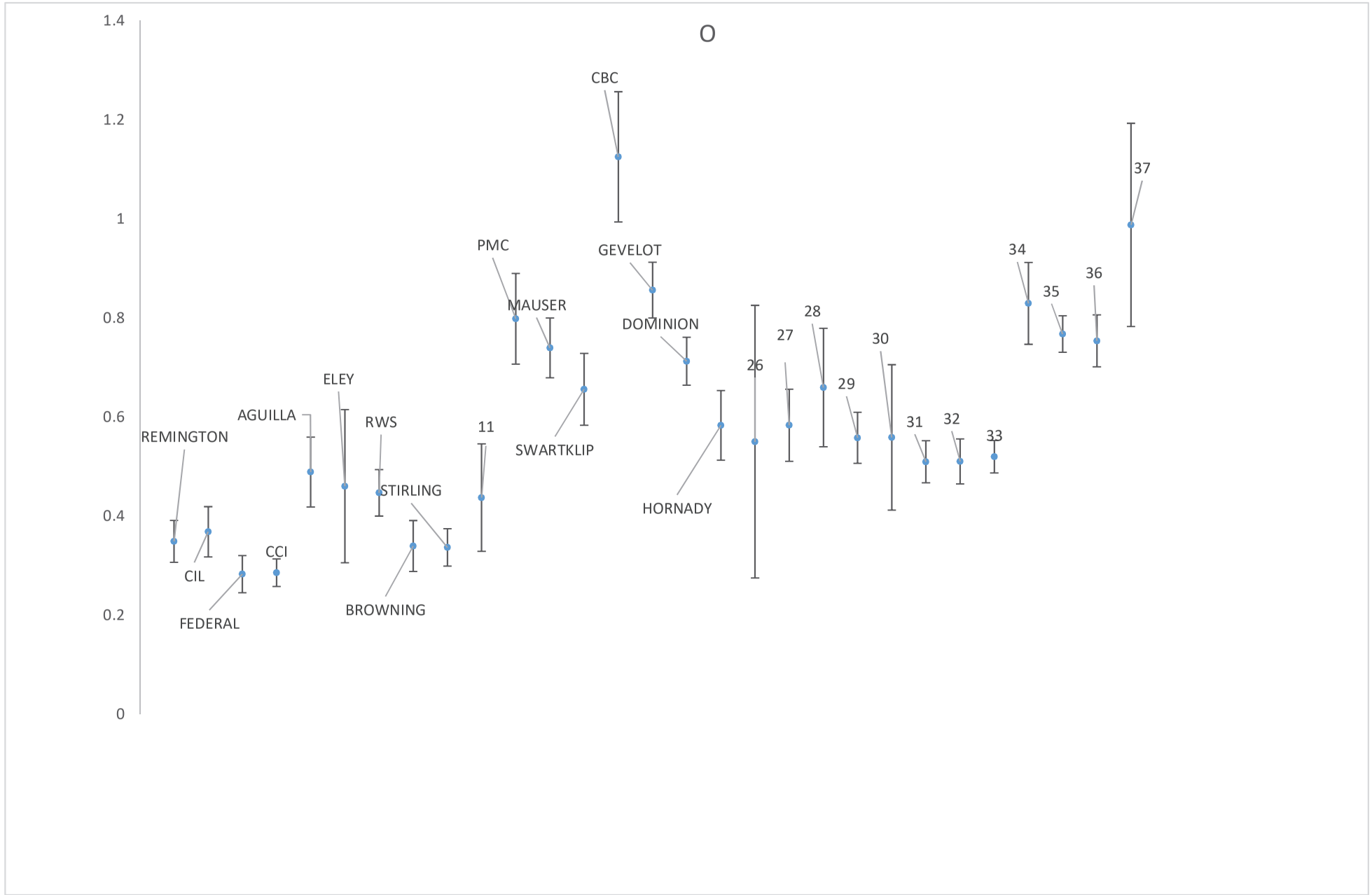
O
1.4
1.2
1
0.8
0.6
0.4
0.2
0
REMINGTON
CIL
FEDERAL
CCI
AGUILLA
ELEY
RWS
STIRLING
BROWNING
11
PMC
MAUSER
SWARTKLIP
CBC
GEVELOT
DOMINION
HORNADY
26
27
28
29
30
31
32
33
34
35
36
37

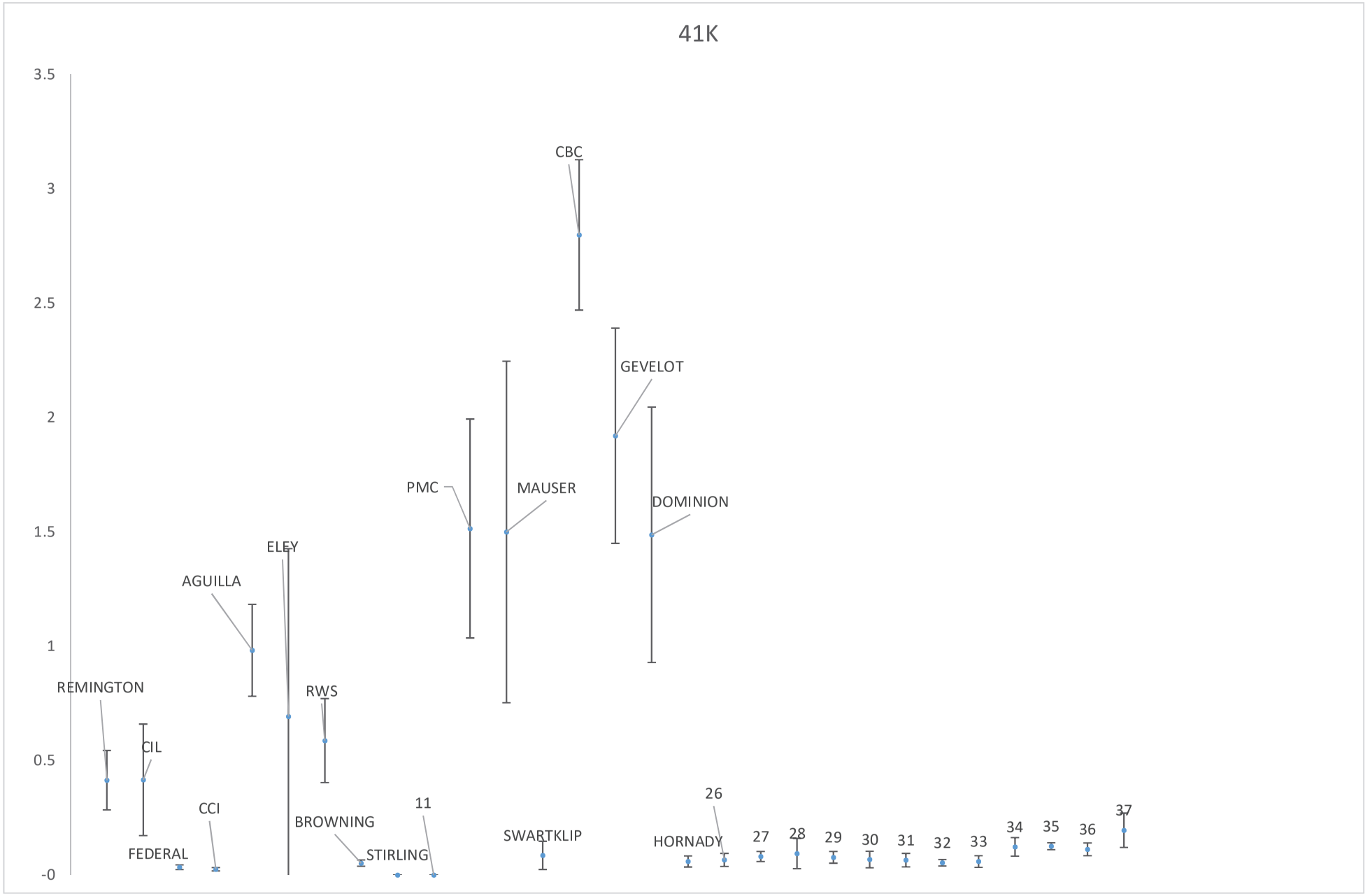
41K
3.5
3
2.5
2
1.5
1
0.5
-0
CBC
GEVELOT
PMC
MAUSER
DOMINION
ELEY
AGUILLA
REMINGTON
RWS
CIL
CCI
BROWNING
11
STIRLING
SWARTKLIP
26
HORNADY
27
28
29
30
31
32
33
34
35
36
37
FEDERAL

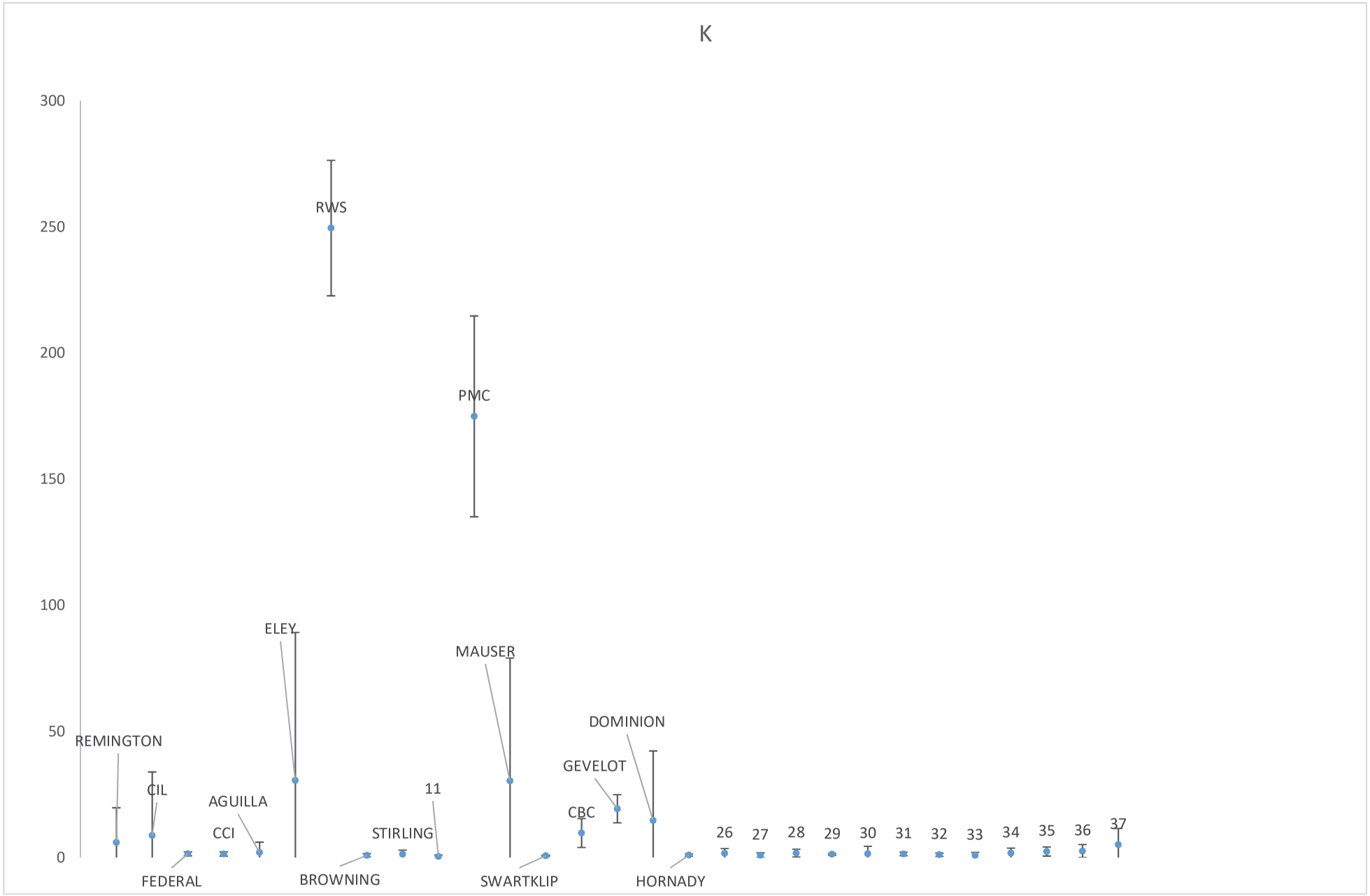
K
300
250
200
150
100
50
0
RWS
PMC
ELEY
MAUSER
DOMINION
GEVELOT
CBC
REMINGTON
CIL
AGUILLA
CCI
STIRLING
11
FEDERAL
BROWNING
SWARTKLIP
HORNADY
26
27
28
29
30
31
32
33
34
35
36
37

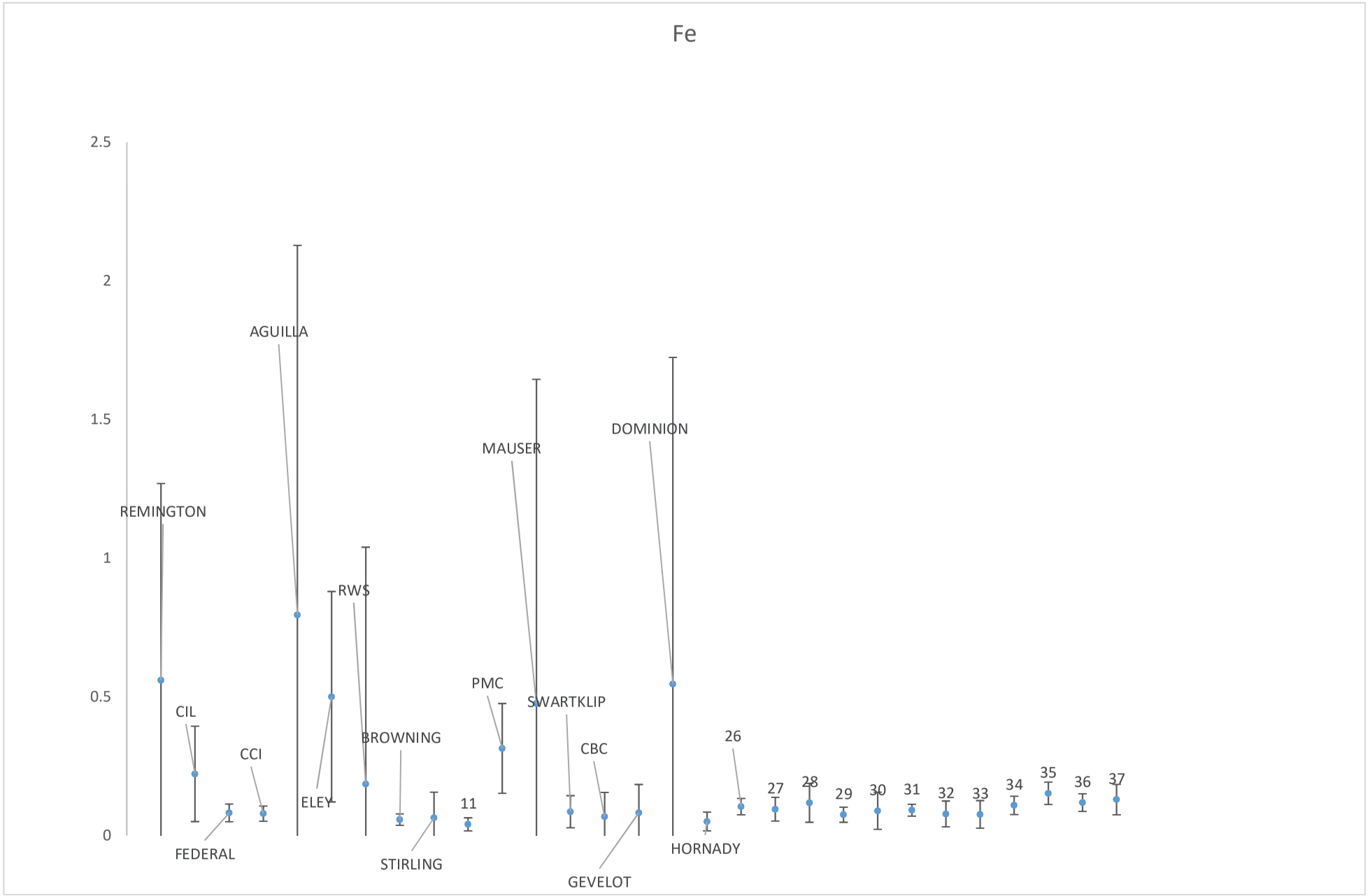
Fe
2.5
2
1.5
1
0.5
0
REMINGTON
CIL
FEDERAL
CCI
AGUILLA
ELEY
RWS
BROWNING
STIRLING
11
PMC
MAUSER
SWARTKLIP
CBC
GEVELOT
DOMINION
HORNADY
26
27
28
29
30
31
32
33
34
35
36
37

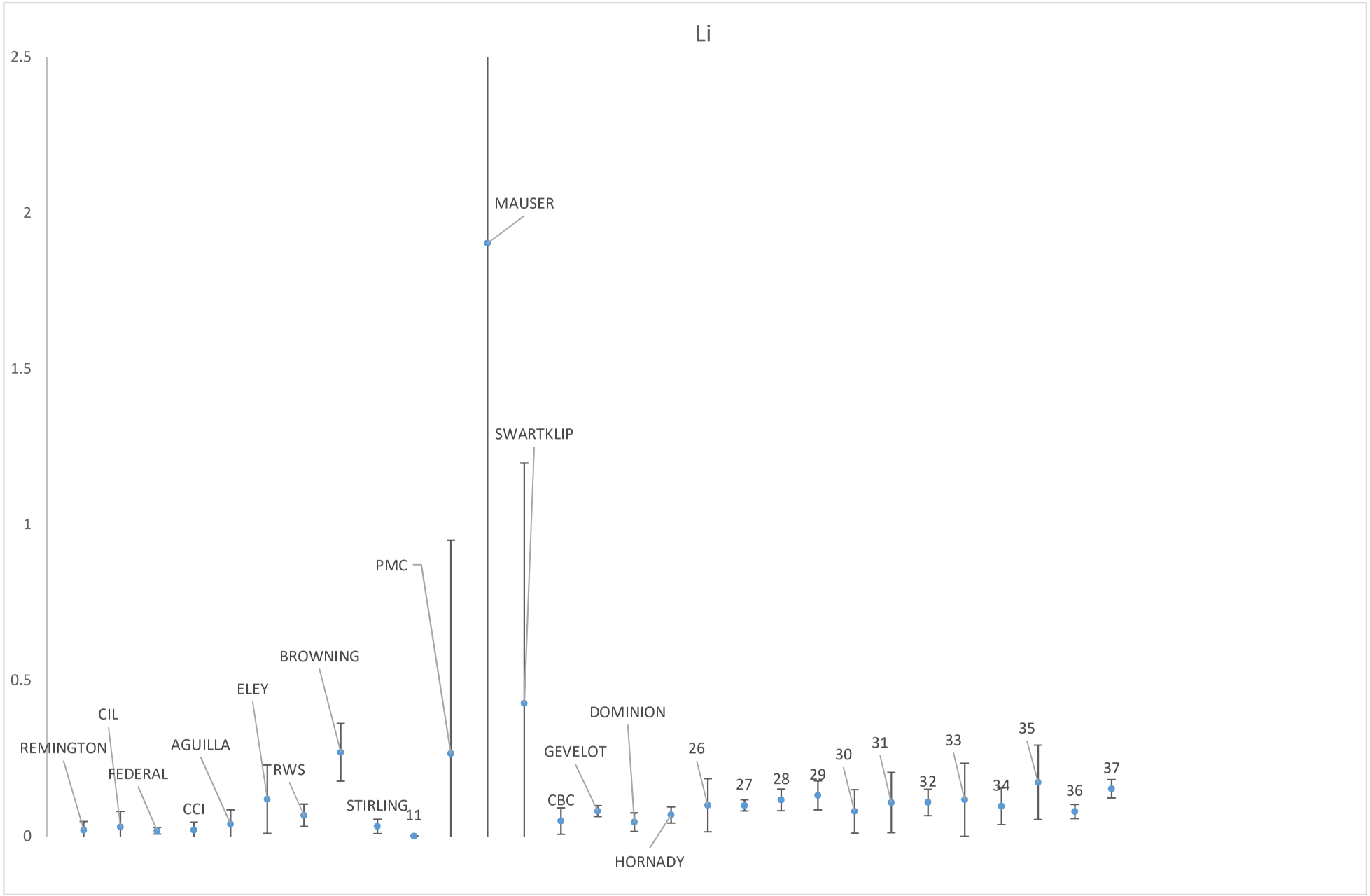
Li
2.5
2
1.5
1
0.5
0
MAUSER
SWARTKLIP
PMC
BROWNING
ELEY
CIL
REMINGTON
AGUILLA
FEDERAL
RWS
CCI
STIRLING
11
DOMINION
GEVELOT
CBC
HORNADY
26
27
28
29
30
31
32
33
34
35
36
37

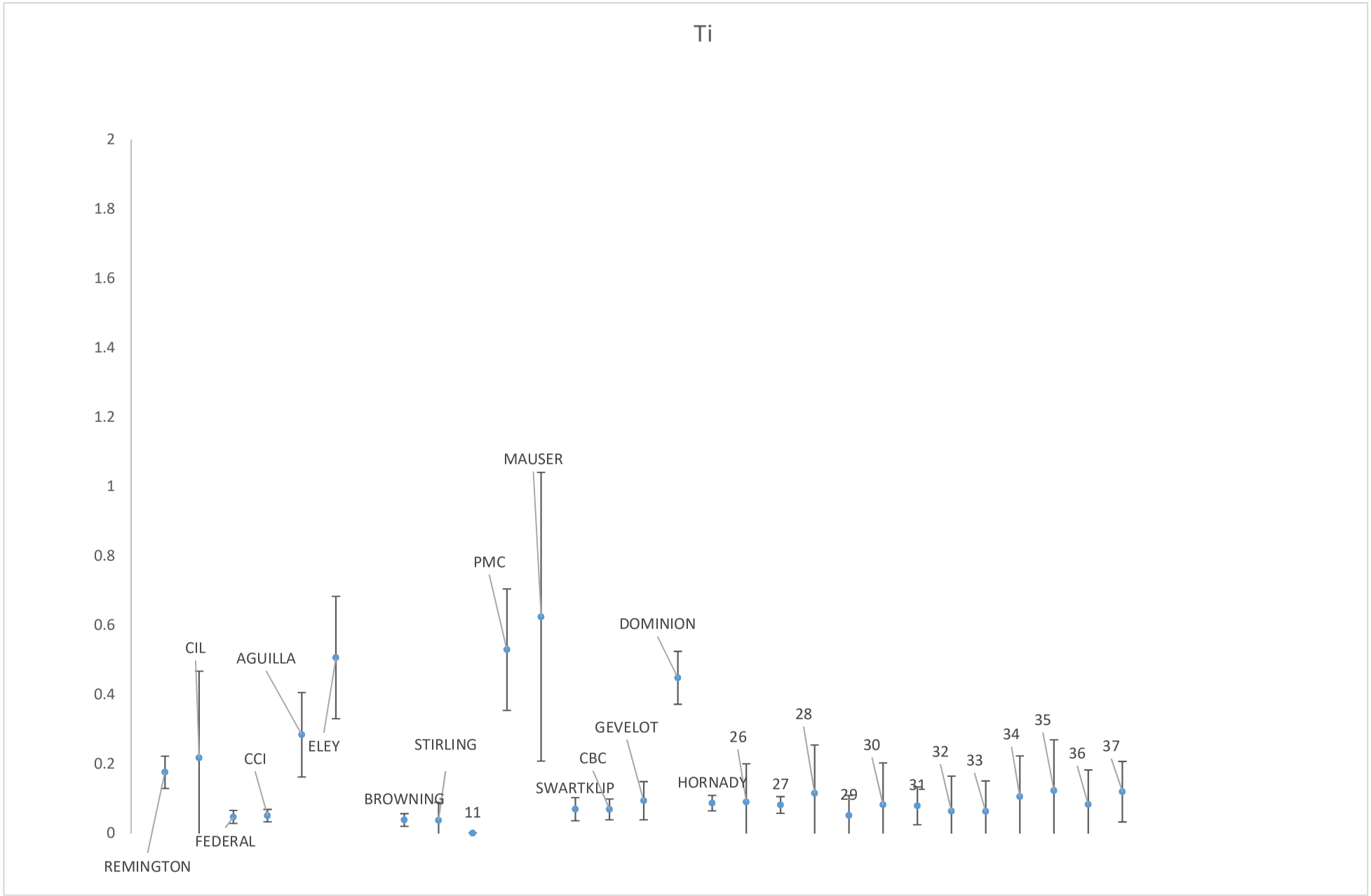
Ti
2
1.8
1.6
1.4
1.2
1
0.8
0.6
0.4
0.2
0
REMINGTON
CIL
FEDERAL
CCI
AGUILLA
ELEY
BROWNING
STIRLING
11
PMC
MAUSER
SWARTKLIP
CBC
GEVELOT
DOMINION
HORNADY
26
27
28
29
30
31
32
33
34
35
36
37

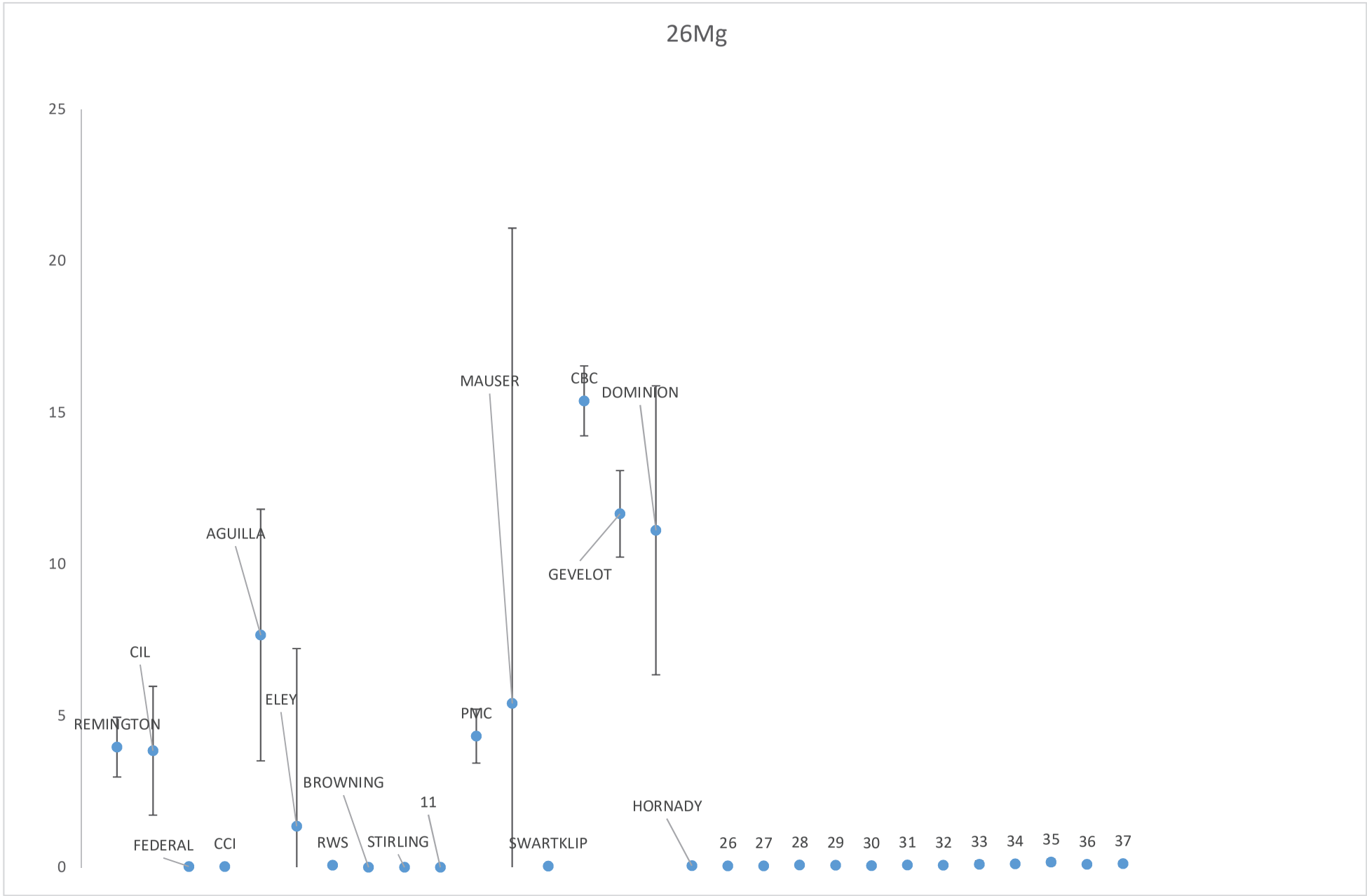
26Mg
25
20
15
10
5
0
REMINGTON
CIL
FEDERAL
CCI
AGUILLA
ELEY
RWS
BROWNING
STIRLING
11
MAUSER
PMC
SWARTKLIP
CBC
DOMINTON
GEVELOT
HORNADY
26
27
28
29
30
31
32
33
34
35
36
37

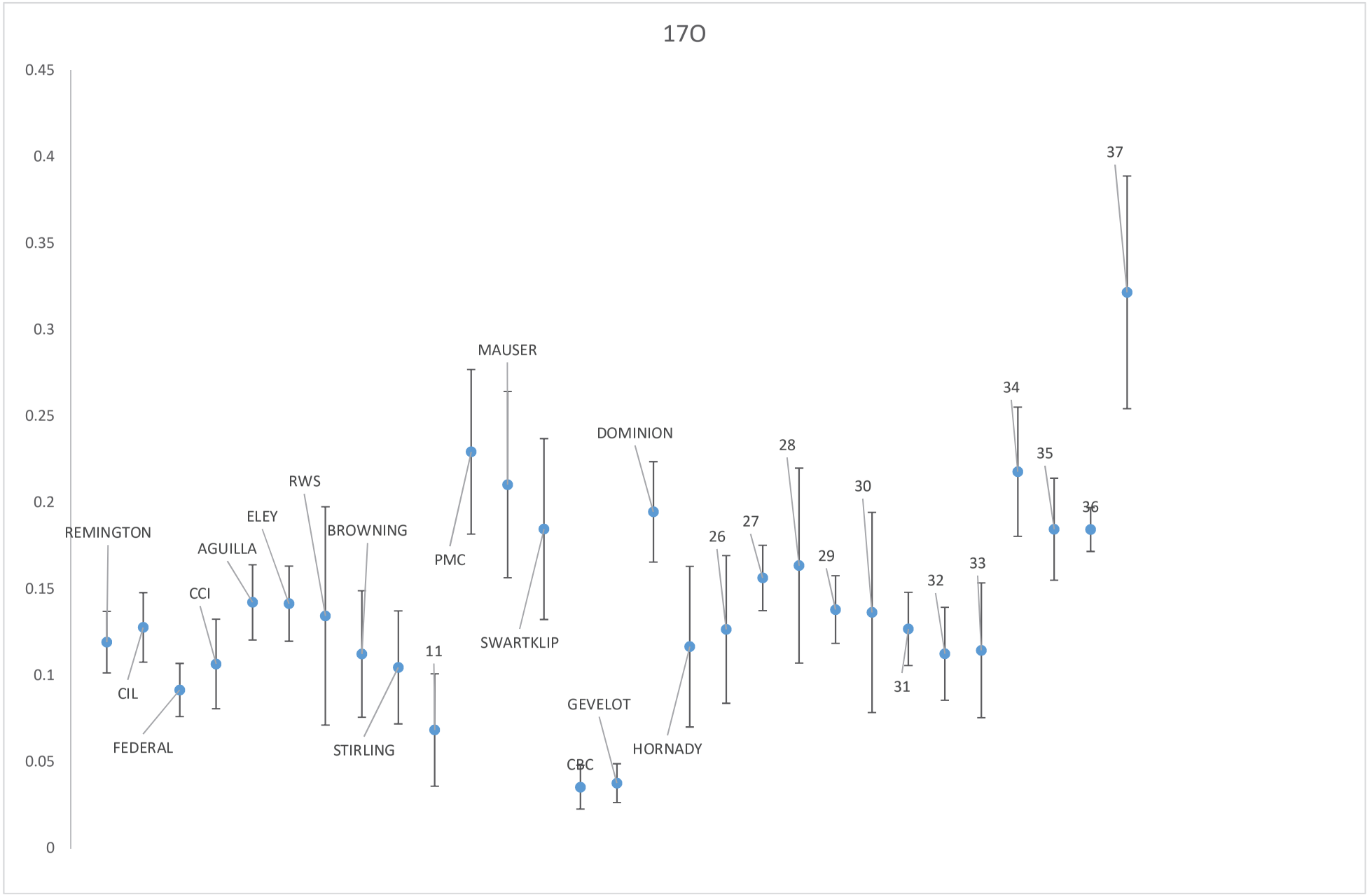
17O
0.45
0.4
0.35
0.3
0.25
0.2
0.15
0.1
0.05
0
REMINGTON
CIL
FEDERAL
CCI
AGUILLA
ELEY
RWS
BROWNING
STIRLING
11
PMC
MAUSER
SWARTKLIP
GEVELOT
CBC
DOMINION
HORNADY
26
27
28
29
30
31
32
33
34
35
36
37

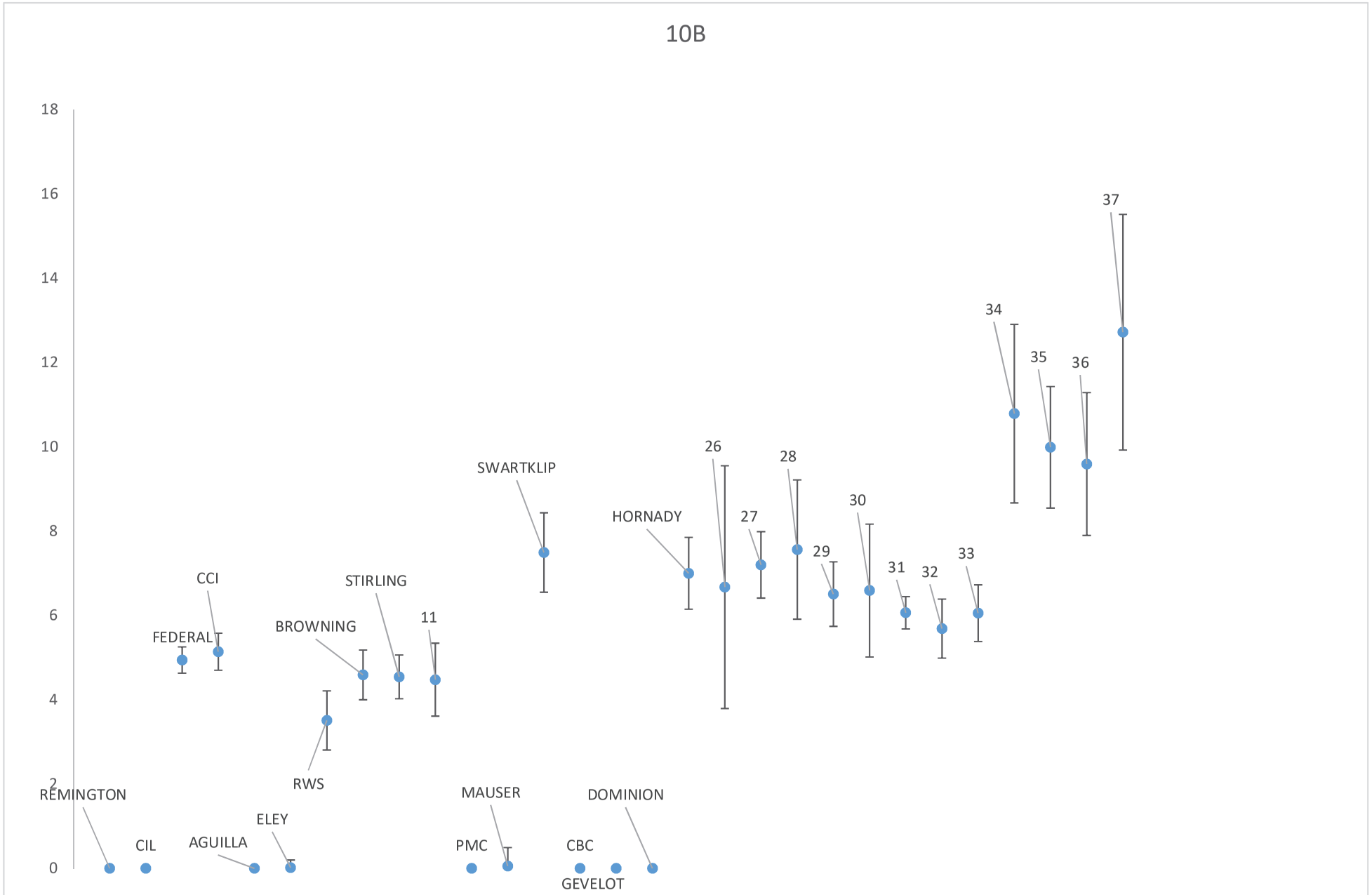
10B
18
16
14
12
10
8
6
4
2
0
REMINGTON
CIL
AGUILLA
ELEY
FEDERAL
CCI
RWS
BROWNING
STIRLING
11
MAUSER
PMC
SWARTKLIP
CBC
GEVELOT
DOMINION
HORNADY
26
27
28
29
30
31
32
33
34
35
36
37

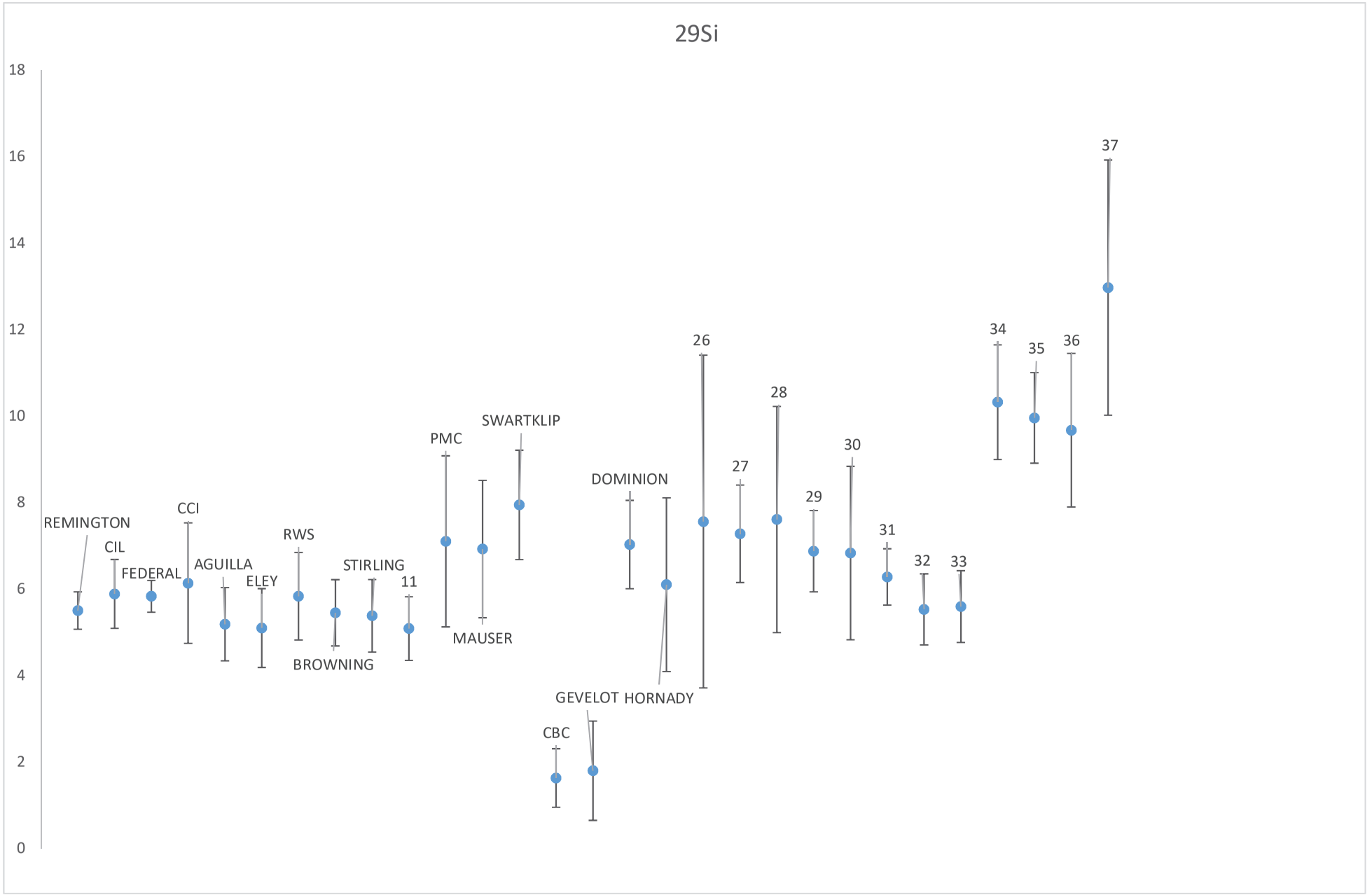
29Si
18
16
14
12
10
8
6
4
2
0
REMINGTON
CIL
FEDERAL
CCI
AGUILLA
ELEY
RWS
BROWNING
STIRLING
11
PMC
MAUSER
SWARTKLIP
CBC
GEVELOT
DOMINION
HORNADY
26
27
28
29
30
31
32
33
34
35
36
37

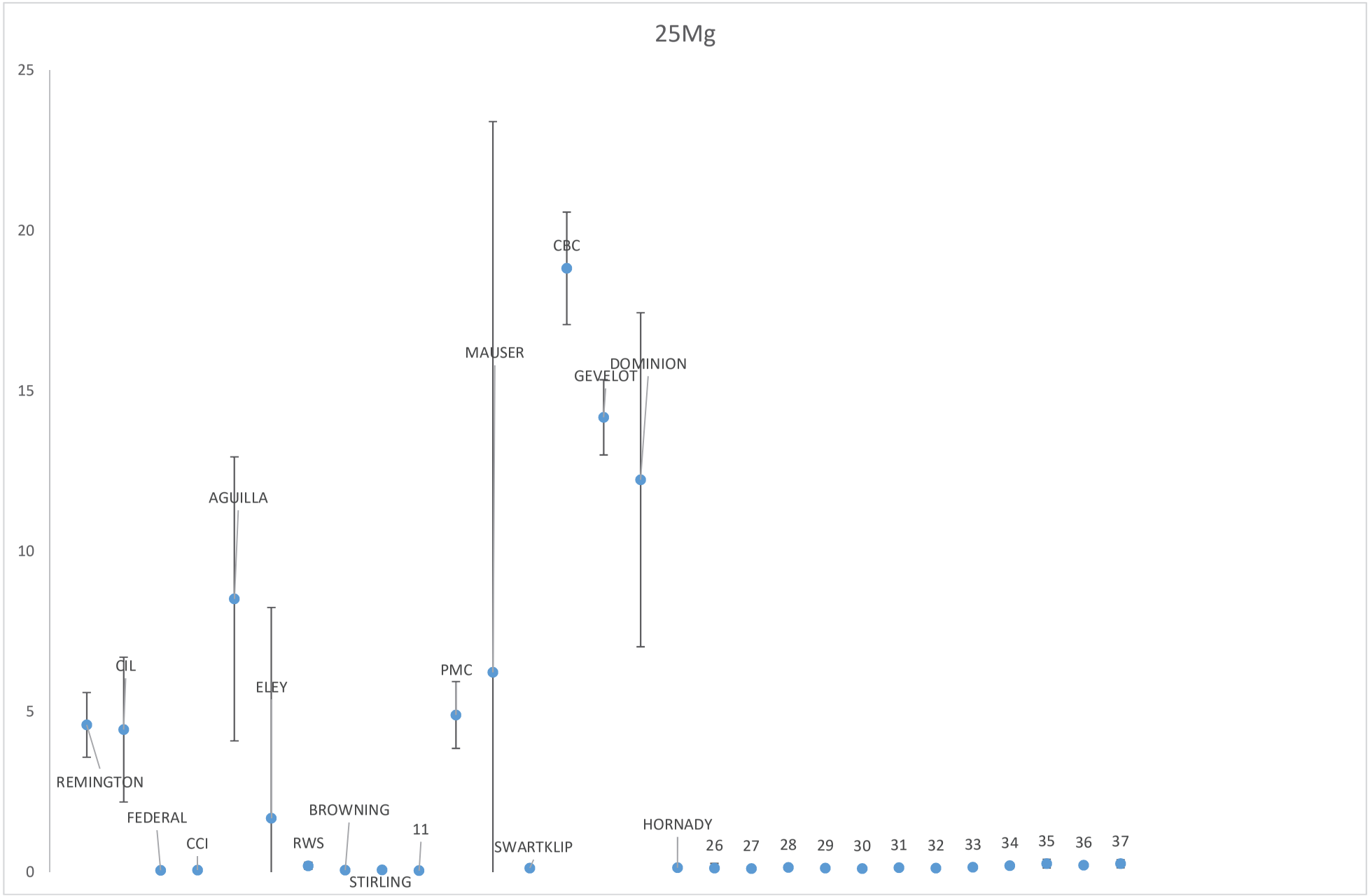
25Mg
25
20
15
10
5
0
CBC
MAUSER
GEVELOT
DOMINION
AGUILLA
CIL
ELEY
PMC
REMINGTON
FEDERAL
CCI
BROWNING
RWS
STIRLING
11
SWARTKLIP
HORNADY
26
27
28
29
30
31
32
33
34
35
36
37

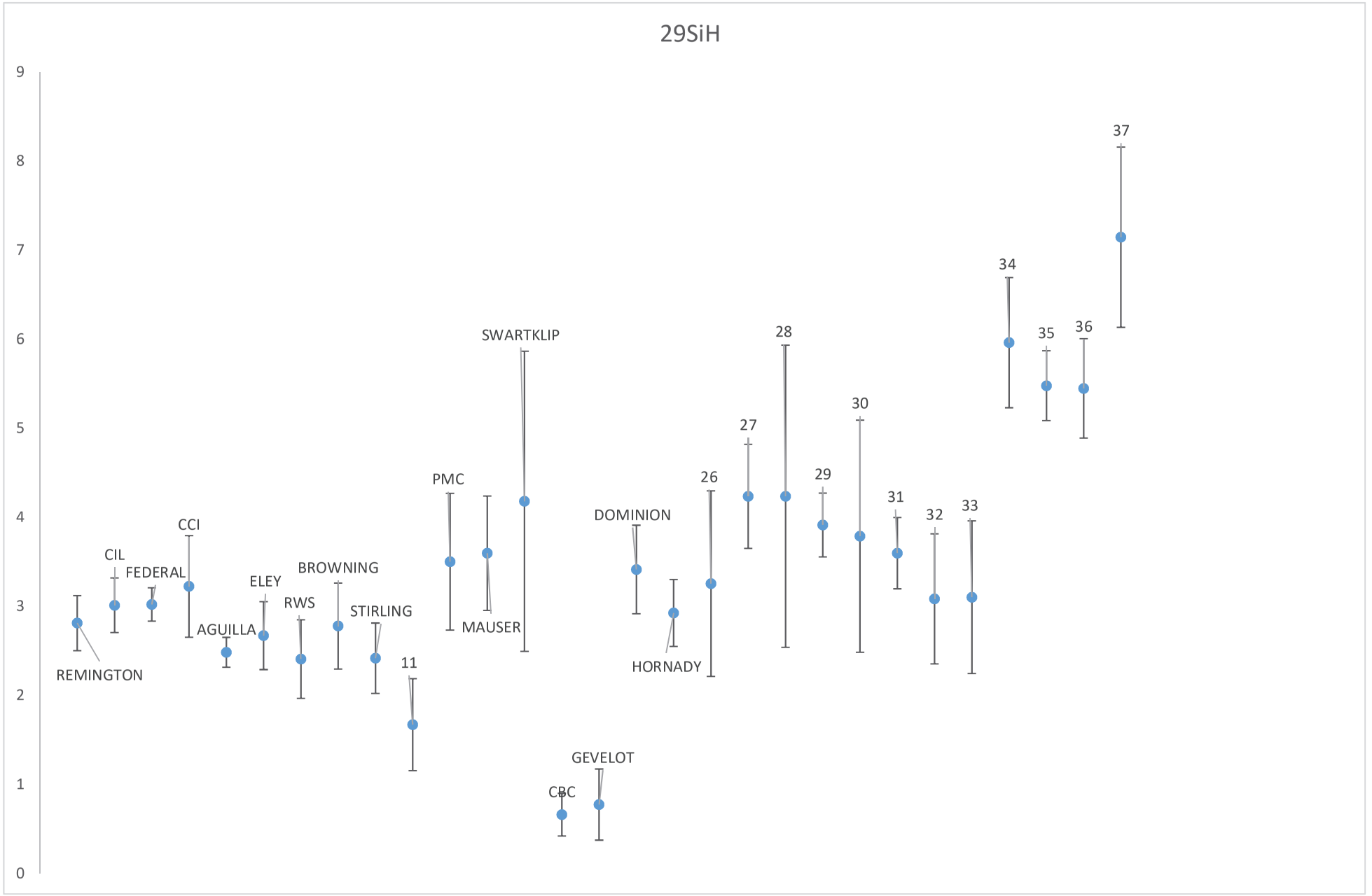
29SiH
9
8
7
6
5
4
3
2
1
0
REMINGTON
CIL
FEDERAL
CCI
AGUILLA
ELEY
RWS
BROWNING
STIRLING
11
PMC
MAUSER
SWARTKLIP
CBC
GEVELOT
DOMINION
HORNADY
26
27
28
29
30
31
32
33
34
35
36
37

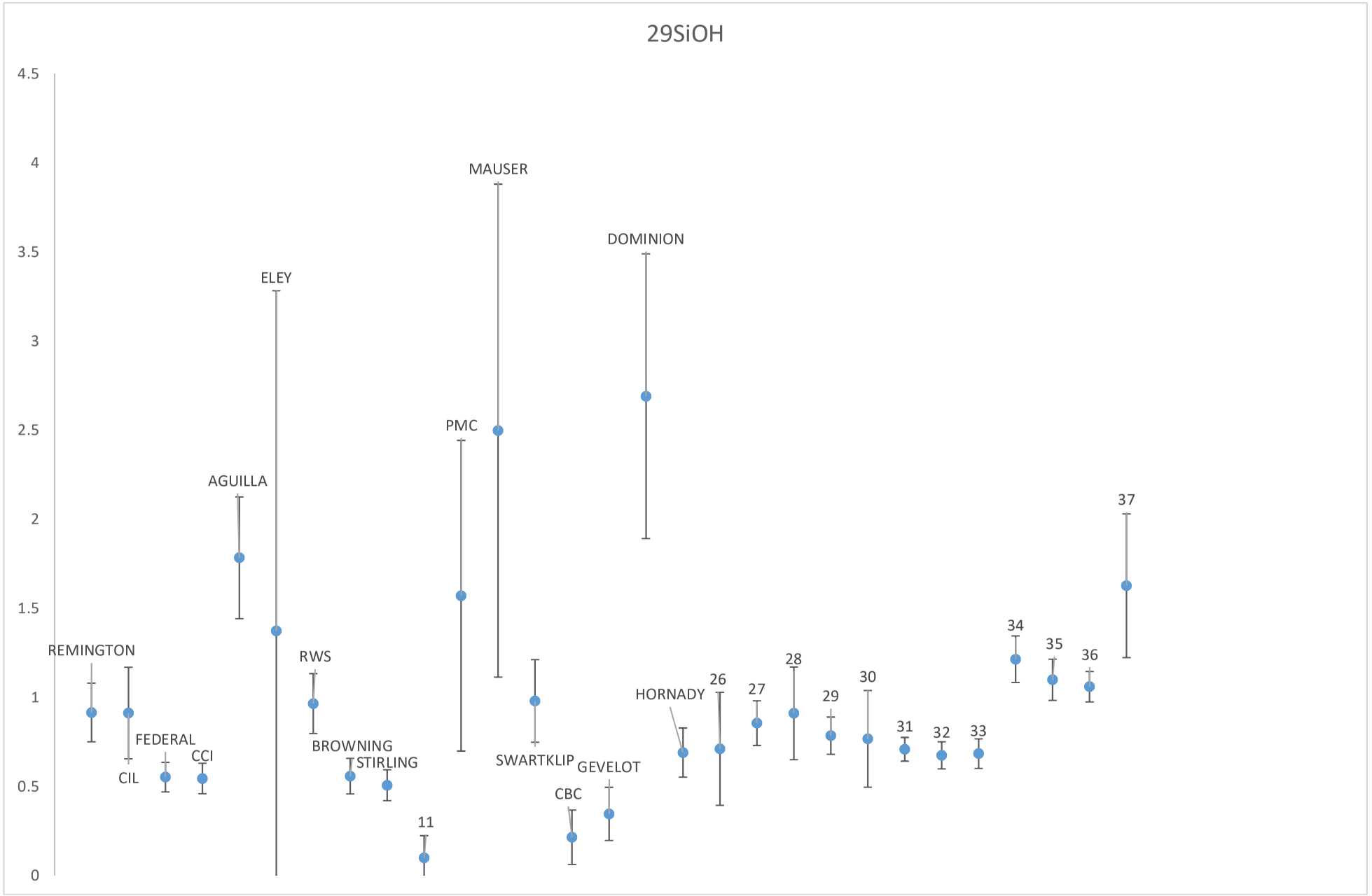
29SiOH
4.5
4
3.5
3
2.5
2
1.5
1
0.5
0
REMINGTON
CIL
FEDERAL
CCI
AGUILLA
ELEY
RWS
BROWNING
STIRLING
11
PMC
MAUSER
SWARTKLIP
CBC
GEVELOT
DOMINION
HORNADY
26
27
28
29
30
31
32
33
34
35
36
37

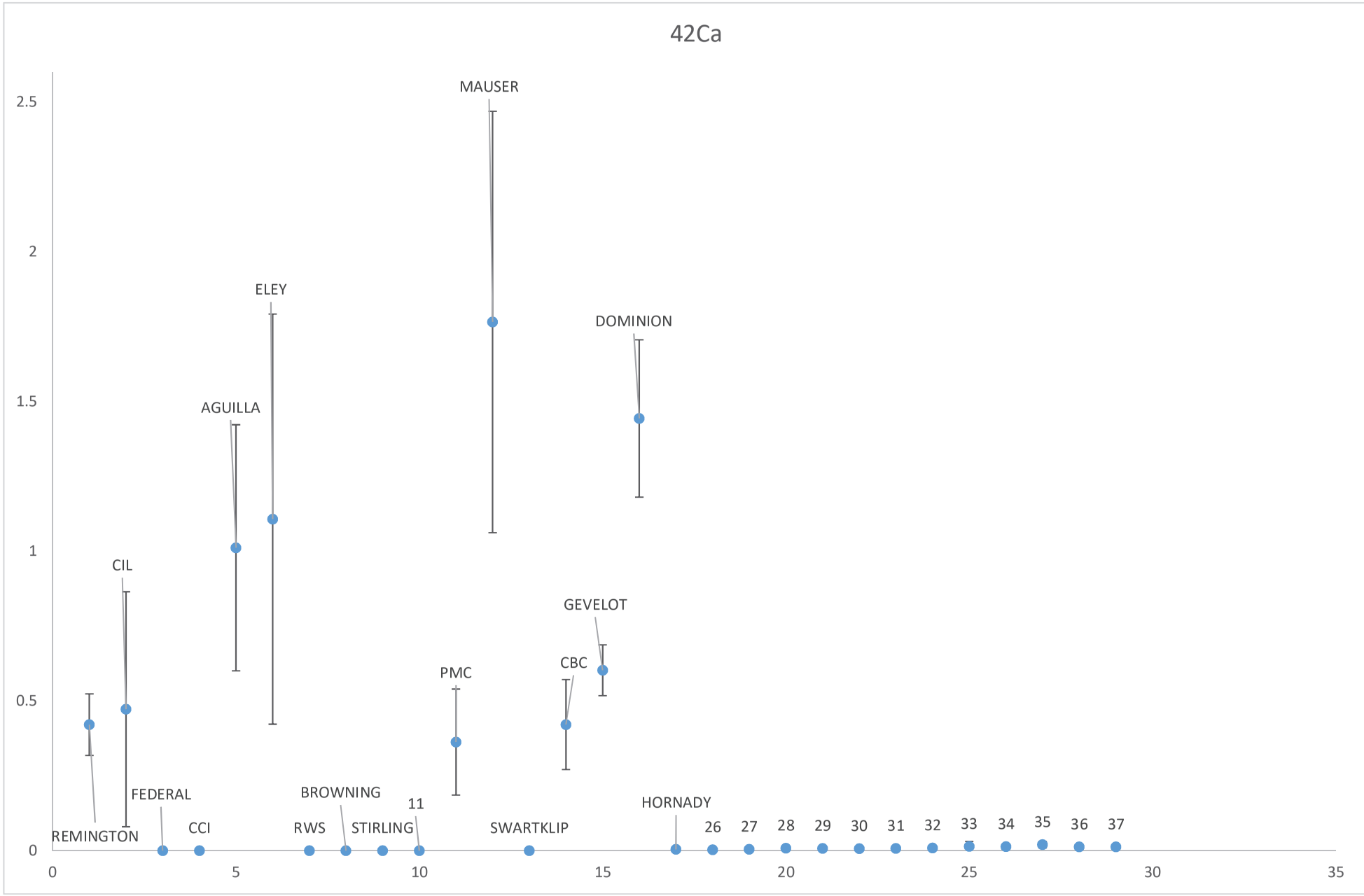
42Ca
MAUSER
ELEY
DOMINION
AGUILLA
CIL
GEVELOT
CBC
PMC
FEDERAL
BROWNING
11
HORNADY
REMINGTON
CCI
RWS
STIRLING
SWARTKLIP
26
27
28
29
30
31
32
33
34
35
36
37
2.5
2
1.5
1
0.5
0
0
5
10
15
20
25
30
35

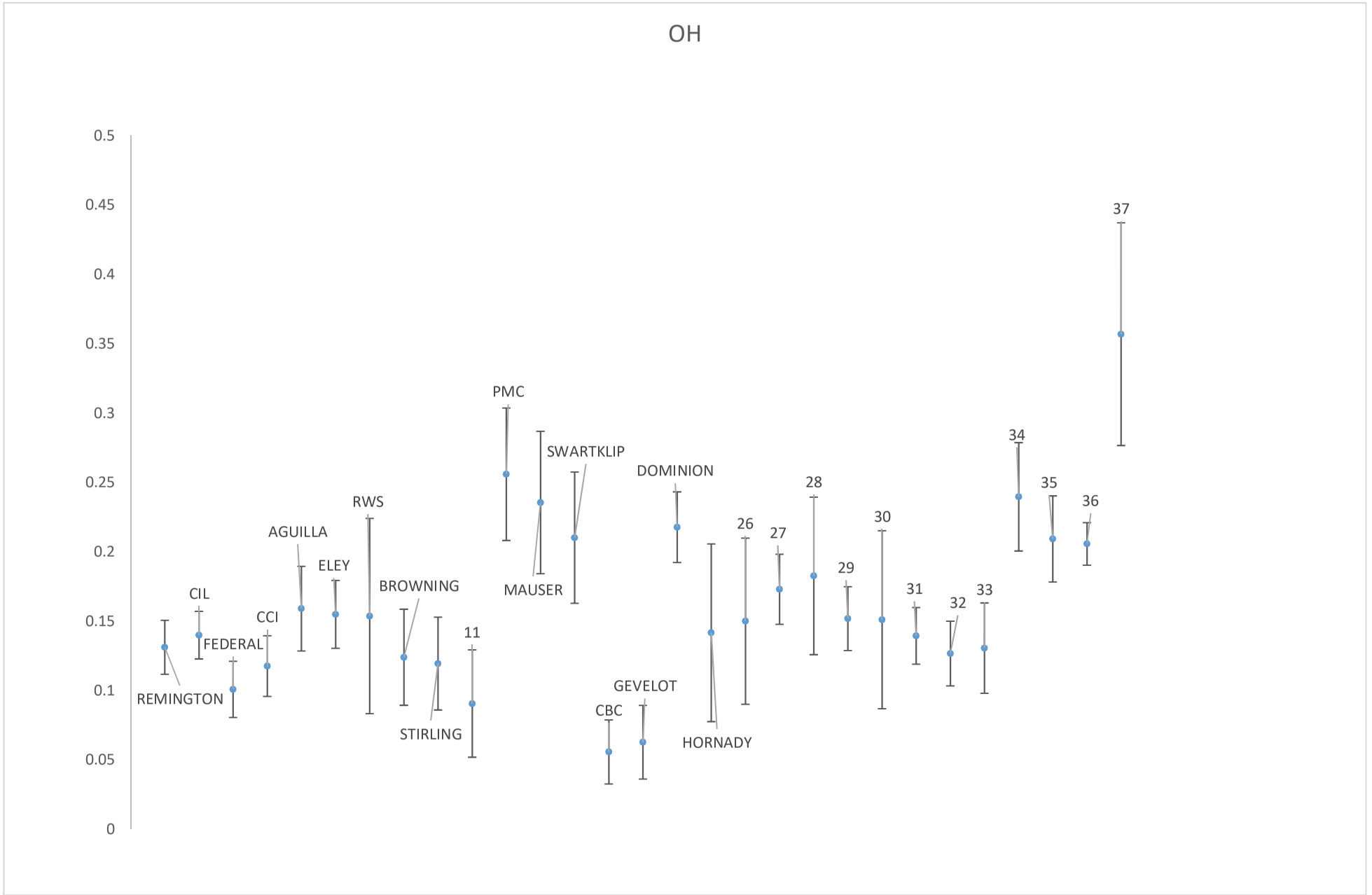
OH
0.5
0.45
0.4
0.35
0.3
0.25
0.2
0.15
0.1
0.05
0
REMINGTON
CIL
FEDERAL
CCI
AGUILLA
ELEY
RWS
BROWNING
STIRLING
11
PMC
MAUSER
SWARTKLIP
CBC
GEVELOT
DOMINION
HORNADY
26
27
28
29
30
31
32
33
34
35
36
37

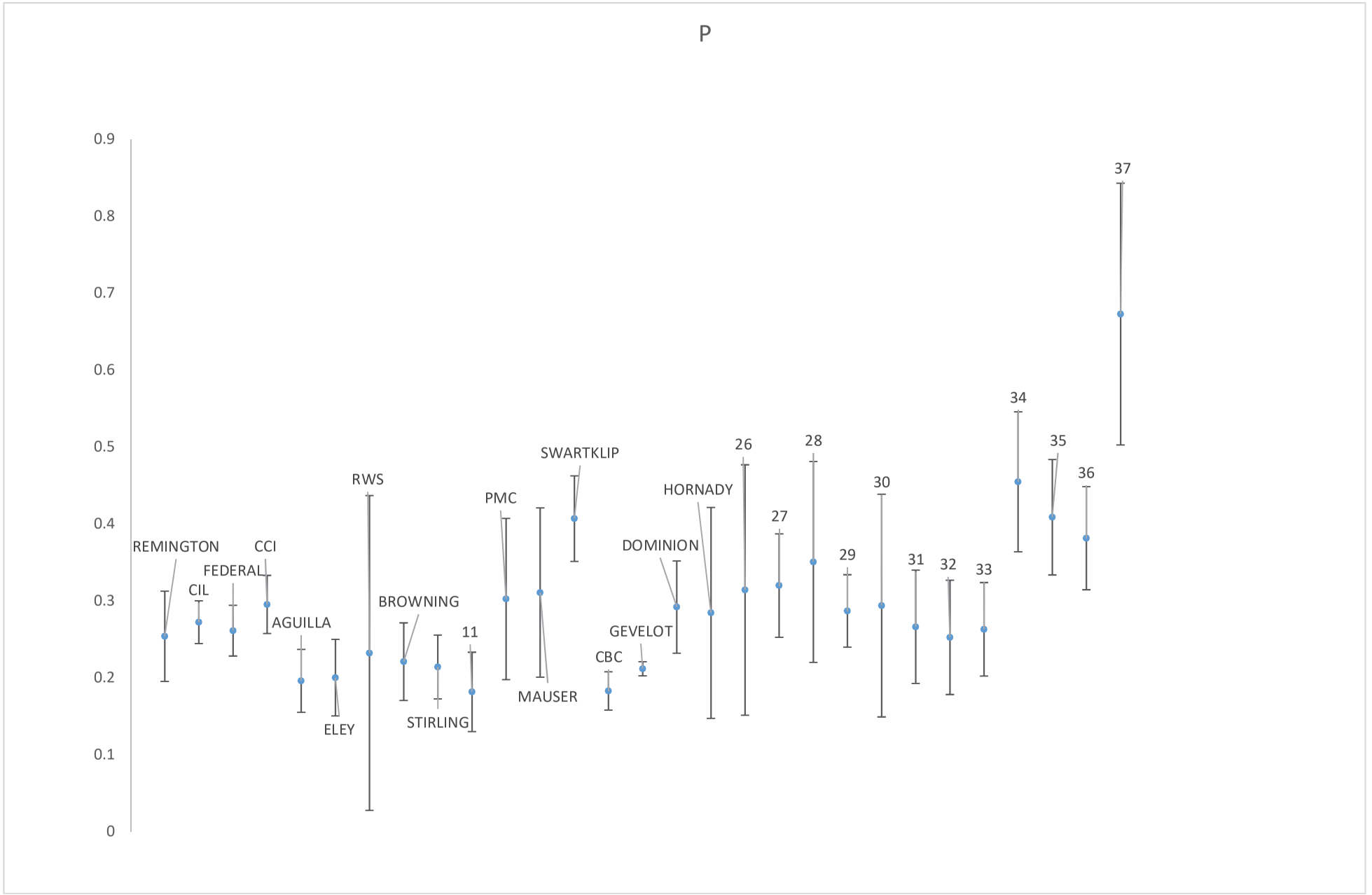
P
0.9
0.8
0.7
0.6
0.5
0.4
0.3
0.2
0.1
0
REMINGTON
CIL
FEDERAL
CCI
AGUILLA
ELEY
RWS
BROWNING
STIRLING
11
PMC
MAUSER
SWARTKLIP
CBC
GEVELOT
DOMINION
HORNADY
26
27
28
29
30
31
32
33
34
35
36
37

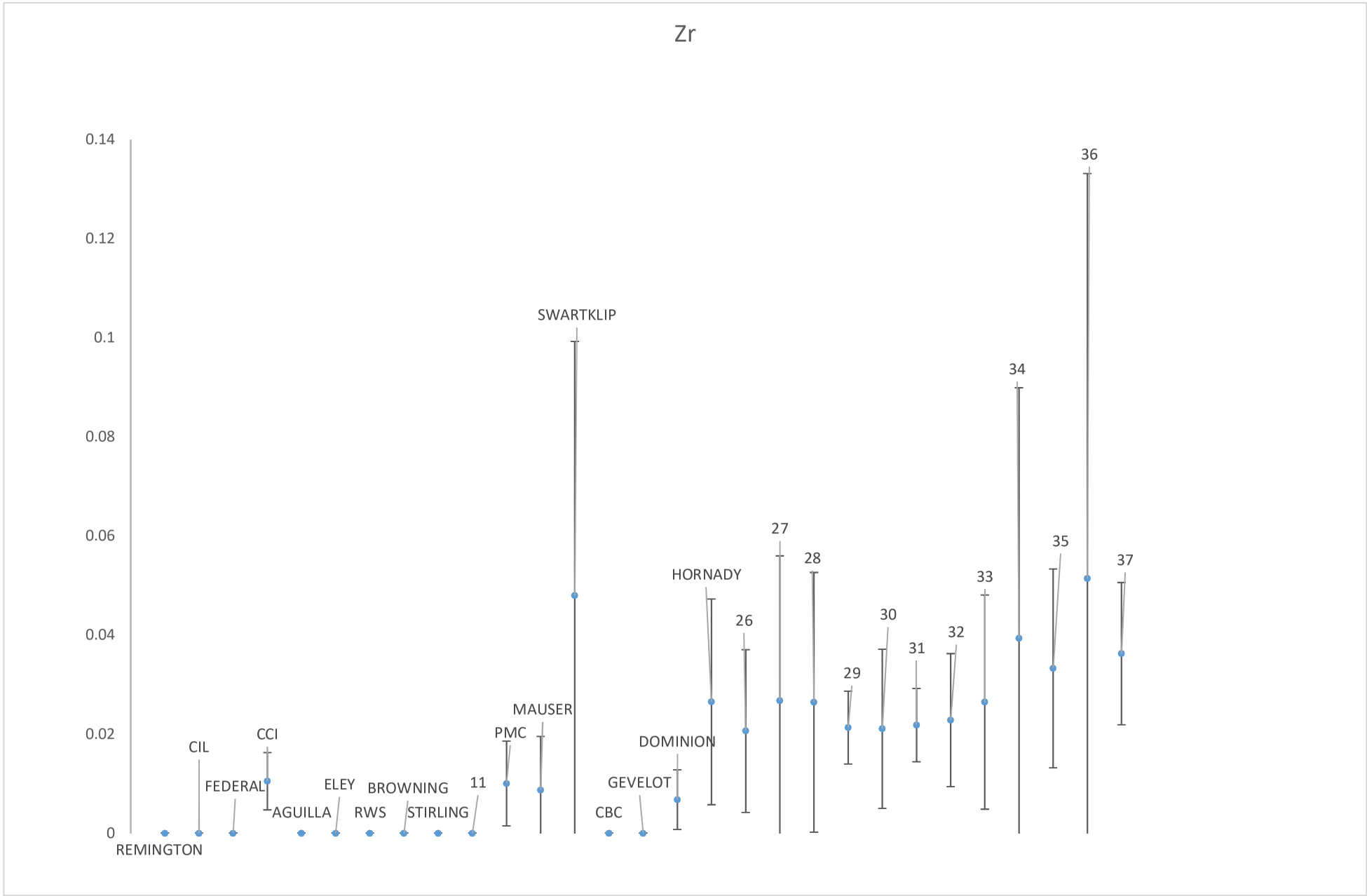
Zr
0.14
0.12
0.1
0.08
0.06
0.04
0.02
0
REMINGTON
CIL
FEDERAL
CCI
AGUILLA
ELEY
RWS
BROWNING
STIRLING
11
PMC
MAUSER
SWARTKLIP
CBC
GEVELOT
DOMINION
HORNADY
26
27
28
29
30
31
32
33
34
35
36
37

## 8.2. Plots of SEM-EDS data with Average Abundance and 99% Confidence Intervals

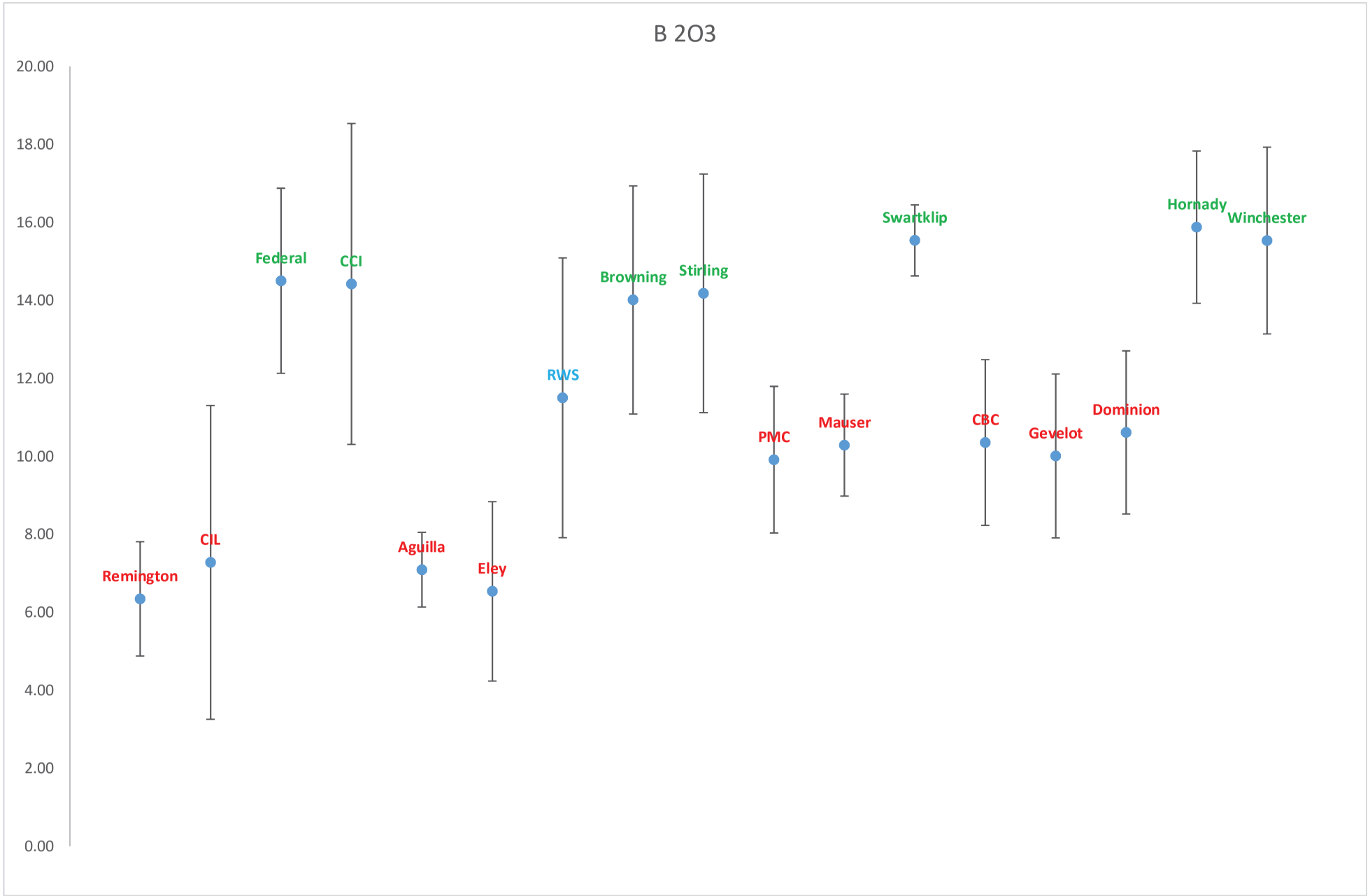
B 2O3
20.00
18.00
16.00
14.00
12.00
10.00
8.00
6.00
4.00
2.00
0.00
Remington
CIL
Federal
CCI
Aguilla
Eley
RWS
Browning
Stirling
PMC
Mauser
Swartklip
CBC
Gevelot
Dominion
Hornady
Winchester

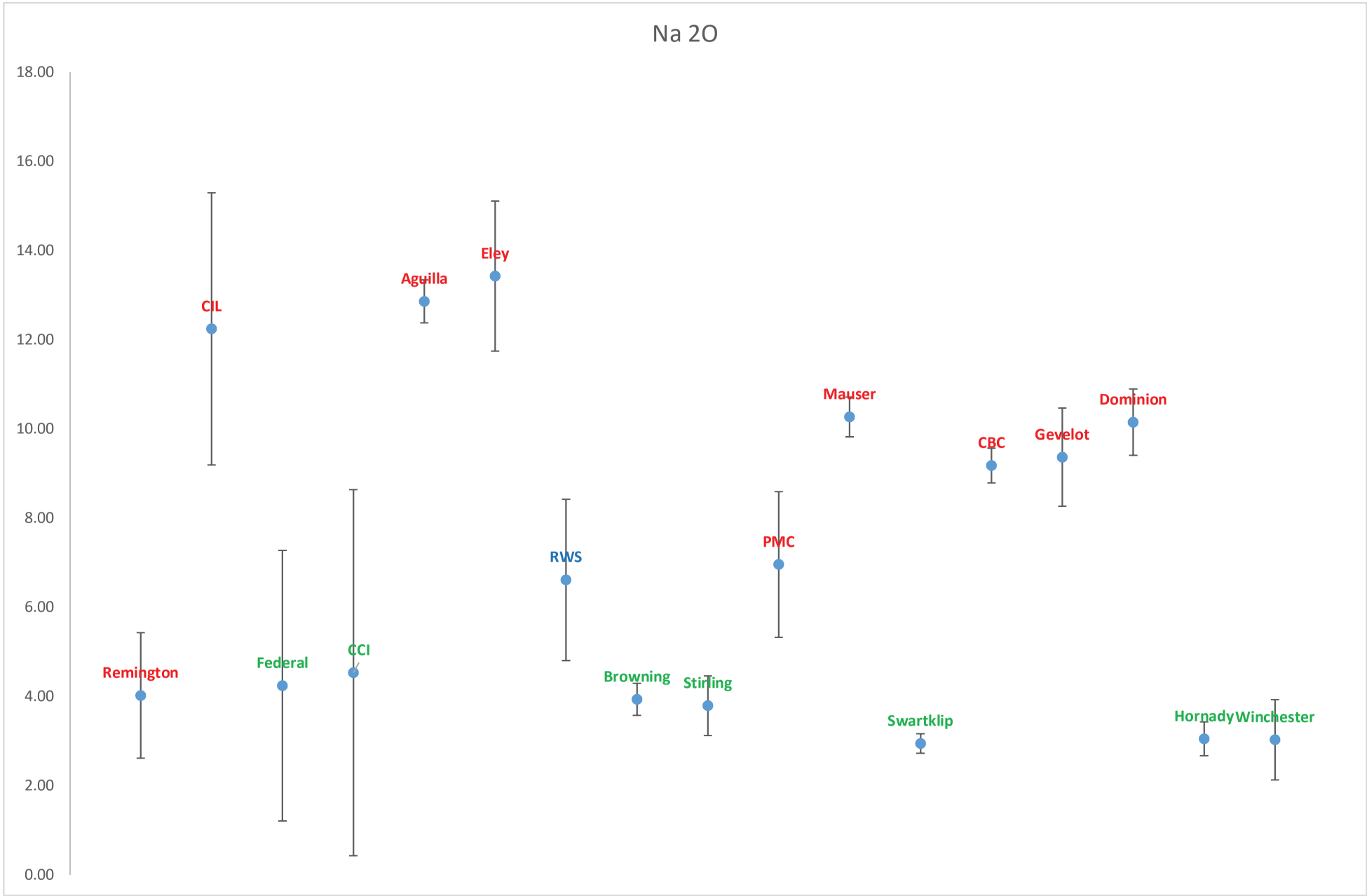
Na 2O
18.00
16.00
14.00
12.00
10.00
8.00
6.00
4.00
2.00
0.00
Remington
CIL
Federal
CCI
Aguilla
Eley
RWS
Browning
Stirling
PMC
Mauser
Swartklip
CBC
Gevelot
Dominion
Hornady
Winchester

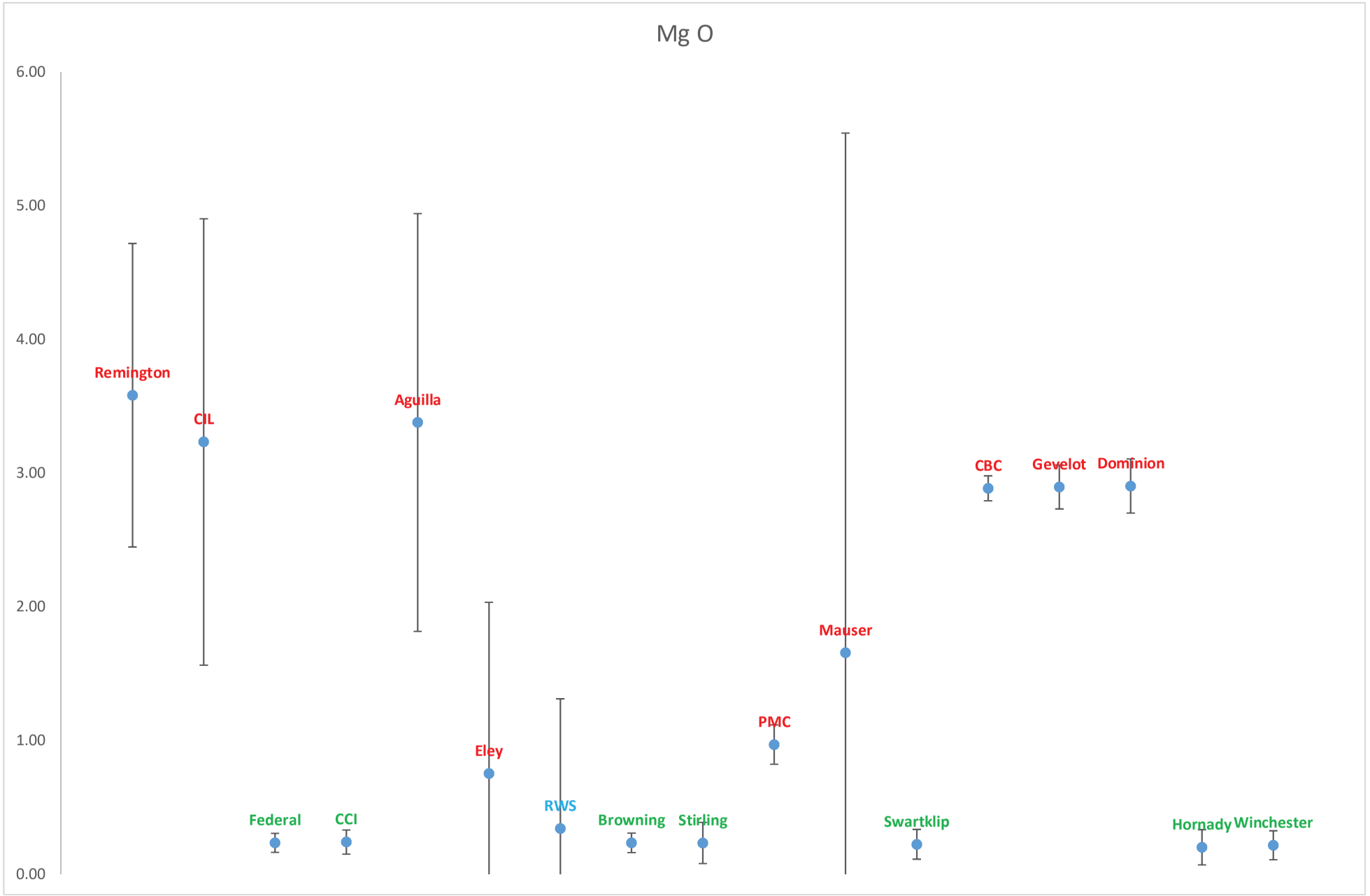
Mg O
6.00
5.00
4.00
3.00
2.00
1.00
0.00
Remington
CIL
Federal
CCI
Aguilla
Eley
RWS
Browning
Stirling
PMC
Mauser
Swartklip
CBC
Gevelot
Dominion
Hornady
Winchester

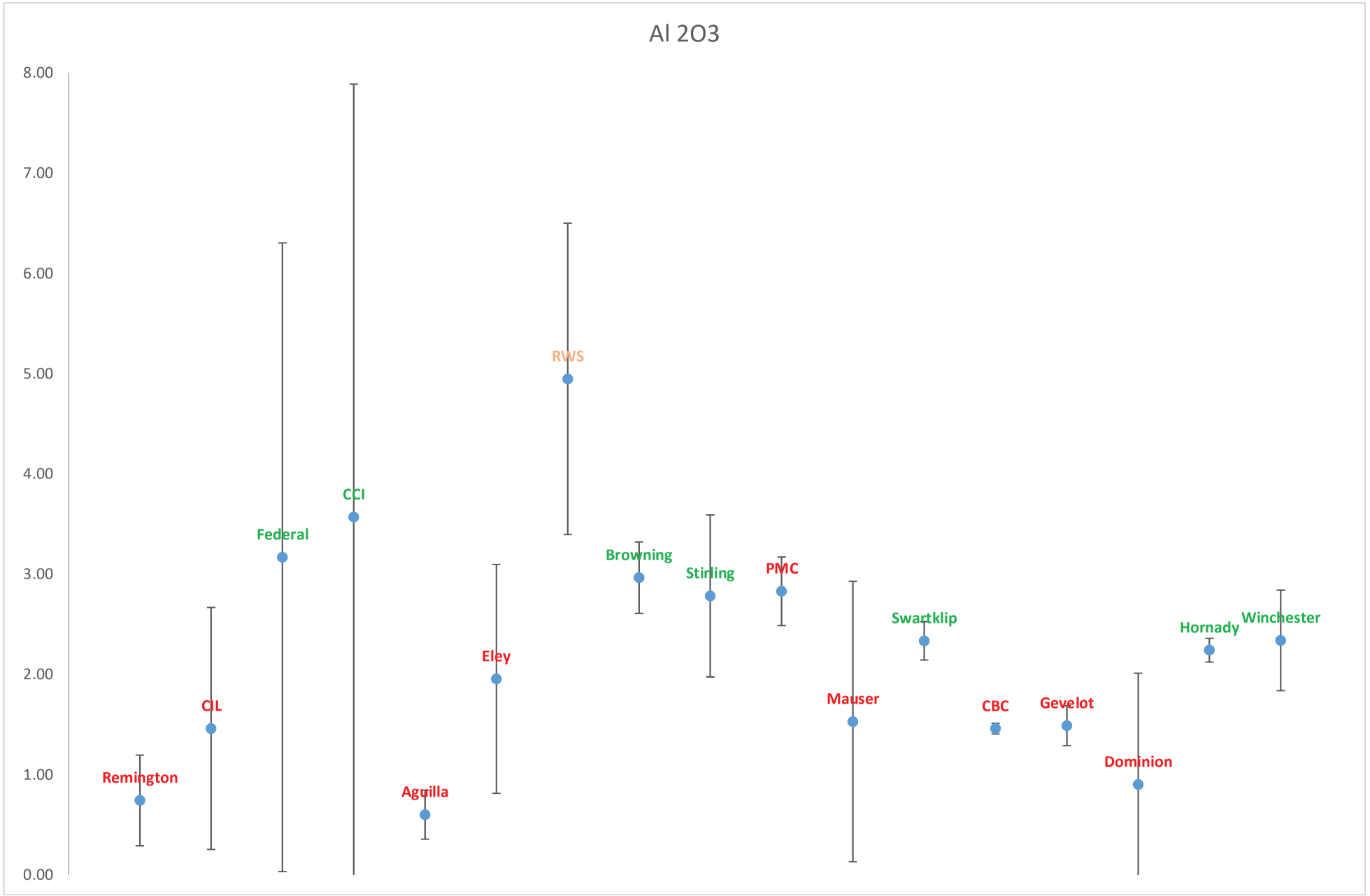
Al 2O3
8.00
7.00
6.00
5.00
4.00
3.00
2.00
1.00
0.00
Remington
CIL
Federal
CCI
Aguilla
Eley
RWS
Browning
Stirling
PMC
Mauser
Swartklip
CBC
Gevelot
Dominion
Hornady
Winchester

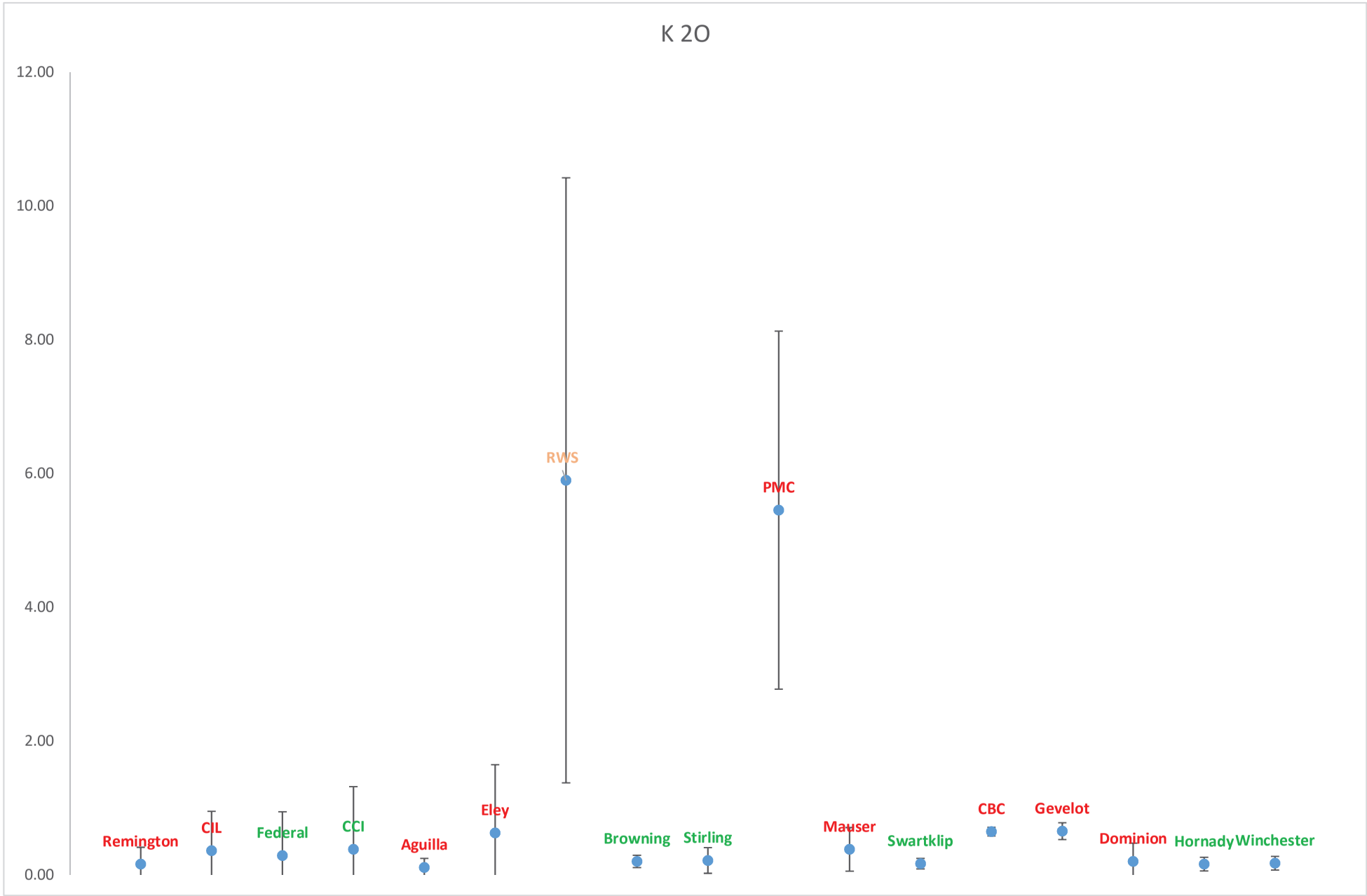
K 2O
12.00
10.00
8.00
6.00
4.00
2.00
0.00
Remington
CIL
Federal
CCI
Aguilla
Eley
RWS
Browning
Stirling
PMC
Mauser
Swartklip
CBC
Gevelot
Dominion
Hornady
Winchester

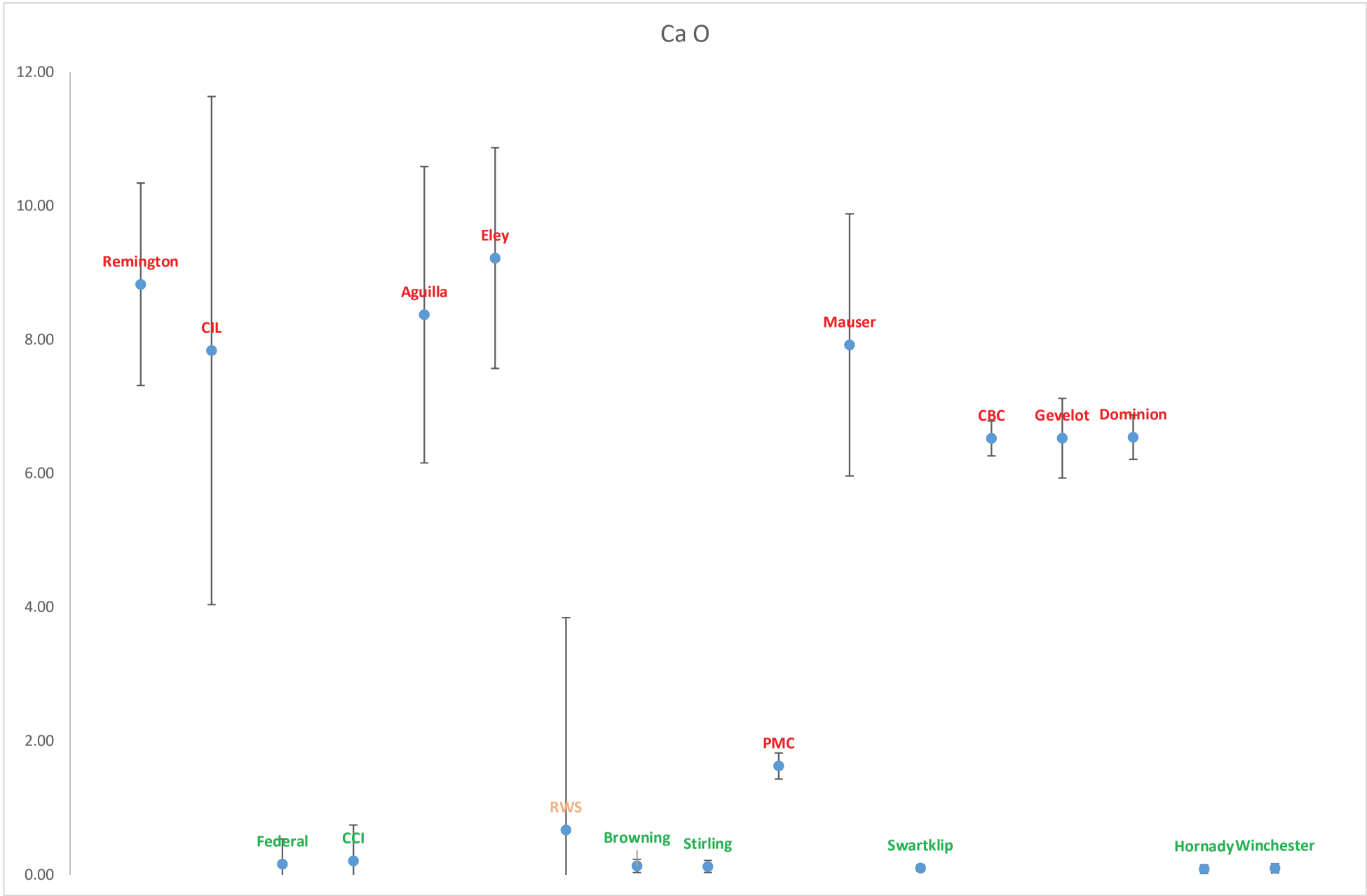
Ca O
12.00
10.00
8.00
6.00
4.00
2.00
0.00
Remington
CIL
Federal
CCI
Aguilla
Eley
RWS
Browning
Stirling
PMC
Mauser
Swartklip
CBC
Gevelot
Dominion
Hornady
Winchester

## 8.3. Particle Count Data from stubs from GSR, automotive sources, nail guns, fireworks and matches

| SAMPLE | PbBaSb | PbBa | BaSb | PbSb | BaCaSi | BaAl | Sb | Ba | | BaS | SbS | SnSb | PbSn | CuZn | Fe | Au | Ni | FeCrNi | Ca |
|---|---|---|---|---|---|---|---|---|---|---|---|---|---|---|---|---|---|---|---|
| 466B | 137 | 35 | 205 | 17 | 11 | 4 | 16 | 140 | 201 | 218 | 13 | 3 | 0 | 2 | 1297 | 9 | 88 | 24 | 331 |
| 535B | 73 | 22 | 83 | 40 | 53 | 17 | 17 | 38 | 846 | 1255 | 8 | 3 | 2 | 1498 | 1562 | 2 | 239 | 53 | 727 |
| 602B | 104 | 25 | 142 | 23 | 22 | 7 | 7 | 70 | 311 | 549 | 2 | 2 | 1 | 3053 | 1825 | 10 | 94 | 43 | 445 |
| 640B | 739 | 61 | 1076 | 203 | 25 | 9 | 45 | 477 | 253 | 1365 | 27 | 2 | 0 | 7 | 1694 | 17 | 197 | 45 | 617 |
| 733B | 710 | 43 | 544 | 356 | 2 | 8 | 17 | 155 | 384 | 209 | 15 | 0 | 3 | 855 | 552 | 4 | 164 | 18 | 0 |
| 767B | 47 | 10 | 71 | 19 | 5 | 6 | 14 | 38 | 298 | 348 | 5 | 0 | 0 | 4 | 1121 | 11 | 129 | 13 | 363 |
| 868B | 752 | 68 | 702 | 475 | 3 | 10 | 49 | 191 | 387 | 483 | 32 | 2 | 1 | 626 | 1269 | 25 | 209 | 86 | 2 |
| 955B | 917 | 86 | 993 | 422 | 7 | 10 | 35 | 217 | 409 | 289 | 45 | 1 | 0 | 0 | 305 | 28 | 131 | 49 | 3 |
| 960B | 41 | 3 | 102 | 10 | 3 | 1 | 8 | 39 | 74 | 313 | 5 | 4 | 1 | 3 | 1855 | 17 | 106 | 30 | 642 |
| **n** | **3520** | **353** | **3918** | **1565** | **131** | **72** | **208** | **1365** | **3163** | **5029** | **152** | **17** | **8** | **6048** | **11480** | **123** | **1357** | **361** | **3130** |
| **%** | **3.70** | **0.37** | **4.12** | **1.65** | **0.14** | **0.08** | **0.22** | **1.44** | **3.33** | **5.29** | **0.16** | **0.02** | **0.01** | **6.37** | **12.08** | **0.13** | **1.43** | **0.38** | **3.29** |
| **ave. per stub** | **391.11** | **39.22** | **435.33** | **173.89** | **14.56** | **8.00** | **23.11** | **151.67** | **351.44** | **558.78** | **16.89** | **1.89** | **0.89** | **672.00** | **1275.56** | **13.67** | **150.78** | **40.11** | **347.78** |

| SAMPLE | Cu | KCl | LaCe | Ti | Sn | W | Bi | Zn | Ag | Zr | Sr | NiCu | BaSn | PbTi | PbCa | CrNi | PbSbSn | AuCu | PbClBr | Hg |
|---|---|---|---|---|---|---|---|---|---|---|---|---|---|---|---|---|---|---|---|---|
| 466B | 2444 | 682 | 3 | 58 | 21 | 0 | 85 | 7 | 2 | 19 | 870 | 157 | 0 | 5 | 1 | 0 | 0 | 9 | 0 | 0 |
| 535B | 3000 | 955 | 7 | 106 | 33 | 2 | 95 | 56 | 5 | 21 | 982 | 81 | 1 | 28 | 7 | 0 | 0 | 1 | 0 | 0 |
| 602B | 3000 | 308 | 6 | 173 | 20 | 3 | 33 | 131 | 5 | 10 | 928 | 26 | 1 | 8 | 0 | 0 | 0 | 1 | 0 | 0 |
| 640B | 2979 | 419 | 11 | 72 | 31 | 0 | 50 | 12 | 3 | 20 | 430 | 185 | 0 | 2 | 0 | 0 | 0 | 3 | 0 | 0 |
| 733B | 3000 | 117 | 6 | 8 | 12 | 1 | 139 | 39 | 1 | 4 | 173 | 293 | 0 | 1 | 1 | 0 | 0 | 4 | 0 | 0 |
| 767B | 3000 | 85 | 4 | 80 | 33 | 0 | 85 | 14 | 34 | 10 | 546 | 71 | 1 | 2 | 0 | 1 | 0 | 0 | 0 | 0 |
| 868B | 3000 | 94 | 11 | 9 | 34 | 0 | 37 | 26 | 1 | 150 | 668 | 304 | 0 | 3 | 0 | 1 | 1 | 4 | 0 | 0 |
| 955B | 3000 | 31 | 7 | 22 | 16 | 3 | 123 | 1 | 4 | 10 | 259 | 288 | 0 | 1 | 1 | 1 | 2 | 2 | 0 | 0 |
| 960B | 3000 | 613 | 50 | 169 | 34 | 0 | 111 | 9 | 1 | 18 | 906 | 29 | 2 | 19 | 0 | 2 | 0 | 7 | 1 | 1 |
| **n** | **26423** | **3304** | **105** | **697** | **234** | **9** | **758** | **295** | **56** | **262** | **5762** | **1434** | **5** | **69** | **10** | **5** | **3** | **31** | **1** | **1** |
| **%** | **27.81** | **3.48** | **0.11** | **0.73** | **0.25** | **0.01** | **0.80** | **0.31** | **0.06** | **0.28** | **6.06** | **1.51** | **0.01** | **0.07** | **0.01** | **0.01** | **0.00** | **0.03** | **0.00** | **0.00** |
| **ave. per stub** | **2935.89** | **367.11** | **11.67** | **77.44** | **26.00** | **1.00** | **84.22** | **32.78** | **6.22** | **29.11** | **640.22** | **159.33** | **0.56** | **7.67** | **1.11** | **0.56** | **0.33** | **3.44** | **0.11** | **0.11** |

| SAMPLE | Unclassified | Total | Classified |
|---|---|---|---|
| 466B | 1887 | 9001 | **7114** |
| 535B | 914 | 12832 | **11918** |
| 602B | 2260 | 13648 | **11388** |
| 640B | 3446 | 14522 | **11076** |
| 733B | 47 | 7885 | **7838** |
| 767B | 1926 | 8394 | **6468** |
| 868B | 149 | 9864 | **9715** |
| 955B | 156 | 7874 | **7718** |
| 960B | 2763 | 10992 | **8229** |
| | | | |
| **n** | **13548** | **95012** | **81464** |
| **%** | **14.26** | **100.00** | **85.74** |
| **ave. per stub** | **1505.33** | **10556.89** | **9051.556** |

| BRAKE PADS | PbBaSb | PbBa | BaSb | PbSb | BaCaSi | BaAl | Sb | Ba | Pb | BaS | SbS | SnSb | PbSn | CuZn | Fe | Au | Ni | FeCrNi | Ca |
|---|---|---|---|---|---|---|---|---|---|---|---|---|---|---|---|---|---|---|---|
| **C1** | 0 | 0 | 4066 | 0 | 12 | 1 | 12 | 28 | 0 | 709 | 228 | 116 | 0 | 54 | 43 | 2 | 0 | 0 | 4 |
| **C2** | 0(5) | 566 | 102 | 2 | 315 | 7 | 14 | 198 | 5 | 2001 | 2 | 1 | 0 | 2 | 706 | 0 | 0 | 0 | 28 |
| **C8** | 0 | 0 | 0 | 0 | 0 | 1 | 0 | 1 | 0 | 13 | 0 | 0 | 0 | 2 | 10000 | 0 | 0 | 0 | 5 |
| **C12** | 0 | 0 | 5 | 0 | 76 | 0 | 0 | 9 | 0 | 918 | 10 | 0 | 0 | 0 | 437 | 0 | 0 | 0 | 9 |
| **C18** | 0 | 0 | 3592 | 0 | 7 | 1 | 23 | 48 | 0 | 1187 | 223 | 72 | 1 | 37 | 19 | 3 | 0 | 0 | 0 |
| **C21** | 0 | 0 | 793 | 0 | 497 | 19 | 2 | 113 | 0 | 2649 | 49 | 3 | 0 | 0 | 163 | 0 | 0 | 1 | 41 |
| **C24** | 0 | 0 | 438 | 0 | 33 | 0 | 87 | 690 | 0 | 727 | 1 | 20 | 0 | 100 | 1255 | 0 | 0 | 0 | 2 |
| **C38** | 0 | 0 | 376 | 0 | 21 | 4 | 66 | 1395 | 1 | 934 | 5 | 56 | 0 | 146 | 1691 | 0 | 0 | 0 | 3 |
| **C42** | 0 | 0 | 1 | 0 | 0 | 0 | 0 | 0 | 0 | 0 | 2 | 0 | 1 | 13 | 10000 | 0 | 1 | 0 | 6 |
| **C46** | 0 | 0 | 1 | 0 | 0 | 0 | 0 | 2 | 1 | 3 | 0 | 0 | 0 | 304 | 4644 | 0 | 0 | 1 | 9 |
| **C57** | 0 | 0 | 0 | 0 | 8 | 1 | 0 | 36 | 2 | 161 | 4 | 0 | 0 | 1 | 10000 | 0 | 0 | 0 | 9 |
| **C60** | 0 | 0 | 0 | 0 | 8 | 0 | 3 | 10 | 1 | 84 | 37 | 0 | 0 | 0 | 6500 | 0 | 0 | 0 | 58 |
| ***Total*** | ***0*** | ***566*** | ***9374*** | ***2*** | ***977*** | ***34*** | ***207*** | ***2530*** | ***10*** | ***9386*** | ***561*** | ***268*** | ***2*** | ***659*** | ***45458*** | ***5*** | ***1*** | ***2*** | ***174*** |
| ***ave. per stub*** | ***0*** | ***47.17*** | ***781.2*** | ***0.17*** | ***81.42*** | ***2.83*** | ***17.25*** | ***210.8*** | ***0.83*** | ***782.2*** | ***46.75*** | ***22.33*** | ***0.17*** | ***54.92*** | ***3788*** | ***0.42*** | ***0.08*** | ***0.17*** | ***14.50*** |
| ***%*** | ***0.00*** | ***0.63*** | ***10.50*** | ***0.00*** | ***1.09*** | ***0.04*** | ***0.23*** | ***2.84*** | ***0.01*** | ***10.52*** | ***0.63*** | ***0.30*** | ***0.00*** | ***0.74*** | ***50.94*** | ***0.01*** | ***0.00*** | ***0.00*** | ***0.19*** |

| BRAKE PADS | Cu | KCl | LaCe | Ti | Sn | W | Bi | Zn | Ag | Zr | Sr | NiCu | BaSn | PbTi | PbCa | CrNi | PbSbSn | AuCu | PbClBr | Hg |
|---|---|---|---|---|---|---|---|---|---|---|---|---|---|---|---|---|---|---|---|---|
| **C1** | 257 | 0 | 0 | 9 | 151 | 0 | 0 | 1 | 0 | 95 | 2 | 0 | 115 | 0 | 0 | 0 | 0 | 0 | 0 | 0 |
| **C2** | 65 | 19 | 0 | 1000 | 2 | 0 | 1 | 3 | 0 | 54 | 0 | 0 | 0 | 579 | 1 | 0 | 0 | 0 | 0 | 0 |
| **C8** | 44 | 0 | 0 | 0 | 85 | 1 | 0 | 2 | 0 | 2 | 0 | 0 | 4 | 0 | 0 | 0 | 0 | 0 | 0 | 0 |
| **C12** | 175 | 0 | 0 | 12 | 0 | 0 | 0 | 1 | 0 | 42 | 0 | 0 | 0 | 0 | 0 | 0 | 0 | 0 | 0 | 0 |
| **C18** | 344 | 0 | 0 | 13 | 242 | 0 | 0 | 0 | 0 | 90 | 0 | 0 | 166 | 0 | 0 | 0 | 0 | 0 | 0 | 0 |
| **C21** | 23 | 0 | 0 | 23 | 40 | 0 | 0 | 7 | 0 | 28 | 0 | 0 | 1000 | 0 | 0 | 0 | 0 | 0 | 0 | 0 |
| **C24** | 380 | 0 | 0 | 0 | 47 | 0 | 0 | 1 | 0 | 689 | 0 | 0 | 58 | 0 | 0 | 0 | 0 | 0 | 0 | 0 |
| **C38** | 527 | 0 | 0 | 0 | 112 | 0 | 0 | 0 | 0 | 681 | 0 | 0 | 96 | 0 | 0 | 0 | 0 | 0 | 0 | 0 |
| **C42** | 34 | 0 | 0 | 0 | 249 | 0 | 0 | 45 | 0 | 2 | 0 | 0 | 2 | 0 | 0 | 0 | 0 | 0 | 0 | 0 |
| **C46** | 577 | 0 | 0 | 1 | 81 | 0 | 32 | 9 | 0 | 1 | 0 | 0 | 0 | 0 | 0 | 0 | 0 | 0 | 0 | 0 |
| **C57** | 1 | 0 | 0 | 0 | 1 | 0 | 0 | 8 | 0 | 61 | 0 | 0 | 0 | 0 | 0 | 0 | 0 | 0 | 0 | 0 |
| **C60** | 2 | 0 | 2 | 2 | 0 | 0 | 0 | 1 | 0 | 6 | 0 | 0 | 0 | 0 | 0 | 0 | 0 | 0 | 0 | 0 |
| ***Total*** | ***2429*** | ***19*** | ***2*** | ***1060*** | ***1010*** | ***1*** | ***33*** | ***78*** | ***0*** | ***1751*** | ***2*** | ***0*** | ***1441*** | ***579*** | ***1*** | ***0*** | ***0*** | ***0*** | ***0*** | ***0*** |
| ***ave. per stub*** | ***202.4*** | ***1.58*** | ***0.17*** | ***88.33*** | ***84.17*** | ***0.08*** | ***2.75*** | ***6.50*** | ***0.00*** | ***145.9*** | ***0.17*** | ***0.00*** | ***120.1*** | ***48.25*** | ***0.08*** | ***0.00*** | ***0.00*** | ***0.00*** | ***0.00*** | ***0.00*** |
| ***%*** | ***2.72*** | ***0.02*** | ***0.00*** | ***1.19*** | ***1.13*** | ***0.00*** | ***0.04*** | ***0.09*** | ***0.00*** | ***1.96*** | ***0.00*** | ***0.00*** | ***1.61*** | ***0.65*** | ***0.00*** | ***0.00*** | ***0.00*** | ***0.00*** | ***0.00*** | ***0.00*** |

| BRAKE PADS | Unclassified | Total |
|---|---|---|
| **C1** | 872 | 6777 |
| **C2** | 1434 | 7107 |
| **C8** | 233 | 10393 |
| **C12** | 969 | 2663 |
| **C18** | 628 | 6696 |
| **C21** | 1315 | 6766 |
| **C24** | 1220 | 5748 |
| **C38** | 839 | 6953 |
| **C42** | 166 | 10522 |
| **C46** | 463 | 6129 |
| **C57** | 2104 | 12397 |
| **C60** | 375 | 7089 |
| | | |
| ***Total*** | ***10618*** | ***89240*** |
| ***ave. per stub*** | ***884.83*** | ***7436.67*** |
| ***%*** | ***11.90*** | ***100.00*** |

| SAMPLE | PbBaSb | PbBa | BaSb | PbSb | BaCaSi | BaAl | Sb | Ba | Pb | BaS | SbS | SnSb | PbSn | CuZn | Fe | Au | Ni | FeCrNi |
|---|---|---|---|---|---|---|---|---|---|---|---|---|---|---|---|---|---|---|
| **W1 Ford Laser** | 0 | 0 | 132 | 0 | 445 | 24 | 3 | 2108 | 1 | 3249 | 6 | 1 | 0 | 0 | 4799 | 0 | 0 | 0 |
| **W2 Ford Forte** | 0 | 0 | 9 | 0 | 6 | 0 | 0 | 1 | 0 | 15 | 0 | 0 | 0 | 0 | 9 | 0 | 0 | 0 |
| **W3 Mazda 3** | 0 | 0 | 0 | 0 | 34 | 1 | 0 | 538 | 0 | 141 | 0 | 0 | 0 | 0 | 4881 | 0 | 0 | 0 |
| **W4 Mitsi LX** | 0 | 0 | 14 | 0 | 37 | 0 | 0 | 2913 | 0 | 1845 | 2 | 0 | 0 | 0 | 2486 | 0 | 0 | 0 |
| **W5 Hyundai iMAX** | 0 | 0 | 2077 | 0 | 611 | 0 | 6 | 352 | 1 | 173 | 2 | 0 | 0 | 11 | 1603 | 2 | 0 | 0 |
| **W6 Toyota Hilux** | 0 | 0 | 0 | 0 | 0 | 0 | 0 | 0 | 0 | 3 | 0 | 0 | 0 | 0 | 330 | 0 | 0 | 0 |
| **W7 Nissan** | 0 | 9 | 2 | 0 | 4 | 2 | 0 | 46 | 33 | 55 | 0 | 0 | 0 | 0 | 1565 | 1 | 0 | 0 |
| **W8 BMW 318i E36** | 0 | 0 | 16 | 0 | 67 | 0 | 0 | 526 | 0 | 322 | 4 | 0 | 0 | 0 | 4275 | 0 | 0 | 0 |
| **W9 Ford Focus** | 0 | 0 | 1 | 0 | 6 | 0 | 0 | 42 | 0 | 198 | 0 | 0 | 0 | 0 | 7297 | 0 | 0 | 0 |
| **W10 Toyota Yaris** | 0 | 0 | 0 | 0 | 0 | 0 | 0 | 4 | 0 | 15 | 0 | 0 | 0 | 2 | 139 | 0 | 0 | 0 |
| **W11 Nissan Pulsar** | 0 | 13 | 288 | 0 | 618 | 15 | 4 | 679 | 20 | 2042 | 2 | 0 | 0 | 0 | 261 | 0 | 0 | 0 |
| **W12 Mazda MX5** | 0 | 0 | 1 | 0 | 1 | 0 | 0 | 25 | 0 | 92 | 2 | 0 | 0 | 0 | 2955 | 0 | 0 | 1 |
| **W13 Subaru Forrester** | 0 | 0 | 1275 | 0 | 385 | 0 | 0 | 117 | 0 | 22 | 0 | 0 | 0 | 0 | 938 | 0 | 0 | 0 |
| **W14 Mistubishi Challenger** | 0 | 0 | 2 | 0 | 0 | 0 | 0 | 12 | 2 | 37 | 0 | 0 | 0 | 1 | 10000 | 0 | 0 | 0 |
| **W15 Nissan Dualis** | 0 | 0 | 0 | 0 | 0 | 0 | 0 | 3 | 0 | 10 | 0 | 0 | 0 | 1 | 2254 | 0 | 0 | 0 |
| **W16 Kia Sorento** | 0 | 0 | 0 | 0 | 1 | 0 | 0 | 18 | 0 | 19 | 0 | 0 | 0 | 0 | 7050 | 0 | 0 | 0 |
| **W17 Ford Territory** | 0 | 0 | 7 | 0 | 90 | 1 | 3 | 2585 | 0 | 612 | 3 | 0 | 0 | 0 | 1792 | 0 | 0 | 0 |
| **W18 Peugeot .307** | 0 | 0 | 0 | 0 | 1 | 0 | 0 | 3 | 1 | 57 | 0 | 0 | 0 | 34 | 6364 | 0 | 0 | 0 |
| **W19 Subaru Forrester 2** | 0 | 1 | 3 | 0 | 41 | 0 | 2 | 478 | 0 | 242 | 3 | 0 | 0 | 0 | 2041 | 0 | 0 | 26 |
| **W20 Mercedes Benz** | 0 | 0 | 0 | 0 | 0 | 0 | 0 | 18 | 0 | 37 | 0 | 0 | 0 | 0 | 11142 | 0 | 0 | 0 |
| **W21 Hyundai Excel** | 0 | 0 | 51 | 0 | 11 | 12 | 0 | 218 | 2 | 470 | 1 | 0 | 0 | 0 | 6198 | 0 | 2 | 1 |
| **W22 Toyota Corolla** | 0 | 0 | 0 | 0 | 0 | 0 | 0 | 7 | 1 | 4 | 0 | 0 | 0 | 0 | 7429 | 0 | 0 | 0 |
| **W23 MG - Zt** | 0 | 0 | 0 | 0 | 0 | 0 | 0 | 5 | 0 | 6 | 0 | 0 | 0 | 0 | 3944 | 0 | 0 | 0 |
| **W24 Toyota Prius** | 0 | 0 | 1 | 0 | 0 | 1 | 1 | 24 | 0 | 13 | 3 | 0 | 0 | 0 | 7842 | 0 | 0 | 0 |
| | | | | | | | | | | | | | | | | | | |
| **Total** | 0 | 23 | 3879 | 0 | 2358 | 56 | 19 | 10722 | 61 | 9679 | 28 | 1 | 0 | 49 | 97594 | 3 | 2 | 28 |
| **%** | 0 | 0.016 | 2.62 | 0 | 1.59 | 0.038 | 0.013 | 7.23 | 0.041 | 6.53 | 0.019 | 0.00067 | 0 | 0.033 | 65.85 | 0.0020 | 0.0013 | 0.019 |
| **ave. per stub** | 0 | 0.96 | 161.63 | 0 | 98.25 | 2.33 | 0.79 | 446.75 | 2.54 | 403.29 | 1.17 | 0.042 | 0 | 2.04 | 4066.4 | 0.13 | 0.083 | 1.17 |

| Ca | Cu | KCl | LaCe | Ti | Sn | W | Bi | Zn | Ag | Zr | Sr | NiCu | BaSn | PbTi | PbCa | CrNi | PbSbSn | AuCu | PbClBr | Hg | Unclass. | Total |
|---|---|---|---|---|---|---|---|---|---|---|---|---|---|---|---|---|---|---|---|---|---|---|
| 1929 | 5 | 1 | 1 | 116 | 0 | 0 | 0 | 3 | 0 | 6 | 1 | 0 | 0 | 0 | 0 | 0 | 0 | 0 | 0 | 0 | 8707 | 21537 |
| 0 | 0 | 0 | 0 | 0 | 0 | 0 | 0 | 0 | 0 | 0 | 0 | 0 | 3 | 0 | 0 | 0 | 0 | 0 | 0 | 0 | 1 | 44 |
| 23 | 25 | 0 | 1 | 34 | 13 | 0 | 1 | 0 | 0 | 130 | 0 | 0 | 11 | 0 | 0 | 0 | 0 | 0 | 0 | 0 | 874 | 6707 |
| 4 | 4 | 0 | 0 | 3 | 0 | 0 | 0 | 0 | 0 | 6 | 0 | 0 | 11 | 0 | 0 | 0 | 0 | 0 | 0 | 0 | 142 | 7467 |
| 35 | 28 | 0 | 4 | 11 | 0 | 0 | 1 | 635 | 0 | 38 | 0 | 0 | 5 | 0 | 0 | 0 | 0 | 0 | 1 | 0 | 935 | 6531 |
| 0 | 0 | 0 | 0 | 0 | 0 | 0 | 0 | 0 | 0 | 1 | 0 | 0 | 0 | 0 | 0 | 0 | 0 | 0 | 0 | 0 | 11 | 345 |
| 0 | 0 | 0 | 2 | 4 | 0 | 0 | 0 | 0 | 0 | 94 | 1 | 0 | 0 | 1 | 0 | 0 | 0 | 0 | 0 | 0 | 34 | 1853 |
| 48 | 4 | 0 | 4 | 9 | 1 | 0 | 0 | 2 | 0 | 5 | 0 | 0 | 0 | 0 | 0 | 0 | 0 | 0 | 0 | 0 | 977 | 6260 |
| 53 | 4 | 0 | 1 | 19 | 4 | 0 | 0 | 12 | 0 | 15 | 0 | 0 | 36 | 0 | 0 | 0 | 0 | 0 | 0 | 0 | 183 | 7871 |
| 1 | 3 | 0 | 3 | 0 | 5 | 0 | 627 | 0 | 0 | 12 | 0 | 0 | 1 | 0 | 0 | 0 | 0 | 0 | 0 | 0 | 103 | 915 |
| 110 | 41 | 0 | 0 | 14 | 0 | 0 | 0 | 12 | 0 | 12 | 0 | 0 | 0 | 0 | 0 | 0 | 0 | 0 | 0 | 0 | 2931 | 7062 |
| 0 | 0 | 0 | 1 | 7 | 0 | 0 | 0 | 0 | 0 | 2 | 0 | 0 | 1 | 0 | 0 | 0 | 0 | 0 | 0 | 0 | 3 | 3091 |
| 0 | 49 | 0 | 0 | 0 | 0 | 0 | 0 | 0 | 0 | 14 | 0 | 0 | 0 | 0 | 0 | 0 | 0 | 0 | 0 | 0 | 278 | 3078 |
| 8 | 1 | 0 | 4 | 9 | 0 | 0 | 0 | 0 | 0 | 1 | 0 | 0 | 0 | 0 | 0 | 0 | 0 | 0 | 0 | 0 | 111 | 10188 |
| 1 | 23 | 0 | 0 | 8 | 6 | 0 | 0 | 68 | 0 | 1 | 0 | 0 | 0 | 0 | 0 | 0 | 0 | 0 | 0 | 0 | 46 | 2421 |
| 0 | 3 | 0 | 0 | 2 | 0 | 0 | 0 | 4 | 0 | 1 | 0 | 0 | 0 | 0 | 0 | 0 | 0 | 0 | 0 | 0 | 6 | 7104 |
| 10 | 11 | 0 | 0 | 17 | 2 | 0 | 0 | 0 | 0 | 175 | 0 | 0 | 20 | 0 | 0 | 0 | 0 | 0 | 0 | 0 | 1806 | 7134 |
| 9 | 27 | 0 | 2 | 3 | 20 | 0 | 0 | 0 | 0 | 0 | 0 | 0 | 1 | 0 | 0 | 0 | 0 | 0 | 0 | 0 | 40 | 6562 |
| 12 | 23 | 0 | 0 | 24 | 0 | 0 | 0 | 3 | 0 | 65 | 0 | 0 | 0 | 0 | 0 | 0 | 0 | 0 | 0 | 0 | 53 | 3017 |
| 1 | 0 | 0 | 0 | 0 | 0 | 0 | 0 | 0 | 0 | 0 | 0 | 0 | 0 | 0 | 0 | 0 | 0 | 0 | 0 | 0 | 25 | 11223 |
| 19 | 4 | 0 | 0 | 12 | 0 | 0 | 0 | 3 | 0 | 3 | 0 | 0 | 0 | 0 | 0 | 0 | 0 | 0 | 0 | 0 | 683 | 7690 |
| 4 | 0 | 0 | 0 | 0 | 0 | 0 | 0 | 0 | 0 | 4 | 0 | 0 | 0 | 0 | 0 | 0 | 0 | 0 | 0 | 0 | 517 | 7966 |
| 5 | 0 | 0 | 0 | 1 | 0 | 0 | 0 | 0 | 0 | 0 | 0 | 0 | 0 | 0 | 0 | 0 | 0 | 0 | 0 | 0 | 43 | 4004 |
| 1 | 2 | 0 | 0 | 0 | 0 | 0 | 0 | 3 | 0 | 0 | 0 | 0 | 0 | 0 | 0 | 0 | 0 | 0 | 0 | 0 | 250 | 8141 |
| | | | | | | | | | | | | | | | | | | | | | | |
| 2273 | 257 | 1 | 23 | 293 | 51 | 0 | 629 | 745 | 0 | 585 | 2 | 0 | 89 | 1 | 0 | 0 | 0 | 0 | 1 | 0 | 18759 | 1E+05 |
| 1.53 | 0.17 | 0.00067 | 0.016 | 0.20 | 0.034 | 0 | 0.42 | 0.50 | 0 | 0.39 | 0.0013 | 0 | 0.060 | 0.00067 | 0 | 0 | 0 | 0 | 0.001 | 0 | 12.66 | 100 |
| 94.71 | 10.71 | 0.042 | 0.96 | 12.21 | 2.13 | 0 | 26.21 | 31.04 | 0 | 24.38 | 0.083 | 0 | 3.71 | 0.042 | 0 | 0 | 0 | 0 | 0.042 | 0 | 781.6 | 6175.5 |

| Sample | PbBa | BaSb | PbSb | BaCaSi | BaAl | Sb | Ba | Pb | BaS | SbS | SnSb | PbSn | CuZn | Fe | Au | Ni | FeCrNi | Ca | Cu | KCl | LaCe | Ti | Sn | W | Bi |
|---|---|---|---|---|---|---|---|---|---|---|---|---|---|---|---|---|---|---|---|---|---|---|---|---|---|
| | 0 | 260 | 0 | 0 | 0 | 0 | 2 | 0 | 1 | 0 | 0 | 0 | 0 | 15 | 0 | 0 | 0 | 0 | 4 | 0 | 0 | 0 | 0 | 0 | 0 |
| R2 | 0 | 0 | 0 | 0 | 0 | 0 | 1 | 0 | 2 | 0 | 0 | 0 | 0 | 60 | 0 | 0 | 0 | 0 | 0 | 0 | 0 | 0 | 1 | 0 | 0 |
| R3 | 0 | 0 | 0 | 0 | 0 | 0 | 0 | 0 | 1 | 0 | 0 | 0 | 1 | 53 | 0 | 0 | 0 | 0 | 5 | 0 | 0 | 0 | 0 | 0 | 0 |
| Total | 0 | 260 | 0 | 0 | 0 | 0 | 3 | 0 | 4 | 0 | 0 | 0 | 1 | 128 | 0 | 0 | 0 | 0 | 9 | 0 | 0 | 0 | 1 | 0 | 0 |
| % | 0 | 59.36 | 0 | 0 | 0 | 0 | 0.68 | 0 | 0.91 | 0 | 0 | 0 | 0.23 | 29.22 | 0 | 0 | 0 | 0 | 2.05 | 0 | 0 | 0 | 0.23 | 0 | 0 |
| ave. per stub | 0 | 86.67 | 0 | 0 | 0 | 0 | 1 | 0 | 1.33 | 0 | 0 | 0 | 0.33 | 42.67 | 0 | 0 | 0 | 0 | 3 | 0 | 0 | 0 | 0.33 | 0 | 0 |

| Zn | Ag | Zr | Sr | NiCu | BaSn | PbTi | PbCa | CrNi | PbSbSn | AuCu | PbClBr | Hg | Unclassified | Total |
|---|---|---|---|---|---|---|---|---|---|---|---|---|---|---|
| 0 | 0 | 1 | 0 | 0 | 0 | 0 | 0 | 0 | 0 | 0 | 0 | 0 | 18 | 301 |
| 0 | 0 | 0 | 0 | 0 | 0 | 0 | 0 | 0 | 0 | 0 | 0 | 0 | 4 | 68 |
| 0 | 0 | 1 | 0 | 0 | 0 | 0 | 0 | 0 | 0 | 0 | 0 | 0 | 8 | 69 |
| | | | | | | | | | | | | | | |
| 0 | 0 | 2 | 0 | 0 | 0 | 0 | 0 | 0 | 0 | 0 | 0 | 0 | 30 | 438 |
| 0 | 0 | 0.46 | 0 | 0 | 0 | 0 | 0 | 0 | 0 | 0 | 0 | 0 | 6.85 | 100 |
| 0 | 0 | 0.67 | 0 | 0 | 0 | 0 | 0 | 0 | 0 | 0 | 0 | 0 | 10 | 146 |

| HANDS | PbBa | BaSb | PbSb | BaCaSi | BaAl | Sb | Ba | Pb | BaS | SbS | SnSb | PbSn | CuZn | Fe | Au | Ni | FeCrNi | Ca | Cu |
|---|---|---|---|---|---|---|---|---|---|---|---|---|---|---|---|---|---|---|---|
| H1 | 0 | 2 | 0 | 4 | 1 | 1 | 4 | 5 | 173 | 9 | 0 | 0 | 7 | 5536 | 0 | 17 | 3 | 151 | 88 |
| H2 | 0 | 17 | 0 | 34 | 7 | 3 | 23 | 5 | 464 | 10 | 0 | 0 | 31 | 8171 | 4 | 34 | 3 | 56 | 95 |
| H3 | 0 | 2 | 19 | 0 | 0 | 32 | 6 | 4 | 147 | 302 | 0 | 0 | 1 | 10000 | 0 | 1 | 2 | 1 | 44 |
| H4 | 6 | 91 | 0 | 100 | 8 | 4 | 137 | 309 | 702 | 14 | 2 | 4 | 200 | 10000 | 4 | 52 | 33 | 910 | 87 |
| H5 | 2 | 15 | 0 | 327 | 0 | 1 | 221 | 3 | 659 | 6 | 0 | 0 | 2 | 4209 | 0 | 1 | 5 | 205 | 61 |
| H6(EM) | 0 | 0 | 0 | 11 | 5 | 0 | 47 | 0 | 165 | 3 | 0 | 0 | 9 | 3609 | 0 | 16 | 8 | 92 | 276 |
| H7(AB) | 0 | 1 | 0 | 50 | 5 | 1 | 62 | 19 | 327 | 11 | 0 | 0 | 34 | 5762 | 0 | 25 | 5 | 5798 | 244 |
| H8(MECH) | 0 | 0 | 0 | 36 | 7 | 0 | 74 | 0 | 329 | 3 | 0 | 0 | 16 | 6553 | 0 | 18 | 15 | 118 | 495 |
| H9(DV) | 0 | 0 | 0 | 11 | 0 | 0 | 11 | 2 | 34 | 0 | 0 | 0 | 0 | 6448 | 0 | 3 | 0 | 11 | 1 |
| H10 (PK) Pulsar | 0 | 82 | 0 | 947 | 1 | 6 | 383 | 2 | 1205 | 8 | 0 | 0 | 6 | 564 | 0 | 1 | 0 | 191 | 74 |
| H11 (PK) Challenger | 0 | 0 | 0 | 16 | 7 | 0 | 96 | 3 | 194 | 0 | 0 | 0 | 3 | 7212 | 0 | 26 | 0 | 103 | 1 |
| ***Total*** | ***8*** | ***210*** | ***19*** | ***1536*** | ***41*** | ***48*** | ***1064*** | ***352*** | ***4399*** | ***366*** | ***2*** | ***4*** | ***309*** | ***68064*** | ***8*** | ***194*** | ***74*** | ***7636*** | ***1466*** |
| ***Freq*** | ***0.01*** | ***0.18*** | ***0.02*** | ***1.33*** | ***0.036*** | ***0.042*** | ***0.92*** | ***0.31*** | ***3.81*** | ***0.32*** | ***0.002*** | ***0.003*** | ***0.27*** | ***59.02*** | ***0.01*** | ***0.17*** | ***0.06*** | ***6.62*** | ***1.27*** |
| ***ave team stub*** | ***0.73*** | ***19.09*** | ***1.73*** | ***139.64*** | ***3.73*** | ***4.36*** | ***96.73*** | ***32.00*** | ***399.91*** | ***33.27*** | ***0.18*** | ***0.36*** | ***28.09*** | ***6187.6*** | ***0.73*** | ***17.64*** | ***6.73*** | ***694.18*** | ***133.27*** |
| HA (whippersnipper&Blank) | 0 | 1 | 0 | 2 | 0 | 0 | 4 | 24 | 39 | 0 | 0 | 0 | 7 | 254 | 43 | 75 | 1 | 0 | 4 |

| KCl | LaCe | Ti | Sn | W | Bi | Zn | Ag | Zr | Sr | NiCu | BaSn | PbTi | PbCa | CrNi | PbSbSn | AuCu | PbClBr | Hg | Unclassified | Total |
|---|---|---|---|---|---|---|---|---|---|---|---|---|---|---|---|---|---|---|---|---|
| 3 | 8 | 3 | 19 | 1 | 3 | 131 | 6 | 19 | 0 | 0 | 1 | 0 | 0 | 1 | 0 | 0 | 0 | 0 | 452 | 6648 |
| 0 | 6 | 12 | 113 | 1 | 1 | 117 | 0 | 27 | 0 | 0 | 8 | 0 | 0 | 4 | 0 | 0 | 0 | 0 | 1178 | 10424 |
| 0 | 5 | 1 | 27 | 6 | 0 | 21 | 0 | 67 | 0 | 0 | 3 | 0 | 0 | 0 | 1 | 1 | 0 | 0 | 128 | 10821 |
| 14 | 10 | 255 | 56 | 6 | 6 | 398 | 1 | 103 | 0 | 4 | 43 | 5 | 6 | 4 | 0 | 3 | 24 | 0 | 1076 | 14677 |
| 0 | 0 | 39 | 1 | 0 | 0 | 32 | 0 | 10 | 0 | 0 | 2 | 0 | 0 | 0 | 0 | 0 | 0 | 0 | 1748 | 7549 |
| 26 | 1 | 15 | 3 | 0 | 0 | 14 | 0 | 36 | 0 | 6 | 0 | 0 | 0 | 0 | 0 | 0 | 0 | 0 | 1705 | 6047 |
| 71 | 3 | 219 | 8 | 3 | 0 | 559 | 0 | 69 | 1 | 5 | 0 | 0 | 0 | 8 | 0 | 0 | 0 | 0 | 10046 | 23336 |
| 34 | 1 | 30 | 2 | 0 | 0 | 19 | 0 | 93 | 0 | 14 | 0 | 0 | 0 | 1 | 0 | 0 | 0 | 0 | 2565 | 10423 |
| 0 | 0 | 21 | 2 | 0 | 0 | 30 | 0 | 0 | 0 | 0 | 0 | 1 | 0 | 0 | 0 | 0 | 1 | 0 | 55 | 6631 |
| 1 | 3 | 33 | 2 | 0 | 0 | 207 | 0 | 5 | 0 | 0 | 0 | 0 | 0 | 0 | 0 | 0 | 0 | 0 | 4854 | 8575 |
| 27 | 2 | 51 | 0 | 0 | 0 | 99 | 0 | 29 | 0 | 0 | 1 | 0 | 0 | 0 | 0 | 0 | 0 | 0 | 2313 | 10183 |
| ***176*** | ***39*** | ***679*** | ***233*** | ***17*** | ***10*** | ***1627*** | ***7*** | ***458*** | ***1*** | ***29*** | ***58*** | ***6*** | ***6*** | ***18*** | ***1*** | ***4*** | ***25*** | ***0*** | ***26120*** | ***115314*** |
| ***0.15*** | ***0.03*** | ***0.59*** | ***0.20*** | ***0.01*** | ***0.01*** | ***1.41*** | ***0.01*** | ***0.40*** | ***0.001*** | ***0.025*** | ***0.05*** | ***0.01*** | ***0.01*** | ***0.02*** | ***0.001*** | ***0.003*** | ***0.022*** | ***0*** | ***22.65*** | ***100*** |
| ***16.00*** | ***3.55*** | ***61.73*** | ***21.18*** | ***1.55*** | ***0.91*** | ***147.91*** | ***0.64*** | ***41.64*** | ***0.09*** | ***2.64*** | ***5.27*** | ***0.55*** | ***0.55*** | ***1.64*** | ***0.09*** | ***0.36*** | ***2.27*** | ***0*** | ***2374.5*** | ***10483*** |

| | | | | | | | | | | | | | | | | | | | | |
|---|---|---|---|---|---|---|---|---|---|---|---|---|---|---|---|---|---|---|---|---|
| 4 | 1 | 2 | 14 | 1 | 2 | 11 | 5 | 5 | 0 | 0 | 0 | 0 | 0 | 2 | 0 | 16 | 0 | 0 | 69 | 586 |

| SAMPLE | PbBaSb | PbBa | BaSb | PbSb | BaCaSi | BaAl | Sb | Ba | Pb | BaS | SbS | SnSb | PbSn | CuZn | Fe | Au | Ni | FeCrNi | Ca | Cu | KCl |
|---|---|---|---|---|---|---|---|---|---|---|---|---|---|---|---|---|---|---|---|---|---|
| Redhead 1 | 0 | 0 | 1 | 0 | 0 | 0 | 0 | 1 | 0 | 1 | 0 | 0 | 0 | 0 | 10 | 0 | 0 | 0 | 26 | 0 | 695 |
| Waterproof 1 | 0 | 0 | 0 | 0 | 0 | 0 | 0 | 1 | 0 | 7 | 0 | 0 | 0 | 0 | 14 | 0 | 0 | 0 | 81 | 0 | 1473 |
| WP2 | 0 | 0 | 0 | 0 | 0 | 0 | 0 | 0 | 1 | 0 | 0 | 0 | 0 | 0 | 5 | 0 | 0 | 0 | 38 | 0 | 8961 |
| Stormproof 1 | 0 | 0 | 0 | 0 | 0 | 0 | 0 | 0 | 0 | 1 | 0 | 0 | 0 | 0 | 114 | 0 | 0 | 0 | 2 | 0 | 295 |
| Street Matches 1 | 0 | 0 | 0 | 0 | 0 | 0 | 0 | 0 | 0 | 0 | 0 | 0 | 0 | 0 | 3 | 0 | 0 | 0 | 0 | 0 | 107 |
| ***Sum of matchesdirect*** | ***0*** | ***0*** | ***1*** | ***0*** | ***0*** | ***0*** | ***0*** | ***2*** | ***1*** | ***9*** | ***0*** | ***0*** | ***0*** | ***0*** | ***146*** | ***0*** | ***0*** | ***0*** | ***147*** | ***0*** | ***11531*** |
| ***% of total Matches*** | ***0*** | ***0*** | ***0.005*** | ***0*** | ***0*** | ***0*** | ***0*** | ***0.01*** | ***0.01*** | ***0.05*** | ***0*** | ***0*** | ***0*** | ***0*** | ***0.77*** | ***0*** | ***0*** | ***0*** | ***0.78*** | ***0*** | ***60.91*** |
| ***ave per stub*** | ***0*** | ***0*** | ***0.2*** | ***0*** | ***0*** | ***0*** | ***0*** | ***0.4*** | ***0.2*** | ***1.8*** | ***0*** | ***0*** | ***0*** | ***0*** | ***29*** | ***0*** | ***0*** | ***0*** | ***29.4*** | ***0*** | ***2306.2*** |

| Hands Matches | PbBaSb | PbBa | BaSb | PbSb | BaCaSi | BaAl | Sb | Ba | Pb | BaS | SbS | SnSb | PbSn | CuZn | Fe | Au | Ni | FeCrNi | Ca | Cu | KCl |
|---|---|---|---|---|---|---|---|---|---|---|---|---|---|---|---|---|---|---|---|---|---|
| EM | 0 | 0 | 0 | 0 | 0 | 0 | 1 | 0 | 0 | 5 | 0 | 0 | 0 | 6 | 2 | 0 | 1 | 0 | 0 | 1 | 6 |
| NL | 0 | 0 | 0 | 0 | 0 | 0 | 0 | 1 | 0 | 17 | 0 | 0 | 0 | 2 | 5 | 1 | 2 | 2 | 0 | 4 | 84 |
| KS | 0 | 0 | 0 | 0 | 0 | 0 | 1 | 0 | 1 | 3 | 0 | 0 | 0 | 5 | 12 | 0 | 0 | 0 | 372 | 6 | 82 |
| ***Sum of matches hands*** | ***0*** | ***0*** | ***0*** | ***0*** | ***0*** | ***0*** | ***2*** | ***1*** | ***1*** | ***25*** | ***0*** | ***0*** | ***0*** | ***13*** | ***19*** | ***1*** | ***3*** | ***2*** | ***372*** | ***11*** | ***172*** |
| ***% of total Matches*** | ***0*** | ***0*** | ***0*** | ***0*** | ***0*** | ***0*** | ***0.27*** | ***0.13*** | ***0.13*** | ***3.34*** | ***0*** | ***0*** | ***0*** | ***1.74*** | ***2.54*** | ***0.13*** | ***0.40*** | ***0.27*** | ***49.67*** | ***1.47*** | ***22.96*** |
| ***ave per stub*** | ***0*** | ***0*** | ***0*** | ***0*** | ***0*** | ***0*** | ***0.67*** | ***0.33*** | ***0.33*** | ***8.33*** | ***0*** | ***0*** | ***0*** | ***4.33*** | ***6.33*** | ***0.33*** | ***1*** | ***0.67*** | ***124*** | ***3.67*** | ***57.33*** |

| LaCe | Ti | Sn | W | Bi | Zn | Ag | Zr | Sr | NiCu | BaSn | PbTi | PbCa | CrNi | PbSbSn | AuCu | PbClBr | Hg | TiZn | U | Unclassified | Total | classified |
|---|---|---|---|---|---|---|---|---|---|---|---|---|---|---|---|---|---|---|---|---|---|---|
| 0 | 7 | 0 | 0 | 0 | 0 | 0 | 694 | 0 | 0 | 0 | 0 | 0 | 0 | 0 | 0 | 0 | 0 | 0 | 0 | 530 | 1965 | 1435 |
| 0 | 3 | 0 | 1 | 0 | 319 | 0 | 1000 | 0 | 0 | 0 | 0 | 0 | 0 | 0 | 0 | 0 | 0 | 12 | 1 | 1084 | 3996 | 2912 |
| 0 | 1 | 0 | 0 | 0 | 892 | 0 | 6 | 0 | 0 | 0 | 0 | 0 | 0 | 0 | 0 | 0 | 0 | 11 | 0 | 1563 | 11478 | 9915 |
| 0 | 0 | 0 | 0 | 0 | 0 | 0 | 800 | 0 | 0 | 0 | 0 | 0 | 0 | 0 | 0 | 0 | 0 | 0 | 0 | 164 | 1376 | 1212 |
| 0 | 2 | 0 | 0 | 0 | 0 | 0 | 0 | 0 | 0 | 0 | 0 | 0 | 0 | 0 | 0 | 0 | 0 | 0 | 0 | 3 | 115 | 112 |
| | | | | | | | | | | | | | | | | | | | | | 0 | 0 |
| ***0*** | ***13*** | ***0*** | ***1*** | ***0*** | ***1211*** | ***0*** | ***2500*** | ***0*** | ***0*** | ***0*** | ***0*** | ***0*** | ***0*** | ***0*** | ***0*** | ***0*** | ***0*** | ***23*** | ***1*** | ***3344*** | ***18930*** | ***15586*** |
| ***0*** | ***6*** | ***0*** | ***0.01*** | ***0*** | ***6.40*** | ***0*** | ***13.21*** | ***0*** | ***0*** | ***0*** | ***0*** | ***0*** | ***0*** | ***0*** | ***0*** | ***0*** | ***0*** | ***0.12*** | ***0.01*** | ***17.67*** | ***100*** | ***82.33*** |
| ***0*** | ***16*** | ***0*** | ***0.2*** | ***0*** | ***242.2*** | ***0*** | ***500*** | ***0*** | ***0*** | ***0*** | ***0*** | ***0*** | ***0*** | ***0*** | ***0*** | ***0*** | ***0*** | ***4.6*** | ***0.2*** | ***668.8*** | ***3786*** | ***3117.2*** |

| LaCe | Ti | Sn | W | Bi | Zn | Ag | Zr | Sr | NiCu | BaSn | PbTi | PbCa | CrNi | PbSbSn | AuCu | PbClBr | Hg | Zn | U | Unclassified | Total | classified |
|---|---|---|---|---|---|---|---|---|---|---|---|---|---|---|---|---|---|---|---|---|---|---|
| 0 | 0 | 4 | 0 | 2 | 5 | 0 | 0 | 0 | 1 | 0 | 0 | 0 | 0 | 0 | 0 | 0 | 0 | 0 | 0 | 12 | 46 | |
| 0 | 0 | 3 | 0 | 0 | 1 | 0 | 0 | 0 | 7 | 0 | 0 | 0 | 0 | 0 | 0 | 0 | 0 | 0 | 0 | 14 | 143 | |
| 0 | 0 | 1 | 0 | 1 | 0 | 3 | 3 | 1 | 0 | 0 | 0 | 0 | 0 | 0 | 0 | 0 | 0 | 0 | 0 | 69 | 560 | |
| | | | | | | | | | | | | | | | | | | | | | 0 | |
| ***0*** | ***0*** | ***8*** | ***0*** | ***3*** | ***6*** | ***3*** | ***3*** | ***1*** | ***8*** | ***0*** | ***0*** | ***0*** | ***0*** | ***0*** | ***0*** | ***0*** | ***0*** | ***0*** | ***0*** | ***95*** | ***749*** | ***654*** |
| ***0*** | ***0*** | ***1.07*** | ***0*** | ***0.40*** | ***0.80*** | ***0.40*** | ***0.40*** | ***0.13*** | ***1.07*** | ***0*** | ***0*** | ***0*** | ***0*** | ***0*** | ***0*** | ***0*** | ***0*** | ***0*** | ***0*** | ***12.68*** | ***100*** | ***87.32*** |
| ***0*** | ***0*** | ***2.67*** | ***0*** | ***1*** | ***2*** | ***1*** | ***1*** | ***0.33*** | ***2.67*** | ***0*** | ***0*** | ***0*** | ***0*** | ***0*** | ***0*** | ***0*** | ***0*** | ***0*** | ***0*** | ***31.67*** | ***249.7*** | ***218*** |

| SAMPLE | PbBaSb | PbBa | BaSb | PbSb | BaCaSi | BaAl | Sb | Ba | Pb | BaS | SbS | SnSb | PbSn | CuZn | Fe |
|---|---|---|---|---|---|---|---|---|---|---|---|---|---|---|---|
| **Control & Air** | | | | | | | | | | | | | | | |
| Control--air (30 min exposure) --2016 | 0 | 0 | 0 | 0 | 0 | 0 | 0 | 0 | 0 | 3 | 0 | 0 | 0 | 0 | 23 |
| AIR -- firework show --2016 | 0 | 0 | 0 | 0 | 0 | 0 | 0 | 0 | 0 | 0 | 0 | 0 | 0 | 3 | 13 |
| ***Sum Control*** | ***0*** | ***0*** | ***0*** | ***0*** | ***0*** | ***0*** | ***0*** | ***0*** | ***0*** | ***3*** | ***0*** | ***0*** | ***0*** | ***3*** | ***36*** |
| ***% of Total Control*** | ***0*** | ***0*** | ***0*** | ***0*** | ***0*** | ***0*** | ***0*** | ***0*** | ***0*** | ***3.66*** | ***0*** | ***0*** | ***0*** | ***3.66*** | ***43.90*** |
| **Hands - observers** | | | | | | | | | | | | | | | |
| NL Hands | 0 | 0 | 0 | 0 | 2 | 0 | 1 | 17 | 3 | 52 | 0 | 7 | 0 | 29 | 411 |
| KN Hands | 0 | 0 | 0 | 0 | 2 | 1 | 0 | 3 | 1 | 70 | 0 | 2 | 0 | 26 | 282 |
| ***Sum FW HandsO*** | ***0*** | ***0*** | ***0*** | ***0*** | ***4*** | ***1*** | ***1*** | ***20*** | ***4*** | ***122*** | ***0*** | ***9*** | ***0*** | ***55*** | ***693*** |
| ***% of Total HandsO*** | ***0*** | ***0*** | ***0*** | ***0*** | ***0.06*** | ***0.02*** | ***0.02*** | ***0.31*** | ***0.06*** | ***1.88*** | ***0*** | ***0.14*** | ***0*** | ***0.85*** | ***10.70*** |
| **Hands - technicians** | | | | | | | | | | | | | | | |
| 18.12.16 -- Tech 1 | 0 | 3 | 0 | 0 | 18 | 22 | 1 | 34 | 42 | 352 | 0 | 1 | 0 | 17 | 1154 |
| 18.12.16-- Tech 2 | 0 | 9 | 1 | 0 | 23 | 16 | 3 | 85 | 256 | 520 | 1 | 0 | 6 | 3 | 1758 |
| 31.12.16 -- Tech 1 | 0 | 7 | 3 | 0 | 50 | 16 | 17 | 133 | 129 | 827 | 3 | 0 | 4 | 6 | 1520 |
| 31.12.16 -- Tech 2 | 0 | 1 | 0 | 0 | 4 | 4 | 23 | 36 | 39 | 245 | 0 | 0 | 1 | 0 | 605 |
| 31.12.16 -- Tech 3 | 0 | 1 | 0 | 0 | 18 | 8 | 2 | 41 | 116 | 354 | 0 | 0 | 6 | 1 | 474 |
| ***Sum FW HandsT*** | ***0*** | ***21*** | ***4*** | ***0*** | ***113*** | ***66*** | ***46*** | ***329*** | ***582*** | ***2298*** | ***4*** | ***1*** | ***17*** | ***27*** | ***5511*** |
| ***% of Total HandsT*** | ***0*** | ***0.08*** | ***0.01*** | ***0*** | ***0.42*** | ***0.24*** | ***0.17*** | ***1.21*** | ***2.14*** | ***8.45*** | ***0.01*** | ***0.00*** | ***0.06*** | ***0.10*** | ***20.26*** |
| ***ave per stub*** | 0 | 4.20 | 0.80 | 0 | 22.60 | 13.20 | 9.20 | 65.80 | 116.40 | 459.60 | 0.8 | 0.2 | 3.4 | 5.4 | 1102.2 |
| **Direct Sampling** | | | | | | | | | | | | | | | |
| 18.12.16 -- small tube | 0 | 0 | 0 | 0 | 0 | 2 | 0 | 0 | 2 | 25 | 0 | 0 | 0 | 2 | 170 |
| 18.12.16 -- mortar tube | 0 | 0 | 0 | 0 | 0 | 0 | 0 | 0 | 139 | 7 | 0 | 0 | 154 | 0 | 17 |
| 18.12.16-- multishot pipes | 0 | 0 | 0 | 0 | 0 | 0 | 0 | 0 | 0 | 14 | 0 | 0 | 0 | 0 | 37 |
| 31.12.16-- firework tube | 0 | 0 | 0 | 0 | 0 | 0 | 0 | 0 | 1 | 0 | 0 | 0 | 0 | 0 | 4 |
| 31.12.16-- mortar | 0 | 0 | 0 | 0 | 1 | 3 | 0 | 1 | 2 | 13 | 1 | 0 | 0 | 0 | 20 |
| 31.12.16-- mines | 0 | 3 | 2 | 0 | 2 | 5 | 0 | 209 | 3 | 243 | 0 | 0 | 0 | 0 | 136 |
| 31.12.16-- cake | 0 | 0 | 0 | 0 | 15 | 7 | 0 | 44 | 17 | 162 | 1 | 1 | 0 | 0 | 235 |
| ***Sum FW direct sample*** | ***0*** | ***3*** | ***2*** | ***0*** | ***18*** | ***17*** | ***0*** | ***254*** | ***164*** | ***464*** | ***2*** | ***1*** | ***154*** | ***2*** | ***619*** |
| ***% of Total direct sample*** | ***0*** | ***0.01*** | ***0.01*** | ***0*** | ***0.08*** | ***0.08*** | ***0*** | ***1.12*** | ***0.72*** | ***2.05*** | ***0.01*** | ***0.00*** | ***0.68*** | ***0.01*** | ***2.73*** |
| ***ave. per stub*** | 0 | 0.43 | 0.29 | 0 | 2.57 | 2.43 | 0 | 36.29 | 23.43 | 66.29 | 0.29 | 0.14 | 22.00 | 0.29 | 88.43 |

| SAMPLE | Au | Ni | FeCrNi | Ca | Cu | KCl | LaCe | Ti | Sn | W | Bi | Zn | Ag | Zr | Sr |
|---|---|---|---|---|---|---|---|---|---|---|---|---|---|---|---|
| **Control & Air** | | | | | | | | | | | | | | | |
| Control--air (30 min exposure) --2016 | 1 | 1 | 1 | 0 | 0 | 0 | 0 | 0 | 0 | 0 | 0 | 0 | 0 | 0 | 0 |
| AIR -- firework show --2016 | 0 | 1 | 0 | 4 | 1 | 7 | 0 | 0 | 0 | 0 | 0 | 0 | 0 | 0 | 0 |
| ***Sum Control*** | ***1*** | ***2*** | ***1*** | ***4*** | ***1*** | ***7*** | ***0*** | ***0*** | ***0*** | ***0*** | ***0*** | ***0*** | ***0*** | ***0*** | ***0*** |
| ***% of Total Control*** | ***1.22*** | ***2.44*** | ***1.22*** | ***4.88*** | ***1.22*** | ***8.54*** | ***0*** | ***0*** | ***0*** | ***0*** | ***0*** | ***0*** | ***0*** | ***0*** | ***0*** |
| **Hands - observers** | | | | | | | | | | | | | | | |
| NL Hands | 2 | 8 | 25 | 17 | 7 | 4501 | 5 | 55 | 5 | 1 | 23 | 1 | 24 | 7 | 1 |
| KN Hands | 1 | 43 | 4 | 80 | 29 | 118 | 2 | 22 | 14 | 0 | 6 | 8 | 74 | 5 | 0 |
| ***Sum FW HandsO*** | ***3*** | ***51*** | ***29*** | ***97*** | ***36*** | ***4619*** | ***7*** | ***77*** | ***19*** | ***1*** | ***29*** | ***9*** | ***98*** | ***12*** | ***1*** |
| ***% of Total HandsO*** | ***0.05*** | ***0.79*** | ***0.45*** | ***1.50*** | ***0.56*** | ***71.32*** | ***0.11*** | ***1.19*** | ***0.29*** | ***0.02*** | ***0.45*** | ***0.14*** | ***1.51*** | ***0.19*** | ***0.02*** |
| **Hands - technicians** | | | | | | | | | | | | | | | |
| 18.12.16 -- Tech 1 | 5 | 7 | 13 | 20 | 70 | 8010 | 8 | 116 | 7 | 17 | 6 | 3 | 15 | 31 | 89 |
| 18.12.16-- Tech 2 | 9 | 3 | 14 | 100 | 49 | 2570 | 13 | 67 | 16 | 2 | 9 | 11 | 1 | 46 | 262 |
| 31.12.16 -- Tech 1 | 8 | 32 | 71 | 31 | 161 | 69 | 41 | 47 | 32 | 1 | 32 | 6 | 1 | 65 | 315 |
| 31.12.16 -- Tech 2 | 6 | 12 | 21 | 4 | 26 | 438 | 12 | 86 | 14 | 0 | 18 | 2 | 2 | 40 | 41 |
| 31.12.16 -- Tech 3 | 1 | 7 | 22 | 0 | 62 | 43 | 20 | 5 | 16 | 1 | 6 | 0 | 0 | 33 | 78 |
| ***Sum FW HandsT*** | ***29*** | ***61*** | ***141*** | ***155*** | ***368*** | ***11130*** | ***94*** | ***321*** | ***85*** | ***21*** | ***71*** | ***22*** | ***19*** | ***215*** | ***785*** |
| ***% of Total HandsT*** | ***0.11*** | ***0.22*** | ***0.52*** | ***0.57*** | ***1.35*** | ***40.92*** | ***0.35*** | ***1.18*** | ***0.31*** | ***0.08*** | ***0.26*** | ***0.08*** | ***0.07*** | ***0.79*** | ***2.89*** |
| ***ave per stub*** | 5.8 | 12.2 | 28.2 | 31 | 73.6 | 2226 | 18.8 | 64.20 | 17.00 | 4.20 | 14.20 | 4.40 | 3.80 | 43.00 | 157.00 |
| **Direct Sampling** | | | | | | | | | | | | | | | |
| 18.12.16 -- small tube | 0 | 129 | 0 | 14 | 209 | 953 | 0 | 17 | 0 | 0 | 1 | 2 | 17 | 4 | 2 |
| 18.12.16 -- mortar tube | 0 | 0 | 0 | 1 | 1 | 137 | 0 | 0 | 30 | 0 | 0 | 0 | 0 | 2 | 1 |
| 18.12.16-- multishot pipes | 0 | 0 | 0 | 228 | 11 | 2087 | 4 | 21 | 0 | 0 | 0 | 0 | 0 | 3 | 2 |
| 31.12.16-- firework tube | 1 | 0 | 0 | 0 | 1 | 46 | 0 | 0 | 0 | 0 | 4 | 0 | 0 | 35 | 2 |
| 31.12.16-- mortar | 0 | 0 | 0 | 85 | 314 | 3670 | 0 | 1 | 0 | 0 | 0 | 0 | 0 | 2 | 3 |
| 31.12.16-- mines | 0 | 0 | 4 | 27 | 0 | 593 | 0 | 11 | 2 | 0 | 0 | 0 | 0 | 4 | 15 |
| 31.12.16-- cake | 0 | 0 | 0 | 683 | 24 | 669 | 5 | 35 | 1 | 0 | 4 | 0 | 0 | 35 | 791 |
| ***Sum FW direct sample*** | ***1*** | ***129*** | ***4*** | ***1038*** | ***560*** | ***8155*** | ***9*** | ***85*** | ***33*** | ***0*** | ***9*** | ***2*** | ***17*** | ***85*** | ***816*** |
| ***% of Total direct sample*** | ***0.00*** | ***0.57*** | ***0.02*** | ***4.58*** | ***2.47*** | ***35.98*** | ***0.04*** | ***0.38*** | ***0.15*** | ***0.00*** | ***0.04*** | ***0.01*** | ***0.08*** | ***0.38*** | ***3.60*** |
| ***ave. per stub*** | 0.14 | 18.43 | 0.57 | 148.29 | 80.00 | 1165.0 | 1.29 | 12.14 | 4.71 | 0 | 1.29 | 0.29 | 2.43 | 12.14 | 116.57 |

| SAMPLE | NiCu | BaSn | PbTi | PbCa | CrNi | PbSbSn | AuCu | PbClBr | Hg | Y | Unclassified | Total | Classified |
|---|---|---|---|---|---|---|---|---|---|---|---|---|---|
| **Control & Air** | | | | | | | | | | | | | |
| Control--air (30 min exposure) --2016 | 0 | 0 | 0 | 0 | 0 | 0 | 0 | 0 | 0 | 0 | 9 | 38 | ***29*** |
| AIR -- firework show --2016 | 0 | 0 | 0 | 0 | 0 | 0 | 0 | 0 | 0 | 0 | 15 | 44 | ***29*** |
| ***Sum Control*** | ***0*** | ***0*** | ***0*** | ***0*** | ***0*** | ***0*** | ***0*** | ***0*** | ***0*** | ***0*** | ***24*** | ***82*** | ***58*** |
| ***% of Total Control*** | ***0*** | ***0*** | ***0*** | ***0*** | ***0*** | ***0*** | ***0*** | ***0*** | ***0*** | ***0*** | ***29.27*** | ***100*** | ***70.73171 U*** |
| **Hands - observers** | | | | | | | | | | | | 0 | ***0*** |
| NL Hands | 0 | 0 | 0 | 0 | 0 | 0 | 0 | 0 | 0 | 0 | 357 | 5561 | ***5204*** |
| KN Hands | 11 | 0 | 0 | 0 | 0 | 0 | 0 | 0 | 0 | 0 | 111 | 915 | ***804*** |
| ***Sum FW HandsO*** | ***11*** | ***0*** | ***0*** | ***0*** | ***0*** | ***0*** | ***0*** | ***0*** | ***0*** | ***0*** | ***468*** | ***6476*** | ***6008*** |
| ***% of Total HandsO*** | ***0.17*** | ***0*** | ***0*** | ***0*** | ***0*** | ***0*** | ***0*** | ***0*** | ***0*** | ***0*** | ***7.23*** | ***100*** | ***92.77332 U*** |
| **Hands - technicians** | | | | | | | | | | | | 0 | ***0*** |
| 18.12.16 -- Tech 1 | 0 | 0 | 0 | 3 | 1 | 1 | 15 | 0 | 0 | 2 | 3179 | 13262 | ***10083*** |
| 18.12.16-- Tech 2 | 1 | 0 | 2 | 1 | 1 | 0 | 3 | 0 | 0 | 3 | 693 | 6557 | ***5864*** |
| 31.12.16 -- Tech 1 | 17 | 0 | 3 | 0 | 2 | 0 | 28 | 0 | 0 | 6 | 378 | 4064 | ***3686*** |
| 31.12.16 -- Tech 2 | 4 | 0 | 0 | 1 | 0 | 0 | 7 | 0 | 0 | 2 | 247 | 1941 | ***1694*** |
| 31.12.16 -- Tech 3 | 1 | 0 | 0 | 0 | 0 | 0 | 2 | 0 | 0 | 2 | 57 | 1377 | ***1320*** |
| ***Sum FW HandsT*** | ***23*** | ***0*** | ***5*** | ***5*** | ***4*** | ***1*** | ***55*** | ***0*** | ***0*** | ***15*** | ***4554*** | ***27201*** | ***22647*** |
| ***% of Total HandsT*** | ***0.08*** | ***0*** | ***0.018*** | ***0.018*** | ***0.015*** | ***0.004*** | ***0.20*** | ***0*** | ***0*** | ***0.055*** | ***16.74*** | ***100*** | ***83.25797*** |
| ***ave per stub*** | 4.60 | 0 | 1.00 | 1.00 | 0.80 | 0.20 | 11 | 0 | 0 | 3 | 910.8 | 5440.2 U | ***4529.4 U*** |
| **Direct Sampling** | | | | | | | | | | | | 0 | ***0*** |
| 18.12.16 -- small tube | 0 | 0 | 0 | 1 | 0 | 0 | 0 | 0 | 0 | 2 | 534 | 2086 | ***1552*** |
| 18.12.16 -- mortar tube | 0 | 0 | 0 | 0 | 0 | 0 | 0 | 0 | 0 | 0 | 373 | 862 | ***489*** |
| 18.12.16-- multishot pipes | 0 | 0 | 0 | 0 | 0 | 0 | 0 | 0 | 0 | 0 | 1320 | 3727 | ***2407*** |
| 31.12.16-- firework tube | 0 | 0 | 0 | 0 | 0 | 0 | 0 | 0 | 0 | 0 | 90 | 184 | ***94*** |
| 31.12.16-- mortar | 0 | 0 | 0 | 0 | 0 | 0 | 0 | 0 | 0 | 0 | 948 | 5064 | ***4116*** |
| 31.12.16-- mines | 0 | 0 | 0 | 0 | 0 | 0 | 0 | 0 | 0 | 1 | 4668 | 5928 | ***1260*** |
| 31.12.16-- cake | 0 | 0 | 0 | 0 | 0 | 0 | 0 | 0 | 0 | 4 | 2082 | 4815 | ***2733*** |
| ***Sum FW direct sample*** | ***0*** | ***0*** | ***0*** | ***1*** | ***0*** | ***0*** | ***0*** | ***0*** | ***0*** | ***7*** | ***10015*** | ***22666*** | ***12651*** |
| ***% of Total direct sample*** | ***0*** | ***0*** | ***0*** | ***0.00*** | ***0*** | ***0*** | ***0*** | ***0*** | ***0*** | ***0.03*** | ***44.19*** | ***100.00*** | ***55.81488*** |
| ***ave. per stub*** | 0 | 0 | 0 | 0.14 | 0 | 0 | 0 | 0 | 0 | 1.00 | 1430.7 | 3238.0 | ***1807.286*** |

| SAMPLE | PbBaSb | PbBa | BaSb | PbSb | BaCaSi | BaAl | Sb | Ba | Pb | BaS | SbS | SnSb | PbSn | CuZn | Fe |
|---|---|---|---|---|---|---|---|---|---|---|---|---|---|---|---|
| **Surfaces** | | | | | | | | | | | | | | | |
| Surface 1 --2016 | 0 | 1 | 9 | 0 | 10 | 1 | 20 | 61 | 10 | 92 | 8 | 16 | 0 | 1 | 4937 |
| Surface 2 -- 2016 | 0 | 1 | 0 | 0 | 51 | 5 | 0 | 48 | 51 | 112 | 2 | 0 | 0 | 1 | 7155 |
| 18.12.16-- bench 3m | 0 | 0 | 0 | 0 | 0 | 0 | 0 | 0 | 3 | 10 | 0 | 0 | 0 | 0 | 28 |
| 18.12.16-- metal casing | 0 | 2 | 0 | 1 | 7 | 19 | 1 | 55 | 60 | 118 | 0 | 0 | 0 | 0 | 750 |
| 18.12.16-- pelican case | 0 | 1 | 0 | 0 | 6 | 0 | 0 | 133 | 3 | 108 | 0 | 0 | 0 | 0 | 81 |
| 31.12.16-- railing 1m | 0 | 0 | 0 | 0 | 1 | 2 | 0 | 12 | 1 | 9 | 0 | 0 | 0 | 1 | 23 |
| ***Sum FW Surfaces*** | ***0*** | ***5*** | ***9*** | ***1*** | ***75*** | ***27*** | ***21*** | ***309*** | ***128*** | ***449*** | ***10*** | ***16*** | ***0*** | ***3*** | ***12974*** |
| ***% of Total Surfaces*** | ***0*** | ***0.01*** | ***0.02*** | ***0.002*** | ***0.16*** | ***0.06*** | ***0.05*** | ***0.68*** | ***0.28*** | ***0.99*** | ***0.02*** | ***0.04*** | ***0*** | ***0.01*** | ***28.53*** |
| ***ave. per stub*** | 0 | 0.833 | 1.5 | 0.167 | 12.5 | 4.5 | 3.5 | 51.5 | 21.33 | 74.83 | 1.67 | 2.67 | 0 | 0.5 | 2162.3 |
| **Hands sec transfer from technician** | 0 | 6 | 1 | 0 | 4 | 5 | 3 | 18 | 45 | 290 | 0 | 0 | 0 | 35 | 797 |
| 18.12.16-- sec transfer to Nick | | | | | | | | | | | | | | | |

| SAMPLE | Au | Ni | FeCrNi | Ca | Cu | KCl | LaCe | Ti | Sn | W | Bi | Zn | Ag | Zr | Sr |
|---|---|---|---|---|---|---|---|---|---|---|---|---|---|---|---|
| **Surfaces** | | | | | | | | | | | | | | | |
| Surface 1 --2016 | 2 | 5 | 4 | 871 | 29 | 0 | 14 | 1000 | 0 | 0 | 5 | 77 | 14 | 63 | 3 |
| Surface 2 -- 2016 | 0 | 1 | 1 | 3854 | 14 | 0 | 36 | 1000 | 2 | 0 | 5 | 622 | 1 | 182 | 8 |
| 18.12.16-- bench 3m | 0 | 0 | 1 | 80 | 27 | 1 | 0 | 386 | 1 | 0 | 1 | 0 | 0 | 14 | 0 |
| 18.12.16-- metal casing | 0 | 0 | 1 | 49 | 25 | 462 | 3 | 60 | 2 | 0 | 1 | 22 | 0 | 18 | 15 |
| 18.12.16-- pelican case | 0 | 0 | 0 | 9 | 29 | 280 | 0 | 5 | 0 | 0 | 0 | 6 | 0 | 5 | 125 |
| 31.12.16-- railing 1m | 0 | 0 | 0 | 47 | 83 | 1078 | 0 | 3 | 1 | 0 | 0 | 1 | 0 | 6 | 1000 |
| ***Sum FW Surfaces*** | ***2*** | ***6*** | ***7*** | ***4910*** | ***207*** | ***1821*** | ***53*** | ***2454*** | ***6*** | ***0*** | ***12*** | ***728*** | ***15*** | ***288*** | ***1151*** |
| ***% of Total Surfaces*** | ***0.004*** | ***0.01*** | ***0.02*** | ***10.80*** | ***0.46*** | ***4.01*** | ***0.12*** | ***5.40*** | ***0.01*** | ***0*** | ***0.03*** | ***1.60*** | ***0.03*** | ***0.63*** | ***2.53*** |
| ***ave. per stub*** | 0.33 | 1 | 1.17 | 818.3 | 34.5 | 303.5 | 8.83 | 409 | 1 | 0 | 2 | 121.3 | 2.5 | 48 | 191.8 |
| **Hands sec transfer from technician** | 6 | 6 | 28 | 103 | 40 | 157 | 11 | 25 | 14 | 3 | 16 | 0 | 126 | 31 | 51 |
| 18.12.16-- sec transfer to Nick | | | | | | | | | | | | | | | |

| SAMPLE | NiCu | BaSn | PbTi | PbCa | CrNi | PbSbSn | AuCu | PbClBr | Hg | Y | Unclassified | Total | Classified |
|---|---|---|---|---|---|---|---|---|---|---|---|---|---|
| **Surfaces** | | | | | | | | | | | | | ***0*** |
| Surface 1 --2016 | 0 | 3 | 1 | 0 | 0 | 0 | 0 | 0 | 0 | 0 | 2382 | 9639 | ***7257*** |
| Surface 2 -- 2016 | 0 | 0 | 3 | 4 | 0 | 0 | 0 | 0 | 0 | 0 | 7763 | 20922 | ***13159*** |
| 18.12.16-- bench 3m | 0 | 0 | 0 | 0 | 0 | 0 | 0 | 0 | 0 | 0 | 1796 | 2348 | ***552*** |
| 18.12.16-- metal casing | 0 | 0 | 2 | 0 | 0 | 0 | 0 | 0 | 0 | 1 | 3120 | 4794 | ***1674*** |
| 18.12.16-- pelican case | 0 | 0 | 0 | 0 | 0 | 0 | 0 | 0 | 0 | 0 | 1540 | 2331 | ***791*** |
| 31.12.16-- railing 1m | 0 | 0 | 0 | 0 | 0 | 0 | 0 | 0 | 0 | 0 | 3166 | 5434 | ***2268*** |
| | | | | | | | | | | | | | ***0*** |
| ***Sum FW Surfaces*** | ***0*** | ***3*** | ***6*** | ***4*** | ***0*** | ***0*** | ***0*** | ***0*** | ***0*** | ***1*** | ***19767*** | ***45468*** | ***25701*** |
| ***% of Total Surfaces*** | ***0*** | ***0.01*** | ***0.01*** | ***0.01*** | ***0*** | ***0*** | ***0*** | ***0*** | ***0*** | ***0.00*** | ***43.47*** | ***100*** | ***56.52547*** |
| ***ave. per stub*** | 0 | 0.5 | 1 | 0.67 | 0 | 0 | 0 | 0 | 0 | 0.17 | 3294.5 | 7578 | ***4283.5*** |
| | | | | | | | | | | | | 0 | ***0*** |
| **Hands sec transfer from technician** | 9 | 1 | 3 | 0 | 0 | 0 | 0 | 0 | 0 | 4 | 291 | 2129 | ***1838*** |
| 18.12.16-- sec transfer to Nick | | | | | | | | | | | | | ***0*** |

**Particle Count Data from stubs from Nail Gun Cartridges**

| SAMPLE | PbBaSb | PbBa | BaSb | PbSb | BaCaSi | BaAl | Sb | Ba | Pb | BaS | SbS | SnSb | PbSn | CuZn | Fe | Au | Ni | FeCrNi | Ca | Cu | KCl | LaCe |
|---|---|---|---|---|---|---|---|---|---|---|---|---|---|---|---|---|---|---|---|---|---|---|
| ***HANDS -- USERS*** | | | | | | | | | | | | | | | | | | | | | | |
| KS HANDS YELLOW | 0 | 1607 | 0 | 0 | 736 | 6 | 0 | 601 | 293 | 13 | 0 | 0 | 0 | 0 | 155 | 0 | 1 | 1 | 155 | 2 | 61 | 0 |
| NL HANDS YELLOW | 0 | 1367 | 0 | 0 | 511 | 2 | 0 | 330 | 192 | 6 | 0 | 0 | 0 | 0 | 87 | 0 | 0 | 0 | 74 | 2 | 4 | 0 |
| VOL#1 YELLOW 10SHOTS | 0 | 1335 | 0 | 0 | 554 | 3 | 0 | 651 | 150 | 18 | 0 | 0 | 0 | 2 | 128 | 0 | 1 | 1 | 121 | 3 | 32 | 0 |
| VOL#2 YELLOW 10SHOTS | 0 | 1160 | 0 | 0 | 283 | 3 | 0 | 600 | 91 | 31 | 0 | 0 | 0 | 2 | 123 | 0 | 0 | 2 | 66 | 1 | 208 | 1 |
| VOL#3 YELLOW 9SHOTS | 0 | 1029 | 0 | 0 | 156 | 0 | 0 | 321 | 350 | 25 | 0 | 0 | 0 | 18 | 99 | 0 | 1 | 1 | 95 | 16 | 13 | 0 |
| VOL#4 YELLOW 10SHOTS | 0 | 1495 | 1 | 0 | 371 | 0 | 0 | 565 | 152 | 57 | 0 | 0 | 0 | 7 | 192 | 1 | 2 | 3 | 330 | 7 | 45 | 4 |
| VOL#5 YELLOW 10SHOTS | 0 | 708 | 0 | 0 | 120 | 0 | 0 | 216 | 93 | 30 | 0 | 0 | 0 | 14 | 88 | 3 | 6 | 4 | 44 | 1 | 45 | 1 |
| VOL#6 YELLOW 10SHOTS | 1 | 1522 | 0 | 0 | 124 | 2 | 1 | 228 | 172 | 15 | 0 | 0 | 0 | 14 | 249 | 6 | 8 | 66 | 25 | 109 | 5 | 0 |
| VOL#7 YELLOW 10SHOTS | 0 | 2183 | 0 | 0 | 182 | 0 | 0 | 466 | 272 | 15 | 0 | 0 | 0 | 0 | 96 | 11 | 4 | 4 | 124 | 24 | 146 | 1 |
| VOL#8 YELLOW 10SHOTS | 0 | 1746 | 0 | 0 | 185 | 2 | 0 | 457 | 210 | 43 | 0 | 0 | 0 | 18 | 327 | 1 | 15 | 6 | 182 | 19 | 563 | 1 |
| VOL#9 YELLOW 10SHOTS | 0 | 2402 | 0 | 0 | 247 | 4 | 0 | 587 | 489 | 12 | 0 | 0 | 0 | 15 | 106 | 2 | 5 | 9 | 59 | 26 | 83 | 0 |
| VOL#10 YELLOW 10SHOTS | 0 | 2603 | 0 | 1 | 281 | 2 | 0 | 529 | 472 | 18 | 0 | 0 | 0 | 17 | 95 | 1 | 0 | 7 | 44 | 14 | 27 | 0 |
| VOL #11 RED 10SHOTS | 0 | 1813 | 0 | 0 | 142 | 1 | 0 | 304 | 371 | 12 | 0 | 0 | 1 | 6 | 67 | 0 | 5 | 4 | 8 | 4 | 81 | 1 |
| VOL#11 RED 10SHOTS | 0 | 200 | 0 | 0 | 34 | 0 | 0 | 38 | 37 | 6 | 0 | 0 | 0 | 1 | 2 | 0 | 0 | 0 | 5 | 1 | 16 | 0 |
| ***Sum Hands*** | ***1*** | ***21170*** | ***1*** | ***1*** | ***3926*** | ***25*** | ***1*** | ***5893*** | ***3344*** | ***301*** | ***0*** | ***0*** | ***1*** | ***114*** | ***1814*** | ***25*** | ***48*** | ***108*** | ***1332*** | ***229*** | ***1329*** | ***9*** |
| ***Average per stub*** | ***0.07*** | ***1512*** | ***0.07*** | ***0.07*** | ***280.4*** | ***1.79*** | ***0.07*** | ***420.9*** | ***238.9*** | ***21.5*** | ***0.00*** | ***0.00*** | ***0.07*** | ***8.14*** | ***129.6*** | ***1.79*** | ***3.43*** | ***7.71*** | ***95.14*** | ***16.36*** | ***94.93*** | ***0.64*** |
| ***% of Total Hands*** | ***0.002*** | ***38.50*** | ***0.00*** | ***0.00*** | ***7.14*** | ***0.05*** | ***0.00*** | ***10.72*** | ***6.08*** | ***0.55*** | ***0.00*** | ***0.00*** | ***0.00*** | ***0.21*** | ***3.30*** | ***0.05*** | ***0.09*** | ***0.20*** | ***2.42*** | ***0.42*** | ***2.42*** | ***0.02*** |
| ***DIRECT SAMPLING*** | | | | | | | | | | | | | | | | | | | | | | |
| TOOL STUB EXT INIT. CONT | 0 | 610 | 0 | 0 | 253 | 2 | 0 | 114 | 308 | 18 | 0 | 0 | 0 | 4 | 232 | 0 | 3 | 1 | 268 | 6 | 6 | 4 |
| Nailgun INT initial | 0 | 1785 | 0 | 0 | 22 | 0 | 0 | 33 | 868 | 0 | 0 | 0 | 0 | 0 | 2 | 0 | 0 | 0 | 0 | 0 | 0 | 0 |
| NAILGUN EXIT PORT | 2 | 567 | 0 | 0 | 139 | 2 | 1 | 121 | 347 | 41 | 0 | 0 | 0 | 16 | 544 | 2 | 3 | 3 | 151 | 7 | 31 | 1 |
| INTERIOR DIRECT SAMPLIN | 0 | 2523 | 0 | 0 | 73 | 0 | 0 | 338 | 427 | 0 | 0 | 0 | 0 | 1 | 105 | 0 | 1 | 0 | 11 | 1 | 0 | 0 |
| FINAL DIRECT SAMPLE | 0 | 3110 | 0 | 0 | 27 | 0 | 0 | 158 | 566 | 0 | 0 | 0 | 0 | 0 | 18 | 0 | 0 | 0 | 4 | 0 | 0 | 0 |
| ***Sum Direct*** | ***2*** | ***8595*** | ***0*** | ***0*** | ***514*** | ***4*** | ***1*** | ***764*** | ***2516*** | ***59*** | ***0*** | ***0*** | ***0*** | ***21*** | ***901*** | ***2*** | ***7*** | ***4*** | ***434*** | ***14*** | ***37*** | ***5*** |
| ***Average per stub*** | ***0.4*** | ***1719*** | ***0*** | ***0*** | ***103*** | ***0.8*** | ***0.2*** | ***153*** | ***503*** | ***11.8*** | ***0*** | ***0*** | ***0*** | ***4.2*** | ***180*** | ***0.4*** | ***1.4*** | ***0.8*** | ***86.8*** | ***2.8*** | ***7.4*** | ***1*** |
| ***% of Direct*** | ***0.01*** | ***39.24*** | ***0.00*** | ***0.00*** | ***2.35*** | ***0.02*** | ***0.00*** | ***3.49*** | ***11.49*** | ***0.27*** | ***0*** | ***0*** | ***0*** | ***0.10*** | ***4.11*** | ***0.01*** | ***0.03*** | ***0.02*** | ***1.98*** | ***0.06*** | ***0.17*** | ***0.02*** |

**Particle Count Data from stubs from Nail Gun Cartridges**



| SAMPLE | PbBaSb | PbBa | BaSb | PbSb | BaCaSi | BaAl | Sb | Ba | Pb | BaS | SbS | SnSb | PbSn | CuZn | Fe | Au | Ni | FeCrNi | Ca | Cu | KCl | LaCe |
|---|---|---|---|---|---|---|---|---|---|---|---|---|---|---|---|---|---|---|---|---|---|---|
| ***Surfaces*** | | | | | | | | | | | | | | | | | | | | | | |
| WOODEN SURFACE RED | 0 | 1596 | 0 | 0 | 39 | 0 | 0 | 83 | 1746 | 2 | 0 | 0 | 0 | 0 | 20 | 0 | 0 | 0 | 23 | 0 | 0 | 0 |
| WOODEN SURFACE YELLOV | 0 | 1760 | 0 | 0 | 31 | 0 | 0 | 71 | 1695 | 0 | 0 | 0 | 0 | 0 | 14 | 0 | 0 | 2 | 29 | 0 | 0 | 0 |
| PLASTIC BOX SAMPLE 1 | 0 | 1797 | 0 | 0 | 172 | 0 | 0 | 135 | 436 | 13 | 0 | 0 | 1 | 1 | 104 | 6 | 0 | 1 | 157 | 1 | 2 | 1 |
| PLASTIC BOX SAMPLE 2 | 0 | 2004 | 0 | 0 | 428 | 0 | 0 | 348 | 484 | 7 | 1 | 0 | 0 | 0 | 128 | 19 | 0 | 1 | 364 | 3 | 0 | 0 |
| ***total surfaces*** | ***0*** | ***7157*** | ***0*** | ***0*** | ***670*** | ***0*** | ***0*** | ***637*** | ***4361*** | ***22*** | ***1*** | ***0*** | ***1*** | ***1*** | ***266*** | ***25*** | ***0*** | ***4*** | ***573*** | ***4*** | ***2*** | ***1*** |
| ***Average per stub*** | ***0*** | ***1431*** | ***0*** | ***0*** | ***134*** | ***0*** | ***0*** | ***127*** | ***872*** | ***4.4*** | ***0.2*** | ***0*** | ***0.2*** | ***0.2*** | ***53.2*** | ***5*** | ***0*** | ***0.8*** | ***115*** | ***0.8*** | ***0.4*** | ***0.2*** |
| ***% of Surfaces*** | ***0*** | ***33.78*** | ***0*** | ***0*** | ***3.16*** | ***0*** | ***0*** | ***3.01*** | ***20.58*** | ***0.10*** | ***0.005*** | ***0*** | ***0.005*** | ***0.005*** | ***1.26*** | ***0.12*** | ***0*** | ***0.02*** | ***2.70*** | ***0.02*** | ***0.009*** | ***0.00*** |
| **HANDS load ONLY** | | | | | | | | | | | | | | | | | | | | | | |
| KS HANDS YELLOW | 0 | 718 | 0 | 0 | 145 | 7 | 0 | 316 | 313 | 12 | 0 | 0 | 0 | 18 | 178 | 1 | 7 | 2 | 69 | 20 | 233 | 0 |
| ***Sum Hands - loading*** | ***0*** | ***718*** | ***0*** | ***0*** | ***145*** | ***7*** | ***0*** | ***316*** | ***313*** | ***12*** | ***0*** | ***0*** | ***0*** | ***18*** | ***178*** | ***1*** | ***7*** | ***2*** | ***69*** | ***20*** | ***233*** | ***0*** |
| ***% of Total Hands - loading*** | ***0*** | ***18.84*** | ***0*** | ***0*** | ***3.80*** | ***0.18*** | ***0.00*** | ***8.29*** | ***8.21*** | ***0.31*** | ***0*** | ***0*** | ***0*** | ***0.47*** | ***4.67*** | ***0.03*** | ***0.18*** | ***0.05*** | ***1.81*** | ***0.52*** | ***6.11*** | ***0*** |

| SAMPLE | Ti | Sn | W | Bi | Zn | Ag | Zr | Sr | NiCu | BaSn | PbTi | PbCa | CrNi | PbSbSn | AuCu | PbClBr | Y | PbBaSn | TiZn | Unclass. | Total |
|---|---|---|---|---|---|---|---|---|---|---|---|---|---|---|---|---|---|---|---|---|---|
| ***HANDS -- USERS*** | | | | | | | | | | | | | | | | | | | | | |
| KS HANDS YELLOW | 10 | 4 | 0 | 0 | 26 | 0 | 16 | 1 | 0 | 1 | 3 | 3 | 0 | 0 | 0 | 0 | 0 | 2 | 0 | 2949 | 6646 |
| NL HANDS YELLOW | 3 | 0 | 0 | 0 | 17 | 0 | 4 | 0 | 0 | 0 | 2 | 1 | 0 | 0 | 0 | 0 | 0 | 0 | 0 | 1102 | 3704 |
| VOL#1 YELLOW 10SHOTS | 15 | 2 | 0 | 0 | 27 | 0 | 0 | 0 | 0 | 0 | 4 | 3 | 0 | 0 | 0 | 0 | 0 | 0 | 0 | 1511 | 4561 |
| VOL#2 YELLOW 10SHOTS | 6 | 1 | 0 | 0 | 19 | 0 | 2 | 1 | 0 | 0 | 1 | 2 | 2 | 0 | 0 | 1 | 0 | 0 | 0 | 745 | 3351 |
| VOL#3 YELLOW 9SHOTS | 3 | 1 | 3 | 0 | 17 | 2 | 0 | 0 | 0 | 0 | 1 | 8 | 0 | 0 | 0 | 0 | 1 | 0 | 0 | 988 | 3148 |
| VOL#4 YELLOW 10SHOTS | 11 | 5 | 2 | 0 | 95 | 3 | 1 | 3 | 0 | 0 | 2 | 14 | 0 | 0 | 1 | 0 | 2 | 0 | 0 | 814 | 4185 |
| VOL#5 YELLOW 10SHOTS | 0 | 13 | 4 | 5 | 83 | 0 | 3 | 0 | 0 | 0 | 0 | 2 | 1 | 0 | 0 | 0 | 0 | 0 | 0 | 316 | 1800 |
| VOL#6 YELLOW 10SHOTS | 44 | 6 | 19 | 0 | 8 | 1 | 2 | 0 | 4 | 1 | 20 | 2 | 0 | 0 | 0 | 0 | 1 | 0 | 0 | 673 | 3328 |
| VOL#7 YELLOW 10SHOTS | 2 | 9 | 0 | 2 | 2 | 0 | 1 | 0 | 0 | 0 | 0 | 1 | 0 | 0 | 0 | 0 | 1 | 0 | 0 | 396 | 3942 |
| VOL#8 YELLOW 10SHOTS | 17 | 6 | 0 | 4 | 41 | 0 | 15 | 0 | 6 | 0 | 1 | 2 | 0 | 0 | 0 | 0 | 1 | 0 | 0 | 1291 | 5159 |
| VOL#9 YELLOW 10SHOTS | 12 | 0 | 0 | 0 | 76 | 0 | 7 | 0 | 1 | 2 | 5 | 2 | 0 | 0 | 0 | 0 | 0 | 0 | 1 | 2035 | 6187 |
| VOL#10 YELLOW 10SHOTS | 4 | 0 | 0 | 1 | 45 | 0 | 10 | 1 | 5 | 0 | 7 | 5 | 0 | 0 | 0 | 0 | 0 | 1 | 0 | 1012 | 5202 |
| VOL #11 RED 10SHOTS | 2 | 11 | 0 | 4 | 101 | 1 | 1 | 0 | 1 | 0 | 0 | 4 | 0 | 0 | 0 | 0 | 0 | 3 | 0 | 329 | 3277 |
| VOL#11 RED 10SHOTS | 1 | 6 | 0 | 0 | 19 | 0 | 0 | 0 | 0 | 0 | 0 | 0 | 0 | 0 | 0 | 0 | 0 | 0 | 0 | 137 | 503 |
| ***Sum Hands*** | ***130*** | ***64*** | ***28*** | ***16*** | ***576*** | ***7*** | ***62*** | ***6*** | ***17*** | ***4*** | ***46*** | ***49*** | ***3*** | ***0*** | ***1*** | ***1*** | ***6*** | ***6*** | ***0*** | ***14298*** | ***54993*** |
| ***Average per stub*** | ***9.29*** | ***4.57*** | ***2.00*** | ***1.14*** | ***41.1*** | ***0.50*** | ***4.43*** | ***0.43*** | ***1.21*** | ***0.29*** | ***3.29*** | ***3.50*** | ***0.21*** | ***0.00*** | ***0.07*** | ***0.07*** | ***0.43*** | ***0.43*** | ***0*** | ***1021*** | ***3928*** |
| ***% of Total Hands*** | ***0.24*** | ***0.12*** | ***0.05*** | ***0.03*** | ***1.05*** | ***0.01*** | ***0.11*** | ***0.01*** | ***0.03*** | ***0.01*** | ***0.08*** | ***0.09*** | ***0.01*** | ***0.00*** | ***0.00*** | ***0.00*** | ***0.01*** | ***0.01*** | ***0*** | ***26.00*** | ***100*** |
| ***DIRECT SAMPLING*** | | | | | | | | | | | | | | | | | | | | | |
| TOOL STUB EXT INIT. CONT | 42 | 3 | 1 | 1 | 292 | 1 | 1 | 1 | 0 | 1 | 4 | 27 | 0 | 0 | 0 | 0 | 0 | 0 | 0 | 1504 | 3707 |
| Nailgun INT initial | 0 | 0 | 0 | 0 | 1 | 0 | 0 | 0 | 0 | 0 | 0 | 1 | 0 | 0 | 0 | 0 | 0 | 0 | 0 | 435 | 3147 |
| NAILGUN EXIT PORT | 46 | 7 | 1 | 0 | 70 | 1 | 17 | 1 | 0 | 0 | 2 | 36 | 0 | 0 | 0 | 0 | 0 | 0 | 0 | 1141 | 3300 |
| INTERIOR DIRECT SAMPLIN | 0 | 0 | 0 | 0 | 68 | 0 | 21 | 0 | 0 | 0 | 7 | 5 | 0 | 0 | 0 | 0 | 0 | 0 | 0 | 2326 | 5907 |
| FINAL DIRECT SAMPLE | 1 | 0 | 0 | 0 | 0 | 0 | 6 | 0 | 0 | 0 | 6 | 2 | 0 | 0 | 0 | 0 | 0 | 0 | 0 | 1942 | 5840 |
| ***Sum Direct*** | ***89*** | ***10*** | ***2*** | ***1*** | ***431*** | ***2*** | ***45*** | ***2*** | ***0*** | ***1*** | ***19*** | ***71*** | ***0*** | ***0*** | ***0*** | ***0*** | ***0*** | ***0*** | ***0*** | ***7348*** | ***21901*** |
| ***Average per stub*** | ***17.8*** | ***2*** | ***0.4*** | ***0.2*** | ***86*** | ***0.4*** | ***9*** | ***0.4*** | ***0*** | ***0.2*** | ***3.8*** | ***14*** | ***0*** | ***0*** | ***0*** | ***0*** | ***0*** | ***0*** | ***0*** | ***1470*** | ***4380*** |
| ***% of Direct*** | ***0.41*** | ***0.05*** | ***0.01*** | ***0.00*** | ***1.97*** | ***0.01*** | ***0.21*** | ***0.01*** | ***0*** | ***0.005*** | ***0.09*** | ***0.32*** | ***0*** | ***0*** | ***0*** | ***0*** | ***0*** | ***0*** | ***0*** | ***33.55*** | ***100*** |

**Particle Count Data from stubs from Nail Gun Cartridges**



| SAMPLE | Ti | Sn | W | Bi | Zn | Ag | Zr | Sr | NiCu | BaSn | PbTi | PbCa | CrNi | PbSbSn | AuCu | PbClBr | Y | PbBaSn | TiZn | Unclass. | Total |
|---|---|---|---|---|---|---|---|---|---|---|---|---|---|---|---|---|---|---|---|---|---|
| ***Surfaces*** | | | | | | | | | | | | | | | | | | | | | |
| WOODEN SURFACE RED | 12 | 0 | 0 | 0 | 10 | 0 | 4 | 1 | 0 | 0 | 13 | 5 | 0 | 0 | 0 | 0 | 0 | 1 | 0 | 2262 | 5817 |
| WOODEN SURFACE YELLOV | 3 | 0 | 0 | 0 | 9 | 0 | 2 | 0 | 0 | 0 | 3 | 14 | 0 | 0 | 0 | 0 | 0 | 0 | 0 | 2099 | 5732 |
| PLASTIC BOX SAMPLE 1 | 8 | 5 | 0 | 0 | 176 | 0 | 1 | 0 | 0 | 0 | 6 | 7 | 0 | 0 | 0 | 0 | 0 | 0 | 0 | 779 | 3809 |
| PLASTIC BOX SAMPLE 2 | 21 | 0 | 0 | 0 | 0 | 0 | 8 | 0 | 0 | 0 | 15 | 34 | 0 | 0 | 0 | 0 | 0 | 0 | 0 | 1963 | 5828 |
| ***total surfaces*** | ***44*** | ***5*** | ***0*** | ***0*** | ***195*** | ***0*** | ***15*** | ***1*** | ***0*** | ***0*** | ***37*** | ***60*** | ***0*** | ***0*** | ***0*** | ***0*** | ***0*** | ***1*** | ***0*** | ***7103*** | ***21186*** |
| ***Average per stub*** | ***8.8*** | ***1*** | ***0*** | ***0*** | ***49*** | ***0*** | ***3.8*** | ***0.25*** | ***0*** | ***0*** | ***9.3*** | ***15*** | ***0*** | ***0*** | ***0*** | ***0*** | ***0*** | ***0.25*** | ***0*** | ***1775.8*** | ***5297*** |
| ***% of Surfaces*** | ***0.21*** | ***0.02*** | ***0*** | ***0*** | ***0.92*** | ***0*** | ***0.07*** | ***0.005*** | ***0*** | ***0*** | ***0.17*** | ***0.28*** | ***0*** | ***0*** | ***0*** | ***0*** | ***0*** | ***0.005*** | ***0*** | ***33.53*** | ***100*** |
| **HANDS load ONLY** | | | | | | | | | | | | | | | | | | | | | |
| KS HANDS YELLOW | 26 | 0 | 0 | 0 | 56 | 2 | 29 | 0 | 1 | 2 | 6 | 5 | 0 | 0 | 1 | 0 | 0 | 0 | 0 | 1645 | 3812 |
| ***Sum Hands - loading*** | ***26*** | ***0*** | ***0*** | ***0*** | ***56*** | ***2*** | ***29*** | ***0*** | ***1*** | ***2*** | ***6*** | ***5*** | ***0*** | ***0*** | ***1*** | ***0*** | ***0*** | ***0*** | ***0*** | ***1645*** | ***3812*** |
| ***% of Total Hands - loading*** | ***0.68*** | ***0*** | ***0*** | ***0*** | ***1.47*** | ***0.05*** | ***0.76*** | ***0*** | ***0.03*** | ***0.052*** | ***0.16*** | ***0.13*** | ***0*** | ***0*** | ***0.03*** | ***0*** | ***0*** | ***0*** | ***0*** | ***43.15*** | ***100*** |

**Particle Count Data from stubs from Nail Gun Cartridges**



| SAMPLE | Classified |
|---|---|
| ***HANDS -- USERS*** | |
| KS HANDS YELLOW | 3697 |
| NL HANDS YELLOW | 2602 |
| VOL#1 YELLOW 10SHOTS | 3050 |
| VOL#2 YELLOW 10SHOTS | 2606 |
| VOL#3 YELLOW 9SHOTS | 2160 |
| VOL#4 YELLOW 10SHOTS | 3371 |
| VOL#5 YELLOW 10SHOTS | 1484 |
| VOL#6 YELLOW 10SHOTS | 2655 |
| VOL#7 YELLOW 10SHOTS | 3546 |
| VOL#8 YELLOW 10SHOTS | 3868 |
| VOL#9 YELLOW 10SHOTS | 4152 |
| VOL#10 YELLOW 10SHOTS | 4190 |
| VOL #11 RED 10SHOTS | 2948 |
| VOL#11 RED 10SHOTS | 366 |
| ***Sum Hands*** | |
| ***Average per stub*** | ***0.00*** |
| ***% of Total Hands*** | ***0.00*** |
| | |
| ***DIRECT SAMPLING*** | |
| TOOL STUB EXT INIT. CONT | 2203 |
| Nailgun INT initial | 2712 |
| NAILGUN EXIT PORT | 2159 |
| INTERIOR DIRECT SAMPLIN | 3581 |
| FINAL DIRECT SAMPLE | 3898 |
| | |
| ***Sum Direct*** | 14553 |
| ***Average per stub*** | ***2910.6*** |
| ***% of Direct*** | **66.45** |

**Particle Count Data from stubs from Nail Gun Cartridges**



| SAMPLE | Classified |
|---|---|
| ***Surfaces*** | |
| WOODEN SURFACE RED | 3555 |
| WOODEN SURFACE YELLOW | 3633 |
| PLASTIC BOX SAMPLE 1 | 3030 |
| PLASTIC BOX SAMPLE 2 | 3865 |
| ***total surfaces*** | 14083 |
| ***Average per stub*** | ***3520.8*** |
| ***% of Surfaces*** | **66.47** |
| | |
| **HANDS load ONLY** | |
| KS HANDS YELLOW | 2167 |
| ***Sum Hands - loading*** | **2167** |
| ***% of Total Hands - loading*** | **56.85** |

## 8.4. Manuscripts published associated with work from this thesis

The following pages contain published papers on which several chapters from this thesis are based.

[1] **K.E. Seyfang,** H.J. Kobus, R.S. Popelka-Filcoff, A. Plummer, C.W. Magee, K.E. Redman, K.P. Kirkbride, Analysis of elemental and isotopic variation in glass frictionators from 0.22 rimfire primers, Forensic Science International 293 (2018) 47-62.
[2] **K.E. Seyfang,** N. Lucas, R.S. Popelka-Filcoff, H. Kobus, K.E. Redman, K.P. Kirkbride, Methods for Analysis of Glass in Glass-Containing Gunshot Residue (gGSR) Particles, Forensic Science International 298 (2019) 359-371.
[3] **K.E. Seyfang,** N. Lucas, K.E. Redman, R.S. Popelka-Filcoff, H.J. Kobus, K.P. Kirkbride, Glass-containing gunshot residues and particles of industrial and occupational origins: Considerations for evaluating GSR traces, Forensic Science International 298 (2019) 284-297.
[4] W. Tucker, N. Lucas, **K.E. Seyfang,** K.P. Kirkbride, R.S. Popelka-Filcoff, Gunshot residue and brake pads: Compositional and morphological considerations for forensic casework, Forensic Science International 270 (2017) 76-82.

[The manuscripts of the publications have been removed for copyright issues]